ペルオキシソームタンパク質輸送機構の解析

二藤　和昌

要旨

高等植物のペルオキシソームは個体の成長段階に合わせて、その酵素群を変化させ様々な生理機能を果たしている。脂肪性種子の発芽段階において、ペルオキシソームは内包する脂肪酸β酸化系とグリオキシル酸回路の諸酵素を用いて、子葉に蓄えられた貯蔵脂肪を糖へと変換するために中心的に機能する。そして、さらに生長が進み光を浴び、緑化すると脂質代謝を担っていた酵素群は減少し、変わって光呼吸に関与する酵素群がペルオキシソーム内に蓄積し機能しはじめる。このようなペルオキシソームの劇的な機能転換には、翻訳後のペルオキシソームタンパク質が適切にペルオキシソームへと輸送されることが重要である。そこで本研究論文では、ペルオキシソームタンパク質輸送の分子メカニズムという視点から、ペルオキシソームの機能獲得について理解するべく研究を進めた。

第1章では、ペルオキシソーム膜タンパク質の *At*Pex14p を欠損した結果、ペルオキシソームの PTS 依存的タンパク質輸送が低下し、そのためペルオキシソーム機能不全となった *ped2* 変異体を足がかりとして、マトリクスタンパク質輸送機構の解明を行った。*At*Pex14p 以外にペルオキシソームへのタンパク質輸送に関わる因子として、PTS1 レセプターと PTS2 レセプターとして機能する可能性が示唆されている *At*Pex5p と *At*Pex7p の cDNA 配列がシロイヌナズナで報告されており、これらも含めて機能を同定した。

ペルオキシソームタンパク質輸送過程における機能分担を明らかにするた

め、*At*Pex14p、*At*Pex5p、*At*Pex7p、PTS1 型タンパク質、PTS2 型タンパク質間の相互作用について解析を行ったところ、以下の結果が得られた。(1) *At*Pex14p は *At*Pex5p と結合するが、*At*Pex7p および PTS1 型タンパク質、PTS2 型タンパク質とは直接結合しない。(2) *At*Pex5p は PTS1 型タンパク質と結合する。(3) *At*Pex7p は PTS2 型タンパク質と結合する。(4) *At*Pex5p は *At*Pex7p と結合する。(5) それぞれの結合領域は互いに重複していない。以上の結果から、新規に合成された PTS1 型タンパク質および PTS2 型タンパク質は細胞質中に存在する *At*Pex5p-*At*Pex7p レセプター複合体によって捕捉された後に、*At*Pex5p を介してペルオキシソーム膜上の *At*Pex14p に結合し、巨大な初期輸送複合体を形成すると考えられる。さらに、*At*Pex7p が *At*Pex5p を介して *At*Pex14p と結合することから、シロイヌナズナにおいて PTS2 型タンパク質の輸送が *At*Pex5p に依存的であり、付加的な経路であることが示された。

また、シロイヌナズナの様々な器官における、これら 3 つの輸送因子の発現をイムノブロットにより解析したところ、*At*Pex14p と *At*Pex5p はほとんどの器官で検出されるのに対して、PTS2 レセプターの *At*Pex7p は限られた器官でのみ検出された。この結果は、PTS2 型タンパク質の発現は高い器官特異性を持っていることを反映しており、これらの発現が植物ペルオキシソームの機能分化を支えている可能性を示唆している。

第 2 章では、マトリクスタンパク質とは異なる経路で輸送されていることが示唆されているペルオキシソーム膜貫通型タンパク質の局在化機構について解析を行った。この解析にはペルオキシソームに局在する 31 kDa 膜貫通型タンパク質であるアスコルビン酸ペルオキシダーゼ（pAPX）を用いて行った。

pAPXの細胞内局在をショ糖密度勾配遠心法により解析したところ、pAPXはペルオキシソーム画分のみならず、小胞体画分にも検出された。しかしながら、マグネシウムシフト法による解析の結果からは、少なくともpAPXが粗面小胞体に局在する可能性は否定され、それ以外の何らかの膜系に局在することがわかった。pAPXがどのような膜構造物に局在しているかを免疫電子顕微鏡観察により解析したところ、pAPXはペルオキシソーム膜に局在するとともに、未同定の膜構造物上にも検出された。この結果はpAPXの局在化に未同定の膜構造物が関与することを示唆している。ペルオキシソーム膜貫通型タンパク質の局在化がこのような膜構造物を介して輸送されているという可能性は、ペルオキシソーム形成における由来や分泌小胞との関連を考察する上で興味深い。

本研究により、高等植物ペルオキシソームへのマトリクスタンパク質、膜貫通型タンパク質両輸送機構の一端が明らかになった。これらの結果は輸送機構のみならず、これまで不明であったペルオキシソームというオルガネラの起源や新規なペルオキシソーム機能に関して新たな知見を与えるものと考えている。

目次

略号

3-AT	: 3-amino triazole
BPB	: bromo phenol blue
BSA	: bovine serum albumin
CAT	: catalase
cDNA	: complementary DNA
2,4-D	: 2,4-dichlorophenoxyacetic acid
2,4-DB	: 2,4-dichlorophenoxybutyric acid
DNA	: deoxyribonucleic acid
DW	: distilled water
EDTA	: ethylenediaminetetraacetic acid
EST	: expressed sequence tag
GFP	: green fluorescent protein
HEPES	: *N*-2-hydroxyethylpiperazine-*N'*-2-ethanesulfonic acid
HPR	: hydroxypyruvate reductase
ICL	: isocitrate lyase
IgG	: immumoglobulin G
kDa	: kilo dalton
mRNA	: messenger RNA
MS	: Murashige and Skoog medium
PBS	: phosphate buffered saline
PCR	: polymerase chain reaction

ped	: peroxisome defective
Pmp	: peroxisome membrane protein
PMSF	: phenylmethanesulfornyl fluoride
poly(A)$^+$ RNA	: polyadenylated RNA
PTS	: peroxisomal targeting signal
PVDF	: polyvinylidene difluoride
RNA	: ribonucleic acid
SDS	: sodium dodecyl sulfate
SDS-PAGE	: SDS-polyacrylamide gel electrophoresis
TBS	: tris buffered saline
Tris	: tris (hydroxymethyl) aminomethane

その他、核酸、アミノ酸の略号として 1 文字表記を用いた。

序論

真核細胞では、様々な代謝機能が生体膜によって区画化されたオルガネラ（細胞内小器官）に存在する。個体が成長する上で、各種のオルガネラが固有の機能を果たしつつ、協調的に働くことが必要不可欠である。これらのオルガネラは決して静的な状態のまま細胞内に存在しているのではなく、細胞の生長分化に伴い生成、変換、消失するなど極めて動的な状態にある。そして、多種多様に分化した真核細胞からなる高等動植物では、個々に分化した細胞内に存在するオルガネラが動的に変化し、それぞれ特殊化した機能を持ち合わせている。逆から見れば、これはオルガネラの機能分化こそが真核細胞の多様化を可能にしているといえる。この事実は、動植物が示す様々な生理現象を解明していく上で、オルガネラレベルでの解析が重要であることを示している。

真核生物細胞に普遍的に存在するオルガネラの内の一つであるペルオキシソームは、1950 年代に発見されて以来長い間、機能をもたないオルガネラと考えられてきた。しかしながら、高等植物のペルオキシソームが脂質代謝に関与するという証明がなされ、更にその後の研究によってこの機能が生物界全般のペルオキシソームに普遍化されることで、注目されるオルガネラとなりつつある。本研究論文では、このペルオキシソームの機能獲得および分化のメカニズムを、ペルオキシソームタンパク質輸送機構の解明という視点から解析を加え、考察する。

高等植物のペルオキシソーム

高等植物細胞のペルオキシソームはそれぞれの機能により少なくとも 3 種類、黄化子葉などに観察されるグリオキシソーム、光合成器官に存在する緑葉ペルオキシソーム、根などの器官にみられる特殊化していないペルオキシソームに細分される(Beevers, 1979)。

高等植物の様々な器官において、これらのペルオキシソームはそれぞれの代謝系に必要な特異的な酵素群を内在している。グリオキシソームは脂肪性種子の発芽段階における胚乳や子葉のような貯蔵器官や老化器官の細胞に存在している(Nishimura et al., 1996)。このグリオキシソームは脂肪酸β酸化とグリオキシル酸回路の酵素群を有しており、貯蔵脂肪からショ糖への変換過程において中心的な役割を担っている。高等植物の発芽段階においてはグリオキシソームに短鎖 acyl-CoA 酸化酵素が蓄積することから、脂肪酸のほとんどがグリオキシソームで分解されていることが示唆されている(Beevers, 1982)。対照的に、緑葉ペルオキシソームは光合成器官の細胞に広く分布している。この緑葉ペルオキシソームにはいくつかの光呼吸系の酵素が含まれており、緑葉ペルオキシソーム、葉緑体、ミトコンドリア間における酵素反応によって光呼吸系を成立させている(Tolbert, 1982)。根や茎などの他の器官に特殊化していないペルオキシソームが存在しているが(Nishimura et al., 1996)、その機能は未だ不明である。

植物ペルオキシソームの機能転換

グリオキシソーム、緑葉ペルオキシソーム、特殊化していないペルオキシソームは環境の変化に応じてその機能を他のペルオキシソームに転換させることが知られている(Nishimura et al., 1996)。たとえば、黄化子葉のグリオキシソームは光照射により子葉が緑化していく過程で、直接緑葉ペルオキシソームへと変化する(Nishimura et al., 1986; Titus and Becker, 1985)。この過程においてイソクエン酸リアーゼ（ICL: isocitrate lyase）やリンゴ酸合成酵素（malate synthase）のようなグリオキシソーム酵素は特異的に分解され、グリコール酸酸化酵素 (glycolate oxidase) やヒドロキシピルビン酸還元酵素 (HPR: hydroxypyruvate reductase）などの緑葉ペルオキシソーム酵素が新規に合成され、それらがペルオキシソームに輸送されることにより、グリオキシソームから緑葉ペルオキシソームへの機能転換が

起こる(Hayashi et al., 1996b; Tsugeki et al., 1993)。逆に、緑化子葉の緑葉ペルオキシソームは子葉の老化の過程において、再びグリオキシソームへと変化する(De Bellis et al., 1991; Nishimura et al., 1993)。このようなタンパク質輸送や分解を伴う高等植物のペルオキシソームの機能転換は遺伝子発現により支配されていると考えられる(Nishimura et al., 1996)。しかしながら、現在のところこの過程を制御する詳細なメカニズムは明らかでない。

ペルオキシソームにおける過酸化水素消去系

ペルオキシソームは 1950 年代初頭、マウスの肝細胞の電子顕微鏡観察により発見されたオルガネラであり、形態学的な知見から当初マイクロボディと呼ばれていた。以降の研究により、高等動物のみならず、植物、菌類、原生動物、無脊椎動物などで発見され、真核生物細胞に普遍的に存在することが知られている。また、生化学的な解析から、このオルガネラには H_2O_2 を生成する一連の酸化酵素群とそれを消去する酵素が局在することが明らかになり、近年ではペルオキシソームと呼ばれることが一般的となりつつある。植物ペルオキシソームはその主な機能である脂肪酸 β 酸化系や光呼吸系の反応過程において、多量の H_2O_2 を副産物として生成する。言うまでもなく H_2O_2 は多くの生体成分を無秩序に酸化し、種々の酸化的障害（酸素毒）をもたらすため、ペルオキシソームは H_2O_2 を即座に分解し酸化的障害から防御する機構を備えている。この防御機構に最も貢献していると考えられているのはカタラーゼ（CAT: catalase）である。カタラーゼはペルオキシソームの標識酵素として頻繁に用いられるように、ペルオキシソームの発見以来すべてのペルオキシソームマトリクスに共通して存在している酵素である。しかしながら、これまでの解析からカタラーゼは H_2O_2 に対する K_m 値が高く(Huang et al., 1983)、低濃度の H_2O_2 の消去には適さないことが明らかにされている。このようなカタラーゼでは消去できない低濃度の H_2O_2 の消去を担っていると考えられているのが一般的に低い K_m 値をもつアスコルビン

酸ペルオキシダーゼ（APX: ascorbate peroxidase）である。植物細胞には 4 種類の APX タンパク質が存在し、それぞれが別々の細胞内局在性を示すことがわかっている。これら APX のうちの 1 つがペルオキシソーム膜に局在する pAPX である。これまでにペルオキシソーム膜局在の pAPX はカボチャ、シロイヌナズナ、綿花、キュウリ、ホウレンソウで酵素学的、生化学的手法により同定されている(Corpas and Trelease, 1998; Ishikawa et al., 1998; Yamaguchi et al., 1995a)。

ペルオキシソームタンパク質輸送シグナル

ペルオキシソーム酵素は細胞質で合成される。そして、翻訳後にペルオキシソームへ輸送されてはじめて機能する。ほとんどの植物ペルオキシソーム酵素はそのアミノ酸配列の中にペルオキシソームへの輸送シグナル（PTSs: peroxisome targeting signals）として同定された 2 つの配列の内のいずれかを有している(Hayashi et al., 2000b)。1 つは PTS1 であり、タンパク質の C 末端に特徴的な 3 アミノ酸配列として存在する(Hayashi et al., 1996a; Trelease et al., 1996)。植物において PTS1 と認識されるアミノ酸の組み合わせは(C/A/S/P)-(K/R)-(I/L/M)である(Hayashi et al., 1997)。もう 1 つの輸送シグナルは、N 末端延長配列内に含まれている(Gietl et al., 1994)。この N 末端延長配列に保存されるアミノ酸配列は(R)-(L/Q/I)-X5-(HL)であり PTS2 と呼ばれている(Kato et al., 1996a; Kato et al., 1998)。これらのタンパク質は N 末端延長配列に伴った高分子量前駆体タンパク質として合成される。この N 末端延長配列をもったタンパク質はペルオキシソームに輸送された後プロセシングされ、成熟型タンパク質となる。PTS1 または PTS2 をもったペルオキシソームタンパク質は細胞質で多量体を形成し、そのままペルオキシソームへと輸送される(Flynn et al., 1998; Kato et al., 1999; Lee et al., 1997)。

ペルオキシソーム膜タンパク質輸送シグナル

一方でペルオキシソーム膜タンパク質の輸送機構についてはほとんど明らかにされていないのが現状である。近年、数種類のペルオキシソームタンパク質において、膜タンパク質の輸送シグナル（mPTS）の解析が進んでいるが、最も研究の進んでいるのは *C. boidinii* の Pmp47（Pmp: peroxisome membrane protein）である(Dyer et al., 1996)。Pmp47 は 6 回貫通している膜タンパク質で N 末端をマトリクス側に向けている。その mPTS は 4 番目と 5 番目の膜貫通領域に挟まれた親水性の領域で、ペルオキシソームマトリクス内にループ構造をとっている 20 アミノ酸に限定されている。同様に、後述するペルオキシン（peroxin）と呼ばれる因子のうちの一部（Pex3p、Pex22p）が mPTS を保有しているとの報告がある(Koller et al., 1999; Wiemer et al., 1996)。Pex3p、Pex22p はいずれも一回貫通型の膜タンパク質であるが、その mPTS はペルオキシソームマトリクス側の 30～40 アミノ酸ほどの領域として同定されている。これらのポリペプチド間に mPTS として保存された領域は見いだされておらず、輸送シグナルとして働くモチーフ構造は未だ明らかでない。ただ、mPTS にはいくつかの塩基性アミノ酸が連なったペプチドの部分構造があること、mPTS が膜貫通領域ではなくペルオキシソームマトリクス内にあることは一致している。よって、mPTS は輸送シグナルとして機能するが、疎水性の高い膜貫通領域により捕捉される輸送停止機構が起こるのではないかと考えられており、これは翻訳後にペルオキシソームへ輸送されるというモデルとも矛盾しない。また、これらの膜貫通型タンパク質にはマトリクスタンパク質のような PTS1、PTS2 が見あたらないことから、膜貫通型タンパク質とマトリクスタンパク質は根本的に局在化機構が異なることが考えられている。最近、ペルオキシンのうちの 1 つ Pex19p が同定されているほとんどのペルオキシソーム膜タンパク質に結合活性があると報告された(Sacksteder et al., 2000)。この報告により Pex19p はペルオキシソーム膜タンパク質の輸送に関わると考えられたが、その膜タンパク質側の Pex19p と

の結合領域は既に報告されていた mPTS とは異なる領域であった(Snyder et al., 2000)。そのため、Pex19p の膜タンパク質への結合が輸送に関わるものなのかは未だ不明であり、今後の解析が待たれている。

ペルオキシソーム形成因子・ペルオキシン

1990 年代から始まった酵母を中心とした遺伝学的解析から、ペルオキシソームの形成維持に関わる因子群の同定が精力的に進められている。酵母はβ酸化系をペルオキシソームにのみ有している。*Saccharomyces cerevisiae* などの脂肪酸資化性酵母は、オレイン酸を単一の炭素源として生育させると、ペルオキシソームが形成され、その際オルガネラ内には脂肪酸β酸化系に必要な酵素が誘導される。*Pichia pastoris*、*Candida boidinii* などのメタノール資化性酵母では、メタノールを単一の炭素源として生育させると、アルコール酸化酵素やカタラーゼなどがペルオキシソーム内に誘導され、ペルオキシソームはその細胞内に占める体積の割合が 80%近くになるまで大きく発達する。メタノール資化性酵母である *Pichia pastoris*、*Candida boidinii* のペルオキシソームはこのようなメタノール代謝系だけではなく、脂肪酸β酸化系も併せてもっているため、オレイン酸などの脂肪酸を炭素源として生育することができる。さらに *Candida boidinii* は、D-アラニンも炭素源として生育でき、D-アミノ酸酸化酵素をもつペルオキシソームを誘導する。このようにペルオキシソーム形成を行うことができない酵母突然変異株は、*Pichia pastoris* では 2 つの炭素源に、*Candida boidinii* では 3 つのペルオキシソーム誘導炭素源に生育できない変異株の中から分離された。ペルオキシソームを誘導し、かつ代謝系としてはあまり関係のない複数の炭素源に生育できるというメタノール資化性酵母の生育特性は、代謝系変異株を排除してペルオキシソーム機能欠損変異体の取得のためのスクリーニング効率を高めることとなった。

一方、哺乳類を対象としたペルオキシソーム形成因子の研究は、ヒトペルオキシソ

ームの機能欠損が重篤な遺伝病を引き起こすことを発端としており、医学的な背景と相まって近年急速に進んでいる。ヒトペルオキシソームの機能欠損による影響は 4 つの臨床上の症状に分類され、それぞれ Zellweger 症候群（ZS: Zellweger syndrome)、新生児型副腎白質ジストロフィー（NALD: neonatal adrenoleukodystrophy)、乳児型 Refsum 病（IRD: infantile Refsum disease)、斑状軟骨形成不全症 II 型（RCDP: rhizomelic chondrodysplasia punctata）と呼ばれている。これらの遺伝病は、重篤な順に ZS、NALD、IRD となっているが、いずれの遺伝病をもつ患者も神経発達の異常、肝機能の低下、頭蓋および顔面の形態異常、低血圧などの痛烈な症状を示し、結果として早期に死に至る。ZS、NALD、IRD の患者における循環器系にはフィタン酸と超長鎖脂肪酸が蓄積し、エーテルリン脂質の 1 種プラズマローゲンの生合成が不十分となっている。これらの患者に対する医学的な予測は冷酷であり、10 才まで生きのびる可能性はわずかだとされている。RCDP は PTS2 型タンパク質の輸送のみが阻害された結果起こる病気であり、そのため ZS、NALD、IRD よりも比較的軽い遺伝病であるが、発育遅延、近接短縮、白内障、骨端石灰化、角化症を引き起こす。RCDP の患者の体内には大量のフィタン酸が蓄積しプラズマローゲンも不足しているが、超長鎖脂肪酸は通常量であることがわかっている(Subramani, 1998)。

以上のような酵母や哺乳類を用いた多種のペルオキシソーム機能不全突然変異体の解析から、ペルオキシソーム形成維持に関わる因子群が同定された。酵母 *Saccharomyces cerevisiae* と *Pichia pastoris* からは PAS 遺伝子(Erdmann and Kunau, 1992; Gould et al., 1992; Kunau et al., 1993)、*Candida boidinii* からは PMP 遺伝子(Sakai et al., 1995)、*Yerrowia lipolytica* からは PAY 遺伝子(Nuttley et al., 1993)、*Hansenula polymorpha* からは PER 遺伝子(Veenhuis et al., 1992)が同定され、哺乳類 *Homo sapiens* と *Mus musculus* からは PAF 遺伝子(Tsukamoto et al., 1994; Tsukamoto et al., 1990)が同定された。このように様々な生物種から多数のペルオキシソーム形成に関わる因子群が同定されたが、当初同一の機能をもつ因子であっても種

間によって名称は異なっており、しばしば混乱を招く原因となっていた。そこで 1996 年ペルオキシソーム形成や維持に関わるタンパク質因子の命名法を全生物について統一することになり、タンパク質因子をペルオキシン（peroxin）、コードしている遺伝子を *PEX* 遺伝子と呼ぶこととなった(Distel et al., 1996)。そして現在までに酵母、哺乳類を含めて 23 種類ものペルオキシンが同定されている。

植物ペルオキシソーム機能欠損変異体

当研究室では植物細胞におけるペルオキシソーム機能制御に関連した遺伝子を同定するため、ペルオキシソーム機能欠損した突然変異体を単離している。このような突然変異体の選抜は、グリオキシソームの脂肪酸 β 酸化系を欠損したシロイヌナズナ突然変異体が 2,4-ジクロロフェノキシ酪酸（2,4-DB: 2,4-dichlorophenoxybutyric acid）に対して耐性を示すことを利用して行った(Hayashi et al., 1998b)。2,4-ジクロロフェノキシ酪酸の酪酸鎖はメチレン基として、グリオキシソームの脂肪酸 β 酸化系に認識をうけ切断される。その結果として、野生型植物体では除草剤である 2,4-ジクロロフェノキシ酢酸（2,4-D: 2,4-dichlorophenoxyacetic acid）に変換する。しかしながら、突然変異体では脂肪酸 β 酸化系が欠損しているためこの変換が行われず、結果として変異個体は生き残る。この選抜方法により、当研究室では 3 つの独立した遺伝子座に分類される 4 つの突然変異体の単離に成功し、それぞれを *ped1*、*ped2*、*ped3* 変異体と名付けた（*ped*: peroxisome defective)。これらの突然変異体はグリオキシソームの脂肪酸 β 酸化系の活性が減少しており、種子に蓄えられた脂肪からショ糖を産生することが妨げられるため、発芽後の成長にショ糖を必要とする。

シロイヌナズナ *ped2* 変異体

これらの突然変異体の内の 1 つ *ped2* 変異体の表現型を詳細に解析した結果、以下のことが明らかとなった(Hayashi et al., 1998b)。

（1）*ped2* 変異体における PTS1 型タンパク質の細胞内輸送

ped2 変異体における PTS1 型タンパク質の細胞内輸送について解析するため、緑色蛍光タンパク質（GFP）と PTS1 型タンパク質との融合タンパク質（GFP-PTS1）(Mano et al., 1999)を *ped2* 変異体内で発現する形質転換シロイヌナズナを作製した。GFP-PTS1 の緑色蛍光は *ped2* 変異体細胞内の細胞質とペルオキシソームの両方に観察された。この結果は GFP-PTS1 の一部がペルオキシソームに輸送されずに細胞質に留まっていることを示している。また、一部はペルオキシソームに観察されたことから、*ped2* 変異体細胞内で一定量の GFP-PTS1 が正しく認識され、ペルオキシソームへと輸送されたことも示された。この結果から、*ped2* 変異体内では PTS1 型タンパク質の細胞内輸送能力が低下していると結論した。

（2）*ped2* 変異体における PTS2 型タンパク質の細胞内輸送

ped2 変異体における PTS2 型タンパク質の細胞内輸送について解析するため、PTS2 型タンパク質であるチオラーゼをイムノブロットにより解析した。その結果、ped2 変異体内には 2 種類のタイプのチオラーゼが検出された。1 つは 45kDa のタンパク質で成熟型チオラーゼに対応しているが、もう 1 つはより大きな分子量（48kDa）のタンパク質であった。この高分子量タンパク質は以前の解析から、細胞質に蓄積したチオラーゼの前駆体タンパク質であることが証明されている(Kato et al., 1996b)。PTS2 型タンパク質はペルオキシソーム内でのみプロセシングされるのでこのデータは、*ped2* 変異体細胞では PTS2 型タンパク質の細胞内輸送活性も低下しており、そのタンパク質合成が盛んな期間は全てのマトリクスタンパク質をペルオキシソームへと輸送する機能が著しく低下していると考えられた。

（3）*ped2* 変異体細胞の形態学的解析

ped2 変異体の様々なペルオキシソームを免疫学的電子顕微鏡観察により解析した。前述したように、高等植物には 3 種類のペルオキシソーム、グリオキシソーム、緑葉ペルオキシソーム、特殊化していないペルオキシソームが存在する。野生型シロイヌナズナではどのペルオキシソームでも直径 0.5-1.0 μm ほどの円形または長円形の構造物として観察される。対照的に、*ped2* 変異体のグリオキシソームはつぶれて萎びたような形態をしていた。同様の形態学的な異常は、*ped2* 変異体の緑葉ペルオキシソーム、特殊化していないペルオキシソームでも観察された。これらのデータから、*ped2* 変異体における変異は 3 種類すべてのペルオキシソームに影響を及ぼし、結果として異常な形態を示していると結論した。

以上（1）～（3）に示したように、*ped2* 変異体はペルオキシソームへの細胞内輸送が低下したためにペルオキシソーム機能不全を引き起こしていると推測された。そこでファインマッピングによる *PED2* 遺伝子座の同定を行った。その結果、*PED2* 遺伝子座が 5 番染色体の P1 クローンの MQB2 に含まれていることが明らかになった（Figure 2A）。P1 クローンの MQB2 には 16 個の推定遺伝子が含まれると予測されていた（http://www.kazusa.or.jp/kaos/）。これら 16 個の推定遺伝子全てをデータベースに送り相同性検索を行ったところ、ペルオキシンのうちの 1 つ Pex14p と相同性のある遺伝子が 1 つだけ、この中に含まれていた。この推定遺伝子は MQB2 の 7734bp の *Xho*I DNA 断片内に存在した（Figure 2B）。野生型シロイヌナズナ（Landsberg *erecta*）と *ped2* 突然変異体においてこの DNA 断片に相当する塩基配列を比較したところ、野生型では 760 番目のシトシンであるところが *ped2* 変異体ではチミンとなるナンセンス変異が起こっていた。この結果は、7734bp の *Xho*I DNA 断片内に *PED2* 遺伝子座が存在することを強く支持していた。

本研究の目的

ペルオキシソームタンパク質輸送因子の特定とその輸送過程における分子機構を明らかにすることは、ペルオキシソームの機能獲得を理解する上で不可避な問題である。上述したように当研究室ではペルオキシソームへのマトリクスタンパク質輸送能が低下したために、ペルオキシソーム機能不全となったと推測される *ped2* 変異体の単離に成功している。そこでまず本論第 1 章では *ped2* 変異体の脂肪酸 β 酸化系以外の表現型の解析をすると共に、*PED2* 遺伝子座が 7734bp の *Xho*I DNA 断片内に存在することを相補実験により証明する。次に *PED2* 遺伝子の翻訳産物の細胞内局在を特定し、ペルオキシソームタンパク質輸送過程における機能を明らかにする。これらの結果から、ペルオキシソームタンパク質輸送の分子メカニズムについて議論する。第 2 章では、第 1 章でのマトリクスタンパク質輸送機構とは異なる膜タンパク質の輸送機構について議論するために、ペルオキシソーム膜タンパク質の内の 1 つであるアスコルビン酸ペルオキシダーゼ（pAPX）について解析を加え、その局在化機構について考察する。

第 1 章　ペルオキシソームマトリクスタンパク質の輸送機構

ペルオキシソームへの PTS 依存的タンパク質輸送が低下したために、ペルオキシソーム機能不全となった *ped2* 変異体を足がかりとして、マトリクスタンパク質輸送機構を解明する。そのために、マッピングの結果から同定された *PED2* 遺伝子座を相補実験にて証明した。続いて *PED2* 遺伝子産物（*At*Pex14p）の細胞内局在を明らかにした。さらに、PTS1 レセプターおよび PTS2 レセプターとして報告されている *At*Pex5p と *At*Pex7p をクローニングし解析に加えた。そして、*At*Pex14p、*At*Pex5p、*At*Pex7p の 3 因子がペルオキシソームへのタンパク質輸送においてどのような役割分担をしているか、タンパク質間相互作用をもとに考察した。

材料と方法

植物材料

シロイヌナズナ（*Arabidopsis thaliana* (landsberg *erecta* and Columbia)）種子を 70%エタノールと滅菌液（2% NaClO, 0.02% Triton X-100）でそれぞれ 5 分間滅菌した。滅菌水で 5 回洗浄した種子をトップアガー（0.4% INA agar (Ina shokuhin, Nagano, Japan)）と共に GM（germination medium: 2.3 g/l MS salt (Wako, Osaka, Japan) 2% sucrose, 100 µg/ml myo-inositol, 1 µg/ml thiamine-HCl, 0.5 µg/ml pyridoxine, 0.5 µg/ml nicotinic acid, 0.5 mg/ml MES-KOH (pH 5.7), 0.8% INA agar (Ina shokuhin, Nagano, Japan)）寒天培地上にまいた。種子の休眠打破のために 2 日間の低温処理をした後、22℃のインキュベーター内で明条件下もしくは暗条件下で発芽生育させた。実験用途に合わせ、発芽 7 日目を経過した植物個体の内いくつかを

バーミキュライト：パーライトを 1: 1 で混合した土に植え継ぎ、22℃、100 μE/m^2/s で 16 時間明所、8 時間暗所で生育させた。

カボチャ種子（*Cucurbita sp.* Kurokawa Amakuri）は種皮をつけたまま、流水で 12 時間浸した後、湿らせた粒状ロックウール（Nitto Boseki, Chiba, Japan）上に播種し、暗所下 25℃において発芽生育させた。また、発芽後 5 日間暗所で生育させた黄化芽生えを白色光下に移し、25℃で更に生育させたものを緑化芽生えとした。

タンパク質試料の調製

電気泳動に用いるタンパク質試料は、植物材料を乳鉢にとり、液体窒素中で磨砕した。これに試料溶解液（2% SDS, 50 mM Tris-HCl (pH 6.8), 5% 2-mercaptoethanol, 0.1% BPB, 10% glycerol）に加えて更に磨砕し、95℃で 5 分間熱処理した。その後 15,000×*g* で 5 分間遠心し、上清をタンパク質試料とした。

cDNA クローニング

明所下で 7 日間発芽生育させたシロイヌナズナ子葉または、3 週間生育させた本葉から、RNeasy Plant Mini Kit（QIAGEN, Hilden, Germany）を用いて全 RNA を抽出した。この全 RNA を鋳型に Preamplification System（Invitrogen, Tokyo, Japan）を用いて逆転写反応を行い first strand cDNA を合成した。*At*Pex14p、*At*Pex5p、*At*Pex7p の ORF をもとに第 1 番目のメチオニンを含むように 5'-末端側プライマーを、ストップコドンを含むように 3'-末端側プライマーを設計し、DNA 合成機（Model 394, Applied Biosystems Inc., Foster City, CA）を用いて化学合成した。これらプライマーには後のサブクローニングのために適当な制限酵素サイトを連結している。これらのプライマーと first strand cDNA を用いて PCR を行い、目的の増幅断片を得た。得られた cDNA 断片を T-ベクター；pBluescript II SK+（Stratagene,

La Jolla, CA）にクローニングし、塩基配列を確認した。塩基配列は BigDye primer Cycle Sequence Kit (Applied Biosystems Inc.) を使用して、DNA シークエンサー (Model 377, Applied Biosystems Inc.) により決定した。制限酵素でクローニングした断片を切り出し、各実験目的に合わせたプラスミドベクターにサブクローニングした。

SDS-PAGE とイムノブロット

SDS-PAGE は Laemmli（1970）の方法に、ナイロン膜（GVHP membrane, Millipore）への転写は Towbin et al.（1979）の方法に準じて行った。タンパク質が転写されたナイロン膜は 3% (w/v) スキムミルクを含む TBS-T (50 mM Tris-HCl (pH 7.5), 150 mM NaCl, 0.05% (w/v) Tween20）で 1 時間ブロッキング処理をした。その後、1,000-10,000 倍希釈した各抗血清を含む TBS-T で 1 時間振とうした。ナイロン膜を TBS-T で 15 分 1 回、5 分 2 回洗浄し、次に 5,000-10,000 倍希釈したペルオキシダーゼ結合ヤギ抗ウサギ IgG 抗体（Amersham Japan, Tokyo, Japan）を含む TBS-T で 1 時間振とうした後に、ナイロン膜を TBS-T で 15 分 1 回、5 分 4 回洗浄した。各抗血清と反応性のあるタンパク質は ECL kit (Amersham Japan, Tokyo, Japan）を用いて検出した。

融合タンパク質の調製と抗体作製

すでに単離された *At*Pex14p、*At*Pex5p、*At*Pex7p それぞれの cDNA を鋳型にして PCR 法により、*At*Pex14p-(^{1}M-^{100}P)、*At*Pex5p-(^{231}K-^{450}D)、*At*Pex7p-(^{1}M-^{317}S)に相当する cDNA 断片を増幅した。得られた cDNA 断片をいったん T-ベクター；pBluescript II SK+（Stratagene, La Jolla, CA）にクローニングし、塩基配列を確認した。それぞれの cDNA 断片に対応した制限酵素で cDNA 断片を切り出し、チオレドキシン（Trx: thioredoxin）と目的タンパク質に加えヒスチジンタグ（6xHis）が融合したタンパク質を構築するための大腸菌発現ベ

クターpET32a（Novagen, USA）にインフレームで連結した後、大腸菌 BL21（DE3）に導入した。大腸菌を終濃度 200 mM になるようカルベニシリンを加えた LB 液体培地で生育させ、OD_{600}=0.6～0.7 になるまで 37℃で振とう培養した。誘導は終濃度 1 mM になるよう IPTG を加え、さらに 3 時間振とう培養した。誘導後の大腸菌を 3,000×*g* で 5 分間の遠心により回収し、開始緩衝液（50 mM sodium phosphate (pH 7.5), 50 mM imidazole, 0.5 M NaCl）に懸濁した。融合タンパク質を抽出するため、超音波処理装置（Model 450D, Branson）を用いて、Output 2～3、50% duty、5 分間の条件で 3 回、氷上にて処理し大腸菌を破砕した。破砕液を 10,000×*g* で 10 分間遠心し、可溶性画分と不溶性画分に分離した。*At*Pex14p-(^{1}M-^{100}P)はこの条件で可溶性画分に抽出されたため、これを精製に用いた。*At*Pex5p-(^{231}K-^{450}D)と *At*Pex7p-(^{1}M-^{317}S)は可溶化されなかったため、沈殿に開始緩衝液に 8 M urea を加えた緩衝液で再懸濁し、10,000×*g* で 10 分間遠心し、尿素可溶性画分と不溶性画分に分離した。*At*Pex5p-(^{231}K-^{450}D)と *At*Pex7p-(^{1}M-^{317}S)は尿素可溶性画分に抽出された。それぞれ可溶化した融合タンパク質を含む粗抽出液を、ニッケルを結合させた HiTrap Chelating カラム（Amersham Japan, Tokyo, Japan）に通し、それぞれを可溶化させた緩衝液で洗浄した後、カラムに結合している融合タンパク質を溶出緩衝液（50 mM sodium phosphate (pH 7.5), 1 M imidazole, 0.5 M NaCl）で溶出精製し、抗原として用いた。

精製融合タンパク質 0.5 mg を含む 1 ml の溶液に、等量の Freund's complete adjuvant（DIFCO Laboratories, USA）を加えよく乳濁化させ、ウサギ背部に皮下注射し第 1 回目の免疫感作とした。4 週間後、同量の融合タンパク質を含む 1 ml の溶液に、今度は等量の Freund's incomplete adjuvant を加えよく乳濁化させ、これを第 2 回目の免疫感作として皮下注射した。以降、1 週間毎に第 5 回目までの追加感作を行った。第 1 回目の免疫感作の直前に少量採血し前血清とした。第 2 回目以降の免疫感作から 3 日後に耳の動脈より採血を行い、抗血清を調製して以降の実験に用いた。

***In vitro* binding experiments**

すでに単離された *At*Pex14p、*At*Pex5p、イソクエン酸リアーゼそれぞれの cDNA を鋳型にして PCR 法により、*At*Pex14p-(^{1}M-^{100}P)、*At*Pex5p-(^{1}M-^{728}L)および PTS1 シグナル (SRM) をもつイソクエン酸リアーゼの C 末端 10 アミノ酸に相当する cDNA 断片を増幅した。得られた cDNA 断片の塩基配列を確認した後に、対応した制限酵素で cDNA 断片を切り出した。この cDNA 断片をチオレドキシン (Trx: thioredoxin) もしくはグルタチオン S トランスフェラーゼ (GST: glutathione S-transferase) と目的タンパク質、さらにヒスチジンタグ (6xHis) が融合したタンパク質を構築するための大腸菌発現ベクターpET32a もしくは pET41a (Novagen, USA) にインフレームで連結した後、大腸菌 BL21 (DE3) に導入した。大腸菌を終濃度 200 mM カルベニシリンまたは 30 mM カナマイシンを加えた LB 液体培地で生育させた。以降に行ったタンパク質の発現誘導および精製は抗体作製時と同様である。10 μg の 2 種類の融合タンパク質を 5 μl のグルタチオンセファロース 4B (glutathione Sepharose 4B, Amersham Japan, Tokyo, Japan) と 1.5 ml チューブ内で混合した後、全体の体積を 100 μl に統一するよう結合緩衝液(50 mM Tris-HCl (pH 7.5), 5 mM $MgCl_2$, 100 mM NaCl, 10% glycerol, 0.5 mg/ml BSA, 5 mM 2-mercaptoethanol) を加えた。これを 4℃で 1 時間、ローテーターにて混和し結合反応を行った後、4℃、10,000×*g* で 10 秒間遠心し上清を捨てた。沈殿に 200 μl の結合緩衝液を加え、軽く撹拌した後、再び 4℃、10,000×*g* で 10 秒間遠心し上清を取り除いた。この洗浄操作を 4 回繰り返した。洗浄後の沈殿に 25 μl の溶出液 (50 mM Tris-HCl (pH 7.5), 5 mM $MgCl_2$, 100 mM NaCl, 10% glycerol, 5 mM 2-mercaptoethanol, 10 mM glutathione) を加え、時々撹拌しながら 20 分間氷上に置き結合タンパク質を溶出した。4℃、10,000×*g* で 10 秒間遠心し上清をとり、等量の試料溶解液 (2% SDS, 50 mM Tris-HCl (pH 6.8), 5% 2-mercaptoethanol, 0.1% BPB, 10% glycerol) を加え、95℃

で 5 分間熱処理した。その後イムノブロットにて結合タンパク質を解析した。

免疫沈降実験

先に作製した *At*Pex5p-(^{231}K-^{450}D)、*At*Pex7p-(^{1}M-^{317}S)に対する抗血清より MabTrap Kit（Amersham Japan, Tokyo, Japan）を用いて、IgG 画分を得た。抗体作製に用いた抗原タンパク質を定法に従い HiTrap NHS-activated HP カラム（Amersham Japan, Tokyo, Japan）に固定化した。IgG 画分を結合緩衝液（20 mM sodium phosphate buffer (pH7.0)）で透析し、抗原を固定化したカラムにそれぞれ通した。カラムに結合した抗原特異的な IgG を酸（0.1 M glycine-HCl (pH 2.7)）で溶出しつつ 500 µl ずつ分画し、各画分 40 µl 中和溶液（1 M Tris-HCl (pH 9.0)）で中和した。このように親和性精製した IgG を HiTrap NHS-activated HP カラム（Amersham Japan, Tokyo, Japan）に固定化し、*At*Pex5p-(^{231}K-^{450}D)、*At*Pex7p-(^{1}M-^{317}S)それぞれの抗体カラムとした。

発芽 4 日目のシロイヌナズナから黄化子葉を切り取り、抽出緩衝液（50 mM sodium phosphate buffer (pH7.5), 100 mM NaCl）と共に乳鉢で磨砕した。これを 15,000×*g* で 5 分間遠心し、上清を総タンパク質試料とした。総タンパク質試料を抗体カラムに通した後、10 ml の抽出緩衝液で洗浄した。最後の 500 µl を洗浄画分として、タンパク質試料を調製した。カラムに結合したタンパク質は酸（0.1 M glycine-HCl (pH 2.7)）で溶出し、各画分 40 µl 中和溶液（1 M Tris-HCl (pH 9.0)）で中和した。これを溶出画分としてタンパク質試料を調製した。それぞれの画分を *At*Pex5p、*At*Pex7p に対する抗体を用いたイムノブロットにより解析した。

酵母 two-hybrid system

酵母 two-hybrid system による解析は Fields and Song（1989）の方法に準じて行った。

実験に用いる遺伝子は Gal4p DNA 結合領域（BD: DNA-binding domain）または Gal4p 活性化領域（AD: activation domain）と融合タンパク質を発現するよう設計し、two-hybrid ベクターの pGBD-C1 または pGAD-C1(James et al., 1996)にサブクローニングした。各遺伝子の部分長を用いる場合はすべて PCR により、cDNA の両端に任意の制限酵素認識部位を付加するよう増幅し、塩基配列を確認した後に two-hybrid ベクターにサブクローニングした。*At*Pex5p の 8 番目の WXXXF 配列を人工的に連結させる方法は Nakajima and Yaoita（1997）に準じて行った。*At*Pex14p と *At*Pex5p に対して行ったアミノ酸置換は QuikChange Site-Directed Mutagenesis Kit（Stratagene, La Jolla, CA）を用いて行った。

それぞれの two-hybrid ベクターを組み合わせ、Gietz らの方法（1995）に従い、宿主菌株 PJ69-4A(James et al., 1996)に導入した。形質転換した酵母は、完全合成培地（2% glucose, 0.67% yeast nitrogen base without amino acids, DIFCO）からトリプトファン、ロイシンを除いた培地上（-WL）で選抜した。タンパク質間相互作用は、さらにヒスチジンを除き終濃度 50 mM になるよう 3-アミノトリアゾール（3-amino triazole）を加えた培地上（-WLH+AT）での生育および β－ガラクトシダーゼ活性の定量測定により検出した。β－ガラクトシダーゼ活性の定量は Miller（1972）の方法に従った。これらの活性は 3 つの独立した酵母株の細胞抽出物を用いて測定し、平均値（unit/mg protein）を算出した。

光化学系 II 最大量子収率の測定

光阻害の影響を低下させるために、各植物個体は弱光条件下（50 μE/m²/s）かつ高濃度二酸化炭素条件下（1000 Pa CO_2）のインキュベーターで 4 週間発芽生育させた。これらの植物個体を通常大気条件下（36 Pa CO_2）で強光下（450 μE/m²/s）に暴露し、0, 30, 60, 120, 240 分間おいた。強光照射が終了した個体はそれぞれ暗黒下に 30 分間静置した（dark adapt）。暗順応させた植物個体の葉の上面より、Mini-PAM（H. Walz, Effeltrich, Germany）を用い

てクロロフィル蛍光を測定し、*Fv/Fm*（variable fluorescence/maximum fluorescence）を算出した。

カボチャ黄化子葉からの無傷ペルオキシソームの単離

発芽5日目のカボチャ黄化子葉100 gに200 mlの緩衝液A（20 mM pyrophosphate-HCl (pH 7.5), 1 mM EDTA, 0.3 M mannitol）を加え、ワーリングブレンダーで3秒間2回破砕し、これを4層のガーゼでろ過し、強く絞った。残渣に200 mlの緩衝液Aを加え、再度3秒間2回破砕し、ろ過した。2回の抽出液を合わせて、1,500×*g*で20分間遠心し、核、プラスチド等を除き、さらに上清を10,000×*g*で20分間遠心した。ここで得られた沈殿を5 mlの緩衝液B（10 mM HEPES-KOH (pH 7.2), 1 mM EDTA, 0.3 M mannitol）で懸濁し、30 mlのPercoll溶液（28% (w/w) Percoll (Amersham Pharmacia Biotech), 10 mM HEPES-KOH (pH 7.2), 1 mM EDTA, 0.3 M raffinose）に上層した。40,000×*g*で30分間遠心した後、遠心管の底部にバンド状に集まったペルオキシソームを駒込ピペットで回収した。回収したペルオキシソーム溶液に4倍量の緩衝液Bを加えてPercollを希釈し、5,000×*g*で10分間遠心して沈殿にした。沈殿に1 mlの緩衝液Aを加え懸濁し、無傷ペルオキシソームとした(Yamaguchi et al., 1995b)。

ペルオキシソーム膜タンパク質の抽出

単離精製した無傷ペルオキシソームを5,000×*g*で10分間の遠心により沈殿させた後、低張液（10 mM HEPES-KOH (pH 7.2)）を加え懸濁、破裂させた。これを100,000×*g*で30分間遠心し、上清を可溶性画分とした。この可溶性画分にはマトリクスタンパク質が抽出される。沈殿には高塩溶液（10 mM HEPES-KOH (pH 7.2), 200 mM KCl）を加えて再懸濁後100,000×*g*で30分間遠心し、上清を塩可溶性画分とした。塩可溶性画分にはイオン結

合などで弱く膜に付着したタンパク質を抽出することができる。さらに沈殿にはアルカリ溶液（100 mM Na_2CO_3）を加えて再懸濁後、100,000×*g* で 30 分間遠心した。その上清を 1 M HCl で中和したものをアルカリ可溶性画分とした。アルカリ可溶性画分には膜貫通型タンパク質以外の膜に強く結合したタンパク質が抽出される。アルカリ溶液でも可溶化しなかった沈殿に低張液を加え、アルカリ不溶性画分とした。これまでの研究からペルオキシソームの膜貫通型タンパク質はアルカリ不溶性画分に検出されることがわかっている。

シロイヌナズナの形質転換

5 番染色体 MQB2 に存在する 7734bp の *Xho*I DNA 断片を植物のバイナリーベクターである Ti-プラスミド pBI121Δ35S の *Xho*I 部位に連結した。この Ti-プラスミドをエレクトロポレーション法によりアグロバクテリウム（*Agrobacterium tumefaciens*）C58C1Rif^R 株に導入した。この形質転換アグロバクテリウムを用いたシロイヌナズナ *ped2* 変異体の形質転換法は Bechtold et al.（1993）の方法に準じて行った。最初に形質転換を行った植物個体を T0 植物とした。T0 植物から T1 種子を回収し、15 mg/l のカナマイシンを含む GM 培地上で形質転換体の選抜を行った。カナマイシン耐性となった T1 植物個体から T2 種子を回収し、さらに次世代のカナマイシン耐性の分離比から、ホモ個体の選抜を行った。得られた形質転換植物に対して、終濃度 0.2 μg/ml の 2,4-DB を含む GM 培地とショ糖を除いた GM 培地を用いて発芽実験を行った。

ショ糖密度勾配遠心

発芽 3 日目または 5 日目のカボチャより黄化子葉を 5 g 切り取り、10 ml の抽出緩衝液（10 mM Tricine-HCl (pH 7.5), 1 mM EDTA, 12% (w/w) sucrose）とともに氷冷したペトリ皿上においた。試料が 2～3 mm 角程になるまでカミソリ刃を用いて破砕し、抽出液を 3

層ガーゼでろ過した。抽出液 1 ml を 16 ml のショ糖密度勾配溶液（30%～60% (w/w), 1 mM EDTA）に上層して、SW 28.1 スイングローター（Beckman, USA）で 85,000×*g*、2.5 時間遠心した。遠心終了後、直ちに fractionator（model 185; ISCO, USA）で 0.5 ml ずつ分画し、それぞれの画分において指標酵素の活性測定および各種抗体によるイムノブロット解析を行った。

その他の方法

プラスミド DNA の調製、制限酵素による DNA の切断、DNA のアガロースゲル電気泳動等の基本操作は Sambrook らの方法（2001）に準じた。

結果

ped2 変異体における光呼吸活性

ペルオキシソームには、植物個体にとって少なくとも 2 つの重要な生理的な役割がある。それは脂質代謝と光呼吸系である。*ped2* 変異体では、ペルオキシソームの脂質代謝能が低下していることがすでに明らかにされている(Hayashi et al., 2000a)。では、*ped2* 変異体において、ペルオキシソームのもう 1 つの機能である光呼吸系はどうなっているのであろうか？通常の大気条件下(36 Pa CO_2)で *ped2* 変異体を生育させた場合、野生型(Figure 1A, WT/air）に比べて黄緑色の葉をした矮性の表現型を示す（Figure 1A, *ped2*/air)。*ped2* 変異体を高濃度の二酸化炭素条件下（1000 Pa CO_2）で生育させた場合、これらの表現型は野生型へと回復した（Figure 1A, *ped2*/CO_2)。同様の現象は光呼吸系を欠損した突然変異体で報告されている(Somerville and Ogren, 1982)。光呼吸系に関わるいくつかの酵素は PTS1 型タンパク質であり、緑葉ペルオキシソームに局在する。よって、*ped2* 変異体では光呼吸活性が低下したために誘導された影響があると仮定した。この仮説を証明するため、光化学系 II の最大量子収率を測定した。光化学系 II の最大量子収率は暗順応したクロロフィル蛍光（*Fv*）と最大クロロフィル蛍光（*Fm*）の割合（*Fv*/*Fm*）から推定することができる(Franklin et al., 1992; Krause, 1988; Öuist et al., 1992)。*ped2* 変異体と野生型シロイヌナズナに加え、ミトコンドリア局在の光呼吸系酵素の 1 つであるセリン－トランスヒドロキシメチラーゼ(serine transhydroxymethylase)を欠損した *stm* 変異体(Somerville and Ogren, 1981)の *Fv*/*Fm* を計測し比較した。

光阻害による影響を軽減するために、各植物個体を高濃度の二酸化炭素条件下（1000 Pa CO_2）および弱光下（50 μE/m^2/s）で 3 週間生育させた。このような条件下では *ped2* 変異体、野生型シロイヌナズナ、*stm* 変異体は正常な生育を示し、*Fv*/*Fm* 値はいずれも 0.8

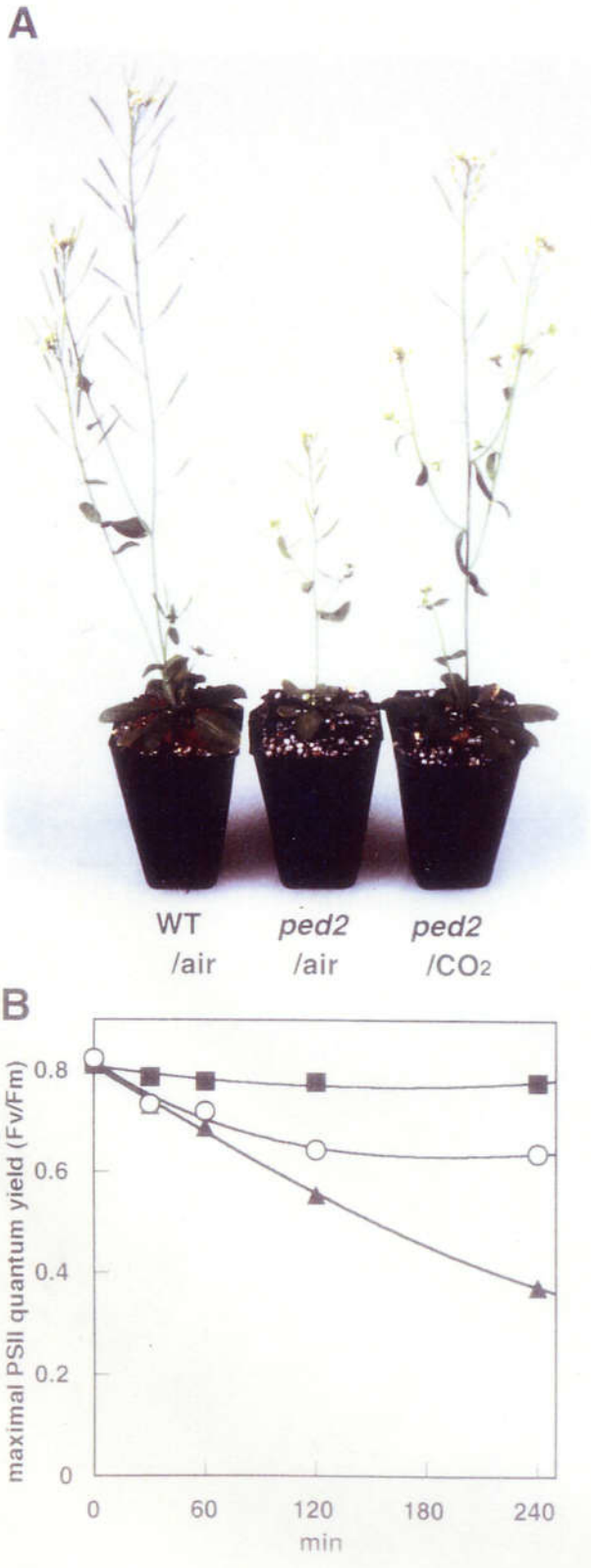

Figure 1. Reduced Activity of Photorespiration in *ped2* Mutant.
(**A**) Effect of CO_2 on the growth of *ped2* mutant. Wild-type Arabidopsis (WT/air) and *ped2* mutant (*ped2*/air) were grown for 8 weeks in a normal atmosphere (36 Pa CO_2) under constant illumination (100 μE m^{-2} sec^{-1}). The *ped2* Mutant was also grown for 8 weeks in an atmosphere containing 1000 Pa CO_2 (*ped2*/CO_2) under constant illumination (50 μE m^{-2} sec^{-1}).
(**B**) Effect of strong irradiation on maximal quantum yield of photosystem II (*Fv/Fm*). Wild-type Arabidopsis (■), *ped2* mutant (○), and stm mutant (▲) were grown for 3 weeks in an atmosphere containing 1000 Pa CO_2 under low light (50 μE m^{-2} sec^{-1}). These plants were illuminated with strong light (450 μE m^{-2} sec^{-1}) in a normal atmosphere (36 Pa CO_2). Maximum quantum yield of photosystem II (*Fv/Fm*) of the leaves at each defined time was measured after these plants were kept for 30 min in the darkness. Each point represents the average *Fv/Fm* measured in six leaves of independent plants.
Standard error of each point is less than 0.01.

前後と計測された（Figure 1B, 0 min）。*Fv/Fm* 値は、光阻害を受けていない葉で 0.8～0.83 くらいの値をとることが知られている。よって、この条件下で育てたそれぞれの植物個体は光阻害をうけていないと判断した。これらの植物個体を通常の大気条件下（36 Pa CO_2）に移し、強光（450 μE/m^2/s）を照射した。このような条件下では RuBisCO（ribulose bisphosphate carboxylase/oxygenase）は光合成における二酸化炭素固定に必要なカルボキシレーション反応に加え、オキシゲネーション反応を行うようになる。オキシゲネーション反応の副産物であるホスホグリコール酸（phosphoglycolate）は光呼吸系酵素群によって代謝され、最終的にカルビン・ベンソンサイクルへと回収される。故に、光呼吸系が相応に機能する野生型シロイヌナズナの *Fv/Fm* 値は、強光照射以後も光阻害が誘導されないため変化がない（Figure 1B, filled squares）。対照的に *ped2* 変異体と *stm* 変異体における *Fv/Fm* 値は、同様の条件下に移した後、減少した（Figure 1B, open circles and filled triangles）。これらの変異体では、光呼吸系に欠損があるためホスホグリコール酸を代謝できずその結果として、強光条件下ではカルビン・ベンソンサイクルの十分な活性が維持できない。カルビン・ベンソンサイクルの活性低下は光合成系の明反応から過度のエネルギー供給を引き起こし、強光下では光阻害の原因となる。つまり、明反応とカルビン・ベンソンサイクル間の不調和が *Fv/Fm* 値の低下を招いていると考えられた。強光照射 120 分後、*ped2* 変異体の *Fv/Fm* 値は定常期に達したが（*Fv/Fm* = 0.64）、*stm* 変異体は減少を続けた。これらの結果は、*ped2* 変異体内の光呼吸活性は部分的に阻害されているが、*stm* 変異体内の活性よりは強いことを示唆している。この結果は、*ped2* 変異体細胞内のペルオキシソームタンパク質輸送能が完全には失われておらず、部分的に輸送されている事実と矛盾しない。

***PED2* 遺伝子座の同定**

5 番染色体 MQB2 に存在する 7734bp の *Xho*I DNA 断片（Figure 2A and B）が *PED2*

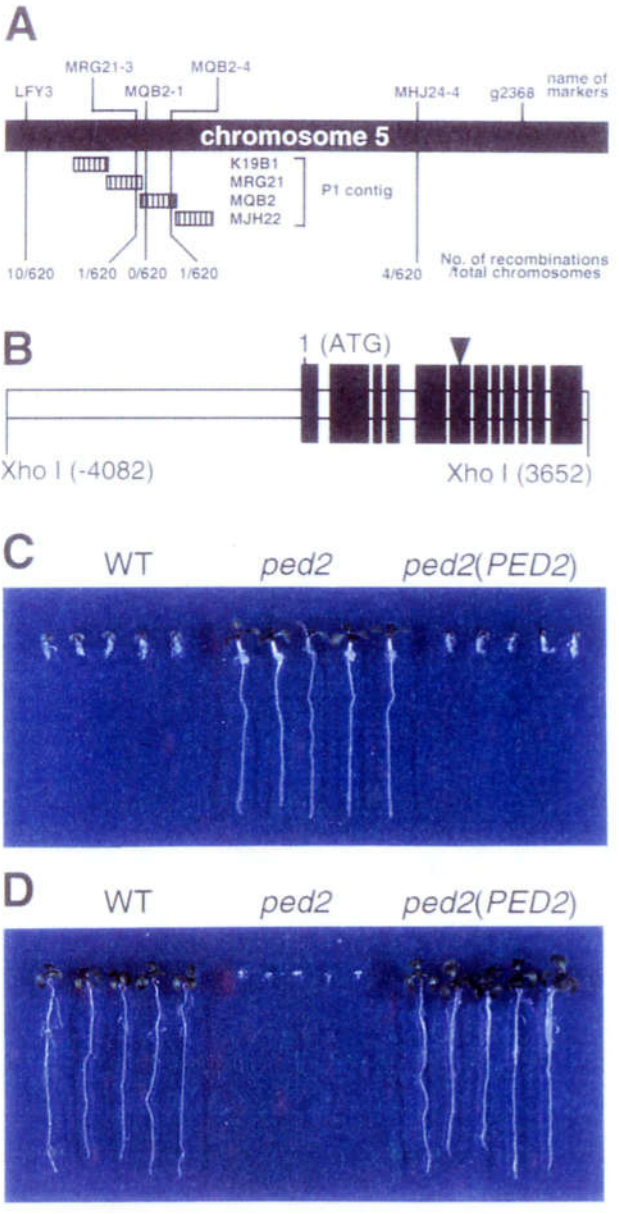

Figure 2. Positional Cloning of the *PED2* Gene.

(**A**) High-resolution mapping of *PED2* on Chromosome 5. Names and positions of the molecular markers used in this study are indicated on the top of the illustration. Hatched bars represent the regions covered by the P1 clones. We analyzed 310 F_2 progenies (620 chromosomes) having homozygous *ped2* alleles. The numbers of recombinations that occurred between the *PED2* locus and the molecular markers are indicated at the bottom of the illustration. Mapping results with a series of molecular markers between LFY3 and MHJ24-4 are summarized schematically and indicate that the *PED2* locus may be located within a single P1 clone, MQB2.

(**B**) Schematic diagram of a 7734-bp *Xho* I-fragment that is involved in the P1 clone, MQB2. The twelve black bars represent protein coding regions determined from the cDNA sequence. The triangle on the sixth black bar indicates the position of a nonsense mutation that occurs in the *ped2* mutant. Nucleotide residue 1 corresponds to an adenine of the first methionine codon.

(**C**) Effects of 2,4-DB on the growth of transgenic *ped2* seedlings (*ped2*(*PED2*)) harboring the 7734 bp *Xho* I-fragment shown in (B). Wild-type Arabidopsis (WT), *ped2* mutant (*ped2*), and *ped2*(*PED2*) were grown for 10 days on growth medium containing 0.2 μg/ml of 2,4-DB under constant illumination. Photographs were taken after the seedlings were removed from the media and rearranged on agar plates.

(**D**) Effects of sucrose on the growth of *ped2*(*PED2*) seedlings. Wild-type Arabidopsis (WT), *ped2* mutant (*ped2*), and *ped2*(*PED2*) were grown for 10 days on growth medium without sucrose under constant illumination. Photographs were taken after the seedlings were removed from the media and rearranged on agar plates.

遺伝子座であることを証明するために、この DNA 断片を植物のバイナリーベクターである pBI121Δ35S にサブクローニングした後、アグロバクテリウムを介した形質転換法(Bechtold et al., 1993)により *ped2* 変異体に導入した。カナマイシン耐性となった T2 世代の個々の種子の中から導入遺伝子についてホモとなった系統を得るため、次世代の種子を播種し、カナマイシン耐性の分離比を評価した。T3 世代でホモ個体が得られた系統について、2,4-DB 耐性と発芽後成長にショ糖を要求するかを検定した。*ped2* 変異体は 2,4-DB に耐性を示し、また発芽後成長にショ糖を要求する（Figure 2C and D, *ped2*）(Hayashi et al., 2000a)。対照的に 7734bp の *Xho*I DNA 断片を導入した *ped2* 変異体では 2,4-DB 感受性となり、発芽後成長にショ糖を要求しなくなった（Figure 2C and D, *ped2*(*PED2*)）。このような表現型は野生型シロイヌナズナと一致する（Figure 2C and D, WT）。さらに Figure 1 で行った実験をこの形質転換体にも行ったところ、通常の大気条件下（36 Pa CO_2）で生育させた場合でも野生型と同様に生育し、強光処理によっても *Fv/Fm* 値の顕著な低下を示さなかった（data not shown）。これらの結果は本研究によって決定されたゲノム配列（DDBJ/EMBL/GenBank: AB037538）が *PED2* 遺伝子であることを示している。

<u>*PED2* 遺伝子の翻訳産物はヒト Pex14p と相同性がある</u>

PED2 遺伝子の cDNA は野生型シロイヌナズナから調製した全 RNA を用いて、RT-PCR 法によりクローニングを行った。5'-プライマーを 5'-UTR 内のインフレームでつながるストップコドンの上流に設計した。これにより cDNA のファーストメチオニンを確認した。*PED2* 遺伝子の cDNA の塩基配列を決定し(DDBJ/EMBL/GenBank: AB037539)、ゲノム DNA の塩基配列と比較したところ *PED2* 遺伝子は 12 のエクソンを含んでいることが明らかとなった（Figure 2B)。また、遺伝子産物から推定されるタンパク質は 507 個のアミノ酸から構成されていた（Figure 3)。*ped2* 変異体では 254 番目のグルタミン（CAA）が 1 塩基

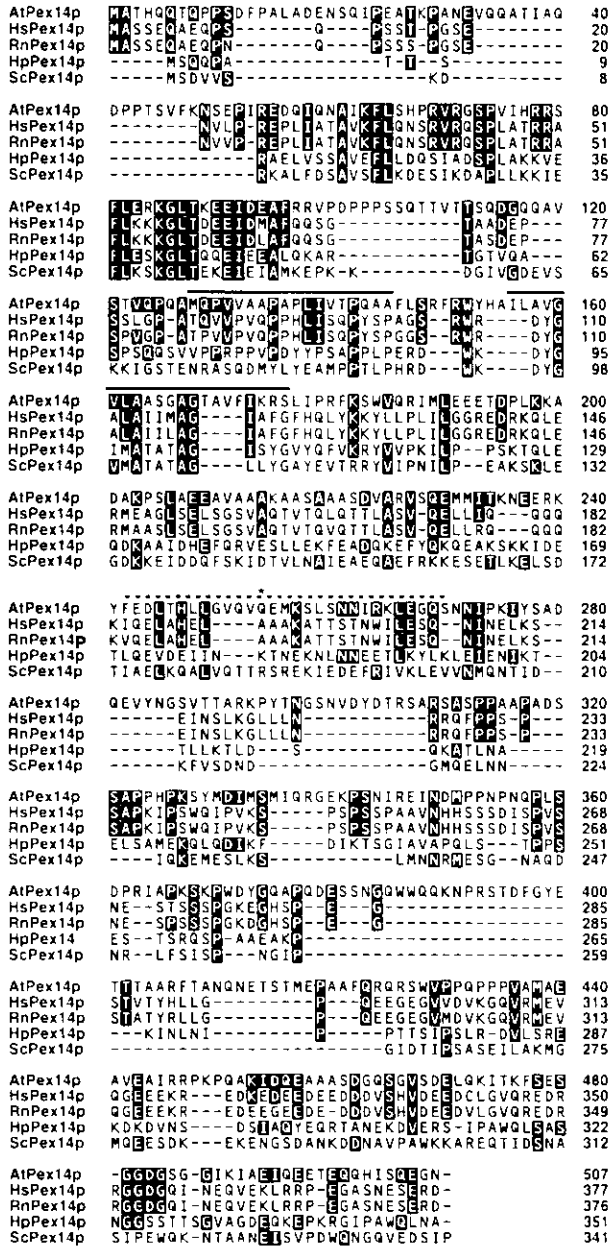

Figure 3. Alignment of Amino Acid Sequences for the *PED2* Gene Product with Mammalian and Yeast Pex14p.

Deduced amino acid sequence of the *PED2* gene product (*At*Pex14p) was compared with Pex14p identified from human (*Hs*Pex14p), rat (*Rn*Pex14p), *H. polymorpha* (*Hp*Pex14p) and *S. cerevisiae* (*Sc*Pex14p). Identical amino acid residues between *At*Pex14p and other Pex14p are highlighted. Amino acid sequence of *At*Pex14p is 29.6 % identical with that of human Pex14p. The asterisk on ^{254}Gln represents the position of a nonsense mutation (CAA to TAA) in the *ped2* gene. Two putative membrane spanning domains are indicated by line. The dashed line represent a putative coiled-coil region.

置換により、終止コドン（TAA）に変わっていた（Figure 3, asterisk）。この遺伝子産物のアミノ酸配列はヒトやカビにおいてペルオキシソームタンパク質輸送機構に関与すると報告されている Pex14p と顕著な類似性が認められた(Albertini et al., 1997; Brocard et al., 1997; Komori et al., 1997; Shimizu et al., 1999; Will et al., 1999)。最も類似性の高いものはヒトの Pex14p であった（Figure 3）。以上の結果から、本タンパク質を *At*Pex14p と命名した。*At*Pex14p は少なくとも 2 つの疎水性領域と coiled-coil 領域をもっていた（Figure 3）。しかしながら酵母 Pex14p で報告されているような SH3 のリガンドとなる class II コンセンサス配列はもっておらず(Albertini et al., 1997)、加えて *At*Pex14p は PTS のような明らかなペルオキシソームへの輸送シグナルももっていないことがわかった。

<u>*At*Pex14p は 75kDa タンパク質として検出される</u>

*At*Pex14p の細胞内局在を解析するため、*At*Pex14p の部分長配列 N 末端 100 アミノ酸（^{1}M-^{100}P）を大腸菌融合タンパク質として調製し、これに対する抗体を作製した。この抗体は、野生型シロイヌナズナの黄化子葉において 75 kDa の単一バンドを検出したが（Figure 4, WT）、*ped2* 変異体ではこのようなバンドは検出されなかった（Figure 4, *ped2*）。これらのデータは、*At*Pex14p が 75 kDa タンパク質であることを指し示している。*At*Pex14p のアミノ酸配列から推定される分子量は 55 kDa であり、この推定分子量と実際にイムノブロット上で検出された分子量との差が何に起因するものかは今のところ不明である。

<u>*At*Pex14p の細胞内局在</u>

植物細胞内の Pex14p の細胞内局在を調査するため、カボチャ黄化子葉より調製したホモジェネートをショ糖密度勾配遠心法により細胞分画した。このようにして得られた各画分をイムノブロット法（Figure 5A）と定量活性測定（Figure 5B）により解析した。*At*Pex14p

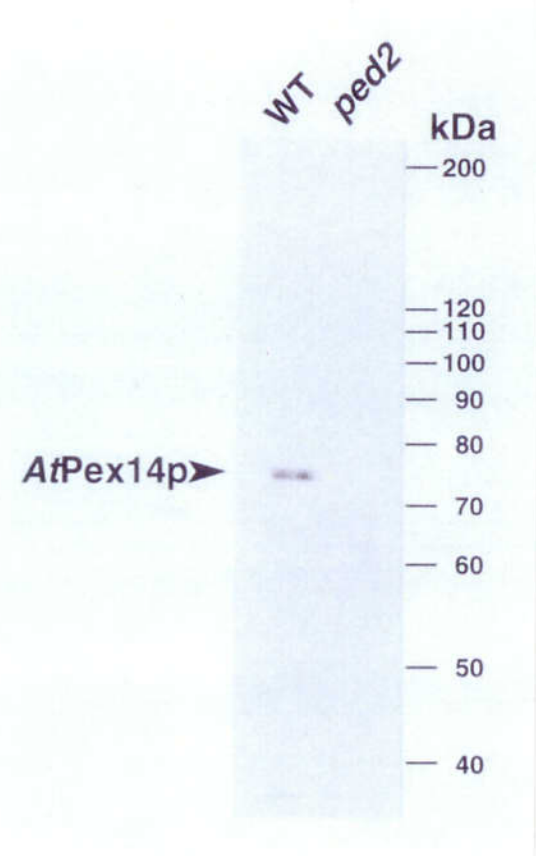

Figure 4. Immunodetection of *At*Pex14p in Etiolated Cotyledons of Wild-Type Arabidopsis and *ped2* Mutant.
Extracts were prepared from 5-day-old etiolated cotyledons of wild-type Arabidopsis (WT), and *ped2* mutant (*ped2*). For each sample, 10 µg of total protein was subjected to SDS-PAGE. Immunoblot analysis was performed using the antibody raised against *At*Pex14p. Markers are shown on the right with molecular masses in kDa.

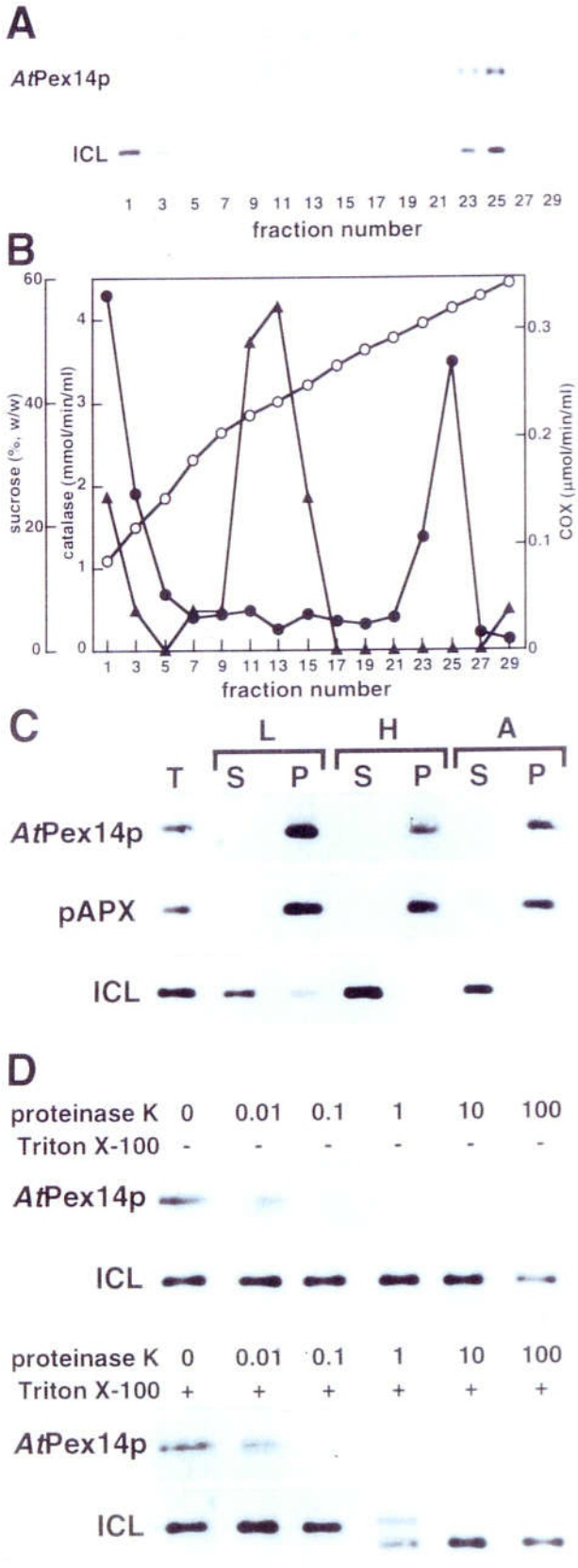

Figure 5. Subcellular Localization of Pex14p in Pumpkin Etiolated Cotyledons.
(**A**) Subcellular fractionation of etiolated pumpkin cotyledons was performed by 30-60 % sucrose density gradient centrifugation. Fraction number 1 represents the top fraction of the gradient. Pex14p and isocitrate lyase in each fraction were detected by immunoblot analyses using antibody raised against *At*Pex14p (*At*Pex14p) and isocitrate lyase (ICL).
(**B**) Sucrose concentration (O), activities of catalase (●) and cytochrome *c* oxidase (COX; ▲) in the same fractions used in (**A**) were also measured.
(**C**) Intact glyoxysomes were resuspended in either low salt buffer (L), high salt buffer (H) or alkaline solution (A). Each buffer consists of 10 mM HEPES-KOH (pH 7.2), 500mM KCl with 10 mM HEPES-KOH (pH 7.2), and 0.1 M Na_2CO_3, respectively. These samples were then centrifuged, and separated into soluble (S) and insoluble (P) fractions. T represents total proteins of the intact glyoxysomes. Pex14p (*At*Pex14p), peroxisomal ascorbate peroxidase (pAPX) and isocitrate lyase (ICL) were detected by immunoblot analysis.
(**D**) The intact glyoxysomes were treated with various concentrations of proteinase K in the absence (-) or presence (+) of Triton X-100. Concentration of proteinase K is indicated in μg/ml on the top of each lane. Pex14p (*At*Pex14p) and isocitrate lyase (ICL) were detected by immunoblot analysis.

は密度 1.25g/cm^3 付近、23～25 番目の画分に検出された。これらの画分はグリオキシソームの標識酵素であるイソクエン酸リアーゼ（ICL）とカタラーゼ（catalase）をも含んでいたが、ミトコンドリアの標識酵素であるチトクロム C オキシダーゼ（cytochrome *c* oxidase）の活性は含んでいなかった（Figure 5A and B）。この結果は、Pex14p がペルオキシソーム局在のタンパク質であることを示している。

次にカボチャ子葉より単離したグリオキシソームを様々な溶液で処理することにより、Pex14p の膜結合性を明らかにすることを試みた。Pex14p とペルオキシソーム膜貫通型タンパク質のアスコルビン酸ペルオキシダーゼ（pAPX: peroxisomal ascorbate peroxidase）(Nito et al., 2001; Yamaguchi et al., 1995a)は共にアルカリ溶液による処理においてさえも不溶性画分に検出された（Figure 5C）。しかしながら、グリオキシソームのマトリクス酵素であるイソクエン酸リアーゼ（ICL）は高塩溶液とアルカリ溶液による処理において完全に可溶性画分に溶出された。この処理によって、Pex14p がアスコルビン酸ペルオキシダーゼと挙動を共にしたことから、Pex14p がペルオキシソーム膜貫通型タンパク質であることが明らかになった。

さらに、ペルオキシソーム膜タンパク質 Pex14p の配向性を明らかにすべく、プロテアーゼによる消化実験を行った。これは無傷グリオキシソームに対してプロテアーゼ K で処理することにより、細胞質側に表在する膜タンパク質は分解されるが、マトリクスタンパク質はプロテアーゼから保護される（接触しない）ことを利用している。対照実験区としてマトリクス酵素のイソクエン酸リアーゼを用いた。ペルオキシソーム膜を人為的に破壊するために Triton X-100 を用いた。その結果、Pex14p は Triton X-100 の存在・非存在下にかかわらず分解された（Figure 5D）。対照的にイソクエン酸リアーゼは Triton X-100 の存在下でのみ分解された。以上の解析から、Pex14p はペルオキシソーム膜タンパク質であり、少なくともポリペプチドの一部分を細胞質側に露出していることが明らかとなった。

酵母 PTS レセプターのシロイヌナズナ orthologue、*At*Pex5p と *At*Pex7p

これまでの *ped2* 変異体の表現型解析から、*At*Pex14p がシロイヌナズナのペルオキシソームタンパク質輸送機構に関わっていることが明らかになっている(Hayashi et al., 2000a)。*At*Pex14p 以外にペルオキシソームへのタンパク質輸送に関わる因子として、Brickner et al.（1998）Schumann et al.（1999）により、*At*Pex5p と *At*Pex7p が酵母や哺乳類ペルオキシンのシロイヌナズナ orthologue として報告されている。酵母や哺乳類の Pex5p と Pex7p はペルオキシソームへのタンパク質輸送過程において、それぞれ PTS1 レセプターと PTS2 レセプターとして機能することが証明されている因子である。高等植物においては、Brickner と Schumann らは *At*Pex5p、*At*Pex7p の cDNA の塩基配列のみを報告するにとどまり、それらレセプターの機能に対する実験的証拠は皆無であった。そこで *At*Pex5p と *At*Pex7p の特徴付けを行うためにまず、*At*Pex5p、*At*Pex7p に対する特異的抗体を作成した。そしてこれらの抗体に加え、*At*Pex14p 抗体を含めてシロイヌナズナにおける発現についてイムノブロット法により解析を行った。

*At*Pex5p 抗体および *At*Pex7p 抗体はシロイヌナズナのホモジェネートに対しそれぞれ 99 kDa と 43 kDa の特異的なバンドを検出した（Figure 6, arrowhead)。PEDANT BLAST Network Service（http://pedant.gsf.de/）を用いてシロイヌナズナゲノムデータベースを検索したところ、シロイヌナズナゲノム上に *At*Pex14p や *At*Pex5p、*At*Pex7p に相同性のある遺伝子は他にはないことがわかった。故にこれらのペルオキシソームタンパク質輸送因子はシロイヌナズナゲノム内にシングルコピーで存在していることが示された。

*At*Pex14p、*At*Pex5p、*At*Pex7p の器官特異的発現

ペルオキシソームタンパク質輸送因子と推測される *At*Pex14p、*At*Pex5p、*At*Pex7p の

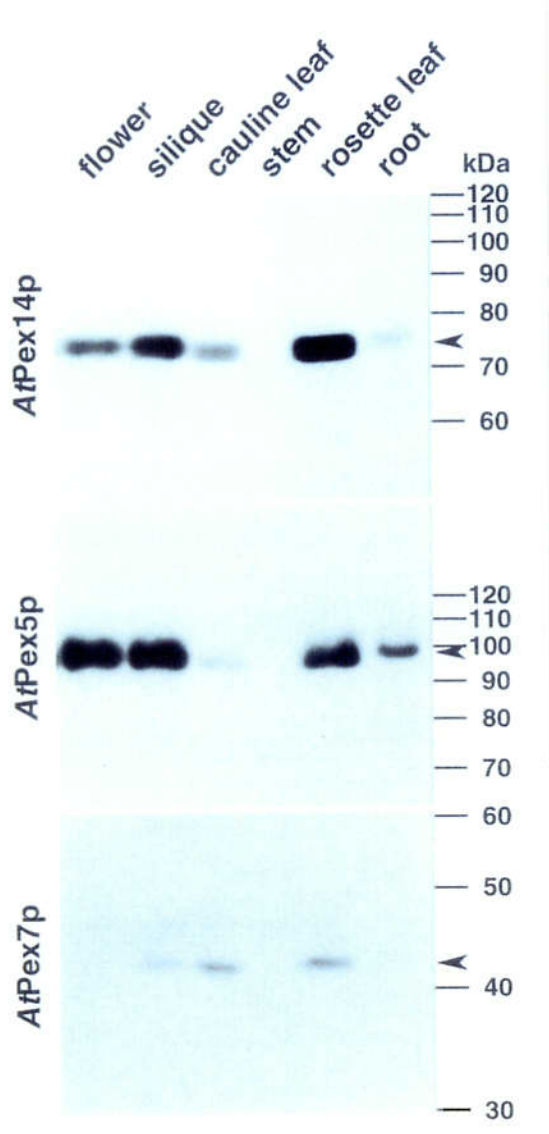

Figure 6. Organ-Specific Expression of *At*Pex14p, *At*Pex5p and *At*Pex7p. Immunoblot analysis of homogenates from various organs was carried out using antibodies against *At*Pex14p, *At*Pex5p and *At*Pex7p. Crude extracts prepared from the flower, silique, cauline leaf, stem, rosette leaf and root, respectively. Equal amounts of total protein, 10 μg for *At*Pex14p and *At*Pex5p and 50 μg for *At*Pex7p, were loaded in each lane. Markers are shown on the right with molecular masses in kDa.

発現パターンを解析するため、シロイヌナズナの様々な器官よりホモジェネートを調製し、*At*Pex14p、*At*Pex5p、*At*Pex7p に対する抗体を用いてイムノブロットにより解析した（Figure 6）。*At*Pex14p は花、鞘、茎生葉、ロゼット葉、根器官において強い発現が認められた。*At*Pex5p もほとんどの器官において発現が認められ、そのパターンは *At*Pex14p のそれとよく似ていた。*At*Pex14p や *At*Pex5p は茎器官では検出されなかったが、検出時間を延長することにより少量の *At*Pex14p と *At*Pex5p が検出された（data not shown）。これらの結果とは対照的に *At*Pex7p の発現パターンは *At*Pex14p や *At*Pex5p のそれとは著しく異なっていた。*At*Pex7p の 43 kDa バンドは鞘、茎生葉、ロゼット葉で著しく発現していたが、花、茎、根器官ではほとんど検出されなかった。

上述したように、*ped2* 変異体の解析から *At*Pex14p は PTS1、PTS2 依存的なタンパク質輸送に必須であることが示されている(Hayashi et al., 2000a)。PTS1 レセプターの *At*Pex5p が *At*Pex14p とほとんど同様の発現パターンを示したことに加え、ペルオキシソームタンパク質として同定されているものの内、多くが PTS1 型輸送シグナルをもつことから、PTS1 経路は高等植物ペルオキシソームタンパク質輸送経路として中心的に機能していることが示唆される。

発芽後成長における *At*Pex14p、*At*Pex5p、*At*Pex7p の量的変動

高等植物のペルオキシソームは個体の成長に伴い、その機能を大きく変化させる。特に顕著な変化は、脂肪性種子を暗所で発芽させた後、明所に移した子葉が緑化していく過程において起こるグリオキシソームから緑葉ペルオキシソームへの機能転換である (Nishimura et al., 1986; Sautter, 1986; Titus and Becker, 1985)。緑化段階の子葉では、ペルオキシソームのマトリクスタンパク質はイソクエン酸リアーゼに代表されるグリオキシソーム酵素は特異的分解をうけ、ヒドロキシピルビン酸還元酵素に代表される緑葉ペルオキシ

ソームへと置き換わる（Figure 7, ICL and HPR）。このような植物ペルオキシソームの機能転換の過程でペルオキシソームタンパク質輸送因子の *At*Pex14p、*At*Pex5p、*At*Pex7p がどのような変動をするのか、シロイヌナズナの実生を用いて解析した（Figure 7）。

種子を暗所で発芽生育させた場合、*At*Pex14p は発芽の早い段階から発現していた。そして、黄化子葉では 5 日目まで蓄積した後急速に減少した。対照的に 4 日目まで暗所で生育させた後明所に移した場合、*At*Pex14p の量は緑化子葉においてほぼ一定量に保たれた。*At*Pex5p の発現は *At*Pex14p に比べてわずかに遅れるが、発芽後およそ 3～5 日目に最大に達し、その後緩やかに減少した。4 日目まで暗所で生育させた後明所に移した場合、*At*Pex5p の量は *At*Pex14p と同様に一定に維持された。以上の結果から、ペルオキシソームタンパク質輸送因子の *At*Pex14p と *At*Pex5p の発芽段階における変動は黄化子葉におけるイソクエン酸リアーゼのようなグリオキシソーム酵素と緑化子葉におけるヒドロキシピルビン酸還元酵素のような緑葉ペルオキシソーム酵素の蓄積と一致することが明らかとなった。よって、*At*Pex14p と *At*Pex5p は 2 種類のペルオキシソームすなわちグリオキシソームと緑葉ペルオキシソームへのタンパク質輸送に関与していると示唆された。また、これらのイムノブロット解析の結果、*At*Pex14p、*At*Pex5p の発現はペルオキシソーム生合成過程におけるペルオキシソームタンパク質の輸送活性が高いことを示すマーカーとなりうるとわかった。対照的に *At*Pex7p の量は黄化子葉において 5 日目に最大に達した後、急速に減少した。また、個体を明条件下に移すと *At*Pex7p の量は *At*Pex14p や *At*Pex5p よりも低いレベルで存在し続けた。これは、PTS2 型タンパク質の発現量が黄化子葉細胞では高いが、緑化子葉細胞では比較的少ないことを意味している。実際、これまでに同定されている PTS2 型タンパク質のすべてがグリオキシソーム酵素であり、緑葉ペルオキシソームにおける PTS2 型タンパク質は未だ同定されていない。このことからも子葉の緑葉ペルオキシソームにおける PTS2 型タンパク質は量的に少ないと考えられる。

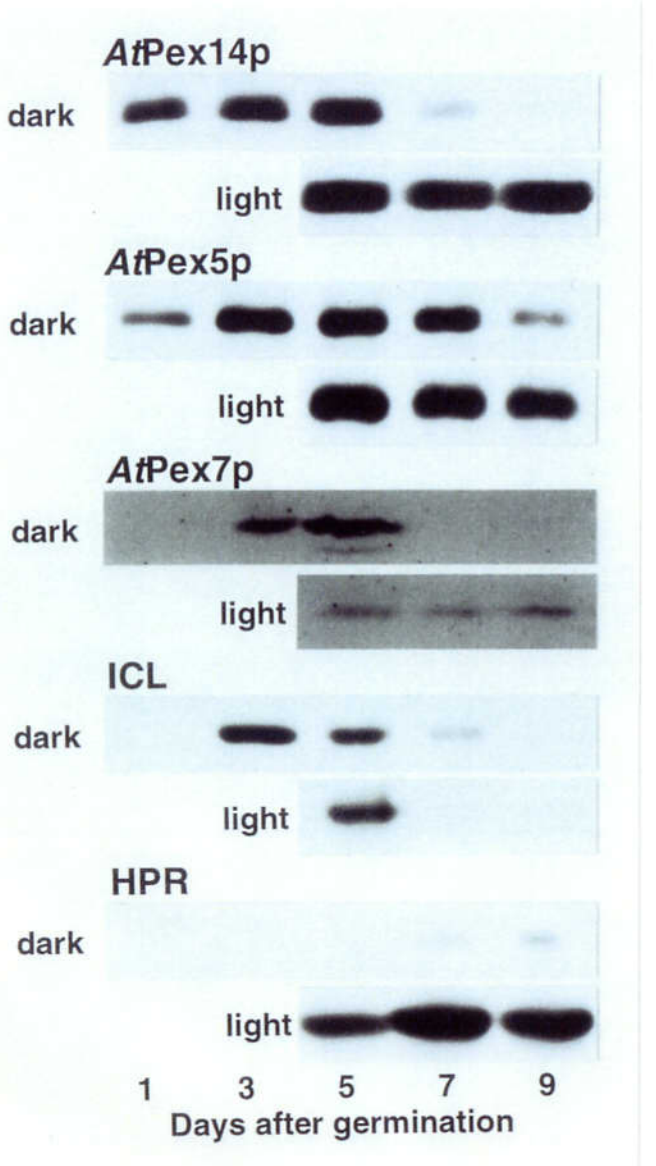

Figure 7. Developmental Changes in the Levels of *At*Pex14p, *At*Pex5p and *At*Pex7p during Germination.
Arabidopsis seeds were grown in continuous darkness for 9 days or in darkness for 4 days then under continuous illumination for 5 days. Immunoblot analysis of homogenates prepared from cotyledons at various stages was carried out using antibodies against *At*Pex14p, *At*Pex5p, *At*Pex7p, isocitrate lyase (ICL), and hydroxypyruvate reductase (HPR). Equal amounts of total protein, 10 µg for *At*Pex14p, *At*Pex5p, ICL and HPR and 50 µg for *At*Pex7p, were loaded in each lane. Number of days after germination is shown at the bottom of each lane.

AtPex14p は AtPex5p と結合する

前述したように、*At*Pex14p はペルオキシソーム膜タンパク質であり、少なくともその一部分を細胞質側に露出していることを明らかにしている（Figure 5)。一方、Pex5p はタバコを材料とした研究から細胞質に局在し、PTS1 型タンパク質を認識する PTS1 レセプターとして同定されている(Kragler et al., 1998; Wimmer et al., 1998)。そこで、ペルオキシソームタンパク質輸送過程における *At*Pex14p、*At*Pex5p、PTS1 型タンパク質間の相互作用について酵母 two-hybrid system による解析を行った。

それぞれのタンパク質を Gal4 activation domain（AD)、もしくは Gal4 DNA binding domain（BD）と融合タンパク質として発現するよう設計し、tester strain の PJ69-4A (James et al., 1996)内で発現させた。タンパク質間相互作用の結合活性は栄養要求性（-histidine + 3-AT 50 mM)とβ－ガラクトシダーゼの定量活性測定により検出した。酵母 two-hybrid system による解析の結果、*At*Pex14p は *At*Pex5p と結合するが、PTS1 型タンパク質とは直接結合しないことが示された（Figure 8A)。また、*At*Pex5p は PTS1 型タンパク質と結合した。これらの相互作用はそれぞれの融合タンパク質を AD もしくは BD と入れ替えた場合にも検出された（data not shown)。また、それぞれのタンパク質を単独で発現させた場合、タンパク質間相互作用を示すレポーター遺伝子の転写活性は上がらず、そのため宿主酵母はヒスチジン非存在下で生育できず、β－ガラクトシダーゼ活性も検出されなかった。ただし、*At*Pex5p を BD との融合タンパク質として発現させた時のみ、レポーター遺伝子の auto-activation が起こったため *At*Pex5p は AD との融合タンパク質のみを用いて相互作用の検出を行った。

酵母 two-hybrid system による結果を *in vitro* binding experiment により追試した。それぞれのタンパク質をチオレドキシン（Trx: thioredoxin）またはグルタチオン S トランスフ

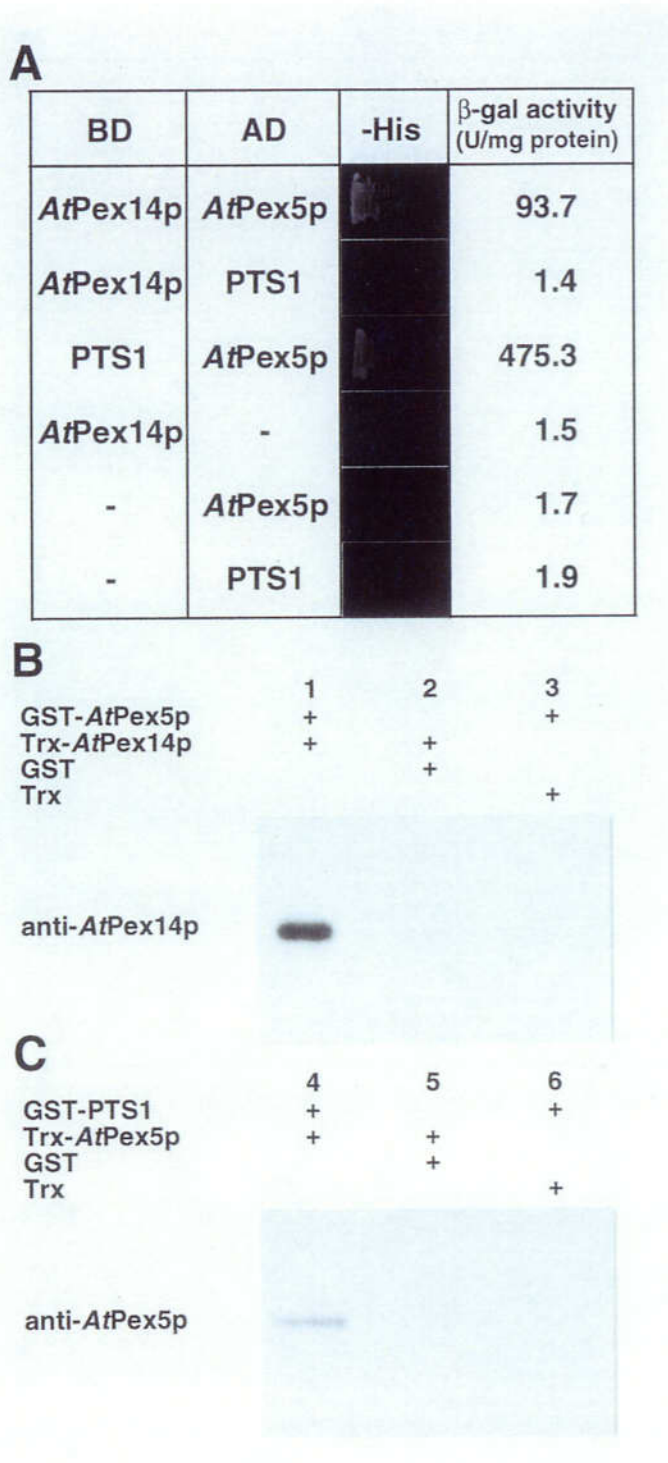

Figure 8. Detection of Interaction among *At*Pex14p, *At*Pex5p and PTS1-Containing Protein.

(**A**) Two-hybrid analysis of *At*Pex14p, *At*Pex5p and PTS1-containing protein. Proteins were fused to Gal4 BD or AD as indicated. Transformants were tested for growth on synthetic medium without histidine (-His) and assayed for quantitative β-galactosidase activity.

(**B**) and (**C**) *In vitro* binding experiments of between *At*Pex14p and *At*Pex5p, *At*Pex5p and PTS1-containing protein. Shown are immunoblots (antibodies are indicated) of proteins recovered in the glutathione Sepharose 4B. The fusion proteins added in each experiment were as indicated.

エラーゼ（GST: glutathione S-transferase）との融合タンパク質として大腸菌発現系にて発現させた。発現させた2種類の融合タンパク質とグルタチオンセファロース4B（glutathione Sepharose 4B）を混合し、グルタチオンセファロース 4B に結合したタンパク質をイムノブロットにて解析した。その結果、GST または Trx との融合タンパク質として発現させた *At*Pex5p は特異的かつ直接的に Trx-*At*Pex14p（Figure 8B; lane 1）と GST-PTS1（Figure 8C; lane 4）に結合した。また、Trx や GST 単独の場合にはこれらの結合は観察されなかった。これらの結果は、*At*Pex5p が真に PTS1 レセプターとしての機能を有していることを示している。さらに *At*Pex14p と *At*Pex5p との間に結合活性があったことから、ペルオキシソーム膜上で *At*Pex14p が細胞質局在の *At*Pex5p に対するレセプターとして機能していると結論した。

<u>*At*Pex14p の２つの領域 ^{58}I-^{65}L と ^{78}R-^{97}R が *At*Pex5p と結合する</u>

*At*Pex14p の *At*Pex5p に対する結合ドメインを決定するため、様々な長さの部分長 *At*Pex14p ポリペプチドを Gal4 BD と融合させ、完全長 *At*Pex5p との結合活性について解析した（Figure 9）。*At*Pex14p をその C 末端側から欠失していくと、*At*Pex14p の N 末端 100 アミノ酸（^{1}M-^{100}P）を発現させた宿主酵母はレポーター遺伝子の転写活性化を示したが、N 末端 50 アミノ酸（^{1}M-^{50}S）を発現させた宿主酵母はレポーター遺伝子の転写活性化をすることができなかった。一方、*At*Pex14p をその N 末端側から欠失していくと、*At*Pex14p の C 末端 482 アミノ酸（^{26}A-^{507}N）を発現させた宿主酵母はレポーター遺伝子の転写活性化を示したが、C 末端 432 アミノ酸（^{76}I-^{507}N）を発現させた宿主酵母はレポーター遺伝子の転写活性化をすることができなかった。さらに、他種由来の Pex14p 間で相同性の高い領域の *At*Pex14p-（^{54}R-^{100}P）（Figure 9 and Figure 10, top column）も *At*Pex5p との結合活性を有していた。以上から、*At*Pex14p の N 末端領域内の ^{54}R-^{100}P が *At*Pex5p との結合活性をも

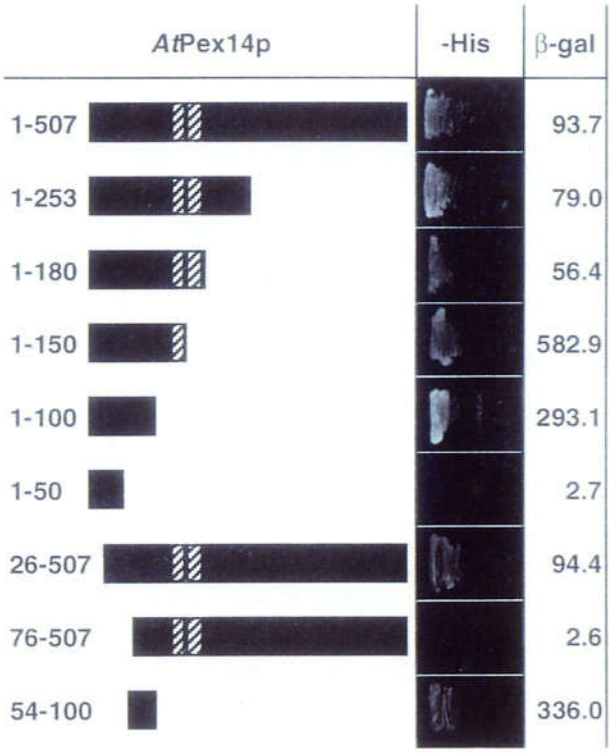

Figure 9. *At*Pex14p-(^{54}R-^{100}P) Interacts with *At*Pex5p.
Various truncated *At*Pex14p were fused to the Gal4p DNA-binding domain and tested for binding activity to *At*Pex5p. Hatched boxes indicate the putative transmembrane domains. Left numbers indicate each length of amino acid sequence. Transformants were tested for growth on synthetic medium without histidine (-His) and assayed for quantitative β-galactosidase activity.

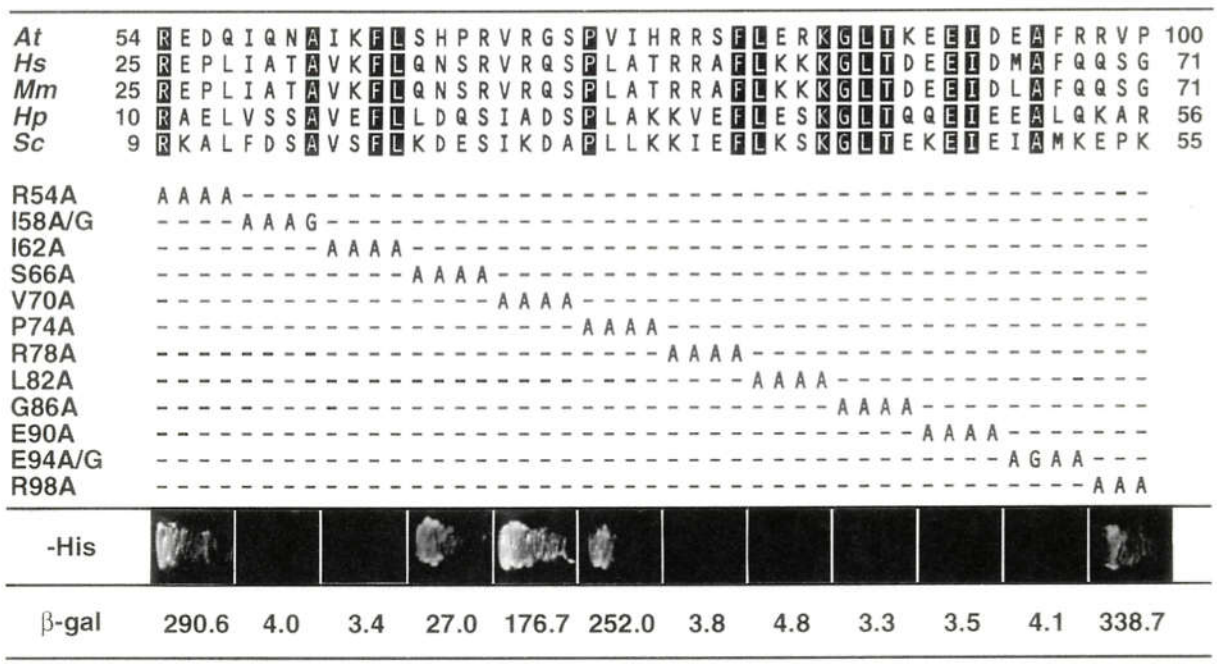

Figure 10. Determination of Binding Domain in *At*Pex14p by Introducing Amino Acid Substitution within ^{54}R-^{100}P.
Top column; Alignment of *At*Pex14p with Pex14ps identified from various species. *At*; *Arabidopsis thaliana*, *Hs*; *Homo sapiens*, *Mm*; *Mus muscuris*, *Hp*; *Hansenula polymorpha*, *Sc*; S*accharomyces cerevisiae*. Conserved amino acids are highlighted.
Middle column; Amino acid sequences of mutated *At*Pex14ps fused to the Gal4p DNA-binding domain. Amino acid substitutions introduced into the fusion proteins are indicated on the right. Name of each fusion protein is indicated on the left.
Bottom column; Result of binding assay for mutated *At*Pex14ps and mutated *At*Pex5p. Transformants were tested for growth on synthetic medium without histidine (-His) and assayed for quantitative β-galactosidase activity.

つと結論した。興味深いことに *ped2* 突然変異体内の翻訳産物と同じ長さの N 末端 253 アミノ酸（^{1}M-^{253}V）は結合活性を残していることがわかった。

*At*Pex14p-(^{54}R-^{100}P)内の *At*Pex5p との結合に重要なアミノ酸残基を特定するために、この領域内のアミノ酸に対して N 末端側より 4 アミノ酸ずつのアラニンもしくはグリシンへの置換を行った（Figure 10, middle column）。そして、アミノ酸置換を導入した *At*Pex14p-(^{54}R-^{100}P)それぞれと、完全長 *At*Pex5p 間の結合活性について解析した。その結果、*At*Pex14p の 2 つの領域、^{58}I-^{65}L および ^{78}R-^{97}R にアミノ酸置換を導入したポリペプチドが *At*Pex5p との結合能を失っていた（Figure 10, bottom column）。この結果から、*At*Pex14p と *At*Pex5p 間のタンパク質間相互作用には *At*Pex14p 側の 2 つの領域、^{58}I-^{65}L および ^{78}R-^{97}R が必要であることが明らかになった。この 2 つの領域を含む *At*Pex14p の N 末端領域を他種由来の Pex14p の N 末端領域と比較した（Figure 10, top column）。*At*Pex14p 全体のアミノ酸配列の相同性は低い（to human; 29.6%）(Will et al., 1999)が、*At*Pex14p-(^{54}R-^{100}P)は他種由来の Pex14p の N 末端部分と相対的に高い相同性をもっていた（to human; 53.2%）。よって、*At*Pex14p の N 末端に保存されたこれらの 2 つの領域は全ての種間に共通の *At*Pex5p の結合ドメインであると推定される。

<u>*At*Pex5p の WXXXF/Y 配列が *At*Pex14p との結合に必須である</u>

次に *At*Pex5p 側の *At*Pex14p に対する結合ドメインの特定を行った。*At*Pex5p には 2 つの特徴的なモチーフが存在する。1 つはタンパク質の C 末端部分に配置されるテトラトリコペプタイドリピート（TPR: tetratricopeptide repeat）であり、酵母 Pex5p を用いた以前の研究から、PTS1 型タンパク質の結合領域であることがわかっている(Brocard et al., 1994)。もう 1 つは WXXXF/Y 繰り返し配列であり、様々な種由来の Pex5p に共通して存在している。しかしながら、この WXXXF/Y 配列は種間によって繰り返し回数や間隔がまちま

ちである。例えば、酵母（*S. cerevisiae*）の Pex5p はこの繰り返し配列がたった 2 回であるのに対し、シロイヌナズナ Pex5p は ^{231}K-^{450}D 内に 9 回も繰り返されている（Figure 11A)。これらのシロイヌナズナ Pex5p に存在する 9 つの WXXXF/Y 配列は ^{231}K-^{450}D 内で N 末端部分の 3 つと C 末端部分の 6 つの配列に別れて存在している。

*At*Pex5p の *At*Pex14p に対する結合ドメインを決定するため、様々な長さの部分長 *At*Pex5p ポリペプチドを Gal4 AD と融合させ、*At*Pex14p-(^{54}R-^{100}P)との結合活性について解析した（Figure 11A)。様々に削りこんだ部分長 *At*Pex5p の内、9 つの WXXXF/Y 配列を含む ^{231}K-^{450}D が *At*Pex14p との結合活性をもつこと、さらにこの ^{231}K-^{450}D 内に別れて存在している N 末端部分の 3 つと C 末端部分の 6 つの WXXXF/Y 配列をそれぞれ含む ^{1}M-^{285}Q、^{336}E-^{728}L の両方が結合活性を有していることから WXXXF/Y 配列が直接 *At*Pex14p との結合に作用している可能性が示された。また、TPR を含む ^{457}H-^{728}L は、酵母 Pex5p の知見と同様に PTS1 型タンパク質と結合活性があることも明らかとなった（data not shown)。*At*Pex14p と PTS1 型タンパク質のそれぞれの結合領域は *At*Pex5p のアミノ酸配列上で重複していなかった。この結果は、*At*Pex14p と *At*Pex5p、PTS1 型タンパク質がペルオキシソームタンパク質輸送において輸送複合体を形成していることを暗示させる。

*At*Pex5p-(^{231}K-^{450}D)に含まれる WXXXF/Y 配列が真に *At*Pex14p の結合ドメインであるか、さらに結合ドメインとして機能しうるならば 9 つの WXXXF/Y 配列それぞれに使い分けがされているのかについて解析した。9 つの WXXXF/Y 配列の内にそれぞれ 1 つずつ AXXXA へのアミノ酸変異をもつよう改変した *At*Pex5p-(^{1}M-^{450}D)と *At*Pex14p 間の結合活性について解析を行った。その結果、変異をもった *At*Pex5p-(^{1}M-^{450}D)はそれぞれ、レポーター遺伝子の β－ガラクトシダーゼ活性がわずかに低下しているものの *At*Pex14p との結合活性を示した（data not shown)。それらの変異 *At*Pex5p-(^{1}M-^{450}D)のうち最も顕著に β－ガラクトシダーゼ活性が低下したものは 8 番目の WXXXF 配列が変異したものであり、

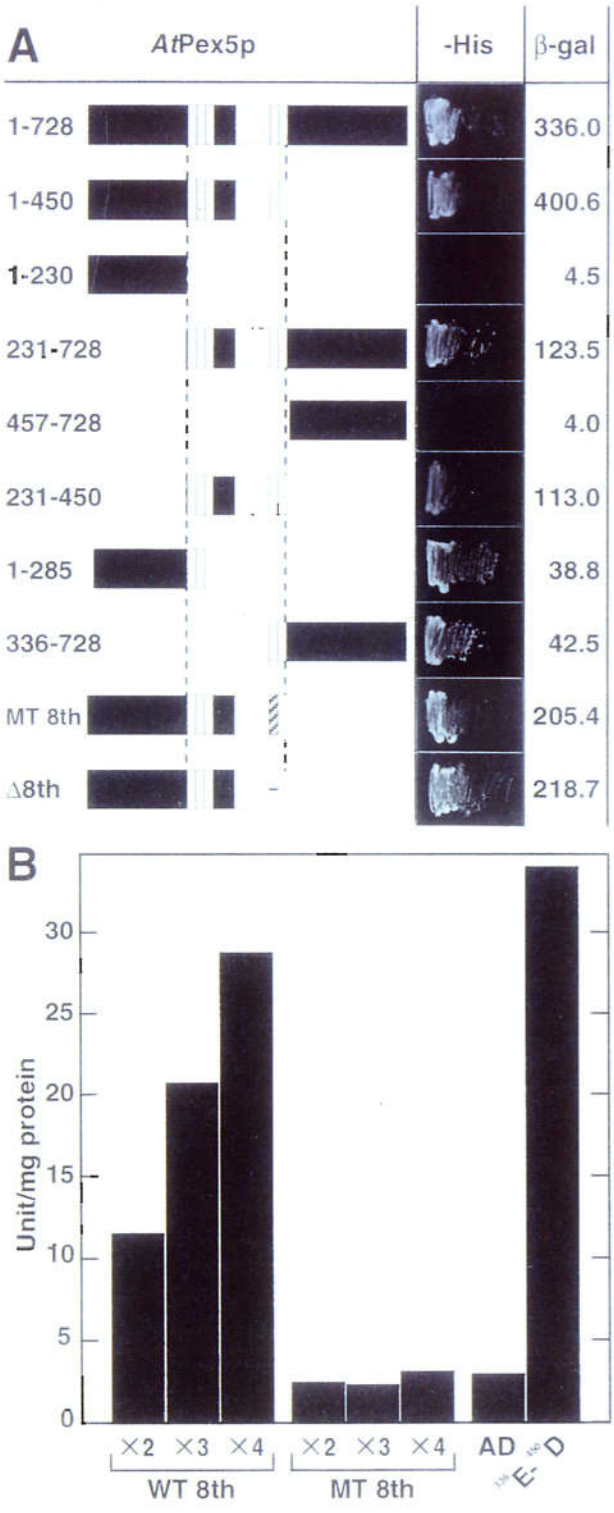

Figure 11. WXXXF/Y Repeats in *At*Pex5p-(^{231}K-^{450}D) Are Required for Binding to *At*Pex14p.

(**A**) Various truncated *At*Pex5p were fused to the Gal4p activation domain and tested for binding activity to *At*Pex14p-(^{54}R-^{100}P). Numbers on the left indicate length of each amino acid sequence. Open boxes indicate WXXXF/Y of the consensus amino acid sequence. Hatched box indicates amino acid substitution of 8th WXXXF to AXXXA.

(**B**) Artificial tandem repeats of 8th WXXXF sequence were tested for binding activity to *At*Pex14p-(^{54}R-^{100}P). WT 8th indicates tandem repeats linked with eighth WXXXF sequence of wild-type. MT 8th indicates tandem repeats linked with AXXXA sequence substituted from eighth WXXXF sequence. AD indicates expression of only Gal4 AD in tester strain. ^{336}E-^{450}D indicates ^{336}E-^{450}D including six WXXXF/Y repeats in *At*Pex5p. Transformants were tested for growth on synthetic medium without histidine (-His) and assayed for quantitative β-galactosidase activity.

野生型 *At*Pex5p-(^{1}M-^{450}D)と比較して 51.3%の値を示した（Figure 11A, MT 8th)。この 8 番目の WXXXF 配列のみを欠損した *At*Pex5p-(^{1}M-^{450}D)も変異を導入したものとほぼ同レベルの結合活性を示した（Figure 11A, Δ8th)。

次に WXXXF/Y 配列が *At*Pex14p との結合モチーフであることを証明するために、8 番目の WXXXF 配列とその前後 5 アミノ酸を含めた合計 15 アミノ酸を複数回連結させたペプチドが、*At*Pex14p との結合活性をもつか調べた。対照実験区として、8 番目の WXXXF 配列の内トリプトファンとフェニルアラニンをアラニンに変異させた AXXXA を同様に連結し、その結合能について解析した。その結果、8 番目の WXXXF 配列の連結個数が 2～4 に増えるのに比例して、結合活性を示すβ－ガラクトシダーゼ活性が増加した（Figure 11B; WT 8th)。対照的に 8 番目の WXXXF に変異を加えた AXXXA は、*At*Pex14p との結合活性を示さなかった（Figure 11B; MT 8th)。この結果は、WXXXF 配列が *At*Pex14p との結合に極めて重要なアミノ酸配列であることを指し示している。加えて、6 つの WXXXF/Y 配列を含む ^{336}E-^{450}D のβ－ガラクトシダーゼ活性はこれらの連結したペプチドの結合活性よりもさらに高かったことから（Figure 11B; ^{336}E-^{450}D)、WXXXF/Y 配列の繰り返し回数が *At*Pex14p との結合効率に影響を及ぼしていると結論した。

***At*Pex7p は *At*Pex5p とは結合するが、*At*Pex14p とは結合しない**

酵母や哺乳類の研究から、ペルオキシソームタンパク質輸送に関わる重要な因子として Pex14p や Pex5p 以外に、PTS2 レセプターとして機能する Pex7p が知られている。この Pex7p はシロイヌナズナゲノム上にも存在する(Schumann et al., 1999)。そこで、*At*Pex7p、*At*Pex14p、*At*Pex5p、PTS2 型タンパク質間の相互作用について、酵母 two-hybrid system により解析することを試みた。それぞれのタンパク質を Gal4 activation domain（AD)、もしくは Gal4 DNA binding domain（BD）と融合タンパク質として発現するよう設計し、tester

strain の PJ69-4A(James et al., 1996)内で発現させた。タンパク質間相互作用の結合活性は栄養要求性（-histidine + 3-AT 50 mM）とβ－ガラクトシダーゼの定量活性測定により検出した。

酵母 two-hybrid system による解析の結果、*At*Pex7p は PTS2 型タンパク質と結合することが、レポーター遺伝子のヒスチジン合成酵素とβ－ガラクトシダーゼの転写活性化により示された（Figure 12A）。これにより、Schumann らの報告している *At*Pex7p が真に PTS2 レセプターとして機能しうることが示された。さらに *At*Pex7p は *At*Pex5p とは結合するが、*At*Pex14p とは直接結合しないことが示された（Figure 12A）。それぞれのタンパク質を単独で発現させた場合、タンパク質間相互作用を示すレポーター遺伝子の転写活性は上がらず、宿主酵母はヒスチジン非存在下で生育できないこと、β－ガラクトシダーゼ活性も検出されないことが確認されている。*At*Pex7p と *At*Pex5p 間の結合は、免疫沈降実験によっても支持された。*At*Pex5p（Figure 12B）もしくは *At*Pex7p（Figure 12C）に対する抗体をアミンカップリング法によりカラムに固定化した。発芽 4 日目のシロイヌナズナ黄化子葉より調製したホモジェネートをこの抗体カラムに通し、結合したタンパク質をイムノブロットにより解析した。この実験において、*At*Pex5p、*At*Pex7p 両タンパク質はそれぞれのカラムから、溶出画分のみに検出されたことから（Figure 12B and C; even lanes）、*At*Pex5p と *At*Pex7p は互いに結合していることが示された。対照実験区に用いた前血清を固定化したカラムからは *At*Pex5p、*At*Pex7p 共に溶出されなかった（data not shown）。すべての溶出画分に IgG のバンドが検出されているが、これは固定化した抗体の一部が剥がれ落ちたためと考えられる。以上の 2 つの実験結果から、*At*Pex5p と *At*Pex7p 間に結合活性があることが証明された。

A

BD	AD	-His	β-gal activity (U/mg protein)
*At*Pex7p	*At*Pex14p		3.7
*At*Pex7p	*At*Pex5p		217.1
*At*Pex7p	PTS2		33.4
*At*Pex7p	-		2.0
-	PTS2		1.5

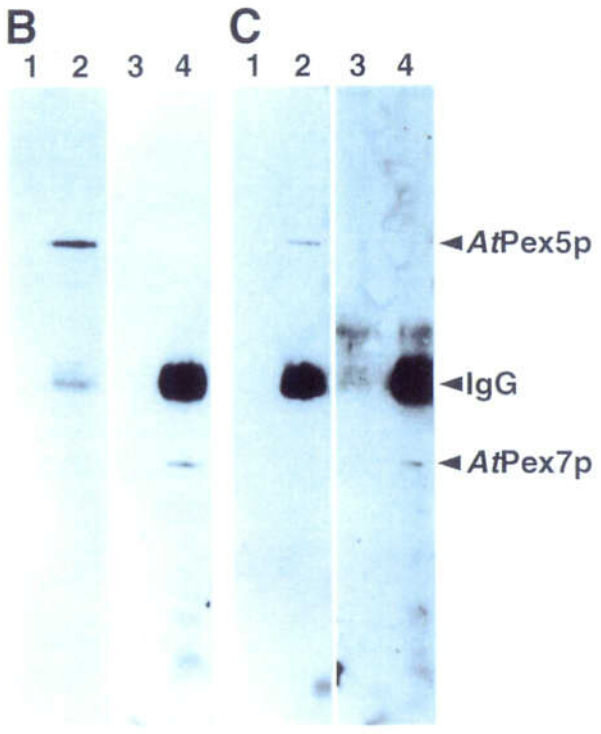

Figure 12. *At*Pex7p Interacts with *At*Pex5p and PTS2-Containing Protein.
(**A**) Two-hybrid analysis of *At*Pex14p, *At*Pex5p, *At*Pex7p and PTS2-containing protein. Proteins were fused to Gal4 BD or AD as indicated. Transformants were tested for growth on synthetic medium without histidine (-His) and assayed for quantitative β-galactosidase activity.
(**B**) and (**C**) Co-immunoprecipitation of *At*Pex5p and *At*Pex7p. Antibodies against *At*Pex5p (**B**) and *At*Pex7p (**C**) were immobilized on column. After total homogenates from etiolated cotyledons were passed over, the columns were washed and then eluted. Wash fraction (odd lanes) and elution fraction (even lanes) were subjected by SDS-PAGE and immunoblotting using antibodies against *At*Pex5p (lane 1, 2) and *At*Pex7p (lane 3, 4). Arrowheads on the right indicate specific bands.

***At*Pex5p の ^{1}M-^{230}V が *At*Pex7p の ^{266}Y-^{317}S と結合する**

*At*Pex5p 側の *At*Pex7p に対する結合ドメインを決定するため、様々な長さの部分長 *At*Pex5p ポリペプチドを Gal4 AD と融合させ、完全長 *At*Pex7p との結合活性について解析した（Figure 13A)。その結果、様々に削りこんだ部分長 *At*Pex5p の内、N 末端側 ^{1}M-^{230}V が *At*Pex7p との結合に必須であることが明らかとなった。この *At*Pex5p の N 末端領域（^{1}M-^{230}V）は *At*Pex14p の結合領域（^{231}K-^{450}D）や PTS1 型タンパク質の結合領域（^{457}H-^{728}L）のいずれとも重複していなかった。一方、*At*Pex7p 側の *At*Pex5p に対する結合ドメインを決定するため、様々な長さの部分長 *At*Pex7p ポリペプチドを Gal4 BD と融合させ、完全長 *At*Pex5p との結合活性について解析した（Figure 13B)。その結果、様々に削りこんだ部分長 *At*Pex7p の内、*At*Pex5p との結合ドメインは *At*Pex7p の C 末端側 ^{266}Y-^{317}S に限定された。この *At*Pex7p の C 末端領域（^{266}Y-^{317}S）は PTS2 型タンパク質の結合領域として同定された WD40 リピート（^{56}S-^{265}D）(Zhang and Lazarow, 1994)と重複していなかった。

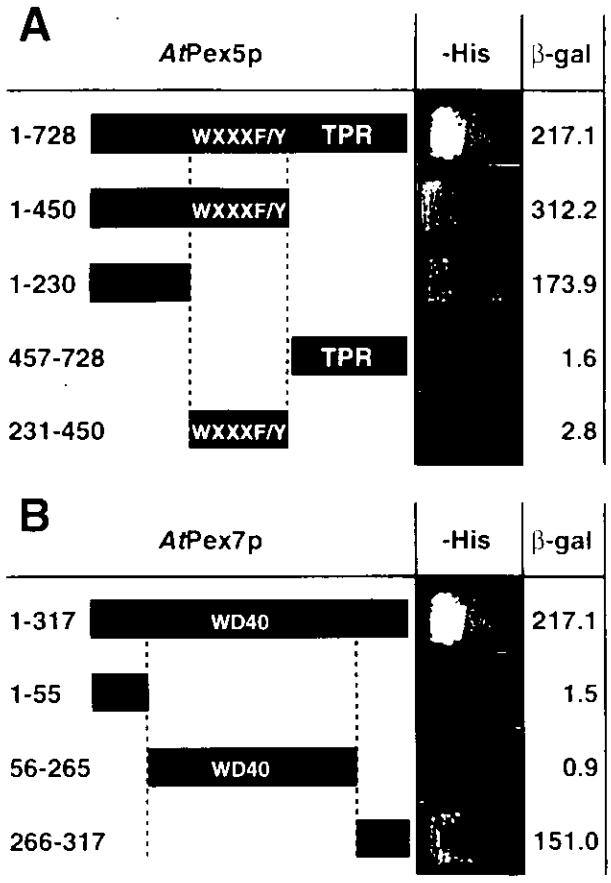

Figure 13. *At*Pex5p-(^{1}M-^{230}V) Interacts with *At*Pex7p-(^{266}Y-^{317}S).
(A) Various truncated *At*Pex5p were fused to the Gal4p activation domain and tested for binding activity to *At*Pex7p. WXXXF/Y indicates 9 repeats of the consensus amino acid sequence. TPR indicates 4 tetratricopeptide repeats.
(B) Various truncated *At*Pex7p were fused to the Gal4p DNA binding domain and tested for binding activity to *At*Pex5p. WD40 indicates 4 WD40 repeats. Numbers on the left indicate length of each amino acid sequence. Transformants were tested for growth on synthetic medium without histidine (-His) and assayed for quantitative β-galactosidase activity.

考察

シロイヌナズナにおけるPTS依存的タンパク質輸送の特徴

現在、酵母や哺乳類を材料とした研究から、20 以上のペルオキシソームの形成維持に関わる遺伝子（PEX）とその遺伝子産物（ペルオキシン）が同定されつつある(Subramani et al., 2000)。これらペルオキシンの内、Pex14p、Pex5p（PTS1 レセプター）、Pex7p（PTS2 レセプター）を含めた複数の因子群が、ペルオキシソームタンパク質輸送装置を構成していることを示唆する論文が報告されているが(Albertini et al., 1997; Marzioch et al., 1994; Van der Leij et al., 1993)、ペルオキシソームタンパク質輸送の分子メカニズムは未だ理解されていない。酵母を用いたペルオキシソーム研究では、Pex14p は Pex5p、Pex7p の両方に結合するが、Pex5p と Pex7p 間に結合活性は認められていない(Albertini et al., 1997)。また、Pex5p もしくは Pex7p を欠損した酵母の突然変異体は、それぞれ PTS1 型タンパク質または PTS2 型タンパク質だけが輸送されなくなる(Marzioch et al., 1994; McCollum et al., 1993)。これらの知見から、酵母において PTS1 型タンパク質輸送経路と PTS2 型タンパク質輸送経路は互いに独立していると考えられている。一方で、哺乳類を用いたペルオキシソーム研究からは酵母とは異なる結果が得られている。ヒト Pex5p の 390 番目のアルギニンにナンセンス変異が起こりストップコドンに変わると PTS1 型タンパク質と PTS2 型タンパク質の両方ともが輸送されなくなる(Braverman et al., 1998)。これはヒト Pex5p が PTS1 型タンパク質だけでなく PTS2 型タンパク質の輸送に関与することを示唆している。ヒトや CHO 細胞（Chinese hamster ovary cell）の Pex5p はオルタネイティブスプライシングにより 2 つのアイソフォームが存在することが報告されており(Braverman et al., 1998; Otera et al., 1998)、各々のアイソフォームはショートフォームとロングフォームの Pex5p と呼ばれている。ヒト Pex5p の 390 番目がストップコドンに変わった変異細胞にロングフォーム

Pex5p を導入すると、PTS1 型タンパク質と PTS2 型タンパク質の両タンパク質輸送が回復する。しかしながら、ショートフォーム Pex5p を導入した場合は PTS1 型タンパク質の輸送のみが回復する。さらに、同じ変異細胞に PTS1 型タンパク質の結合領域を変異させたロングフォーム Pex5p を導入すると PTS2 型タンパク質の輸送のみが回復し、PTS1 型タンパク質は輸送されない。これらの結果は、ヒト Pex5p の 2 つのアイソフォームの内、ロングフォームは PTS2 型タンパク質の輸送にも関与していることを強く示している (Braverman et al., 1998; Otera et al., 1998)。故に、ヒトの PTS2 型タンパク質の輸送は PTS1 レセプターである Pex5p に部分的に依存しているといえる。今回の研究において、シロイヌナズナ *At*Pex5p は *At*Pex14p、*At*Pex7p の両方に結合すること、*At*Pex14p は *At*Pex7p とは結合しないことが証明された。このシロイヌナズナのペルオキシソームタンパク質輸送因子間の結合様式は、ヒトのロングフォーム Pex5p のそれとよく似ている。しかしながら、イムノブロット解析（Figure 6 and 7）および RT-PCR（data not shown）の結果において、*At*Pex5p は単一のバンドとして検出されており、シロイヌナズナ *At*Pex5p がオルタネイティブスプライシングをうけ、複数のアイソフォームが存在する可能性は低い。よってこれらの解析結果は、シロイヌナズナにおける PTS2 型タンパク質の輸送が PTS1 レセプターである *At*Pex5p に完全に依存的であり、それはヒトの場合とは異なった様式であることを示唆している（Figure 14）。

ペルオキシソーム輸送シグナル PTS1 と PTS2 について

様々な種において同定されたペルオキシソームマトリクスタンパク質のほとんどは、ペルオキシソームへの輸送シグナルとして PTS1 か PTS2 のどちらかをもっている(Olsen, 1998)。本研究は、*At*Pex14p と *At*Pex5p がほとんどの植物器官において発現していることを明らかにし、これをもとに *At*Pex5p に依存する PTS1 経路がペルオキシソームへのタン

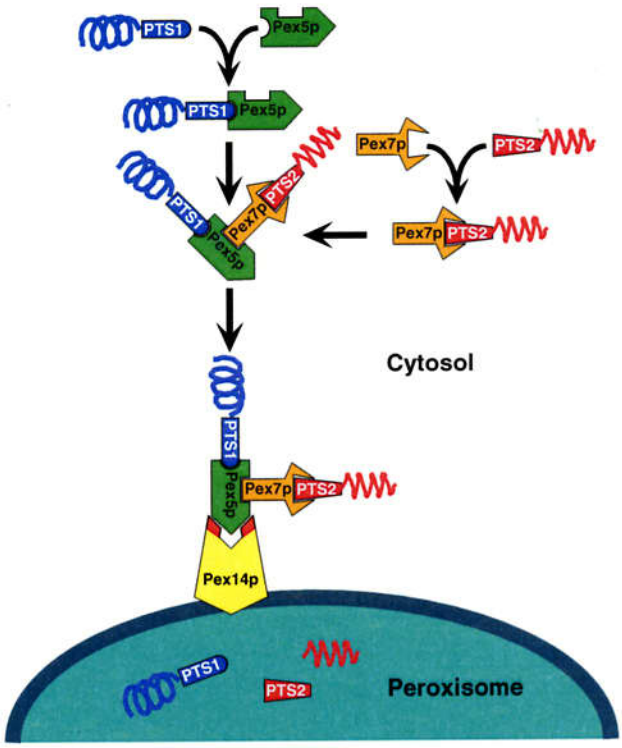

Figure 14. A Schematic Model of Peroxisomal Protein Import in Arabidopsis. Pex5p and Pex7p, PTS1 receptor and PTS2 receptor, which are localized in the cytosol are bound to PTS1- and PTS2-containing proteins (cargo), respectively. Both protein complexes bind between ^{1}M-^{230}V of *At*Pex5p and ^{266}Y-^{317}S of *At*Pex7p. The receptor-cargo import complex consisting of Pex5p, Pex7p, PTS1- and PTS2-containing protein binds then to the peroxisomal membrane via interaction between WXXXF/Y repeats of *At*Pex5p and ^{58}I-^{65}L and ^{78}R-^{97}R of *At*Pex14p. All binding domains do not overlap in the process of peroxisomal protein import.

パク質輸送経路として中心的に機能していると推測した（Figure 6）。この結果は、ヒト Pex14p と Pex5p がほとんどの組織で発現している事実とも一致している(Wiemer et al., 1995; Will et al., 1999)。一方で、PTS2 レセプターである *At*Pex7p が *At*Pex5p に比べて限られた器官でのみ発現していたことから、PTS2 経路がペルオキシソームへのタンパク質輸送経路として付加的な経路であると推測できる。この仮説が正しいとするならば、PTS2 型タンパク質の発現は PTS1 型タンパク質のそれと比べて、より器官特異性が高いともいえる。現在までに同定されているグリオキシソーム酵素、緑葉ペルオキシソーム酵素を含めたほとんどのペルオキシソーム酵素は PTS1 をもっている。対照的に PTS2 を輸送シグナルを保有していることが明らかになっている高等植物のタンパク質はチオラーゼ(Kato et al., 1996b)、リンゴ酸脱水素酵素(Kato et al., 1998)、クエン酸合成酵素(Kato et al., 1995)、長鎖アシル CoA 酸化酵素(Hayashi et al., 1998a)の 4 つのみである。これらのペルオキシソームタンパク質は主にグリオキシソームに蓄積しており、緑葉ペルオキシソームでは顕著でない。現在までに高等植物において PTS2 をもった緑葉ペルオキシソーム局在のタンパク質は同定されていない。ところが本研究の結果、緑葉ペルオキシソームをもつ茎生葉、ロゼット葉では他器官に比べて PTS2 レセプターである *At*Pex7p の発現が顕著であった（Figure 6）。PEDANT BLAST Network Service（http://pedant.gsf.de/）を用いてシロイヌナズナゲノムデータベースを検索したところ、シロイヌナズナゲノムには 49 個もの未同定な PTS2 型タンパク質が存在すると予測されていた。この予測結果は、未同定な PTS2 型タンパク質が茎生葉やロゼット葉などで発現し、新規の植物ペルオキシソームの代謝機能に寄与している可能性が高いことを示すものと考えている。今後、PTS をもつと予測されるタンパク質を中心にマイクロアレイによる網羅的な解析を行う予定であり、この解析結果が未知のペルオキシソームタンパク質が関わる新規な代謝系の発見の端緒になると期待される。

AtPex14p の 2 つの結合領域、^{58}I-^{65}L および ^{78}R-^{97}R

酵母やほ乳類の研究から得られたデータによれば、Pex14p はペルオキシソーム膜上に局在し、PTS1 型タンパク質を捕捉した Pex5p をペルオキシソーム膜上に引き寄せる為に中心的に働いていると言われている(Brocard et al., 1997; Will et al., 1999)。ヒト Pex14p では、その N 末端 78 アミノ酸が Pex5p との結合領域であることが特定されている(Schliebs et al., 1999)。シロイヌナズナ *At*Pex14p のアミノ酸配列はヒト Pex14p よりも若干長く、そのためシロイヌナズナ *At*Pex14p の N 末端 100 アミノ酸はヒト Pex14p の N 末端 71 アミノ酸に相当することが配列の相同性から示された（Figure 10, top column)。さらに本研究において、*At*Pex14p の N 末端 100 アミノ酸内に存在する 2 つの領域、^{58}I-^{65}L および ^{78}R-^{97}R が *At*Pex5p の結合ドメインであることが証明された（Figure 10, bottom column)。タンパク質のアミノ酸配列から、*At*Pex14p の 2 次構造を予測させたところ(Garnier et al., 1978)、これら 2 つの領域は、複数の β 構造によって構成された複雑な構造をとっていると予測された（Figure 15)。この予測は、2 つの領域が結合ポケットを形成し機能している可能性を示している。この結合ポケットが全ての種由来の Pex14p に共通に存在し、ペルオキシソーム膜上で Pex5p を繋留しているのかもしれない。

ped2 変異体の表現型の解釈

シロイヌナズナの突然変異体 *ped2* の以前の解析から、*ped2* 変異体では *At*Pex14p の 254 番目のグルタミンをコードする CAA コドンがストップコドン TAA に塩基置換を起こしていることが明らかにされている。またこの突然変異体内では、PTS1 型、PTS2 型両タンパク質輸送が共に不完全となっていることがわかっている(Hayashi et al., 2000a)。本研究結果から、*ped2* 変異体内における *At*Pex14p の推定部分長配列に相当する ^{1}M-^{253}V は *At*Pex5p

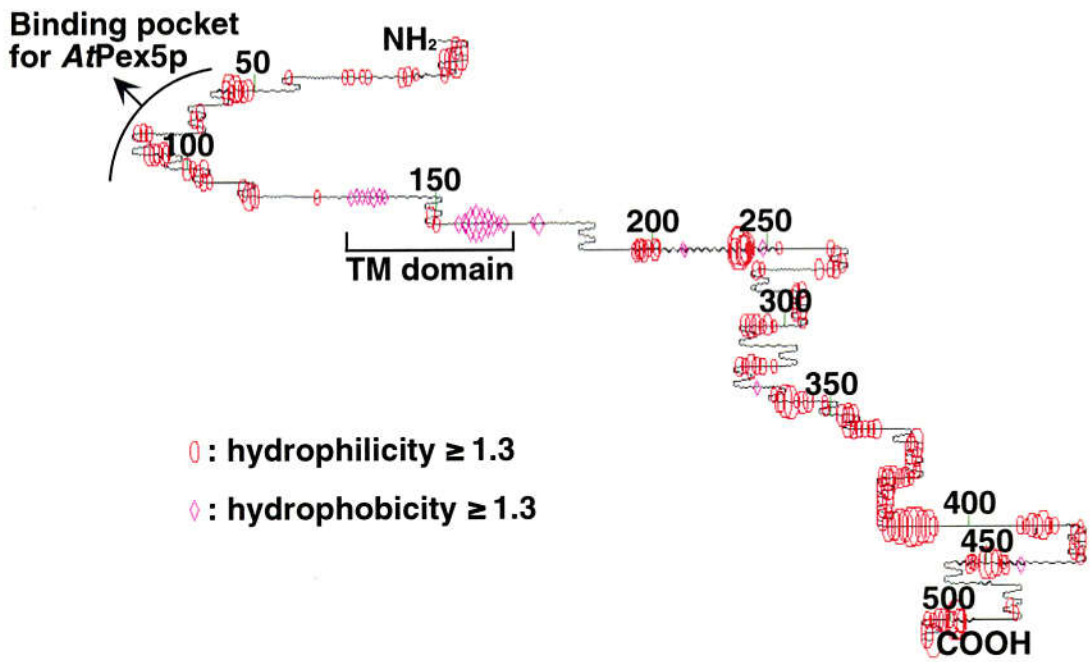

Figure 15. Two N-terminal domains, ^{58}I-^{65}L and ^{78}R-^{97}R of *At*Pex14p might form a putative binding pocket for *At*Pex5p.
Deduced secondary structure for the amino acid sequence of *At*Pex14p according to Garnier-Robson method (Garnier et al., 1978). Wavy, straight and curved lines indicate α-helix, β-structure and β-turn, respectively. Red circles and Magenta diamonds represent hydrophilic and hydrophobic regions, respectively. TM domain indicates a putative transmembrane domain.

との結合活性を残していることが示された（Figure 9）。イムノブロット解析では、この *At*Pex14p の N 末端 253 アミノ酸（^{1}M-^{253}V）を *ped2* 変異体内に検出することはできなかったが（data not shown）、C 末端の欠失により本来の安定性を失った部分長 *At*Pex14p がわずかに存在している可能性もある。*ped2* 変異体の表現型である PTS1 型および PTS2 型タンパク質の部分的なペルオキシソームへの輸送は、この部分長 *At*Pex14p が一部輸送能力を残しているためと考えられる。もし、このような部分長 *At*Pex14p が *ped2* 変異体内で機能していないと仮定すると、シロイヌナズナでは *At*Pex14p に非依存的なマイナーな別の輸送経路が存在している可能性が生じるが、現在までにこれを支持するような結果は、植物はもとより酵母、哺乳類を用いた研究からも得られていない。

Pex5p の WXXXF/Y 配列はなぜ植物に多いのか？

*At*Pex5p 側の *At*Pex14p の結合ドメインについても解析した結果、*At*Pex14p の結合ドメインは *At*Pex5p の 9 つある WXXXF/Y 配列であり、この WXXXF/Y 配列の数が *At*Pex14p と *At*Pex5p 間の親和性を規定していることが証明された（Figure 11）。この WXXXF/Y 配列は様々な種由来の Pex5p のアミノ酸配列上に繰り返し回数や間隔は異なるものの、共通して見受けられる(Schliebs et al., 1999)。例えば、シロイヌナズナとスイカの Pex5p は 9 つの WXXXF/Y 配列をもつが、ヒトでは 7 つ、酵母ではたったの 2 つである。このように高等植物の WXXXF/Y 配列の数は他の生物種に比べ多い傾向にある。一方で、ヒトを用いた最新の解析から、Pex5p は 4 量体構造を形成していることが報告されている(Schliebs et al., 1999)。もし、この様な 4 量体が *At*Pex5p でも形成されているならば、*At*Pex5p のレセプター4 量体は *At*Pex14p の結合ドメインとして 36 もの WXXXF/Y 配列をもつことになる。この事実は、高等植物の Pex5p は他の生物種由来の Pex5p より Pex14p に対して高い親和性をもち、結果として高いペルオキシソームタンパク質輸送能力を持つことを想像させる。

高等植物は発芽段階において生長エネルギーを得るために素早く貯蔵脂肪を分解する必要がある。さらに生長の進んだ高等植物個体では、ペルオキシソームは光呼吸活性を得るためにその機能を素早く転換させなければならない。このような生長の一過程における大量の脂質代謝や機能転換は高等植物固有の現象であり、酵母や哺乳類では観察されない。故に、高等植物は素早く大量の代謝酵素を入れ換えられるように適応し、その結果として高い輸送能をもったPex5pを生み出したのかもしれない。

ペルオキシソームタンパク質輸送複合体

Pex5pとPex7pはペルオキシソームタンパク質輸送における重要な因子として様々な種において同定されている。これらのレセプターは細胞質に局在しそれぞれPTS1レセプターおよびPTS2レセプターとして機能する(Subramani, 1998)。本研究において、*At*Pex5pと*At*Pex7pがペルオキシソームタンパク質輸送過程でPTS1-PTS2レセプター複合体を形成していることを示す結果が得られた。これらレセプター間の互いの結合ドメインはそれぞれ*At*Pex5pのN末端側^{1}M-^{230}Vと、*At*Pex7pのC末端側^{266}Y-^{317}Sであった（Figure 13)。これらの結合ドメインとは別に、それぞれのレセプターは当然PTS1型タンパク質、PTS2型タンパク質を捕捉するための結合ドメインをも有している。Pex5pでは、荷物タンパク質の結合ドメインとしてアミノ酸配列のC末端領域にtetratricopeptide repeat（TPR）モチーフをもっており(Gatto et al., 2000)、*At*Pex5pでは^{457}H-^{728}Lに相当する。Pex7pでは、このような結合ドメインとしてWD40 repeatをもっており(Shimozawa et al., 1999)、*At*Pex7pでは^{56}S-^{265}Dに相当する。本研究結果から、これら輸送因子の荷物タンパク質を認識するための結合ドメインおよびレセプター間の結合ドメイン、さらに*At*Pex14pと結合する*At*Pex5pの^{231}K-^{450}Dを含めて、少なくともアミノ酸配列上は重複していなかった。これらの結果に加えて、いくつかのPTS1またはPTS2をもつペルオキシソームタンパク質は翻

訳後、細胞質でオリゴマーを形成し、そのままペルオキシソームへと輸送されていることを示唆する結果が得られている(Kato et al., 1999; Subramani, 1998)。これらの事実から、ペルオキシソームタンパク質輸送因子 *At*Pex14p、*At*Pex5p、*At*Pex7p に加え、荷物タンパク質の PTS1 型、PTS2 型タンパク質はペルオキシソームタンパク質輸送過程において非競合的であり、それ故ペルオキシソーム膜上でこれらのタンパク質は巨大なタンパク質輸送複合体を形成していることを想像させる。このような巨大な輸送複合体が本当に形成されているかについては、化学的な架橋剤などを用いて複合体の構成因子間を架橋した後に複合体ごと免疫沈降させ、質量分析によって複合体の構成因子を同定し確認をすることが必要である。この実験系では新たな複合体構成因子を検出することも可能であり、ペルオキシソームタンパク質輸送機構をより理解するために重要である。一方で、ペルオキシソームへのタンパク質輸送機構はミトコンドリアや葉緑体のそれとは大きく異なるといわれている。その最も特徴的な点は、PTS さえ結合していれば直径 9 nm の巨大な金粒子がペルオキシソーム膜を通してマトリクスに輸送されるということであろう(Walton et al., 1995)。このような特徴的なペルオキシソームタンパク質輸送における現象は、おそらくタンパク質輸送因子 *At*Pex14p、*At*Pex5p、*At*Pex7p に加え、PTS1 型および PTS2 型タンパク質が形成する巨大な輸送複合体を取り込む能力を反映しており（Figure 14)、今後この膜透過の分子機構を解明することが、ペルオキシソームというオルガネラの輸送機構の特殊性を理解する上で重要である。

ペルオキシソームタンパク質輸送解析の課題

本研究において、ペルオキシソームタンパク質輸送因子 *At*Pex14p、*At*Pex5p、*At*Pex7p 間の結合ドメインは少なくとも 1 次構造上は重複していないことを明らかにした。しかしながら、これらの輸送因子間の結合が 3 次構造上も重複していないのかは未だ不明である。

今後、これら輸送因子間の結合ドメインの立体構造解析を行うことで、ペルオキシソームタンパク質輸送過程における輸送因子の協調関係が理解されるようになるだろう。

本研究結果を基にシロイヌナズナにおけるペルオキシソームへのタンパク質輸送モデルを提唱した（Figure 14)。このモデルの中で、輸送因子と荷物タンパク質は巨大な輸送複合体を形成している。しかしながら、本研究で行った *in vitro* binding experiment では 3 つ以上の因子で構成された輸送複合体を検出することに成功していない。この原因はおそらくこれらの輸送因子間の結合効率が低いためと考えられる。一般的には、3 つ以上の因子が関わるタンパク質間相互作用では、それぞれの結合がアロステリック効果により制御されている実験結果も数多く報告されており(Drees et al., 2001; Kone, 2000; Kukkonen et al., 2001; Uetz et al., 2000; Zhang and Yuan, 1998)、ペルオキシソームタンパク質輸送においても同様の現象が起きている可能性がある。例えば、PTS1 型タンパク質を捕捉した *At*Pex5p と単体の *At*Pex5p が *At*Pex14p に対して親和性が変化するという可能性であり、このようなメカニズムが働かなければペルオキシソームへのタンパク質輸送は大変非効率的なものとなってしまう。従って、3 つ以上の因子間における相互作用による親和性変化の解析と、その結果をから予測される輸送複合体構成因子の変化を解明することは、今後の重要な課題である。

最近、ヒト Pex5p を用いた研究から、Pex5p は細胞質で PTS1 型タンパク質を捕捉した後に、荷物タンパク質と共にペルオキシソームマトリクスに入り、再び細胞質にリサイクルバックされるということが証明された(Dammai and Subramani, 2001)。本研究結果からも推測されるように、それぞれの輸送因子は他の輸送因子との結合解離を巧妙に制御されることで荷物タンパク質をペルオキシソームへと輸送していると考えられる。しかしながら、この過程において Pex5p などのレセプターと PTS1 型タンパク質の結合解離のメカニズムは未だに明らかでない。また、*At*Pex14p、*At*Pex5p、*At*Pex7p 以外のペルオキシソー

ムタンパク質輸送因子が存在する可能性もあり、それらとの相互作用が結合解離のメカニズムを制御しているのかもしれない。事実、酵母や哺乳類の解析から、Pex13p や Pex17p がペルオキシソーム膜上のタンパク質輸送因子として同定されている。シロイヌナズナの Pex13p や Pex17p は未だ機能的に同定されておらず、このような他の輸送因子の同定と、これらによって構成された輸送複合体が荷物タンパク質とどのようにして結合解離を行っているのか、これらの問題も今後のペルオキシソーム研究の焦点となってくるだろう。

第２章　ペルオキシソーム膜貫通型タンパク質・アスコルビン酸ペルオキシダーゼの局在化機構

ペルオキシソーム膜貫通型タンパク質の局在化機構の解析を行うために、最初にこれまであまり解析の進んでいないペルオキシソーム膜タンパク質の同定を行い、その特徴について明らかにすることにした。この結果、グリオキシソームに局在する 31 kDa 膜貫通型タンパク質のアスコルビン酸ペルオキシダーゼ(pAPX)の同定に成功した。この pAPX の細胞内局在性の詳細な検討および、免疫細胞生化学的解析から pAPX の局在化に未知の膜構造物が関与することを見いだしたので報告する。

材料と方法

植物材料

シロイヌナズナ（*Arabidopsis thaliana* (landsberg *erecta* and Columbia)）種子を 70%エタノールと滅菌液（2% NaClO, 0.02% Triton X-100）でそれぞれ 5 分間滅菌した。滅菌水で 5 回洗浄した種子をトップアガー（0.4% INA agar (Ina shokuhin, Nagano, Japan)）と共に GM（germination medium: 2.3 g/l MS salt (Wako, Osaka, Japan) 2% sucrose, 100 µg/ml myo-inositol, 1 µg/ml thiamine-HCl, 0.5 µg/ml pyridoxine, 0.5 µg/ml nicotinic acid, 0.5 mg/ml MES-KOH (pH 5.7), 0.8% INA agar (Ina shokuhin, Nagano, Japan)）寒天培地上にまいた。種子の休眠打破のために 2 日間の低温処理をした後、22℃のインキュベーター内で明条件下もしくは暗条件下で発芽生育させた。実験用途に合わせ、発芽 7 日目を経過した植物個体の内いくつかを

バーミキュライト：パーライトを 1: 1 で混合した土に植え継ぎ、22℃、100 μE/m^2/s で 16 時間明所、8 時間暗所で生育させた。

カボチャ種子（*Cucurbita sp.* Kurokawa Amakuri）は種皮をつけたまま、流水で 12 時間浸した後、湿らせた粒状ロックウール（Nitto Boseki, Chiba, Japan）上に播種し、暗所下 25℃において発芽生育させた。また、発芽後 5 日間暗所で生育させた黄化芽生えを白色光下に移し、25℃で更に生育させたものを緑化芽生えとした。

カボチャ黄化子葉からの無傷ペルオキシソームの単離

発芽 5 日目のカボチャ黄化子葉 100 g に 200 ml の緩衝液 A（20 mM pyrophosphate-HCl (pH 7.5), 1 mM EDTA, 0.3 M mannitol）を加え、ワーリングブレンダーで 3 秒間 2 回破砕し、これを 4 層のガーゼでろ過し、強く絞った。残渣に 200 ml の緩衝液 A を加え、再度 3 秒間 2 回破砕し、ろ過した。2 回の抽出液を合わせて、1,500×*g* で 20 分間遠心し、核、プラスチド等を除き、さらに上清を 10,000×*g* で 20 分間遠心した。ここで得られた沈殿を 5 ml の緩衝液 B（10 mM HEPES-KOH (pH 7.2), 1 mM EDTA, 0.3 M mannitol）で懸濁し、30 ml の Percoll 溶液（28% (w/w) Percoll (Amersham Pharmacia Biotech), 10 mM HEPES-KOH (pH 7.2), 1 mM EDTA, 0.3 M raffinose）に上層した。40,000×*g* で 30 分間遠心した後、遠心管の底部にバンド状に集まったペルオキシソームを駒込ピペットで回収した。回収したペルオキシソーム溶液に 4 倍量の緩衝液 B を加えて Percoll を希釈し、5,000×*g* で 10 分間遠心して沈殿にした。沈殿に 1 ml の緩衝液 A を加え懸濁し、無傷ペルオキシソームとした(Yamaguchi et al., 1995b)。

ペルオキシソーム膜タンパク質の抽出

単離精製した無傷ペルオキシソームを 5,000×*g* で 10 分間の遠心により沈殿させた後、

低張液（10 mM HEPES-KOH (pH 7.2)）を加え懸濁、破裂させた。これを 100,000×*g* で 30 分間遠心し、上清を可溶性画分とした。この可溶性画分にはマトリクスタンパク質が抽出される。沈殿には高塩溶液（10 mM HEPES-KOH (pH 7.2), 200 mM KCl）を加えて再懸濁後 100,000×*g* で 30 分間遠心し、上清を塩可溶性画分とした。塩可溶性画分にはイオン結合などで弱く膜に付着したタンパク質を抽出することができる。さらに沈殿にはアルカリ溶液（100 mM Na_2CO_3）を加えて再懸濁後、100,000×*g* で 30 分間遠心した。その上清を 1 M HCl で中和したものをアルカリ可溶性画分とした。アルカリ可溶性画分には膜貫通型タンパク質以外の膜に強く結合したタンパク質が抽出される。アルカリ溶液でも可溶化しなかった沈殿に低張液を加え、アルカリ不溶性画分とした。これまでの研究からペルオキシソームの膜貫通型タンパク質はアルカリ不溶性画分に検出されることがわかっている。

カボチャ黄化子葉ライブラリーの作製

暗所で 4 日間発芽生育させたカボチャ黄化子葉から、SDS/phenol 法によって全 RNA を抽出した。この全 RNA をオリゴ（dT）セルロースカラムクロマトグラフィにより精製し、poly (A)$^+$RNA を調製した(Mori et al., 1991)。

プラスミド pTTQ18（Amersham Japan, Tokyo, Japan）を *Pst*I 部位で切断して直鎖状にし、50±10 残基のオリゴ（dT）を末端に連結した。これをさらに *Xba*I 部位で切断した後、オリゴ（dA）セルロースカラムクロマトグラフィにて精製し、これをベクタープライマーとして用いた。

1 μg のベクタープライマーpTTQ18 と 10 μg の poly (A)$^+$RNA に 15 unit の Moloney murine leukemia virus reverse transcriptase（Amersham Japan, Tokyo, Japan）、1st-strand 反応緩衝液（50 mM Tris-HCl (pH 8.3 at 37℃), 2 mM dNTPs, 8 mM $MgCl_2$, 30 mM KCl, 10 mM dithiothreitol）を加えて、37℃1 時間で 1st-strand DNA を合成した。2nd-strand DNA は 2nd-

strand 反応緩衝液（20 mM Tris-HCl (pH 7.5), 4 mM $MgCl_2$, 100 mM KCl, 50 μg/ml bovine serum albumin）に、20 unit の DNA polymerase I と 30 unit の RNase H を加え、16℃2 時間で合成した。反応を 65℃10 分間の保温により停止させた。cDNA と結合したベクターを平滑末端化した後、自己環状化させた。これを大腸菌株 DH5αに導入した。

In-gel digestion 法による pAPX 内部アミノ酸配列の決定

カボチャ 31 kDa 膜タンパク質（pAPX）のトリプシン消化および、得られたペプチドの N 末端アミノ酸配列の解析は、Shevchenco et al.（1996）の方法に従って行った。無傷ペルオキシソームより膜タンパク質を抽出し、SDS-PAGE によって分離した。ゲルを CBB 染色し、31 kDa タンパク質のバンドを切り出し、100 μl の脱染脱水液（0.2 M ammonium bicarbonate (pH 8.0), 50% acetonitrile）中で 30 分振とうした。この操作を数回繰り返した後、上清を捨てゲルを減圧乾燥させた。ゲルを 10 μl の膨潤液（0.2 M ammonium bicarbonate (pH 8.0)）で 5 分間おき、10 μl の 0.2 mg/ml のトリプシン溶液と 20 μl の膨潤液を加えて、37 度で一晩反応させた。停止液（10% trifluoric acetate）を 4 μl 加え反応を停止させた。これに溶出液（0.1% trifluoric acetate, 60% acetonitrile）を 100 μl 加え 30 分振とうし、ペプチドを溶出させた。上清を回収し、1/3 量になるまで減圧濃縮したものを 0.22 μm フィルター（Millipore）でろ過し、逆相クロマトグラフィでペプチドを分取した。逆相クロマトグラフィには、SMART system (Amersham Japan, Tokyo, Japan) を、カラムはμRPC C2/C18 PC3.2/3 を用いた。各ペプチドはアミノ酸シークエンサー（Model 492, Applied Biosystems）を用いて Edman 法により配列を解析した。

タンパク質試料の調製

電気泳動に用いるタンパク質試料は、植物材料を乳鉢にとり、液体窒素中で磨砕し

た。これに試料溶解液（2% SDS, 50 mM Tris-HCl (pH 6.8), 5% 2-mercaptoethanol, 0.1% BPB, 10% glycerol）に加えて更に磨砕し、95℃で 5 分間熱処理した。その後 15,000×*g* で 5 分間遠心し、上清をタンパク質試料とした。

融合タンパク質の調製と抗体作製

すでに単離された pAPX の cDNA を鋳型にして PCR 法により、pAPX-(^{1}M-^{90}L)、pAPX-(^{147}M-^{286}K)に相当する cDNA 断片を増幅した。得られた cDNA 断片を T-ベクター；pBluescript II SK+（Stratagene, La Jolla, CA）にクローニングし、塩基配列を確認した。それぞれの cDNA 断片に対応した制限酵素で cDNA 断片を切り出し、チオレドキシン（Trx: thioredoxin）と目的タンパク質に加えヒスチジンタグ（6xHis）が融合したタンパク質を構築するための大腸菌発現ベクターpET32a（Novagen, USA）にインフレームで連結した後、大腸菌 BL21（DE3）に導入した。大腸菌を終濃度 200 mM になるようカルベニシリンを加えた LB 液体培地で生育させ、OD_{600}=0.6～0.7 になるまで 37℃で振とう培養した。誘導は終濃度 1 mM になるよう IPTG を加え、さらに 3 時間振とう培養した。誘導後の大腸菌を 3,000×*g* で 5 分間の遠心により回収し、開始緩衝液（50 mM sodium phosphate (pH 7.5), 50 mM imidazole, 0.5 M NaCl）に懸濁した。融合タンパク質を抽出するため、超音波処理装置（Model 450D, Branson）を用いて、Output 2～3、50% duty、5 分間の条件で 3 回、氷上にて処理し大腸菌を破砕した。破砕液を 10,000×*g* で 10 分間遠心し、可溶性画分と不溶性画分に分離した。pAPX-(^{1}M-^{90}L)と pAPX-(^{147}M-^{286}K)はこの条件で可溶性画分に抽出されたため、これを精製に用いた。それぞれ可溶化した融合タンパク質を含む粗抽出液を、ニッケルを結合させた HiTrap Chelating カラム（Amersham Japan, Tokyo, Japan）に通し、開始緩衝液で洗浄した後、カラムに結合している融合タンパク質を溶出緩衝液（50 mM sodium phosphate (pH 7.5), 1 M imidazole, 0.5 M NaCl）で溶出精製し、抗原として用いた。

精製融合タンパク質 0.5 mg を含む 1 ml の溶液に、等量の Freund's complete adjuvant（DIFCO Laboratories, USA）を加えよく乳濁化させ、ウサギ背部に皮下注射し第 1 回目の免疫感作とした。4 週間後、同量の融合タンパク質を含む 1 ml の溶液に、今度は等量の Freund's incomplete adjuvant を加えよく乳濁化させ、これを第 2 回目の免疫感作として皮下注射した。以降、1 週間毎に第 5 回目までの追加感作を行った。第 1 回目の免疫感作の直前に少量採血し前血清とした。第 2 回目以降の免疫感作から 3 日後に耳の動脈より採血を行い、抗血清を調製して以降の実験に用いた。pAPX-(^{1}M-^{90}L)を抗原として用いた抗血清はカボチャ pAPX に特異的に反応し、カボチャの他の APX アイソザイムやシロイヌナズナ pAPX には反応しなかった。一方、pAPX-(^{147}M-^{286}K)を抗原とした抗血清は細胞質局在の cAPX と強く反応し、pAPX に弱く反応した。よって、pAPX-(^{1}M-^{90}L)に対する抗血清は pAPX を、pAPX-(^{147}M-^{286}K)に対する抗血清は cAPX を検出するために用いた。

SDS-PAGE とイムノブロット

SDS-PAGE は Laemmli（1970）の方法に、ナイロン膜（GVHP membrane, Millipore）への転写は Towbin et al.（1979）の方法に準じて行った。タンパク質が転写されたナイロン膜は 3%（w/v）スキムミルクを含む TBS-T（50 mM Tris-HCl (pH 7.5), 150 mM NaCl, 0.05% (w/v) Tween20）で 1 時間ブロッキング処理をした。その後、1,000-10,000 倍希釈した各抗血清を含む TBS-T で 1 時間振とうした。ナイロン膜を TBS-T で 15 分 1 回、5 分 2 回洗浄し、次に 5,000-10,000 倍希釈したペルオキシダーゼ結合ヤギ抗ウサギ IgG 抗体（Amersham Japan, Tokyo, Japan）を含む TBS-T で 1 時間振とうした後に、ナイロン膜を TBS-T で 15 分 1 回、5 分 4 回洗浄した。各抗血清と反応性のあるタンパク質は ECL kit（Amersham Japan, Tokyo, Japan）を用いて検出した。

ショ糖密度勾配遠心

発芽 3 日目または 5 日目のカボチャより黄化子葉を 5 g 切り取り、10 ml の抽出緩衝液（10 mM Tricine-HCl (pH 7.5), 1 mM EDTA, 12% (w/w) sucrose）とともに氷冷したペトリ皿上においた。試料が 2～3 mm 角程になるまでカミソリ刃を用いて破砕し、抽出液を 3 層ガーゼでろ過した。抽出液 1 ml を 16 ml のショ糖密度勾配溶液（30%～60% (w/w), 1 mM EDTA）に上層して、SW 28.1 スイングローター（Beckman, USA）で 85,000×*g*、2.5 時間遠心した。遠心終了後、直ちに fractionator（model 185; ISCO, USA）で 0.5 ml ずつ分画し、それぞれの画分において指標酵素の活性測定および各種抗体によるイムノブロット解析を行った。

マグネシウムシフト

発芽 5 日目のカボチャより黄化子葉を 5 g 切り取り、20 ml の抽出緩衝液（50 mM HEPES-NaOH (pH 7.0), 10% (w/w) sucrose, 2 mM EDTA or 5 mM $MgCl_2$）とともに氷冷したペトリ皿上においた。試料が 2～3 mm 角程になるまでカミソリ刃を用いて破砕し、抽出液を 3 層ガーゼでろ過した。10,000×*g* で 10 分間遠心し、核、プラスチド等の主要なオルガネラを沈殿除去した上清を得た。この上清を更に 100,000×*g* で 1 時間遠心し、マイクロソーム画分を沈殿させた。沈殿に同じ抽出緩衝液を 0.5 ml 加えて懸濁し、16 ml のショ糖密度勾配溶液（15%～45% (w/w), 2 mM EDTA or 5 mM $MgCl_2$）に上層して、SW 28.1 スイングローター（Beckman, USA）で 110,000×*g*、2.5 時間遠心した。遠心終了後、直ちに fractionator（model 185; ISCO, USA）で 0.5 ml ずつ分画し、それぞれの画分において抗 pAPX 抗体と抗 BiP 抗体によるイムノブロット解析を行った。

形質転換シロイヌナズナの作出

pAPX の全長 cDNA を制限酵素 *Sma*I/*Hin*dIII で切り出し、T4 DNA polymerase で平滑末端化した。この DNA 断片を Ti-プラスミド pBI121-Hm の *Sma*I 部位に連結した。これにより cDNA は cauliflower mosaic virus 35S プロモーターにより発現させられる。この Ti-プラスミドをエレクトロポレーション法によりアグロバクテリウム（*Agrobacterium tumefaciens*）EHA101 株に導入した。この形質転換アグロバクテリウムを用いたシロイヌナズナの形質転換法は Bechtold et al.（1993）の方法に準じて行った。最初に形質転換を行った植物個体を T0 植物とした。T0 植物から T1 種子を回収し、100 mg/l のカナマイシンを含む GM 培地上で形質転換体の選抜を行った。カナマイシン耐性となった植物個体を明条件下で発芽生育させ、7 日間を経た個体から緑化子葉を 1 枚切り取り、イムノブロットにて pAPX の発現量が高い個体を選抜した。pAPX の過剰発現が認められた個体の残るもう 1 枚の子葉を用いて、免疫電子顕微鏡観察を行った。

免疫電子顕微鏡観察

カボチャ pAPX を過剰発現した形質転換シロイヌナズナを、明所下で発芽生育させ 8 日間を経た個体の緑化子葉を Nishimura et al.（1993）の方法に従い免疫電子顕微鏡観察を行った。試料を固定液（4% paraformaldehyde, 1% glutaraldehyde, 0.05 M sodium-cacodylate (pH 7.4), 0.06 M sucrose）に浸し、1 時間減圧浸透処理した後に 1 mm 角以下に細切し、新しい固定液でさらに 2 時間処理し固定化した。同じ固定液で洗浄した後、ジメチルホルムアミド濃度勾配系列により-20℃で脱水した。固定化試料は LR-White 樹脂（London Resin Co. Ltd., Basingtoke, Hampshire, UK）に包埋し、紫外線重合装置（Dohan EM）を用いて、-20℃で 24 時間重合させた。ミクロトーム（Reichrt Ultramicrotome）で超薄切片を作製し、ニッケルグリッドにマウントした。切片をブロッキング液（1% BSA in PBS）で 1 時間処理した後、ブロッキング液で 200 倍希釈した pAPX 抗血清と 4℃で一晩反応させた。PBS で洗浄後、

切片をブロッキング液で 20 倍希釈した protein A-金コロイド液（Amersham Pharmacia Biotech）で、室温 30 分間処理した。切片を DW で洗浄し、4%酢酸ウランとクエン酸鉛で染色した。観察は染色後切片を透過型電子顕微鏡（1200EX, JEOL Ltd., Tokyo, Japan）を使用して 80 kV で行った。

その他の方法

プラスミド DNA の調製、制限酵素による DNA の切断、DNA のアガロースゲル電気泳動等の基本操作は Sambrook（2001）の方法に準じた。

結果

ペルオキシソーム膜タンパク質の調製

ペルオキシソーム膜タンパク質の輸送メカニズムを解析するため、最初にカボチャグリオキシソーム膜に局在するタンパク質の同定を試みた。発芽 5 日目のカボチャ黄化子葉よりグリオキシソームを単離し、まず低張液を加えグリオキシソームを膨圧により破裂させた。以降、順に高塩溶液、アルカリ溶液で処理し、アルカリ溶液でもほとんど可溶化しなかったタンパク質をペルオキシソーム膜貫通型タンパク質の候補とした。これらの候補膜タンパク質の内、31 kDa タンパク質（Figure 16; arrowhead）を以降の解析に用いた。

31 kDa タンパク質の cDNA クローニング

31 kDa タンパク質の cDNA を得るために、SDS-PAGE により分離した本タンパク質を抗原として作製した抗体と、プラスミドベクターpTTQ18 に構築されたカボチャ黄化子葉の cDNA ライブラリー(Mori et al., 1991)を用いてイムノスクリーニングを行った。ここで得られた最も長い cDNA 断片を鋳型に用いたコロニーハイブリダイゼーションにより、同じライブラリーに対してスクリーニングを行った。最も長い cDNA を含んでいたクローンを選び、塩基配列を特定した。得られた cDNA は全長 1,133bp でその中に 858bp からなるオープンリーディングフレーム（ORF）を含んでいた。また、この ORF の 5'-非翻訳領域にインフレームでつながるストップコドンの存在を確認している。これにコードされるタンパク質の推定アミノ酸配列は 286 アミノ酸で構成され、推定分子量は 31,527 Da であった（Figure 17A)。一方で、グリオキシソームより抽出した 31 kDa タンパク質をトリプシンにより消化し、得られた 2 つのペプチド断片からその内部配列を決定した。31 kDa タンパク質由来の 2 つのペプチド断片のアミノ酸配列は、スクリーニングの結果得られた

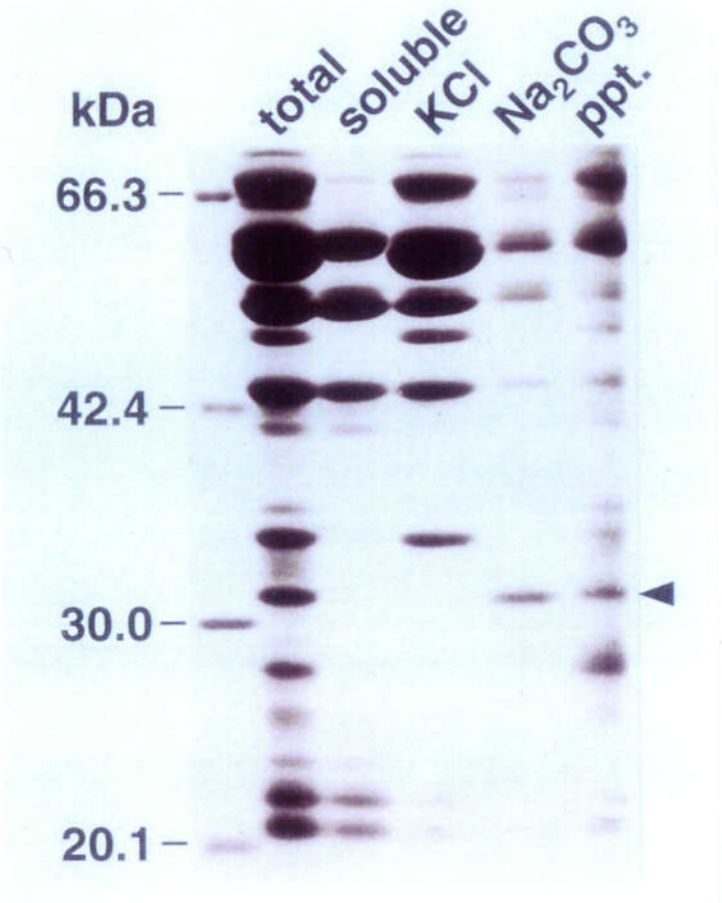

Figure 16. SDS-PAGE of Major Membrane Proteins of Glyoxysomes Isolated from Germinating Pumpkin Cotyledons.
Total, water-soluble (soluble), salt-soluble (KCl), alkali-soluble (Na_2CO_3) and alkali-insoluble (ppt.) fractions of glyoxysomal membrane proteins were prepared as described in "Materials and Methods" and were subjected to SDS-PAGE. Arrowhead indicates 31-kDa protein localized on glyoxysomal membranes. Markers are shown on the left with molecular masses in kDa.

A

```
MALPVVDTEYLKEIEKARRDLRALIANRNC  30
APIMLRLAWHDAGTYDVSTKTGGPNGSIRN  60
QEEYSHGSNNGLKKAIDFCEEVKSKHPKIT  90
YADLYQLAGVVAVEVTGGPTIDFVSGRKDS 120
RISPREGRLPDAKKGAPHLRDIFYRMGLSD 150
KDIVALSGGHTLGRAHPERSGFDGPWTEDP 180
LKFDNSYFVELLKGESEGLLKLPTDKALLE 210
DPEFRPYVELYAKDEDAFFKDYAESHKKLS 240
ELGFTPGSARAIANDSTVLAQGAVGVAVAA 270
AVVILSYFYEIRKNLK                286
```

B

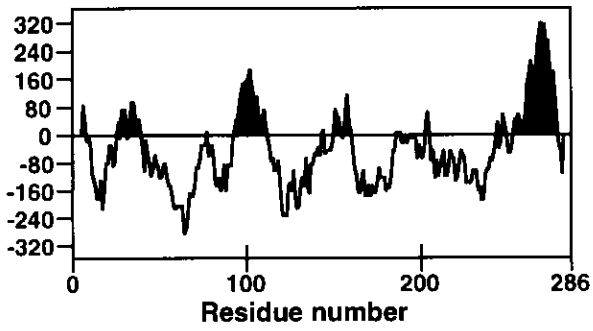

Figure 17. Amino Acid Sequence Encoded by a cDNA for Pumpkin pAPX.
(A) Deduced amino acid sequence of pumpkin pAPX cDNA
(B) Hydropathy profile of pAPX.
Internal amino acid sequences of pAPX that were determined directly are underlined.
Hydropathy indexes were calculated according to Kyte and Doolittle (1982).

cDNA に含まれる ORF の推定アミノ酸配列の一部と一致した（Figure 17A, underline)。故に、この cDNA クローンは 31 kDa タンパク質の cDNA を含んでいると結論した。

31 kDa タンパク質はペルオキシソーム膜局在のアスコルビン酸ペルオキシダーゼである

31 kDa タンパク質の推定アミノ酸配列は既知の植物のアスコルビン酸ペルオキシダーゼ（APX）と高い相同性を示した。別の研究から、無傷ペルオキシソームを精製する過程で APX 活性が濃縮されること、またその活性はマトリクスではなくペルオキシソーム膜にあることが報告されていたため(Yamaguchi et al., 1995a)、本タンパク質がカボチャペルオキシソーム膜局在のアスコルビン酸ペルオキシダーゼ（pAPX）であると結論した。pAPX のアミノ酸配列は既に報告されているカボチャ由来のチラコイド膜局在型 APX（tAPX）(Yamaguchi et al., 1996)、ストロマ局在型 APX（sAPX）(Mano et al., 1997)、シロイヌナズナ由来の細胞質局在型 APX（cAPX）(Kubo et al., 1992)とそれぞれ、30%、34%、53%、の相同性を示した（Figure 18)。pAPX は cAPX と高い相同性を示したが、両者における明白な違いは、pAPX の C 末端には cAPX にはみられない 39 アミノ酸からなる延長配列が存在することであった。pAPX の疎水性プロットを行ったところ(Kyte and Doolittle, 1982)、この C 末端配列は非常に疎水性が高く膜貫通領域であることが予測された（Figure 17B)。以上の結果から、pAPX は C 末端部分をペルオキシソーム膜に埋め込んだ状態で存在していることが示唆された。

発芽後成長における pAPX の量的変動

pAPX の発芽段階における量的な変動を明らかにするため、イムノブロットによる解析を行った。APX の cDNA クローニングに用いた抗体は、それほど力価が高くなく、し

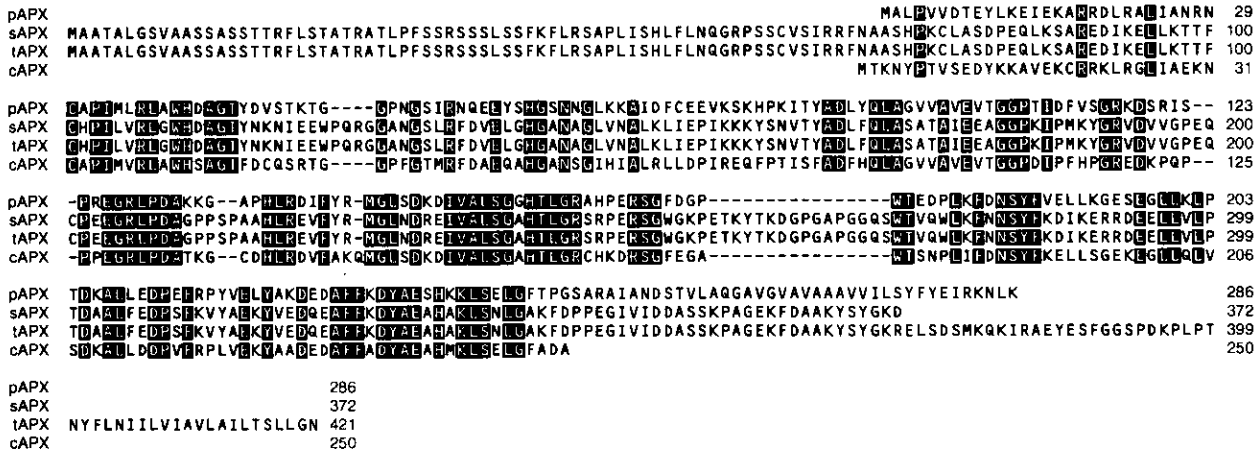

Figure 18. Alignment among APX Isoforms in Higher Plant.
Deduced amino acid sequence of the pumpkin pAPX was compared with APX isozymes identified from stroma (sAPX) and thylakoid-bound (tAPX) ascorbate peroxidases of pumpkin, and cytosolic ascorbate peroxidase (cAPX) of *Arabidopsis*. Identical amino acid residues among all APX are highlighted. Amino acid sequence of pAPX is 53% identical with that of Arabidopsis cAPX.

かも他の APX アイソザイムにも反応性を示すことから、以降の解析には、大腸菌発現系をにより発現精製した pAPX の部分長ペプチドを抗原として作製した pAPX 特異的抗体を用いた。カボチャ種子を暗所にて発芽させた場合、pAPX の量は発芽 5 日目に最大に達し、その後緩やかに減少した（Figure 19, pAPX)。しかしながら、発芽 5 日目の黄化子葉を明条件下に移したところ、pAPX の量は急速に減少した。カボチャ子葉内のイソクエン酸リアーゼやクエン酸合成酵素などのグリオキシソーム酵素の量はグリオキシソームから緑葉ペルオキシソームへの転換の際、同様の変動パターンを示す(Kato et al., 1995; Mano et al., 1996)。対照的に緑葉ペルオキシソーム酵素のヒドロキシピルビン酸還元酵素は暗条件下ではその発現は顕著でないが、明条件下に移すと強く発現が誘導されることが知られている(Hayashi et al., 1996b)。これらの結果は、カボチャ pAPX の量が他のグリオキシソーム酵素の変動と同様に制御されていることを示唆している。

子葉の老化過程における pAPX の量的変動

実生の発達がさらに進み本葉が展開することには、緑化子葉はだんだんと老化してやがて枯死する。この老化の過程において、ペルオキシソームは再びグリオキシソーム酵素を内包しはじめ、緑化過程とは逆の緑葉ペルオキシソームからグリオキシソームへの転換を行う(De Bellis et al., 1991)。この老化段階における pAPX の変動を、植物個体より切り離した緑化子葉を暗所に静置し老化を誘導する *in vitro* senescence の系にて解析した(Gut and Matile, 1988)。発芽 20 日目のカボチャ緑化子葉を切り取り暗所に静置したところ、pAPX はわずかに存在しているが増減はほとんどなく一定量が存在し続けた（Figure 20, pAPX)。同様の過程において緑葉ペルオキシソーム酵素のヒドロキシピルビン酸還元酵素はわずかに減少し、対照的にグリオキシソーム酵素のイソクエン酸リアーゼは著しく増加した。

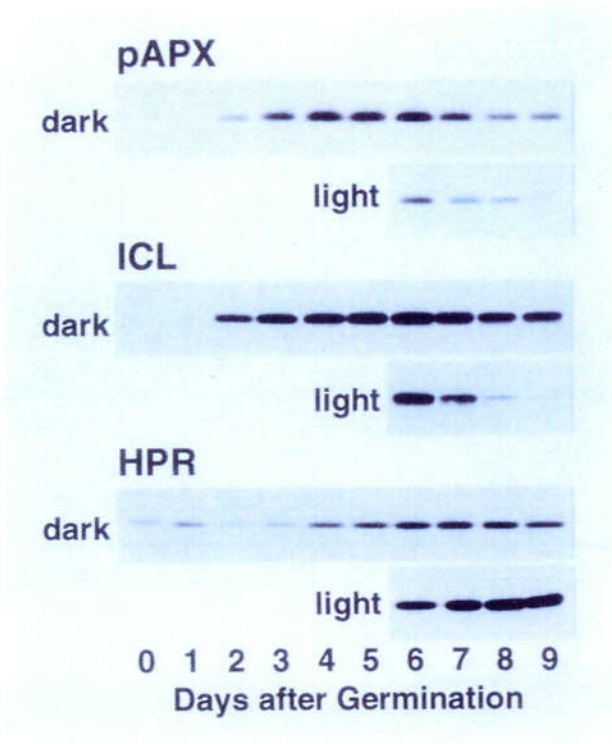

Figure 19. Developmental Changes in the Levels of Peroxisomal Proteins in Pumpkin Cotyledons during the Peroxisomal Transition from Glyoxysomes to Leaf Peroxisomes. Pumpkin seeds were grown in continuous darkness for 9 days or in darkness for 5 days then under continuous illumination for 4 days. Immunoblot analysis of homogenates prepared from cotyledons at various stages was carried out using antibodies against pAPX, isocitrate lyase (ICL), and hydroxypyruvate reductase (HPR). Equal amounts of total protein, 10 μg for pAPX, ICL and HPR, were loaded in each lane. Number of days after germination is shown at the bottom of each lane.

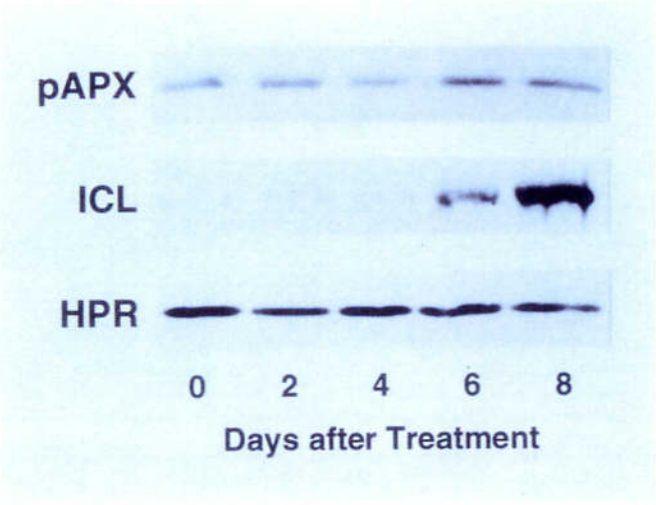

Figure 20. Developmental Changes in the Levels of Peroxisomal Proteins in Pumpkin Cotyledons after Induction of *In Vitro* Senescence.
Green cotyledons of pumpkin were harvested and were incubated in continuous darkness for 0, 2, 4, 6 and 8 days. Immunoblot analysis of homogenates prepared from cotyledons at various stages was carried out using antibodies against pAPX, isocitrate lyase (ICL), and hydroxypyruvate reductase (HPR). Equal amounts of total protein, 10 μg for pAPX, ICL and HPR, were loaded in each lane. Number of days after treatment is shown at the bottom of each lane.

pAPX の細胞内局在

pAPX の細胞内局在を解析するため、発芽 5 日目のカボチャ黄化子葉をショ糖密度勾配遠心法により細胞分画し、pAPX とともに各オルガネラの標識酵素の分布をそれぞれの特異的抗体を用いたイムノブロットにより検出した（Figure 21A)。標識酵素の分布から、グリオキシソームははっきりと細胞質画分および小胞体画分と分離されている。ショ糖密度勾配の上部画分（2 番目の画分）に検出されたカタラーゼ、イソクエン酸リアーゼ、BiP（binding protein）はサンプル調製時にダメージを与えてしまったオルガネラより流出したものである。pAPX のピークはイムノブロットにより検出されたバンドが示すように、密度勾配の底面に近くショ糖密度 1.25g/cm^3 の 24 番目の画分であった（Figure 21A, arrow)。このピークはグリオキシソームの標識酵素であるカタラーゼやイソクエン酸リアーゼのピークをも含むため、グリオキシソームを含む画分であることが示された。このピーク以外に、pAPX はグリオキシソーム画分とは異なる密度勾配の上部に近い 4 番目の画分にも検出された（Figure 21A, arrowhead)。小胞体の標識酵素である BiP の一部は可溶化して細胞質画分に検出されていること、さらにサンプル調製時にダメージを受けたオルガネラから放出されたカタラーゼやイソクエン酸リアーゼは 2 番目の画分のみに検出されたことから、4～6 番目の画分が小胞体画分であることが示唆される。よって、4 番目の画分に検出された pAPX のピークは小胞体と共存していることが明らかとなった。

グリオキシソームの生合成は初期発芽段階の方がより盛んである。そこで初期発芽段階における小胞体及びグリオキシソーム画分に存在する pAPX の分布を比較するため、発芽 3 日目のカボチャ黄化子葉を同様に細胞分画し解析した（Figure 21B)。その結果、種子の発芽初期において細胞内全ての pAPX の内、小胞体画分に存在する pAPX の割合が、発芽後期（発芽 5 日目）のそれに比べて多いことが明らかとなった。この結果は、発芽に際して pAPX が小胞体を経由してグリオキシソームへと輸送される可能性を示唆している。

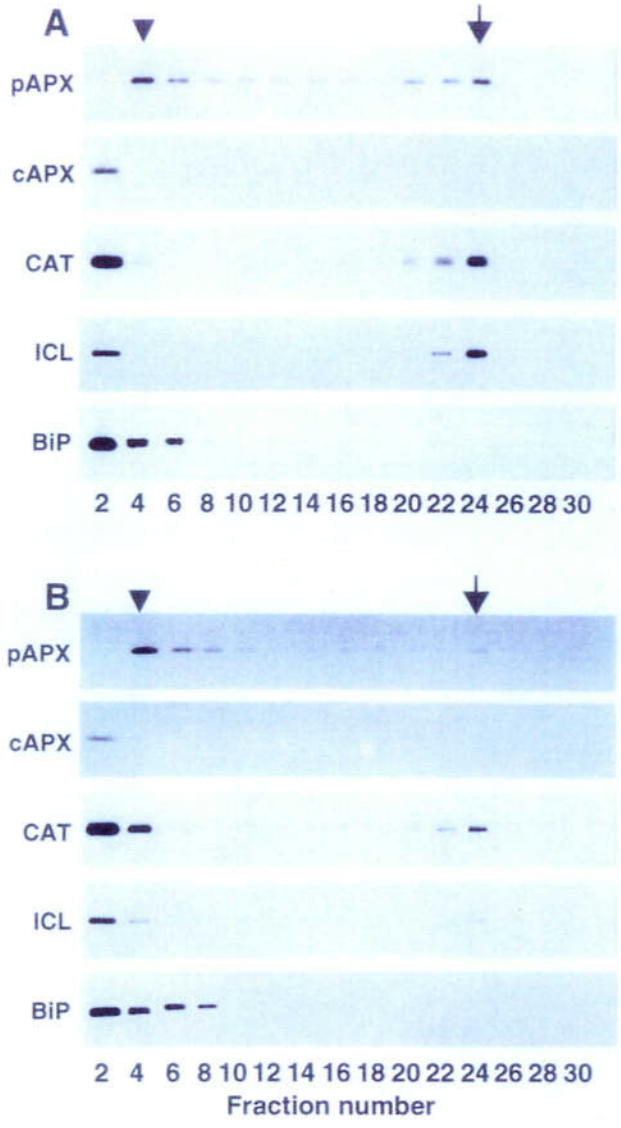

Figure 21. Subcellular Distribution of pAPX in Pumpkin Etiolated Cotyledons. Subcellular fractionation of etiolated pumpkin cotyledons was performed by 30-60 % sucrose density gradient centrifugation.
(A) Homogenate from 5-day-old pumpkin cotyledons
(B) Homogenate from 3-day-old pumpkin cotyledons
Fractions were numbered from the top of the gradient. pAPX, catalase (CAT) and isocitrate lyase (ICL) in each fraction were detected by immunoblot analyses using antibody raised against pAPX, cAPX, CAT, ICL and BiP. Arrows indicate the peak of the peroxisome. Arrowheads indicate the peak of the ER.

pAPX は粗面小胞体には局在しない

小胞体画分に存在している pAPX が真に小胞体に局在しているのかを明らかにするため、カボチャ黄化子葉よりマイクロソーム膜系を調製し、マグネシウム存在・非存在下においてショ糖密度勾配遠心法により分画した。そして、各画分をイムノブロット法により解析した（Figure 22)。マグネシウム非存在下（-Mg^{2+}; +2 mM EDTA）において分画した場合、pAPX のほとんどがショ糖密度 35%（w/w）の画分に検出された。同一の画分内における BiP の分布を調べたところ、BiP は pAPX とおおよそ同一のショ糖密度の画分に検出された。マグネシウム存在下（+Mg^{2+}; 5 mM $MgCl_2$）で同様のショ糖密度勾配で分画したところ、pAPX のピークはより低いショ糖密度の画分（29%）へ移動した。対照的に BiP のピークはより高いショ糖密度の画分（>42%）へ移動した。マグネシウム依存的な密度の変化は粗面小胞体の特徴の一つである。粗面小胞体上に存在するリボゾームはマグネシウム依存的に小胞体上に結合している。そのためマグネシウム存在下では粗面小胞体として密度の高い画分に分画されるが、マグネシウム非存在下ではリボゾームが解離し結果として滑面小胞体と同等の密度の低い画分に分画される。pAPX はマグネシウム存在・非存在下において BiP との挙動を共にしなかった。よって、pAPX は粗面小胞体以外の何らかの膜系に局在することが示唆された。

pAPX はペルオキシソーム膜と未知の膜構造物上に局在する

pAPX がどのような膜構造物に局在しているかを、免疫電子顕微鏡観察を用いた形態学的観察から解析することを考えた。シロイヌナズナのホモジェネートに対してカボチャ pAPX 抗体を用いてイムノブロットを行った場合、シロイヌナズナ pAPX に対してカボチャ pAPX 抗体は反応しなかった（data not shown)。またシロイヌナズナおよびカボチャの子葉を用いて免疫電子顕微鏡観察を行った場合も、タンパク質の局在を示す金粒子は特異

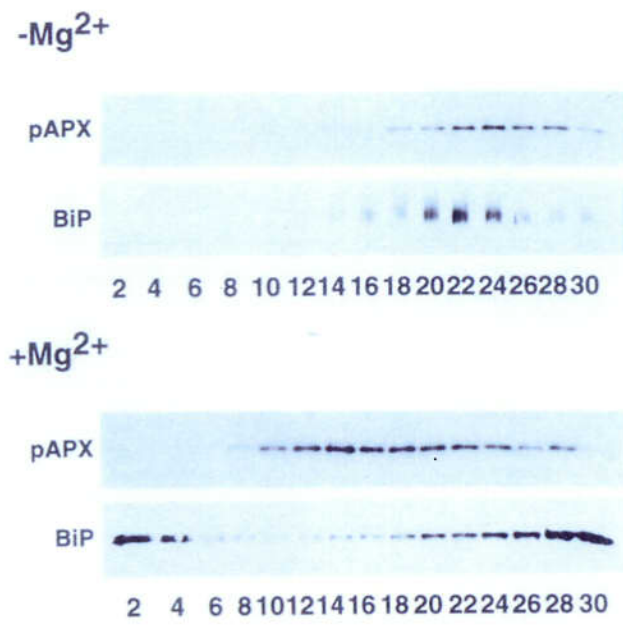

Figure 22. Mg^{2+}-Induced Shift Analysis of Microsomal Fraction from Pumpkin Etiolated Cotyledons.
Microsomal membrane fractions were prepared under 2 mM EDTA ($-Mg^{2+}$) or 5 mM $MgCl_2$ ($+Mg^{2+}$) conditions. Fractions were numbered from the top of the gradient. Each fraction of the gradient was subjected to SDS-PAGE followed by immunoblotting using antibodies against pAPX and BiP.

的な局在を示さなかった（data not shown)。故に、免疫電子顕微鏡観察を行うためにカボチャ pAPX を過剰発現させた形質転換シロイヌナズナを作成し、これを用いた。形質転換シロイヌナズナを連続明条件下で発芽生育させ、8 日間経たものの子葉から超薄切片を調製し、カボチャ pAPX 抗体を金粒子に結合させたものを用いて免疫染色を行った（Figure 23)。形質転換シロイヌナズナの緑化子葉において発現したカボチャ pAPX はペルオキシソーム膜上に局在するとともに（Figure 23A)、未知の膜構造物上にも検出された（Figure 23B)。しかし、粗面小胞体やミトコンドリア、葉緑体などの他のオルガネラには検出されなかった。この免疫電子顕微鏡観察の結果は、Figure 21 and 22 で示した結果を支持し、pAPX がペルオキシソーム膜のみならず、粗面小胞体以外の未知の膜構造物上に局在していることを示唆している。

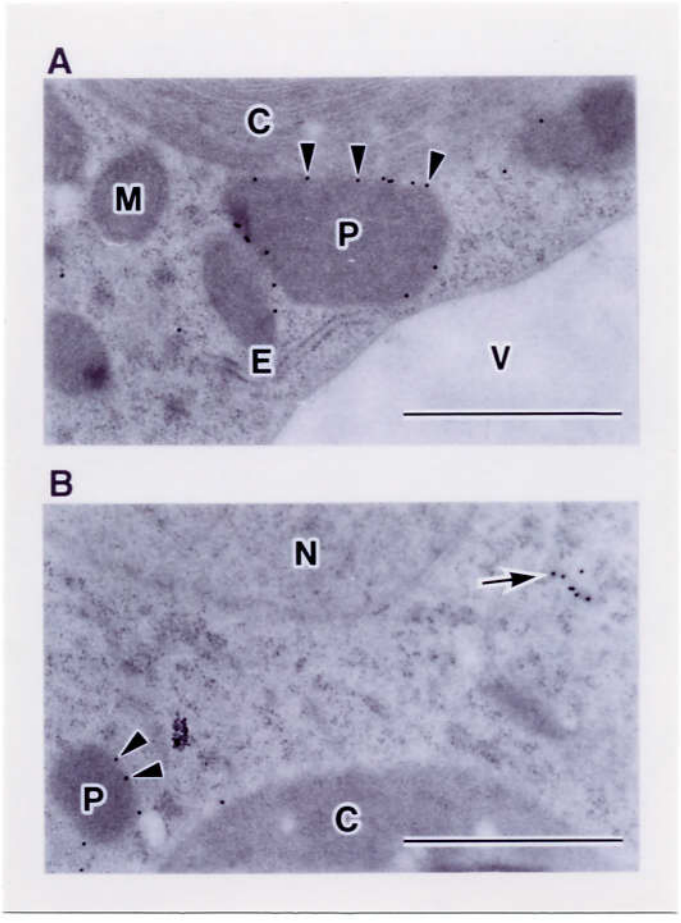

Figure 23. Immunocytochemical Localization of pAPX in Transgenic *Arabidopsis* That Expressed Pumpkin pAPX.
Ultra-thin sections of cotyledons of *Arabidopsis* were immunogold labeled with an antibody against pAPX.
(A) and **(B)** Arrowheads indicate gold particles on peroxisomal membranes.
(B) Arrows indicate gold particles localized on the unknown membranous structure.
C, chloroplast; E, rough ER; M, mitochondrion; N, nucleus; P, peroxisome; V, vacuole.
Bars represent 1 μm.

考察

ペルオキシソーム膜タンパク質

植物ペルオキシソームは一重膜によって隔離された内部（マトリクス）で脂肪酸の分解や光呼吸などの重要な代謝を行っている。ペルオキシソーム膜はマトリクスを細胞質と隔てると同時に各種膜タンパク質をもっており、これらを介して特定の物質交換を行っている。植物ペルオキシソームのこれまでの研究は、主にマトリクス酵素の解析にその焦点がおかれ、その膜タンパク質はあまり注目されておらず解析は進んでいなかった。よって、ペルオキシソーム膜タンパク質の同定とその局在化機構を明らかにすることは、マトリクスタンパク質を用いたペルオキシソーム研究とは異なった視点から、ペルオキシソーム機能分化を理解できるものと期待される。

ペルオキシソームにおける H_2O_2 消去機構

発芽段階の脂肪性種子において、グリオキシソームは貯蔵脂肪を分解しショ糖を産生する過程で重要な役割を担っている。このような植物の成長段階において、イソクエン酸リアーゼやリンゴ酸合成酵素のようなグリオキシソーム酵素の発現量は上昇し、グリオキシソーム内に蓄積する。そしてこれらの酵素群の働きにより、子葉細胞内にリピッドボディの形で細胞内を埋め尽くしていた貯蔵脂肪はショ糖へと変換され、極めて短期間のうちにリピッドボディは消失する。その一方で、このようなグリオキシソーム内での急速な脂質代謝過程において、細胞毒性のある H_2O_2 が大量に発生している。また、緑化以降の植物細胞内に観察される緑葉ペルオキシソームにおいても、その主な代謝系である光呼吸系が機能する過程で同様に H_2O_2 が発生している。このようにペルオキシソームがその機能を果たす過程では、細胞毒性をもつ H_2O_2 が発生する宿命にあり、そのためにペルオキ

シソームはこれを消去する機能をも兼ね備えている。H_2O_2 消去機構の中心的役割を果たすのが、全てのペルオキシソームに共通のマトリクス酵素として存在するカタラーゼである。カタラーゼは特に発芽段階の子葉細胞中に多量に検出されることからも、貯蔵脂肪の転流過程で発生する H_2O_2 を積極的に消去していると考えられている。しかしながら、このカタラーゼにも弱点がある。それはカタラーゼの H_2O_2 に対する K_m 値が高いため（K_m= 1 M）に低濃度の H_2O_2 を消去することに適さないことである(Huang et al., 1983)。

APX も細胞内で H_2O_2 を消去することに関わる抗酸化酵素であり、細胞内に局在の異なるアイソザイムとして複数存在している(Shigeoka et al., 1998)。APX は抗酸化剤として細胞内に豊富に存在しているアスコルビン酸を用いて、H_2O_2 を還元しその結果としてモノデヒドロアスコルビン酸と水を生じる。その他の APX の酵素学的特徴はアスコルビン酸特異的に反応し、還元型グルタチオン、チトクロム *c*、NAD(P)H および脂肪酸とは反応しないこと、アスコルビン酸非存在下で非常に不安定であり、特に葉緑体型（sAPX および tAPX）の失活の半減期はアスコルビン酸非存在下において数十秒であることが知られている。更に重要な知見は、APX の K_m 値はカタラーゼよりも低く（K_m= 30～80 μM）(Chen and Asada, 1989; Koshiba, 1993)、低濃度の H_2O_2 の消去に向いている点である。本研究において、pAPX は疎水性の高い C 末端をペルオキシソーム膜に貫通させた状態で存在していることが明らかになった（Figure 17)。また、最近の無傷ペルオキシソームを用いた研究から pAPX の触媒部位が細胞質側に露出していることが示されている(Yamaguchi et al., 1995a)。以上の事実から、ペルオキシソーム内で発生した H_2O_2 のほとんどはカタラーゼにより消去されるが、これを逃れた H_2O_2 がペルオキシソーム膜を透過して漏れ出た場合に、pAPX が機能しペルオキシソーム膜上で H_2O_2 を消去していると考えられる。

子葉の老化段階おける pAPX の役割

pAPX は光呼吸をその主な機能とする緑葉ペルオキシソームにおいても、低いレベルで存在し続ける（Figure 19)。また、さらに光合成器官としての葉がその役割を終え老化する過程においても、pAPX は低いレベルで存在していた（Figure 20)。この枯死する過程にある組織で pAPX が存在している意味はなんであろうか？老化段階にある子葉組織では、緑葉ペルオキシソームからグリオキシソームへの逆機能転換が起きており、ペルオキシソーム内には再び脂質代謝に関わる酵素群が蓄積されている。これらの酵素群は老化している器官をソースとして利用し、他の栄養器官（シンク）に無駄なく転流するために機能していると言われている。よって、老化器官における pAPX の機能は、ソース器官で転流に関わる酵素群を H_2O_2 から保護しているものと考えられる。

ペルオキシソーム膜貫通型タンパク質輸送シグナル

ペルオキシソームは自ら DNA をもたないため、全ての遺伝情報を核 DNA に依存し制御されている。これまでの研究からペルオキシソームタンパク質は細胞質の遊離リボソームで翻訳後、直接ペルオキシソームへと運ばれる。本論文第 1 章に報告したように、多くのマトリクスタンパク質はペルオキシソーム輸送シグナルとして PTS1 もしくは PTS2 をもっており、これを認識するレセプターによりペルオキシソームへと輸送される。しかし、pAPX を含めたペルオキシソーム膜貫通型タンパク質にはそのような明らかな輸送シグナルはもっておらず、マトリクスタンパク質輸送系とは全く異なる経路で輸送されている可能性が高い。ペルオキシソーム膜貫通型タンパク質の輸送シグナル mPTS についても積極的な研究がなされているが、これまでのところ必要十分条件を満たすモチーフ構造は特定されていない。ところが極めて最近、タバコ培養細胞 BY2 に綿花由来の pAPX を発現させる系を用いて、pAPX の輸送シグナルを特定する研究が行われた(Mullen and Trelease, 2000)。その結果、綿花 pAPX の C 末端側に存在する塩基性アミノ酸（リジンおよびアル

ギニン）で構成されるクラスター（RKRMK）が少なくとも綿花 pAPX の輸送に必要であることが示された。このクラスターは綿花 pAPX がペルオキシソーム膜に局在した際マトリクス側に位置しているが、この配列だけでは充分でなく、そのクラスター側から見て細胞質側に膜貫通領域が存在することも重要であるらしい。興味深いことに、綿花 pAPX で特定された塩基性アミノ酸クラスターは、これまで報告されているペルオキシソーム膜貫通型タンパク質のいずれもマトリクス側に共通に存在していることから、mPTS として機能している可能性が高い。本研究において同定されたカボチャ pAPX にも C 末端に RKNLK というアミノ酸配列が存在しており、かつその N 末端方向には膜貫通領域と推定される領域がある（Figure 17）。よって、この配列がカボチャ pAPX においても輸送に重要である可能性が高い。

ペルオキシソーム膜貫通型タンパク質の局在化機構

本研究から、カボチャ pAPX が粗面小胞体には局在しないが何らかの膜系に局在しうることが明らかとなった（Figure 22）。さらに免疫電子顕微鏡観察による結果もこれを支持した（Figure 23B）。カボチャ pAPX が局在するこの膜構造物が何であるかは、今のところ不明であるが、一つの可能性として滑面小胞体もしくは特殊化した小胞体であると推測している。Mullen（1999）の行った間接蛍光抗体法による解析から、綿花 pAPX はタバコ培養細胞 BY2 内で、網目状または環状のネットワークを形成しているが、小胞体の標識タンパク質の BiP、calreticulin、calnexin などとは局在を共にしないことが示された。彼らは綿花 pAPX が局在したこの構造物を、小胞体のサブドメインであると報告し pER（peroxisomal ER）と名付けている。Figure 23B で観察された未知の膜構造物は、その pER と同一の構造物なのかもしれない。そして、このような膜構造物を介してペルオキシソームへと輸送されているのかもしれない。同様に小胞体を介した輸送経路をたどるとされる

膜貫通型タンパク質は他にも報告されている(Baerends et al., 1996; Elgersma et al., 1997)。ペルオキシソームの膜系がペルオキシソームの分裂や肥大化の際にどのように供給形成されるのか、未だ答えは得られていないが、ペルオキシソーム膜貫通型タンパク質の輸送経路が解明されることにより、膜系の由来や分泌系小胞輸送との関連が明らかになると考えられる。

大変興味深いことに、前述した mPTS をもつとされているペルオキシソーム膜貫通型タンパク質の内、いくつかはマトリクスタンパク質と同様に細胞質で翻訳された後直接ペルオキシソーム膜へと運ばれるが、あるものは翻訳後まず特殊化した小胞体へ輸送されそれから、ペルオキシソームへと運ばれることが報告されている。同じ膜貫通型タンパク質でありながらどうして輸送経路が異なるのか？さらにその選別にはどのような機構が存在するのか？が、今後の研究課題となっている。

総合討論

本研究論文では、高等植物におけるペルオキシソームへのマトリクスタンパク質及び膜タンパク質の輸送機構について実験、解析を行った。その結果、マトリクスタンパク質と膜タンパク質の輸送機構は大きく異なることが示された。これらの結果から、ペルオキシソームの生合成過程と今後の展望について考察する。

ペルオキシソームの誘導

これまでの研究から脂肪性種子を暗所で発芽させた場合、ペルオキシソーム内にはグリオキシソーム酵素が著しく増加し、さらに生長が進み個体が光を受けるようになるとグリオキシソーム酵素は分解され、今度は緑葉ペルオキシソーム酵素が蓄積する。このようなペルオキシソーム酵素の増減には、吸水や光といった外部刺激により誘導制御を受けていることが示唆されている。また、これらの因子以外による調節因子として、遺伝子の発現が糖の存在により制御されていることを示唆する知見がグリオキシル酸サイクル酵素のリンゴ酸合成酵素とイソクエン酸リアーゼについて報告されている。プロモーターの解析から、これらの酵素をコードする遺伝子には発芽と糖の応答に関する 2 つのシス制御配列があり、これらの配列は種間でよく保存されていることが明らかになっている(De Bellis et al., 1997; Graham et al., 1994; Reynolds and Smith, 1995a; Reynolds and Smith, 1995b; Sarah et al., 1996)。このような因子によってペルオキシソーム酵素が誘導される条件では、当然これを輸送する因子群も必要とされるはずであり、今回同定した *At*Pex14p、*At*Pex5p、*At*Pex7p も発現している可能性が高い。しかしながら、これまでのところペルオキシソームを誘導する因子からのシグナルがどのように伝達されてくるのかは明らかでない。

近年、このようなシグナル伝達を行うものの候補の 1 つとして、哺乳類の研究から

発見されたペルオキシソーム増殖剤活性化受容体（PPAR: peroxisome proliferator-activated receptor）が注目されている(Issemann and Green, 1990)。動物細胞においては、脂肪酸分解系は細胞内の脂肪量のホメオスタシスに適応して機能すること、細胞内の脂肪の蓄積が主な要因となりペルオキシソームの増殖が誘導されることが確認されている。PPAR は医学分野において抗高脂血剤などのペルオキシソーム増殖剤のレセプターとしてクローニングされた因子であり、増殖剤の添加によりペルオキシンの発現を誘導することが知られている。さらにそれらに対する生理的リガンドとして脂肪酸の一種であるアラキドン酸 J_2(Forman et al., 1995)やロイコトリエン B_4(Devchand et al., 1996)も同定されている。PPAR の研究は肥満や糖尿病との関連性も高いことから、この分野の発展は著しい。このように PPAR は細胞内の脂肪酸量をモニターして下流にペルオキシソーム生合成のシグナルを伝達していると考えられている。

高等植物にもペルオキシソーム生合成を制御する PPAR のような因子が存在し、下流で *At*Pex14p、*At*Pex5p、*At*Pex7p を含めたペルオキシンの発現制御をしているのであろうか？シロイヌナズナのゲノムデータベースを検索したが、これに該当する遺伝子の存在は今のところ確認できていない。しかしながら、工業的に重要な中鎖脂肪酸を植物に合成させる試みの過程で、中鎖脂肪酸合成系に関与する酵素である Lauroyl-acyl carrier protein thioesterase を過剰発現させた植物個体では、同時に脂肪酸 β 酸化系酵素の acyl-CoA oxidase の発現が誘導されることが報告されている(Eccoleston and Ohlrogge, 1998)。さらにこの知見によれば、Lauroyl-acyl carrier protein thioesterase の過剰発現が確認されているにもかかわらず、脂肪酸組成に大きな変化が見られなかった。このことは植物細胞内においても、脂肪酸量を感知し適宜脂肪酸 β 酸化系を用いて脂肪酸量を調節する機構が存在することを示唆している。今後、このようなペルオキシソームの生合成を調節する機構の解明のために、脂肪酸代謝機能を欠損した *ped* 変異体を用いたマイクロアレイによる解析を行うこと

で、何らかの調節因子群が同定されることが期待できる。

ペルオキシソームの形成における由来

ペルオキシソームが細胞内でどのように形成され、維持されるのか長い間議論の対象となっていた。1970 年代に提唱された一般的なペルオキシソームの生合成モデルは、粗面小胞体の特殊化した領域からの出芽（budding）によってペルオキシソームが形成されるというものであった。この小胞体出芽モデル（ER-vesiculation model）の前提は、ペルオキシソームのマトリクス及び膜タンパク質の翻訳が小胞体で行われているというものである。小胞体中で合成されたペルオキシソームタンパク質は、翻訳後膨張した滑面小胞体膜中に集まり、そこから出芽し成熟したペルオキシソームになると考えられていた。しかしながら、1980 年代に入り様々な研究結果から、ペルオキシソームタンパク質は小胞体上で合成されるのではなく、細胞質中の遊離ポリソームで合成されることが示されると、ペルオキシソームと小胞体の直接的な因果関係はなくなり、小胞体出芽モデルは賛同を得られなくなっていった。そこで次に登場したモデルは、実験的な観察からペルオキシソームが肥大化と分裂するというモデル（growth and division model）である。このモデルはペルオキシソームがミトコンドリアや葉緑体と同様に、ペルオキシソームタンパク質の翻訳後の輸送に伴い、その大きさを肥大化させ、最終的に成熟化したペルオキシソームの分裂により増殖するというものである(Lazarow and Fujiki, 1985)。このモデルは、PTS1 型および PTS2 型タンパク質に代表されるペルオキシソームのマトリクスタンパク質が細胞質での翻訳以後にペルオキシソーム内へと輸送されることが証明されることによって、広く一般に受け入れられた。

ところがごく最近の研究から、ペルオキシソーム膜貫通型タンパク質の合成及び局在化の研究から肥大化と分裂モデルを一部改変し、再びペルオキシソームの生合成に小胞

体が関与するという説が浮上しつつある。最初に小胞体を経てペルオキシソームへと輸送されると報告されたのはペルオキシソーム膜貫通型タンパク質の *Sc*Pex15p である。*Sc*Pex15p の過剰発現は小胞体膜の異常増殖を誘導する。また、*Sc*Pex15p の 384 アミノ酸の内、C 末端から 55 アミノ酸を除去すると、*Sc*Pex15p は小胞体へ運ばれ、12 アミノ酸を残しておくとペルオキシソームへと輸送される(Elgersma et al., 1997; Subramani, 1996)。この報告は後に、*Sc*Pex15p の小胞体への局在は過剰発現による影響であるとの反対論文も出されたが(Hettema et al., 2000)、*Sc*Pex15p 以外にも小胞体を経由して輸送されるという可能性をもったペルオキシソーム膜タンパク質は続々と報告されている(Baerends et al., 1996; Bodnar and Rachubinski, 1991; Mullen et al., 1999; Titorenko et al., 1997; Titorenko and Rachubinski, 1998)。本論文第 2 章に示したように、ペルオキシソーム膜貫通型タンパク質の pAPX も小胞体またはこれの準ずる膜構造物を経由して輸送されると考えている。残念なことに、これらの膜貫通型タンパク質が小胞体を経由して輸送されるという決定的な証明は未だなされていない。しかし、膜タンパク質が膜構造物を介して輸送されるという可能性は、新規の小胞輸送系の存在とペルオキシソームというオルガネラの起源がどこに由来するものなのかを考察する上で大変興味深い。

シロイヌナズナのペルオキシンと他生物種のペルオキシン

現在までに全生物種において同定されているペルオキシンは 23 にものぼる。これらのペルオキシンは、少なくともこの因子の欠損によりペルオキシソーム形成が阻害されることが証明されている。しかしながら、これまでに報告されている 23 個のペルオキシンが全ての生物種に共通に保存されているわけではないようである（Table 1)。*Yl*Pex9p、*Sc*Pex15p、*Yl*Pex20p、*Sc*Pex21p、*Yl*Pex23p については、1 生物種のみで同定されているペルオキシンであり、これまでのところ他の生物種では見つかっていない。ゲノムプロジェ

Table 1. Registered Peroxins from Various Species in NCBI Data Base

	PEX1	PEX2	PEX3	PEX4	PEX5	PEX6	PEX7	PEX8	PEX9	PEX10	PEX11	PEX12
A. thaliana	○	○	○	○	○	○	○			○	○	○
H. sapiens	○	○	○		○	○	○			○	○	○
S. cerevisiae	○	○	○	○	○	○	○	○		○	○	○
P. pastoris	○	○	○	○	○	○	○	○		○		○
Y. lipolytica	○	○				○			○	○	○	
C. elegans	○				○	○						
X. laevis			○		○	○						○
D. melanogaster					○							○

	PEX13	PEX14	PEX15	PEX16	PEX17	PEX18	PEX19	PEX20	PEX21	PEX22	PEX23
A. thaliana	○	○		○	○		○				
H. sapiens	○	○		○		○	○				
S. cerevisiae	○	○	○		○	○	○		○	○	
P. pastoris	○	○			○		○			○	
Y. lipolytica				○	○		○	○		○	○
C. elegans	○						○				
X. laevis	○										
D. melanogaster											

(Dec. 7. 2001)

クトが終了している酵母 *S. cerevisiae* やシロイヌナズナにおいても、それらに対応するホモログは確認されていない。さらに酵母 *S. cerevisiae* では PTS2 型タンパク質輸送に関わるペルオキシンとして Pex7p、Pex18p、Pex21p の存在が明らかにされているが、線虫 *C. elegans* のゲノムデータベースにはこれらに対応する因子は存在しない。この線虫 *C. elegans* に PTS2 型タンパク質を発現させたところ、細胞質に留まりペルオキシソームへは輸送されないという結果が得られたことから、線虫 *C. elegans* には PTS2 依存的なタンパク質輸送経路自体が失われていることが証明された(Motley et al., 2000)。このような事実から、ペルオキシソームの生合成過程に関わる因子は、それぞれの種によって進化または淘汰され、様々であることが示唆されている。

高等植物においてペルオキシソームの形成維持に関わることが証明されているペルオキシンは、今回の研究結果を含めても Pex14p、Pex5p、Pex7p、Pex16p のみであるが(Hayashi et al., 2000a; Lin et al., 1999)、これら以外に NCBI データベース上には、Pex1p、Pex2p、Pex3p、Pex4p、Pex6p、Pex10p、Pex11p、Pex12p、Pex13p、Pex17p、Pex19p の合計 11 のペルオキシンホモログの存在が予測されている（Table 1）(Mullen et al., 2001)。これらの予測された因子の中には、本研究で同定した *At*Pex14p、*At*Pex5p、*At*Pex7p と同様にペルオキシソームタンパク質輸送に関わるとされる因子も含まれている。これらの新規因子がどのような機能を有しているか、*At*Pex14p、*At*Pex5p、*At*Pex7p とどのように関わりペルオキシソームへのタンパク質輸送を成立させているか、非常に興味深い点である。今後、これらの高等植物のペルオキシンホモログがペルオキシソームの生合成に関わる因子であることを、RNAi 効果もしくは T-DNA タグラインから遺伝子発現が低下したシロイヌナズナを入手しその表現型から証明を行いたい。また酵母や哺乳類から同定されたペルオキシンにはこれらの因子間で特異的なタンパク質間相互作用が報告されているので、シロイヌナズナのペルオキシンにも同様のタンパク質間相互作用が見られるか検討することも有効であると

思われる。一方で、*ped* 変異体をさらに選抜することで、新規なペルオキシンの同定を進めることも重要である。前述したように高等植物のペルオキシソームには他の生物種と比べて特徴的な点が多く観察されているため、高等植物固有のペルオキシンが存在する可能性は高いと考えている。

ペルオキシソームの機能分化

本論文第 1 章において、*At*Pex14p、*At*Pex5p がシロイヌナズナのペルオキシソームへのタンパク質輸送において中心的に機能することを証明し、故にこの 2 つのタンパク質輸送因子が発現している器官ではペルオキシソームへのタンパク質輸送が盛んであることを考察した。このことを鑑みた上で、シロイヌナズナの様々な器官における発現パターンを見直すと、花、鞘、茎生葉、ロゼット葉、根器官および黄化子葉、緑化子葉での発現が高くペルオキシソームへのタンパク質輸送が盛んであることがわかる。高等植物にはグリオキシソーム、緑葉ペルオキシソーム、特殊化していないペルオキシソームの 3 種類が存在するが、花及び根器官でのペルオキシソームは機能が不明な特殊化していないペルオキシソームに分類されており、これまでのところ特異的な代謝経路は見いだされていない。

最近、紫外線の照射や障害などの様々なストレスによって誘導される植物ホルモンであるジャスモン酸の合成系にペルオキシソームの脂肪酸 β 酸化系が深く関与していることが報告された。また、ジャスモン酸合成の中間段階で脂肪酸 β 酸化系に送る基質を生成する酵素 OPR3（12-oxophytodienoate reductase）（OPDA（12-oxophytodienoic acid）から OPC 8: 0（3-oxo-2-(2'-Z-pentenyl)-cyclopentane-1-octanoic acid）を生成する）はそのアミノ酸配列の C 末端に PTS1 をもっており、OPR3 もペルオキシソーム局在の可能性が示唆されている(Stintzi and Browse, 2000)。大変興味深いことに、この OPR3 を欠損したシロイヌナズナ変異体 *delayed dehiscence1* では葯の開裂が野生型の比べて遅れ、結果として雄性不稔の

表現型を示すが、ジャスモン酸の添加により野生型へと回復することが報告されている(Sanders et al., 2000)。この報告とペルオキシソームへの積極的なタンパク質輸送を示す *At*Pex14p、*At*Pex5p の花器官における発現は、花序器官細胞内でのペルオキシソームの果たす役割を考察する上で非常に重要な知見である。

一方、根器官におけるペルオキシソームの役割を示す結果はあまり多くはないが、唯一マメ科植物の根粒細胞のペルオキシソームにウリカーゼ（uricase）が存在していることが知られている(Kaneko and Newcomb, 1987; Kaneko and Newcomb, 1990)。ウリカーゼは尿素合成系の最終酵素の内の一つであり、尿酸+O_2+2H_2O→尿素+H_2O_2+CO_2 の反応を触媒する。このような事実から、根粒のペルオキシソームは窒素固定に関わることが示唆されている。根粒以外の根にもペルオキシソームは存在するが、グリオキシソームや緑葉ペルオキシソームの様な際だった生理的機能は明らかにされていない。

Figure 7 に示すように *At*Pex7p はロゼット葉や茎生葉に特に強い発現が認められた。これはこれらの器官において PTS2 型タンパク質の発現量が多く、その輸送活性が高いことを示している。その一方で光照射以後の子葉では *At*Pex7p の発現はあまり顕著でなく（Figure 6)、PTS2 に依存したタンパク質輸送経路はそれほど機能していないことが示唆された。これまで緑化した光合成器官に存在するペルオキシソームは、すべて緑葉ペルオキシソームと呼び光呼吸系に関わるものとして同一視されてきた。しかし、本研究結果から、子葉の緑葉ペルオキシソームと本葉（ロゼット葉や茎生葉）の緑葉ペルオキシソームでは PTS2 型タンパク質の組成が異なり、従来のように同一の緑葉ペルオキシソームとして分類することができない可能性が示唆された。また、pAPX の様なペルオキシソーム膜タンパク質の同定についても、これまでは黄化もしくは緑化子葉のペルオキシソームについてのみ解析がされており、花や根器官ではもちろん本葉のペルオキシソーム膜タンパク質についても全く手つかずの状態となっている。さらに近年、植物ペルオキシソームの機

能不全が種子貯蔵物質の組成に影響を及ぼしたり(Lin et al., 1999)、花序の形態に異常を生じさせるなど(Richmond and Bleecker, 1999)、これまでに知られているペルオキシソーム機能からは説明のつかない事象が報告されている。これらの事象は高等植物のペルオキシソームに、未知の生理機能が存在することを予感させる。以上のことから、植物の多様な器官におけるペルオキシソームの機能分化とその生理機能を理解する上で、それぞれのペルオキシソームがどのようなタンパク質で構成されているかを明らかにすることは重要な課題である。これを解決する手段として考えられるのが無傷ペルオキシソームを用いたプロテオーム解析である。今後、各器官から無傷ペルオキシソームを調製し、その構成タンパク質を同定することで、より様々に分化した植物ペルオキシソームの実体が明らかにされることを期待している。

今後の展望

本研究論文では *ped2* 変異体を出発点としてペルオキシソームタンパク質輸送に中心的に関わる *At*Pex14p および PTS1、PTS2 レセプターとして機能する *At*Pex5p、*At*Pex7p を同定した。しかしながら、ペルオキシソームへのタンパク質輸送過程において *At*Pex14p だけが全てを行っているとは考えにくく、*At*Pex14p を補助するような複数の因子の存在が予測される。そこでこのような新規因子を同定するための一つの手法として、酵母 two-hybrid system を用いたライブラリースクリーニングが有効であると考えている。*At*Pex14p を囮タンパク質にしてこれと相互作用する因子を網羅的に得るという実験は既に進行中であり、これまでに 2 つのポジティブクローンを得ている。この 2 つの因子の内の 1 つは、シロイヌナズナのゲノムデータベース上の予測からリン酸化酵素である可能性が高い。本論文では特に触れなかったが、酵母 Pex14p はオレイン酸などでペルオキシソーム形成を誘導した場合にリン酸化されるということが報告されている(Komori et al., 1999)。今後、

スクリーニングによって得られた因子をさらに解析することにより、*At*Pex14p のリン酸化がペルオキシソームへのタンパク質輸送においてどのような生理的意義があるのか解明できるものと期待している。

引用文献

Albertini, M., Rehling, P., Erdmann, R., Girzalsky, W., Kiel, J. A., Veenhuis, M., and Kunau, W. H. (1997). Pex14p, a peroxisomal membrane protein binding both receptors of the two PTS-dependent import pathways, Cell 89, 83-92.

Baerends, R. J. S., Rasmussen, S. W., Hilbrands, R. E., van der Heide, M., Faber, K. N., Reuvekamp, P. T. W., Kiel, J. A. K. W., Cregg, J. M., van der Klei, I. J., and Veenhuis, M. (1996). The *Hansenula polymorpha* PER9 gene encodes a peroxisomal membrane protein essential for peroxisome assembly and integrity., J Biol Chem 271, 8887-8894.

Bechtold, N., Ellis, J., and Pelletier, G. (1993). In planta Agrobacterium mediated gene transfer by infiltration of adult *Arabidopsis thaliana* plants., C R Acad Sci Paris, Life sciences 316, 1194-1199.

Beevers, H. (1979). Microbodies in higher plants., Annu Rev Plant Physiol 30, 159-193.

Beevers, H. (1982). Glyoxysomes in higher plants., Ann N Y Acad Sci 386, 243-251.

Bodnar, A. G., and Rachubinski, R. A. (1991). Characterization of the integral membrane polypeptides of rat liver peroxisomes isolated from untreated and clofibrate-treated rats., Biochem Cell Biol 69, 499-508.

Braverman, N., Dodt, G., Gould, S. J., and Valle, D. (1998). An isoform of Pex5p, the human PTS1 receptor, is required for the import of PTS2 proteins into peroxisomes, Hum Mol Genet 7, 1195-1205.

Brickner, D. G., Brickner, J. H., and Olsen, L. J. (1998). Sequence analysis of a cDNA encoding Pex5p, a peroxisomal targeting signal type 1 receptor from *Arabidopsis thaliana*, Plant Physiol 118, 330.

Brocard, C., Kragler, F., Simon, M. M., Schuster, T., and Hartig, A. (1994). The tetratricopeptide repeat-domain of the PAS10 protein of *Saccharomyces cerevisiae* is essntial for binding the peroxisomal targeting signal -SKL, Biochem Biophys Res Comm 204, 1016-1022.

Brocard, C., Lametschwandtner, G., Koudelka, R., and Hartig, A. (1997). Pex14p is a member of the protein linkage map of Pex5p, EMBO J 16, 5491-5500.

Chen, G., and Asada, K. (1989). Ascorbate peroxidase in tea leaves: occurrence of two isozymes and the differences in their enzymatic and molecular properties, Plant Cell Physiol 30, 987-998.

Corpas, F. J., and Trelease, R. N. (1998). Differential expression of ascorbate peroxidase and a putative molecular chaperone in the boundary membrane of differentiating cucumber seedling peroxisomes, Plant Physiol 153, 332-338.

Dammai, V., and Subramani, S. (2001). The human peroxisomal targeting signal receptor, Pex5p, is translocated into the peroxisomal matrix and recycled to the cytosol, Cell 105, 187-196.

De Bellis, L., Baden, C. S., and Nishimura, M. (1991). Development of enzymes of the glyoxylate cycle during senescence of pumpkin cotyledons., Plant Cell Physiol 32, 555-561.

De Bellis, L., Ismail, I., Reynolds, S. J., Barrett, M. D., and Smith, S. M. (1997). Distinct cis-acting sequences are required for the germination and suger responses of the cucumber isocitrate lyase gene., Gene 197, 375-378.

Devchand, P. R., Keller, H., Peters, J. M., Vazques, M., Gonzalez, F. J., and Wahli, W. (1996). The PPAR alpha-leukotriene B4 pathway to inflammation control., Nature 384, 39-43.

Distel, B., Erdmann, R., Gould, S. J., Blobel, G., Crane, D. I., Cregg, J. M., Dodt, G., Fujiki, Y., Goodman, J. M., Just, W. W., et al. (1996). A unified nomenclature for peroxisome biogenesis factors., J Cell Biol 135, 1-3.

Drees, B. L., Sundin, B., Brezeau, E., Caviston, J. P., Chen, G. C., Guo, W., Kozminski, K. G., Lau, M. W., Moskow, J. J., Tong, A., Schenkman, L. R., McKenzie, A., Brennwald, P., Longtine, M., Bi, E., Chan, C., Novick, P., Boone, C., Pringle, J. R., Davis, T. N., Fields, S., and Drubin, D. G. (2001). J Cell Biol 154, 549-571.

Dyer, J. M., McNew, J. A., and Goodman, J. M. (1996). The sorting sequence of the peroxisomal integral membrane protein PMP47 is contained within a short hydrophobic loop., J Cell Biol 133, 269-280.

Eccoleston, V. S., and Ohlrogge, J. B. (1998). Expression of lauroyl-acyl carrier protein thioesterase in *Brassica napus* seeds induces pathway for both fatty acid oxidation and biosynthesis and implies a set point for triacylglycerol accumulation., Plant Cell 10, 613-622.

Elgersma, Y., Kwast, L., van den Berg, M., Snyder, W. B., Distel, B., Subramani, S., and Tabak, H. F. (1997). Overexpression of Pex15p, a phosphorylated peroxisomal integral membrane protein required for peroxisome assembly in *S. cerevisiae*, causes proliferation of the endoplasmic reticulum membrane, EMBO J 16, 7326-7341.

Erdmann, R., and Kunau, W. H. (1992). A genetic approach to the biogenesis of peroxisomes in the yeast *Saccharomyces cerevisiae*., Cell Biochem Funct 10, 167-174.

Field, S., and Song, O. K. (1989). A novel genetic system to detect protein-protein interactions, Nature 340, 245-246.

Flynn, C. R., Mullen, R. T., and Trelease, R. N. (1998). Mutational analyses of a type 2 peroxisomal targeting signal that is capable of directing oligomeric protein import into tobacco BY-2 glyoxysomes., Plant J 16, 709-720.

Forman, B. M., Tontonoz, P., Chen, J., Brun, R. P., Spiegelman, B. M., and Evans, R. M. (1995). 15-Deoxy-delta 12, 14-prostaglandin J2 is a ligand for the adipocyte determination factor

PPAR gamma., Cell 83, 803-812.

Franklin, L. A., Levavasseur, G., Osmond, C. B., Henley, W. J., and Ramus, J. (1992). Two components of onset and recovery during photoinhibition of Ulva rotundata., Planta 187, 399-408.

Garnier, J., Osguthorpe, D. J., and Robson, B. (1978). Analysis of the accuracy and implication of simple methods for predicting the secondary structure of globular proteins., J Mol Biol 120, 97-120.

Gatto, G. J., Geisberecht, B. V., Gould, S. J., and Berg, J. M. (2000). Peroxisomal targeting signal-1 recognition by the TPR domains of human PEX5, Nat Struct Biol 7, 1091-1095.

Gietl, C., Faber, K. N., Vanderklei, I. J., and Veenhuis, M. (1994). Mutational analysis of the N-terminal topogenic signal of watermelon glyoxysomal malate dehydrogenase using the heterologous host *Hansenula polymorpha*., Proc Natl Acad Sci USA 91, 3151-3155.

Gietz, R. D., Schiestl, R. H., Willems, A. R., and Woods, R. A. (1995). Studies on the Transformation of Intact Yeast Cells by the LiAc/SS-DNA/PEG Procedure, YEAST 11, 355-360.

Gould, S. J., McCollum, D., Spong, A. P., Heyman, J. A., and Subramani, S. (1992). Development of the yeast *Pichia pastoris* as a model organism for a genetic and molecular analysis of peroxisome assembly, YEAST 8, 613-628.

Graham, I. A., Baker, C. J., and Leaver, C. J. (1994). Analysis of the cucumber malate synthase gene promoter by transient expression and gel retardation assays., Plant J 6, 893-902.

Gut, H., and Matile, P. (1988). Apparent induction of key enzymes of the glyoxylic acid cycle in senescent barley leaves, 176, 548-550.

Hayashi, H., De Bellis, L., Yamaguchi, K., Kato, A., Hayashi, M., and Nishimura, M. (1998a). Molecular characterization of a glyoxysomal long chain acyl-CoA oxidase that is synthesized as a precursor of higher molecular mass in pumpkin, J Biol Chem 273, 8301-7.

Hayashi, M., Aoki, M., Kato, A., Kondo, M., and Nishimura, M. (1996a). Transport of chimeric proteins that contain a carboxy-terminal targeting signal into plant microbodies, Plant J 10, 225-34.

Hayashi, M., Aoki, M., Kondo, M., and Nishimura, M. (1997). Changes in targeting efficiencies of proteins to plant microbodies caused by amino acid substitutions in the carboxy-terminal tripeptide, Plant Cell Physiol 38, 759-68.

Hayashi, M., Nito, K., Toriyama-Kato, K., Kondo, M., Yamaya, T., and Nishimura, M. (2000a). *At*Pex14p maintains peroxisomal functions by determining protein targeting to three kinds of plant peroxisomes, EMBO J 19, 5701-10.

Hayashi, M., Toriyama, K., Kondo, M., Kato, A., Mano, S., De Bellis, L., Hayashi-Ishimaru, Y., Yamaguchi, K., Hayashi, H., and Nishimura, M. (2000b). Functional transformation of plant peroxisomes, Cell Biochem Biophys 32, 295-304.

Hayashi, M., Toriyama, K., Kondo, M., and Nishimura, M. (1998b). 2,4-Dichlorophenoxybutyric acid-resistant mutants of Arabidopsis have defects in glyoxysomal fatty acid beta-oxidation, Plant Cell 10, 183-95.

Hayashi, M., Tsugeki, R., Kondo, M., Mori, H., and Nishimura, M. (1996b). Pumpkin hydroxypyruvate reductases with and without a putative C-terminal signal for targeting to microbodies may be produced by alternative splicing, Plant Mol Biol 30, 183-9.

Hettema, E. H., Girzalsky, W., van den Berg, M., Erdmann, R., and Distel, B. (2000). *Saccharomyces cerevisiae* Pex3p and Pex19p are required for proper localization and stability of peroxisomal membrane proteins, EMBO J 19, 223-33.

Huang, A. H. C., Trelease, R. N., and Moore, T. S. (1983). Plant peroxisomes, Academic Press, New York, 89-94.

Ishikawa, T., Yoshimura, K., Sakai, K., Tamoi, M., Takeda, T., and Shigeoka, S. (1998). Molecular characterization and physiological role of a glyoxysome-bound ascorbate peroxidase from spinach, Plant Cell Physiol 39, 23-34.

Issemann, I., and Green, S. (1990). Activation of a member of the steroid hormone receptor superfamily by peroxisome proliferators., Nature 347, 645-650.

James, P., J., H., and Craig, E. A. (1996). Genomic libraries and s host strain designed for highly efficient two-hybrid selection in yeast., Genetics 144, 1425-1436.

Kaneko, Y., and Newcomb, E. H. (1987). Cytochemical localization of uricase and catalase in developing root nodules of soybean., Protoplasma 140, 1-12.

Kaneko, Y., and Newcomb, E. H. (1990). Specialization for ureide biogenesis in the root nodules of black locust (*Robinia pseudoacacia*), an amide exporter., Protoplasma 157, 102-111.

Kato, A., Hayashi, M., Kondo, M., and Nishimura, M. (1996a). Targeting and processing of a chimeric protein with the N-terminal presequence of the precursor to glyoxysomal citrate synthase, Plant Cell 8, 1601-11.

Kato, A., Hayashi, M., Mori, H., and Nishimura, M. (1995). Molecular characterization of a glyoxysomal citrate synthase that is synthesized as a precursor of higher molecular mass in pumpkin, Plant Mol Biol 27, 377-90.

Kato, A., Hayashi, M., and Nishimura, M. (1999). Oligomeric proteins containing N-terminal targeting signals are imported into peroxisomes in transgenic Arabidopsis, Plant Cell Physiol 40, 586-91.

Kato, A., Hayashi, M., Takeuchi, Y., and Nishimura, M. (1996b). cDNA cloning and expression of a gene for 3-ketoacyl-CoA thiolase in pumpkin cotyledons, Plant Mol Biol 31, 843-52.

Kato, A., Takeda-Yoshikawa, Y., Hayashi, M., Kondo, M., Hara-Nishimura, I., and Nishimura, M. (1998). Glyoxysomal malate dehydrogenase in pumpkin: cloning of a cDNA and functional analysis of its presequence, Plant Cell Physiol 39, 186-195.

Koller, A., Snyder, W. B., Faber, K. N., Wenzel, T. J., Rangell, L., Keller, G. A., and Subramani, S. (1999). Pex22p of *Pichia pastoris*, essential for peroxisomal matrix protein import, anchors the ubiquitin-conjugating enzyme, Pex4p, on the peroxisomal membrane, J Cell Biol 146, 99-112.

Komori, M., Kiel, J. A. K. W., and Veenhuis, M. (1999). The peroxisomal membrane protein Pex14p of *Hansenula polymorpha* is phosphorylated in vivo., FEBS Lett 457, 397-399.

Komori, M., Rasmussen, S. W., Kiel, J. A. K. W., Baerends, R. J. S., Cregg, J. M., van der Klei, I. J., and Veenhuis, M. (1997). The *Hansenula polymorpha* PEX14 gene encodes a novel peroxisomal membrane protein essential for peroxisome biogenesis., EMBO J 16, 44-53.

Kone, B. C. (2000). Protein-protein interactions controlling nitric oxide synthases., Acta Physiol Scand 168, 27-31.

Koshiba, T. (1993). Cytosolic ascorbate peroxidase in seedings and leaves of maize, Plant Cell Physiol 34, 713-721.

Kragler, F., Lametschwandtner, G., Christmann, J., Hartig, A., and Harada, J. J. (1998). Identification and analysis of the plant peroxisomal targeting signal 1 receptor *Nt*PEX5, Proc Natl Acad Sci 95, 13336-13341.

Krause, G. H. (1988). Photoinhibition of photosynthesis. An evaluation of damaging and protective mechanisms., Physiol Plant 74, 566-574.

Kubo, A., Saji, H., Tanaka, K., and Kondo, N. (1992). Cloning and sequencing of a cDNA encoding ascorbate peroxidase from *Arabidopsis thaliana*, Plant Mol Biol 18, 691-701.

Kukkonen, J. P., Nasman J., and Akerman K. E. (2001) Modelling of promiscuous receptor-Gi/Gs-protein coupling and effector response., Trend Pharmacol Sci 22, 616-622

Kunau, W. H., Beyer, A., Franken, T., Gotte, K., Marzioch, M., Saidowsky, J., Skaletz-rorowski, A., and Wiebel, F. F. (1993). Two complementary approaches to study peroxisome biogenesis in *Saccharomyces cerevisiae*: forward and reversed genetics., Biochimie 75, 209-224.

Kyte, J., and Doolittle, R. F. (1982). A simple method for displaying the hydropathic character of a protein., J Mol Biol 157, 105-132.

Laemmli, U. K. (1970). Cleavage of structural protein during the assembly of the head of bacteriophage T4., Nature 227, 680-685.

Lazarow, P. B., and Fujiki, Y. (1985). Biogenesis of peroxisomes., Annu Rev Cell Biol 1, 489-530.

Lee, M. S., Mullen, R. T., and Trelease, R. N. (1997). Oilseed isocitrate lyase lacking their essential type 1 peroxisomal targeting signal are piggybacked to glyoxysomes., Plant Cell 9, 185-197.

Lin, Y., Sun, L., Nguyen, L. V., Rachubinski, R. A., and Goodman, H. M. (1999). The Pex16p homolog SSE1 and storage organelle formation in *Arabidopsis* seeds., science 284, 328-330.

Mano, S., Hayashi, M., Kondo, M., and Nishimura, M. (1996). cDNA cloning and expression of a gene for isocitrate lyase in pumpkin cotyledons, Plant Cell Physiol 37, 941-948.

Mano, S., Hayashi, M., and Nishimura, M. (1999). Light regulates alternative splicing of hydroxypyruvate reductase in pumpkin, Plant J 17, 309-320.

Mano, S., Yamaguchi, K., Hayashi, M., and Nishimura, M. (1997). Stromal and thylakoid-bound ascorbate peroxidases are produced by alternative splicing in pumpkin, FEBS Lett 413, 21-26.

Marzioch, M., Erdmann, K. S., Veenhuis, M., and Kunau, W.-H. (1994). PAS7 encodes a novel yeast member of the WD-40 protein family essential for import of 3-oxoacyl-CoA thiolase, a PTS2-containing protein, into peroxisomes, EMBO J 13, 4908-4918.

McCollum, D., Monosov, E., and Subramani, S. (1993). The pas8 mutant of *Pichia pastoris* exhibit the peroxisomal protein import deficiencies of Zellweger syndrome cells--the PAS8 protein binds to the COOH-terminal tripeptide peroxisomal targeting signal, and is a member of the TPR protein family, J Cell Biol 121, 761-774.

Mori, H., Takeda-Yoshikawa, Y., Hara-Nishimura, I., and Nishimura, M. (1991). Pumpkin malate synthase, Eur J Biochem 197, 331-336.

Motley, A. M., Hettema, E. H., Ketting, R., Plasterk, R., and Tabak, H. (2000). Caenorhabditis elegans has a single pathway to target matrix protein to peroxisomes, EMBO reports 1, 40-46.

Mullen, R. T., Flynn, C. R., and Trelease, R. N. (2001). How are peroxisomes formed? The role of the endoplasmic reticulum and peroxins., TRENDS in Plant Sci 6, 256-261.

Mullen, R. T., Lisenbee, C. S., Miernyk, J. A., and Trelease, R. N. (1999). Peroxisomal membrane ascorbate peroxidase is sorted to a membranous network that resembles a subdomain of the endoplasmic reticulum., Plant Cell 11, 2167-86.

Mullen, R. T., and Trelease, R. N. (2000). The sorting signals for peroxisomal membrane-bound ascorbate peroxidase are within its C-terminal tail., J Biol Chem 275, 16337-16344.

Nakajima, K., and Yaoita, T. (1997). Construction of multiple-epitope tag sequence by PCR for sensitive western blot analysis, Nucleic Acids Res 25, 2231-2232.

Nishimura, M., Hayashi, M., Kato, A., Yamaguchi, K., and Mano, S. (1996). Functional transformation of microbodies in higher plant cells, Cell Struct Funct 21, 387-93.

Nishimura, M., Yamaguchi, J., Mori, H., Akazawa, T., and Yokota, S. (1986).

Immunocytochemical analysis shows that glyoxysomes are directly transformed to leaf peroxisomes during greening of pumpkin cotyledons., Plant Physiol 80, 313-316.

Nishimura, N., Takeuchi, Y., De Bellis, L., and Hara-Nishimura, I. (1993). Leaf peroxisomes are directly transformed to glyoxysomes during senescence of pumpkin cotyledons., Protoplasma 175, 131-137.

Nito, K., Yamaguchi, K., Kondo, M., Hayashi, M., and Nishimura, M. (2001). Pumpkin peroxisomal ascorbate peroxidase is localized on peroxisomal membranes and unknown membranous structures, Plant Cell Physiol 42, 20-7.

Nuttley, W. M., Brade, A. M., Gaillardin, C., Eitzen, G. A., Glover, J. R., Aitchison, J. D., and Rachubinski, R. A. (1993). Rapid identification and characterization of peroxisomal assembly mutants in *Yarrowia lipolytica*., YEAST 9, 507-517.

Olsen, L. J. (1998). The surprising complexity of peroxisome biogenesis, Plant Mol Biol 38, 163-189.

Otera, H., Okumoto, K., Tateishi, K., Ikoma, Y., Matsuda, E., Nishimura, M., Tsukamoto, T., Osumi, T., Ohashi, K., Higuchi, O., and Fujiki, Y. (1998). Peroxisome targeting signal type 1 (PTS1) receptor is involved in import of both PTS1 and PTS2: studies with PEX5-defective CHO cell mutants, Mol Cell Biol 18, 388-399.

Reynolds, S. J., and Smith, S. M. (1995a). The isocitrate lyase gene of cucumber: isolation, characterization and expression in cotyledons following seed germination., Plant Mol Biol 27, 487-497.

Reynolds, S. J., and Smith, S. M. (1995b). Regulation of expression of the cucumber isocitrate lyase gene in cotyledons upon seed germination and by sucrose, Plant Mol Biol 29, 885-896.

Richmond, T. A., and Bleecker, A. B. (1999). A defect in b-oxidation causes abnormal

inflorescence development in Arabidopsis, Plant Cell 11, 1911-1924.

Sacksteder, K. A., Jones, J. M., South, S. T., Li, X., Liu, Y., and Gould, S. J. (2000). PEX19 binds multiple peroxisomal membrane proteins, is predominantly cytoplasmic, and is required for peroxisome membrane synthesis., J Cell Biol 148, 931-944.

Sakai, K., Matsuo, H., He, K.-Z., Saiganji, A., Yurimoto, H., Takabe, K., Sakai, H., and Kato, N. (1995). Isolation and characterization of mutants of the methylotrophic yeast *Candida boidinii* S2 that are impared in growth on peroxisome-inducing carbon sources, Biosci Biotech Biochem 59, 869-875.

Sambrook, J. (2001). Molecular Cloning: A Laboratory Manual (New York, Cold Spring Harbor Laboratory Press).

Sanders, P. M., Lee, P. Y., Biesgen, C., Boone, J. D., Beals, T. P., Weiler, E. W., and Goldberg, R. B. (2000). The Arabidopsis DELAYED DEHISCENCE1 gene encodes an enzyme in the jasmonic acid synthesis pathway., Plant Cell 12, 1041-1061.

Sarah, C. J., Graham, I. A., Reynolds, S. J., Leaver, C. J., and Smith, S. M. (1996). Distinct cis-acting elemants direct the germination and suger responses of the cucumber malate synthase gene., Mol Gen Genet 250, 153-161.

Sautter, C. (1986). Microbody transition in greening watermelon cotyledons. Double immunocytochemical labeling of isocitrate lyase and hydroxypyruvate reductase., Planta 167, 491-503.

Schliebs, W., Saidowsky, J., Agianian, B., Dodt, G., Herberg, F. W., and Kunau, W.-H. (1999). Recombinant human peroxisomal targeting signal receptor PEX5, J Biol Chem 274, 5666-5673.

Schumann, U., Gietl, C., and Schmid, M. (1999). Sequence analysis of a cDNA encoding

Pex7p, a peroxisomal targeting signal 2 receptor from *Arabidopsis thaliana*, Plant Physiol 120, 339.

Shevchenko, A., Wilm, M., Vorm, O., and Mann, M. (1996). Mass spectrometric sequencing of proteins silver-stained polyacrylamide gels., Anal Chem 68, 850-858.

Shigeoka, S., Ishikawa, T., Takeda, T., and Tamoi, M. (1998). [Molecular mechanism of defense system against photooxidative damage in photosynthetic organisms--possibility of creation of plants with tolerance to photooxidative damage], Tanpakushitsu Kakusan Koso 43, 634-48.

Shimizu, N., Itoh, R., Hirono, Y., Otera, H., Ghaedi, K., Tateishi, K., Tamura, S., Okumoto, K., Harano, T., Mukai, S., and Fujiki, Y. (1999). The peroxin Pex14p. cDNA cloning by functional complementation on a Chinese hamster ovary cell mutant, characterization, and functional analysis, J Biol Chem 274, 12593-604.

Shimozawa, N., Suzuki, Y., Zhang, Z., Miura, K., Matsumoto, A., Nagaya, M., Castillo-Taucher, S., and Kondo, N. (1999). A novel nonsense mutation of the PEX7 gene in a patient with rhizomelic chondrodysplasia punctata, J Hum Genet 44, 123-125.

Snyder, W. B., Koller, A., Choy, A. J., and Subramani, S. (2000). The peroxin Pex19p interacts with multiple, integral membrane proteins at the peroxisomal membrane, J Cell Biol 149, 1171-8.

Somerville, C. R., and Ogren, W. L. (1981). Photorespiration-deficient mutants of *Arabidopsis thaliana* lacking mitochondrial serine transhydroxymethylase activity., Plant Physiol 67, 666-671.

Somerville, C. R., and Ogren, W. L. (1982). Genetic modification of photorespiration., Trends Biochem Sci 7, 171-174.

Stintzi, A., and Browse, J. (2000). The *Arabidopsis* male-sterile mutant, opr3, lacks the 12-oxophytodienoic acid reductase required for jasmonate synthesis., Proc Natl Acad Sci USA 97, 10625-10630.

Subramani, S. (1996). Protein translocation into peroxisomes, J Biol Chem 271, 32483-32486.

Subramani, S. (1998). Components involved in peroxisome import, biogenesis, proliferation, turnover, and movement, Physiol Rev 78, 171-88.

Subramani, S., Koller, A., and Snyder, W. B. (2000). Import of peroxisomal matrix and membrane proteins, Annu Rev Biochem 69, 399-418.

Titorenko, V. I., Ogrydziak, D. M., and Rachubinski, R. A. (1997). Four distinct secretory pathways serve protein secretion, cell surface growth, and peroxisome biogenesis in yeast *Yarrowia lipolytica.*, Mol Cell Biol 17, 5210-5226.

Titorenko, V. I., and Rachubinski, R. A. (1998). Mutants of the yeast *Yarrowia lipolytica* defective in protein exit from the endoplasmic reticulum are also defective in peroxisome biogenesis., Mol Cell Biol 18, 2789-2803.

Titus, D. E., and Becker, W. M. (1985). Investigation of the glyoxysome-peroxisome transition in germinating cucumber cotyledons using double-label immunoelectron microscopy, J Cell Biol 101, 1288-99.

Tolbert, N. E. (1982). Leaf peroxisomes., Ann N Y Acad Sci 386, 254-268.

Towbin, H., Staehelin, T., and Gordon, J. (1979). Electrophoretic transfer of proteins from polyacrylamide gels to nitrocellulose sheets: procedure and some applications., Proc Natl Acad Sci USA 76, 4350-4354.

Trelease, R. N., Lee, M. S., Banjoko, A., and Bunkelmann, J. (1996). C-terminal polypeptides are necessary and sufficient for in vivo targeting of transiently-expressed proteins to peroxisomes in suspension-cultured plant cells., Protoplasma 195, 156-167.

Tsugeki, R., Hara-Nishimura, I., Mori, H., and Nishimura, M. (1993). Cloning and sequencing of cDNA for glycolate oxidase from pumpkin cotyledons and northern blot analysis, Plant Cell

Physiol 34, 51-57.

Tsukamoto, T., Shimozawa, N., and Fujiki, Y. (1994). Peroxisome assembly factor 1: nonsense mutation in a peroxisome-deficient Chinese hamster ovary cell mutant and deletion analysis., Mol Cell Biol 14, 5458-5465.

Tsukamoto, T., Yokota, S., and Fujiki, Y. (1990). Isolation and characterization of chinese hamster ovary cell mutants defective in assembly of peroxisomes., J Cell Biol 110, 651-660.

Uetz, P., Giot, L., Cagney, G., Mansfield, T. A., Judson, R. S., Knight, J. R., Lockshon, D., Narayan, V., Srinivasan, M., Pochart, P., Qureshi-Emili, A., Li, Y., Godwin, B., Conover, D., Kalbfleisch, T., Vijayadamodar, G., Yang, M., Jhonston, M., Fields, S., Rothberg, J. M. (2000) A comprehensive analysis of protein-protein interactions in Saccharomyces cerevisiae., Nature 403, 623-627.

Öuist, G., Chow, W. S., and Andersson, J. M. (1992). Photoinhibition of photosynthesis represents a mechanism for the long term regulation of photosystem II., Planta 186, 450-460.

Van der Leij, I., Franse, M. M., Elgersma, Y., Distel, B., and Tabak, H. F. (1993). PAS10 is tetratricopeptide-repeat protein that is essential for the import of most matrix proteins into peroxisomes of *Saccharomyces cerevisiae*, Proc Natl Acad Sci 90, 11782-6.

Veenhuis, M., van der Klei, I. J., Titorenko, V., and Harder, W. (1992). *Hansenula polymorpha*: an attractive model organism for molecular studies of peroxisome biogenesis and function., FEMS Microbiol lett 79, 393-403.

Walton, P. A., Hill, P. E., and Subramani, S. (1995). Import of stably folded proteins into peroxisomes, Mol Biol Cell 6, 675-683.

Wiemer, E., Luerst, G., Faber, K., T., Veenhuis, M., and Subramani, S. (1996). Isolation and characterization of Pas2p, aperoxisomal membrane protein essential for peroxisome biogenesis in

the methylotrophic yeast *Pichia pastoris*, J Biol Chem 271, 18973-18980.

Wiemer, E. A. C., Nuttley, W. M., Bertolaet, B. L., Li, X., Francke, U., Wheelock, M. J., Anne, U. K., Johnson, K. R., and Subramani, S. (1995). Human peroxisomal targeting signal-1 receptor restores peroxisomal protein import in cells from patients with fatal peroxisomal disorders, J Cell Biol 130, 51-65.

Will, G. K., Soukupova, M., Hong, X., Erdmann, K. S., Kiel, J. A. K. W., Dodt, G., Kunau, W.-H., and Erdmann, R. (1999). Identification and characterization of the human orthologue of yeast Pex14p, Mol Cell Biol 19, 2265-2277.

Wimmer, C., Schmid, M., Veenhuis, M., and Gietl, C. (1998). The plant PTS1 receptor: similarities and differences to its human and yeast counterparts, Plant J 16, 453-464.

Yamaguchi, K., Hayashi, M., and Nishimura, M. (1996). cDNA cloning of thylakoid-bound ascorbate peroxidase in pumpkin and its characterization, Plant Cell Physiol 37, 405-409.

Yamaguchi, K., Mori, H., and Nishimura, M. (1995a). A novel isoenzyme of ascorbate peroxidase localized on glyoxysomal and leaf peroxisomal membranes in pumpkin, Plant Cell Physiol 36, 1157-62.

Yamaguchi, K., Takeuchi, Y., Mori, H., and Nishimura, M. (1995b). Development of microbody membrane proteins during the transformation of glyoxysomes to leaf peroxisomes in pumpkin cotyledons, Plant Cell Physiol 36, 455-464.

Zhang, J. W., and Lazarow, P. B. (1994). PEB1 (PAS7) in *Saccharomyces cerevisiae* encodes a hydrophilic, intraperoxisomal protein which is a member of the WD repeat family and is essential for the import of thiolase into peroxisomes, J Cell Biol 129, 65-80.

Zhang, M., and Yuan, T. (1998). Molecular mechanisms of calmodulin's functional versatility, Biochem Cell Biol 76, 313-323.

謝辞

本研究を遂行するにあたり、終始ご指導とご鞭撻を頂きました西村幹夫教授に心から感謝いたします。また、常日頃適切なご助言とご指導を頂きました林誠助教授に深く感謝いたします。山口勝司技官にはオルガネラ分画およびタンパク質の N 末端アミノ酸解析をして頂き、近藤真紀技官には免疫電子顕微鏡観察をして頂きました。ここに深く感謝いたします。さらに、研究者生活において多くの激励とご助言を頂いた西村いくこ教授（京都大学）、加藤朗助教授（新潟大学）、真野昌二助手、嶋田知生助手（京都大学）、鳥山可菜子氏をはじめ細胞機構研究部門の職員、学生の皆様に深く感謝いたします。酵母 two-hybrid system による解析を行うためのクローニングベクターと宿主酵母を快く御供与してくださった Philip James 氏（University of Wisconsin）に感謝いたします。ヒマ ICL 抗体を御供与して頂いた前島正義教授（名古屋大学）に感謝いたします。また、大量に塩基配列決定をして頂いた遺伝子第一研究部門の職員の方々に感謝いたします。

最後に、ここに至るまでの間、常に物心両面から支えてくださった両親、妹に深く感謝いたします。

報文目録

Hayashi, M., Nito, K., Toriyama-Kato, K., Kondo, M., Yamaya, T. and Nishimura, M. (2000). *At*Pex14p maintains peroxisomal functions by determining protein targeting to three kinds of plant peroxisomes, EMBO J. 19, 5701-10

Nito, K., Yamaguchi, K., Kondo, M., Hayashi, M. and Nishimura, M. (2001). Pumpkin peroxisomal ascorbate peroxidase is localized on peroxisomal membranes and unknown membranous structures, Plant Cell Physiol. 42, 20-7

Nito, K., Hayashi, M. and Nishimura, M. (2002) Direct interaction and determination of binding domains among peroxisomal import factors in *Arabidopsis thaliana*, Plant Cell Physiol. 43, 355-366

The EMBO Journal Vol. 19 No. 21 pp. 5701–5710, 2000

*At*Pex14p maintains peroxisomal functions by determining protein targeting to three kinds of plant peroxisomes

Makoto Hayashi[1,2], Kazumasa Nito[1,3], Kanako Toriyama-Kato[1], Maki Kondo[1], Tomoyuki Yamaya[2] and Mikio Nishimura[1,3,4]

[1]Department of Cell Biology, National Institute for Basic Biology, Okazaki 444-8585, [2]Department of Applied Plant Science, Graduate School of Agricultural Sciences, Tohoku University, 1-1 Tsutsumidori-Amamiyamachi, Aoba-ku, Sendai 981-8555 and [3]Department of Molecular Biomechanics, School of Life Science, Graduate University of Advanced Studies, Okazaki 444-8585, Japan

[4]Corresponding author at first address
e-mail: mikosome@nibb.ac.jp

We previously isolated an *Arabidopsis* peroxisome-deficient *ped2* mutant by its resistance to 2,4-dichlorophenoxybutyric acid. Here, we describe the isolation of a gene responsible for this deficiency, called the *PED2* gene, by positional cloning and confirmed its identity by complementation analysis. The amino acid sequence of the predicted protein product is similar to that of human Pex14p, which is a key component of the peroxisomal protein import machinery. Therefore, we decided to call it *At*Pex14p. Analyses of the *ped2* mutant revealed that *At*Pex14p controls intracellular transport of both peroxisome targeting signal (PTS)1- and PTS2-containing proteins into three different types of peroxisomes, namely glyoxysomes, leaf peroxisomes and unspecialized peroxisomes. Mutation in the *PED2* gene results in reduction of enzymes in all of these functionally differentiated peroxisomes. The reduction in these enzymes induces pleiotropic defects, such as fatty acid degradation, photorespiration and the morphology of peroxisomes. These data suggest that the *At*Pex14p has a common role in maintaining physiological functions of each of these three kinds of plant peroxisomes by determining peroxisomal protein targeting.

Keywords: β-oxidation/peroxisome/*pex14*/photorespiration/protein targeting

Introduction

Peroxisomes in higher plant cells are known to differentiate into at least three different classes, namely glyoxysomes, leaf peroxisomes and unspecialized peroxisomes (Beevers, 1979). Each organelle contains a unique set of enzymes that provides special functions in various organs in higher plants. Glyoxysomes are present in cells of storage organs, such as endosperms and cotyledons during post-germinative growth of oil-seed plants, as well as in senescent organs (Nishimura *et al.*, 1996). They contain enzymes for fatty acid β-oxidation and the glyoxylate cycle, and play a pivotal role in the conversion of lipid into sucrose. It has been suggested that fatty acids are exclusively degraded in glyoxysomes (i.e. not in mitochondria) during germination and post-germinative growth (Beevers, 1982). In contrast, leaf peroxisomes are found widely in cells of photosynthetic organs. It has been shown that some of the enzymes responsible for photorespiration are localized in leaf peroxisomes even though the entire photorespiratory process involves a combination of enzymic reactions that occur in chloroplasts, leaf peroxisomes and mitochondria (Tolbert, 1982). Other organs, such as roots and stems, contain unspecialized peroxisomes whose function is still obscure (Nishimura *et al.*, 1996).

Glyoxysomes, leaf peroxisomes and unspecialized peroxisomes are known to be converted into one another under certain conditions (Nishimura *et al.*, 1996). For example, glyoxysomes in etiolated cotyledons are transformed directly into leaf peroxisomes during the greening of cotyledons (Titus and Becker, 1985; Nishimura *et al.*, 1986). During this process, glyoxysomal enzymes, such as malate synthase, are specifically degraded (Mori and Nishimura, 1989), and leaf peroxisomal enzymes, such as glycolate oxidase and hydroxypyruvate reductase, are newly synthesized and transported into the organelle as it is being transformed from a glyoxysome to a leaf peroxisome (Tsugeki *et al.*, 1993; Hayashi *et al.*, 1996b). Leaf peroxisomes in green cotyledons are subsequently converted to glyoxysomes when the cotyledons undergo senescence (De Bellis and Nishimura, 1991; Nishimura *et al.*, 1993). It has been suggested that the functional transformation of plant peroxisomes is controlled by gene expression, protein translocation and protein degradation, although the detailed mechanisms underlying these processes still need to be clarified (Nishimura *et al.*, 1996).

To identify the genes responsible for regulation of peroxisomal function in plant cells, we isolated mutants with defective peroxisomes. To screen such mutants, we used 2,4-dichlorophenoxybutyric acid (2,4-DB) as a compound for detecting *Arabidopsis* mutants with defects in glyoxysomal fatty acid β-oxidation (Hayashi *et al.*, 1998). We expected that two methylene groups of the butyric side chain in 2,4-DB would be removed by the action of glyoxysomal fatty acid β-oxidation to produce a herbicide, 2,4-dichlorophenoxyacetic acid (2,4-D), in wild-type plants, whereas the mutants no longer produce a toxic level of 2,4-D from 2,4-DB because of the defect in fatty acid β-oxidation. We succeeded in identifying four mutants that were classified as carrying alleles at three independent loci. We designated these loci as *ped1*, *ped2* and *ped3*, respectively, where *ped* stands for *p*eroxisome *d*efective. These mutants required sucrose for post-germinative growth, because the reduced activity of glyoxysomal fatty acid β-oxidation prevented the production of sucrose from the lipid reserves in seeds. One of these mutants, *ped2*, has been demonstrated previously to

have a defect in the intracellular transport of 3-ketoacyl CoA thiolase, an enzyme participating in fatty acid β-oxidation, from the cytosol to glyoxysomes (Hayashi *et al.*, 1998).

Peroxisomal enzymes are synthesized in the cytosol, and function after their post-translational transport into peroxisomes. Most of the plant peroxisomal enzymes have been shown to contain one of two peroxisome targeting signals (PTSs) within their amino acid sequences (Hayashi, 2000). One type of targeting signal (PTS1) is a unique tripeptide sequence found in the C-terminus of the proteins (Hayashi *et al.*, 1996a; Trelease *et al.*, 1996). The permissible combinations of tripeptide sequence for plant PTS1 are (C/A/S/P)-(K/R)-(I/L/M) (Hayashi *et al.*, 1997). Another type of targeting signal is involved in a cleavable N-terminal presequence (Gietl *et al.*, 1994). The N-terminal presequences contain a consensus sequence (R)-(L/Q/I)-X5-(H)-(L) (X stands for any amino acid) called PTS2 (Kato *et al.*, 1996a, 1998). These proteins are synthesized as precursor proteins, which show a higher molecular mass due to the N-terminal presequence. The N-terminal presequence is processed to form the mature protein after its transport into peroxisomes. These peroxisomal proteins with PTS1 or PTS2 are imported into peroxisomes with oligomeric forms (Lee *et al.*, 1997; Flynn *et al.*, 1998; Kato *et al.*, 1999).

Here we report the identification and analysis of the *PED2* gene, and present evidence that the gene product of *PED2* is a component of the protein targeting machinery involved in each of the three kinds of plant peroxisome. We discuss the pleiotropic defects in the *ped2* mutant based upon the predicted function of the *PED2* gene product.

Results

High-resolution mapping of the PED2 locus

The *Arabidopsis ped2* mutant, which has a Landsberg *erecta* ecotype background, was identified by its resistance to the presence of 2,4-DB. This mutant requires sucrose for post-germinative growth, because of its reduced activity for fatty acid β-oxidation. Our initial mapping of *PED2* located it to the lower arm of chromosome 5, between two molecular markers, LFY3 and g2368 (Hayashi *et al.*, 1998). We outcrossed the *ped2* mutant (which has a Landsberg *erecta* ecotype background) to wild-type *Arabidopsis*, which has a Columbia ecotype background, and identified 310 F_2 progenies that have homozygous *ped2* alleles for high-resolution mapping. These progenies were subsequently scored according to their genetic background at a series of molecular markers using the cleaved amplified polymorphic sequence (CAPS) mapping procedure described by Konieczny and Ausubel (1993) (Figure 1A). The number of chromosomes that showed a Columbia background represents the number of recombinations that occurred between the *PED2* locus and the position of each molecular marker, since the genomic DNA of the *ped2* mutant has a Landsberg *erecta*

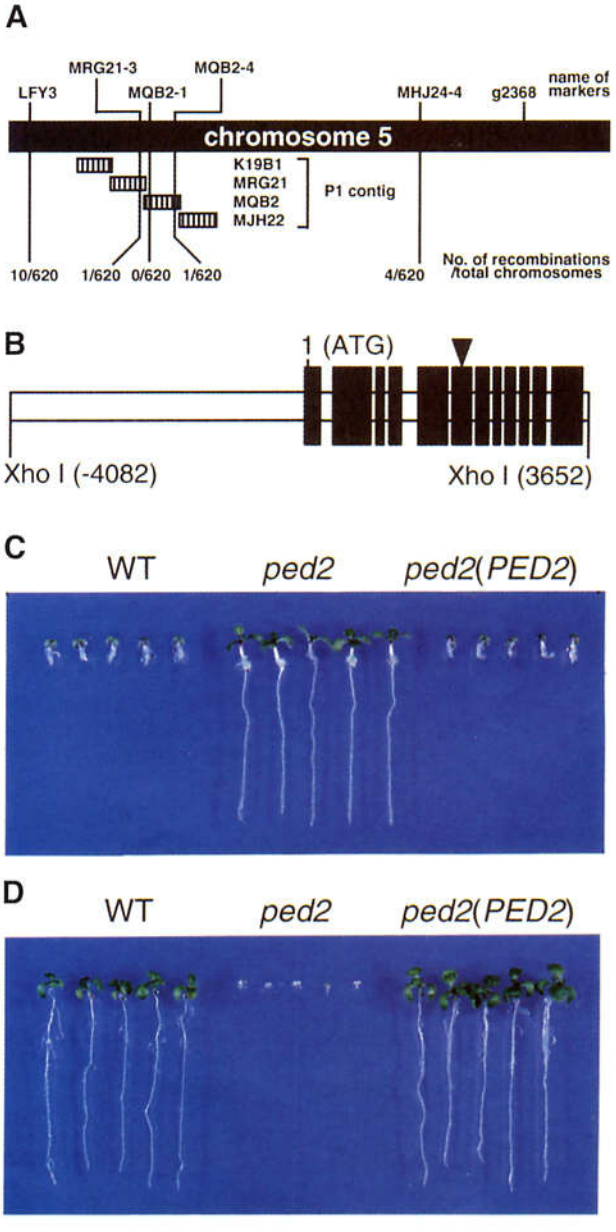

Fig. 1. Positional cloning of the *PED2* gene. (**A**) High-resolution mapping of *PED2* on chromosome 5. Names and positions of the molecular markers used in this study are indicated on the top of the illustration. Hatched bars represent the regions covered by the P1 clones. We analyzed 310 F_2 progeny (620 chromosomes) having homozygous *ped2* alleles. The numbers of recombinations that occurred between the *PED2* locus and the molecular markers are indicated at the bottom of the illustration. Mapping results with a series of molecular markers between LFY3 and MHJ24-4 are summarized schematically and indicate that the *PED2* locus may be located within a single P1 clone, MQB2. (**B**) Schematic diagram of a 7734 bp *Xho*I fragment that is involved in the P1 clone, MQB2. The 12 black bars represent protein coding regions determined from the cDNA sequence. The triangle on the sixth black bar indicates the position of a nonsense mutation that occurs in the *ped2* mutant. Nucleotide residue 1 corresponds to an adenine of the first methionine codon. (**C**) Effects of 2,4-DB on the growth of transgenic *ped2* seedlings [*ped2*(*PED2*)] harboring the 7734 bp *Xho*I fragment shown in (B). Wild-type *Arabidopsis* (WT), *ped2* mutant (*ped2*) and *ped2*(*PED2*) were grown for 10 days on growth medium containing 0.2 μg/ml 2,4-DB under constant illumination. Photographs were taken after the seedlings were removed from the media and rearranged on agar plates. (**D**) Effects of sucrose on the growth of *ped2*(*PED2*) seedlings. Wild-type *Arabidopsis* (WT), *ped2* mutant (*ped2*) and *ped2*(*PED2*) were grown for 10 days on growth medium without sucrose under constant illumination. Photographs were taken after the seedlings were removed from the media and rearranged on agar plates.

background. To identify the genetic background of chromosome 5 between LFY3 and g2368, we generated four molecular markers, MRG21-3, MQB2-1, MQB2-4, MHJ24-4, based on the nucleotide sequences of P1 contigs that have been reported by the Kazusa DNA Institute, Chiba, Japan (http://www.kazusa.or.jp/kaos/). As summarized in Figure 1A, high-resolution mapping revealed that the *PED2* locus is located between MRG21-3 and MQB2-4. The closest molecular marker to the *PED2* locus is MQB2-1. This result strongly suggests that the *PED2* gene is contained within a single P1 clone, MQB2.

Identification of the PED2 gene

MQB2 is reported to contain 16 predicted genes (http://www.kazusa.or.jp/kaos/). Based on the nucleotide sequences, we designed a set of oligonucleotide primers that could amplify one of the predicted genes by using the PCR. This gene is located within the 7734 bp *Xho*I fragment contained in MQB2 (Figure 1B). DNA fragments were amplified from genomic DNAs of wild-type *Arabidopsis* (ecotype Landsberg *erecta*) and the *ped2* mutant, using this primer set, and were fully sequenced. The nucleotide sequences of the two fragments are identical except for one nucleotide substitution, from C in the wild-type plant to T in the *ped2* mutant (Figure 1B, arrowhead). This result strongly indicated that the 7734 bp *Xho*I fragment contained the *PED2* gene.

To confirm this result, the 7734 bp *Xho*I fragment isolated from the MQB2 clone was inserted into a plant binary vector, pBI121Δ35S, and then transformed into the *ped2* mutant by *Agrobacterium*-mediated transformation (Bechtold *et al.*, 1993). Seeds from individual kanamycin-resistant T_2 progenies were scored for kanamycin resistance to identify the lines that are homozygous for the transgene. The homozygous T_3 lines were assayed for 2,4-DB resistance and a sucrose requirement during post-germinative growth. As we have previously reported, the *ped2* mutant was resistant to a toxic level of 2,4-DB, while it was sensitive to the absence of sucrose in the growth medium (Figure 1C and D, *ped2*). In contrast, the *ped2* mutant transformed with the 7734 bp *Xho*I fragment became sensitive to a toxic level of 2,4-DB, whereas it was resistant to the absence of sucrose in the growth medium [Figure 1C and D, *ped2(PED2)*]. These phenotypes are identical to wild-type plants (Figure 1C and D, WT). These data indicated that the genomic sequence determined in this study corresponds to the *PED2* gene. The nucleotide sequence data of *PED2* are available in the DDBJ/EMBL/GenBank nucleotide sequence databases (AB037538).

PED2 encodes a protein similar to Pex14p

A cDNA clone of the *PED2* gene was generated using RT–PCR with total RNA isolated from wild-type plants. The first methionine that appeared in this cDNA represents the start of the open reading frame, since the 5′ primer used for the PCR was designed to hybridize with the 5′ untranslated region including an in-frame stop codon. We determined the nucleotide sequence of the cDNA (DDBJ/EMBL/GenBank accession No. AB037539). Comparison of the cDNA and genomic DNA sequences showed that the *PED2* gene contains 12 exons (Figure 1B). The deduced amino acid sequence of the gene product is

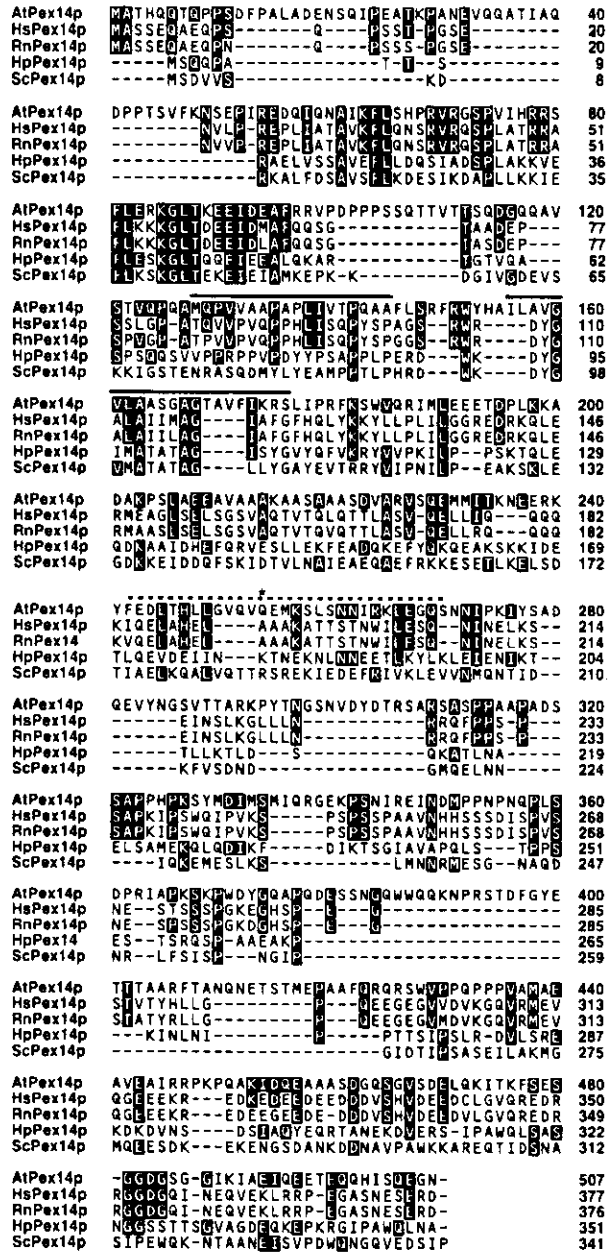

Fig. 2. Alignment of amino acid sequences for the *PED2* gene product with mammalian and yeast Pex14p. Deduced amino acid sequence of the *PED2* gene product (AtPex14p) was compared with Pex14p identified from human (HsPex14p), rat (RnPex14p), *H.polymorpha* (HpPex14p) and *Saccharomyces cerevisiae* (ScPex14p). Identical amino acid residues between AtPex14p and other Pex14p are highlighted. Amino acid sequence of AtPex14p is 29.6% identical to that of human Pex14p. The asterisk on Gln254 represents the position of a nonsense mutation (CAA to TAA) in the *ped2* gene. Two putative membrane spanning domains are indicated by a line. A dashed line represents a putative coiled-coil region.

composed of 507 amino acid residues (Figure 2). A nucleotide substitution occurred in the *ped2* mutant, converting a CAA codon encoding Gln254 of the gene product to a stop codon (TAA) (Figure 2, asterisk). The amino acid sequence of the gene product shows significant similarity to mammalian and fungal Pex14p, one of the peroxisomal membrane proteins involved in the peroxisomal protein targeting machinery (Albertini *et al.*, 1997; Brocard *et al.*, 1997; Komori *et al.*, 1997; Shimizu *et al.*,

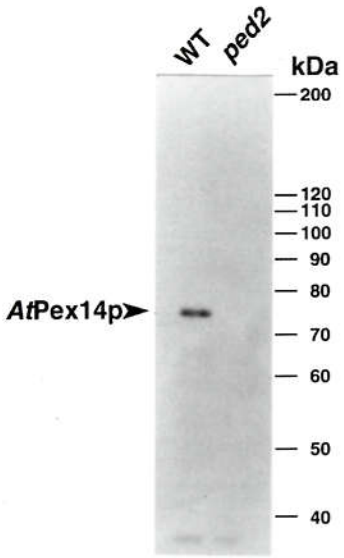

Fig. 3. Immunodetection of *At*Pex14p in etiolated cotyledons of wild-type *Arabidopsis* and *ped2* mutant. Extracts were prepared from 5-day-old etiolated cotyledons of wild-type *Arabidopsis* (WT) and *ped2* mutant (*ped2*). For each sample, 10 μg of total protein were subjected to SDS–PAGE. Immunoblot analysis was performed using the antibody raised against *At*Pex14p. Markers are shown on the right with molecular masses in kDa.

1999; Will *et al.*, 1999), and is most similar to that of human Pex14p (Figure 2). Therefore we decided to call it *At*Pex14p. *At*Pex14p contains at lease two hydrophobic segments and a coiled-coil region (Figure 2). Although two yeast Pex14p are known to contain the class II SH3 ligand consensus sequence (Albertini *et al.*, 1997), *At*Pex14p does not contain such a motif. In addition, there is no obvious PTS.

Subcellular localization of AtPex14p

To analyze the subcellular localization of *At*Pex14p, we prepared an antiserum raised against a fusion protein containing a partial amino acid sequence of *At*Pex14p (Met1–Pro100). This antiserum recognized a 75 kDa protein in wild-type plant (Figure 3, WT), while no cross-reactive band was detected in the *ped2* mutant (Figure 3, *ped2*). These data indicate that *At*Pex14p is the 75 kDa protein.

To investigate the subcellular localization of Pex14p in plant cells, homogenates prepared from pumpkin etiolated cotyledons were subjected to sucrose density gradient centrifugation. Fractions thus obtained were analyzed using an immunoblotting technique with the antibody raised against *At*Pex14p (Figure 4A). The 75 kDa protein was detected in fractions 23–25, whose densities were 1.25 g/cm^3. These fractions also contained other glyoxysomal marker enzymes, such as isocitrate lyase and catalase, while they did not contain a mitochondrial marker enzyme (cytochrome *c* oxidase) activity (Figure 4A and B).

Figure 4C represents the result of the extensive subfractionation studies performed by the treatment of intact glyoxysomes with various solutions. Pex14p and ascorbate peroxidase, a marker enzyme for peroxisomal membranes (Yamaguchi *et al.*, 1995), were found in the

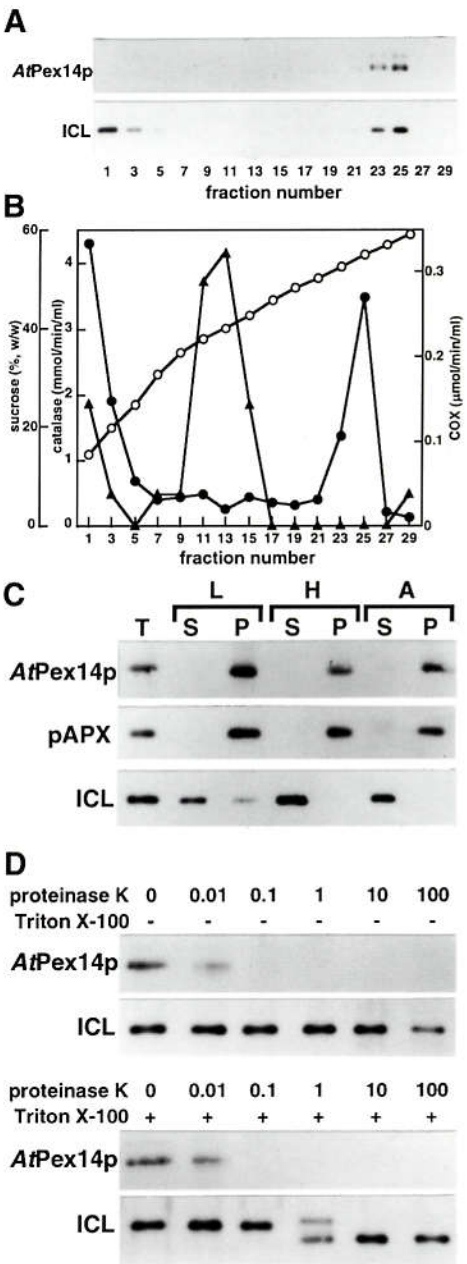

Fig. 4. Subcellular localization of Pex14p in pumpkin etiolated cotyledons. (**A**) Subcellular fractionation of etiolated pumpkin cotyledons was performed by 30–60% sucrose density gradient centrifugation. Fraction number 1 represents the top fraction of the gradient. Pex14p and isocitrate lyase in each fraction were detected by immunoblot analyses using antibody raised against *At*Pex14p (*At*Pex14p) and isocitrate lyase (ICL). (**B**) Sucrose concentration (open circles), activities of catalase (filled circles) and cytochrome *c* oxidase (COX; filled triangles) in the same fractions as used in (A) were also measured. (**C**) Intact glyoxysomes were resuspended in either low salt buffer (L), high salt buffer (H) or alkaline solution (A). Each buffer consists of 10 mM HEPES–KOH pH 7.2, 500 mM KCl with 10 mM HEPES–KOH pH 7.2 and 0.1 M Na_2CO_3, respectively. These samples were then centrifuged and separated into soluble (S) and insoluble (P) fractions. T represents total proteins of the intact glyoxysomes. Pex14p (*At*Pex14p), peroxisomal ascorbate peroxidase (pAPX) and isocitrate lyase (ICL) were detected by immunoblot analysis. (**D**) The intact glyoxysomes were treated with various concentrations of proteinase K in the absence (–) or presence (+) of Triton X-100. The concentration of proteinase K is indicated in μg/ml on the top of each lane. Pex14p (*At*Pex14p) and isocitrate lyase (ICL) were detected by immunoblot analysis.

insoluble fraction even after treatment with alkaline solution. However, isocitrate lyase, a marker enzyme for the glyoxysomal matrix, was dissolved completely both in high-salt buffer and alkaline solution. In addition, Pex14p in intact glyoxysomes was sensitive to the digestion of proteinase K both in the absence and presence of Triton X-100, whereas isocitrate lyase was degraded only in the presence of Triton X-100 (Figure 4D). Overall results suggest that the 75 kDa protein is a peroxisomal membrane-associated protein, and that at least a part of the polypeptide is located in the cytosol.

Intracellular transport of PTS1-containing proteins in the ped2 mutant

To analyze the intracellular transport of PTS1-containing proteins in the *ped2* mutant, we generated plants expressing a jellyfish green fluorescent protein (GFP)–PTS1 fusion protein (GFP–PTS1) in a *ped2* background, as described previously (Mano *et al.*, 1999). GFP–PTS1 consisted of GFP fused to a dodecapeptide containing serine-lysine-leucine at the C-terminal end. These plants were created by outcrossing the *ped2* mutant with transgenic *Arabidopsis* expressing GFP–PTS1. Additional control plants were created by outcrossing the *ped2* mutant with transgenic *Arabidopsis* expressing only GFP. When GFP–PTS1 is expressed in cells of the F_3 progeny that are homozygous for the *ped2* allele, green fluorescence was observed both in the periphery of the cells (Figure 5A, arrow) and in small spots distributed diffusely throughout the periphery (Figure 5A, arrowhead). The fluorescence detected in the periphery indicated that a part of the GFP–PTS1 remains in the cytosol, since GFP without PTS1 showed a similar fluorescent pattern in the *ped2* mutant (Figure 5B, arrow) and in wild-type plants (data not shown). In Figure 5A and B, the dark space surrounded by the cytosol corresponds to a central vacuole. The fluorescent spots distributed in the cytosol indicate that a significant amount of GFP–PTS1 was recognized correctly and transported into the peroxisomes in the cells of the *ped2* mutant. In contrast, only punctate fluorescence was observed when GFP–PTS1 was expressed in wild-type plants (Figure 5C). These data indicate that the ability for intracellular transport of PTS1-containing proteins is reduced in the *ped2* mutant.

Intracellular transport of PTS2-containing proteins in the ped2 mutant

To analyze intracellular transport of PTS2-containing proteins in the *ped2* mutant, two PTS2-containing proteins, 3-ketoacyl CoA thiolase (Figure 6A, *ped2*) and malate dehydrogenase (Figure 6B, *ped2*), were analyzed in 3- and 5-day-old etiolated cotyledons and 7-day-old green cotyledons by using an immunoblotting technique. As shown in Figure 6A, 3-day-old etiolated cotyledons contained two types of 3-ketoacyl CoA thiolase. One of these corresponds to the mature form of 3-ketoacyl CoA thiolase (45 kDa) (Figure 6A, arrowhead), whereas the other was an additional protein with a higher molecular mass (48 kDa) (Figure 6A, arrow). We have demonstrated previously that the larger protein corresponded to the precursor form of 3-ketoacyl CoA thiolase that accumulated in the cytosol (Kato *et al.*, 1996a; Hayashi *et al.*, 1998). In addition, 3-day-old etiolated cotyledons contained the mature form of malate dehydrogenase (33 kDa) (Figure 6B, arrowhead) and the precursor form of the enzyme (37 kDa) (Figure 6B, arrow). In contrast, the wild-type plants did not contain detectable amounts of the precursor proteins during any stages of post-germinative growth (Figure 6A and B, WT). The precursor proteins detected in 3-day-old etiolated cotyledons of the *ped2* mutant rapidly disappeared, whereas the amounts of the mature proteins remained at similar levels during subsequent seedling growth. 3-Ketoacyl CoA thiolase and malate dehydrogenase are known to be actively synthesized in cells of etiolated cotyledons but not in the green cotyledons (Kato *et al.*, 1996a, 1998). Accumulation of the precursors for PTS2-containing proteins in the *ped2* mutant occurred only during the period of active protein

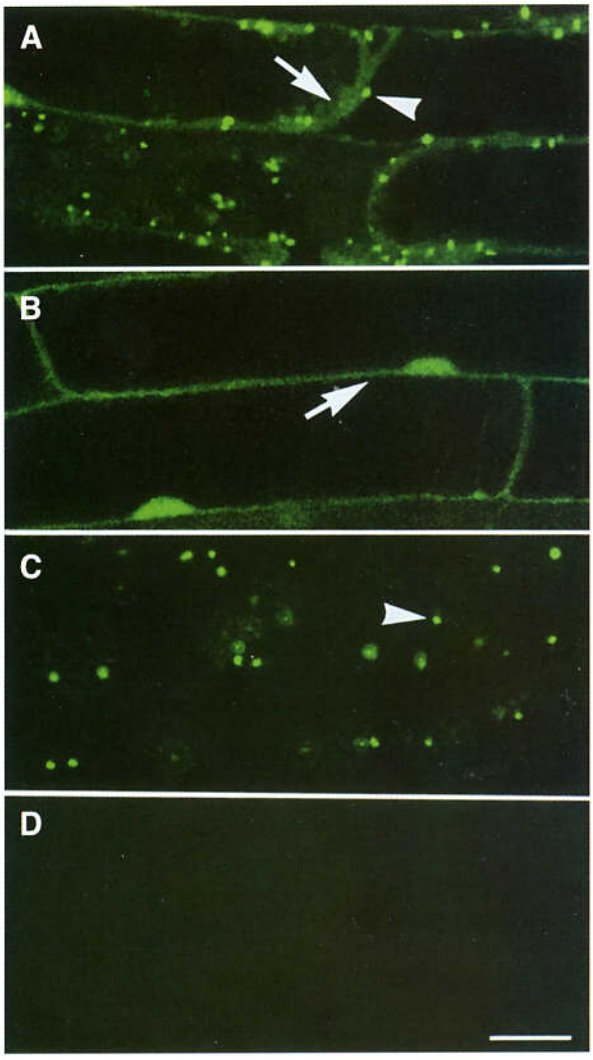

Fig. 5. Subcellular localization of GFP–PTS1 fusion protein in *ped2* mutant. Seedlings were grown under continuous illumination for 10 days. Images of the green fluorescence derived from GFP in root cells were taken by a confocal laser microscope as single optical sections. (**A**) Subcellular localization of GFP–PTS1 expressed in the cells of a *ped2* mutant. (**B**) Subcellular localization of GFP expressed in the cells of a *ped2* mutant. (**C**) Subcellular localization of GFP–PTS1 expressed in the cells of a wild-type plant. (**D**) No fluorescence was observed in non-transformed cell of a *ped2* mutant. Arrowheads indicate fluorescence detected in peroxisomes, whereas the arrows indicate fluorescence detected in the cytosol. Bar in (D), 20 μm. Magnifications of (A)–(D) are the same.

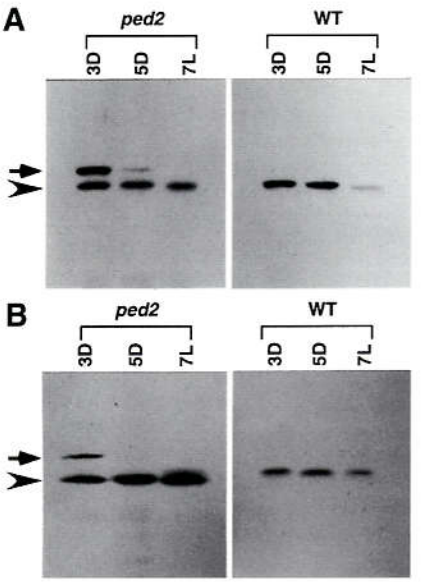

Fig. 6. Immunodetection of thiolase and malate dehydrogenase in cotyledonary cells of *ped2* mutants. Seedlings of the *ped2* mutant (*ped2*) and wild-type plant (WT) were grown in continuous darkness for 3 days (3D), 5 days (5D) or under continuous illumination for 7 days (7L). Ten micrograms of total protein prepared from the cotyledons were subjected to immunoblotting using an antibody raised against 3-ketoacyl CoA thiolase (**A**) and malate dehydrogenase (**B**). Arrowheads indicate the positions of the mature proteins, whereas the arrows indicate the positions of the precursors.

synthesis. These data indicate that the *ped2* mutant has reduced activity for the intracellular transport of PTS2-containing proteins, and is not able to import all of the PTS2-containing proteins when these proteins are actively synthesized.

Morphology of glyoxysomes, leaf peroxisomes and unspecialized peroxisomes in the ped2 mutant

Figure 7 shows an immunoelectron microscopic analysis of various peroxisomes in wild-type plants and the *ped2* mutant. As mentioned above, there are three types of plant peroxisomes: glyoxysomes, leaf peroxisomes and non-specialized peroxisomes. In wild-type plants, these peroxisomes have similar morphologies (Nishimura *et al.*, 1996). As shown in Figure 7A, glyoxysomes found in the 5-day-old etiolated cotyledons of wild-type plants are ~0.5 μm in diameter and have a round or oval shape containing a uniform matrix. The glyoxysomes contain enzymes for fatty acid β-oxidation. When cells were immunogold labeled using antibodies raised against one of these enzymes, 3-ketoacyl CoA thiolase, the gold particles were exclusively localized on the glyoxysomes (Figure 7A). In contrast, the peroxisomes in the *ped2* mutant showed an abnormal morphology (Figure 7B–E). Glyoxysomes found in the etiolated cotyledons of the *ped2* mutant were shrunken and not round (Figure 7B). Therefore, they looked very different from the glyoxysomes of wild-type plants. A small but significant number of gold particles were detected when the glyoxysomes of the *ped2* mutant were stained with antibodies raised against 3-ketoacyl CoA thiolase. In contrast, the number of gold particles detected in the cytosol was not significant, in spite of the fact that the precursor of 3-ketoacyl CoA

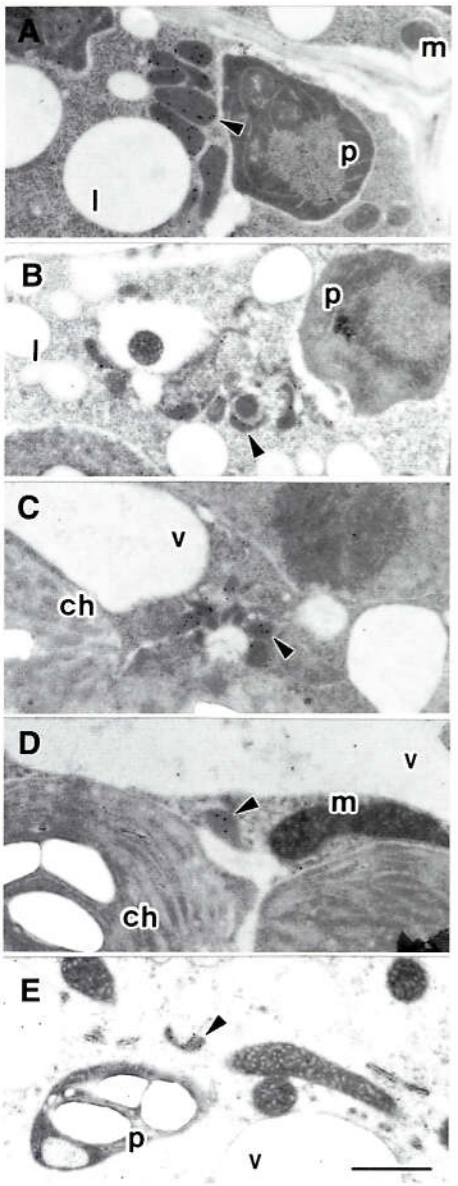

Fig. 7. Electron microscopic analysis of peroxisomes in the cells of the *ped2* mutant. (**A**) Etiolated cotyledon of wild-type *Arabidopsis*, grown for 5 days in darkness, was stained with 3-ketoacyl CoA thiolase-specific antibody. (**B**) Etiolated cotyledon of *ped2* mutant, grown for 5 days in darkness, was stained with 3-ketoacyl CoA thiolase-specific antibody. (**C**) Green cotyledon of *ped2* mutant, grown for 7 days under continuous illumination, was stained with hydroxypyruvate reductase-specific antibody. (**D**) Leaf of *ped2* mutant, grown for 14 days under continuous illumination, was stained with hydroxypyruvate reductase-specific antibody. (**E**) Root of *ped2* mutant, grown for 14 days under continuous illumination, was stained with catalase-specific antibody. Arrowhead, peroxisome; m, mitochondrion; l, lipid body; p, plastid; ch, chloroplast; v, vacuole. Bar in (E), 1 μm. Magnification of (A)–(E) is the same.

thiolase is accumulated in the cytosol. This may be because the concentration of the precursor that accumulated in the cytosol was not sufficient to be clearly detected. A similar abnormal morphology was detected in leaf peroxisomes found in cells of green cotyledons (Figure 7C) and leaves (Figure 7D), as well as in unspecialized peroxisomes found in cells of root (Figure 7E). Since the leaf peroxisomes contain photorespiration enzymes, such as hydroxypyruvate reductase, the leaf peroxisomes were

stained using antibodies raised against hydroxypyruvate reductase (Figure 7C and D). However, fewer gold particles were detected in the leaf peroxisomes of the *ped2* mutant than in those of the wild-type plant (data not shown). A similar phenomenon was observed when unspecialized peroxisomes in root cells were stained with antibodies raised against catalase (Figure 7E). These data indicate that all three kinds of peroxisome in the *ped2* mutant have abnormal morphologies, and contain fewer enzymes than do the peroxisomes of wild-type plants.

Reduced activity of photorespiration in ped2 mutant

When *ped2* mutants were grown in a normal atmosphere (36 Pa CO_2), they always had yellow-green leaves and showed a dwarf phenotype (Figure 8A, *ped2*/air) compared with wild-type plants (Figure 8A, WT/air). No such phenotypes were observed in transgenic *ped2* mutants transformed with the wild-type *PED2* gene (data not shown). These phenotypes were recovered when the *ped2* mutant was grown under high CO_2 conditions (1000 Pa CO_2) (Figure 8A, *ped2*/CO_2). A similar phenomenon was observed in mutants with alterations in the photorespiratory pathway (Somerville and Ogren, 1982). Since some enzymes involved in the photorespiratory pathway are PTS1-containing proteins that are located in leaf peroxisomes, we assumed that these effects are induced by the reduced activity of photorespiration in the *ped2* mutant. We tested this hypothesis by measuring the maximal quantum yield of photosystem II, which can be estimated from the ratio of the variable fluorescence of dark-adapted chlorophyll a to the maximum fluorescence (F_v/F_m) (Krause, 1988; Franklin *et al.*, 1992; Öquist *et al.*, 1992). We compared the F_v/F_m of dark-adapted leaves of the *ped2* mutant with that of wild-type plants. We also compared it with the F_v/F_m of the *stm* mutant, which lacks one of the enzymes for photorespiration, a mitochondrial serine transhydroxymethylase (Somerville and Ogren, 1981).

To reduce the effect of photoinhibition, plants were grown for 3 weeks in an atmosphere containing high CO_2 (1000 Pa) under low light (50 μE/m²/s). Under these conditions, the *ped2* mutant, the wild-type plant and the *stm* mutant showed normal growth, and had similar F_v/F_m values of ~0.8 (Figure 8B, 0 min). These plants were then transferred to a normal atmosphere (36 Pa CO_2), where they were illuminated with a strong light (450 μE/m²/s). Under these conditions, ribulose bisphosphate carboxylase/oxygenase (RuBisCO) has an oxygenase activity in addition to its carboxylase activity, which is necessary for CO_2 fixation in photosynthesis. Phosphoglycolate, a byproduct of the oxygenase reaction, is metabolized by

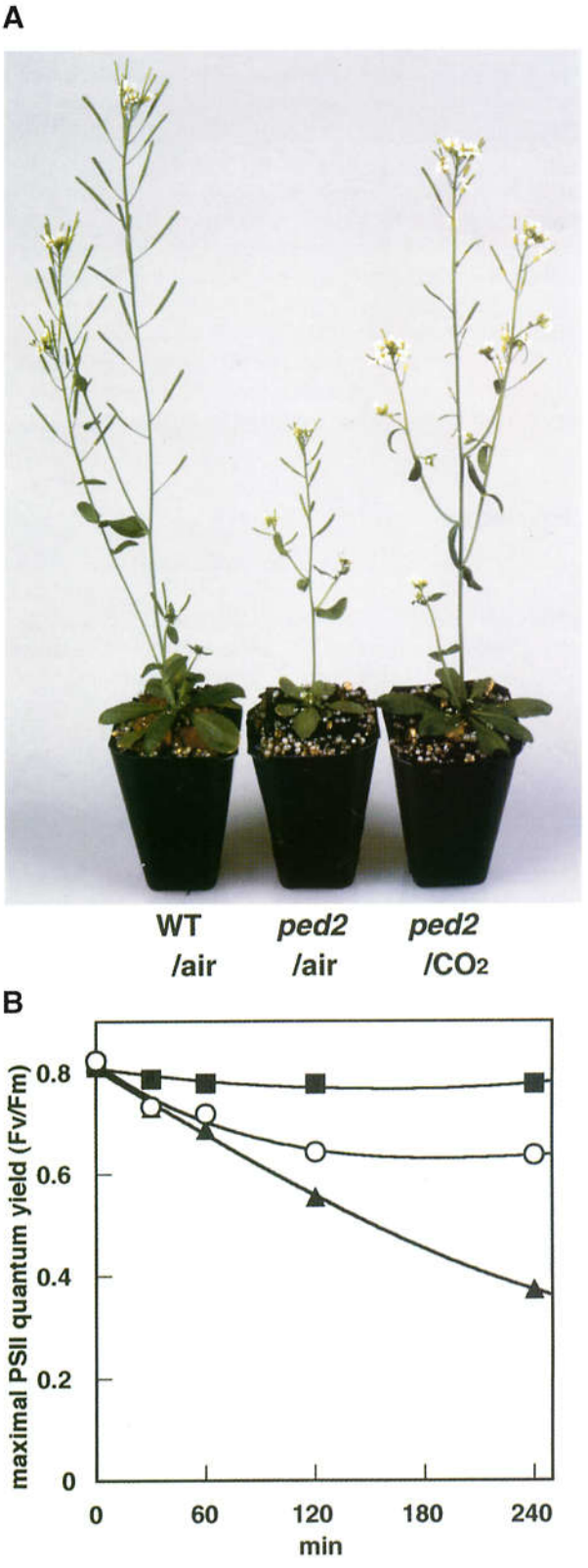

Fig. 8. Reduced activity of photorespiration in *ped2* mutant. (**A**) Effect of CO_2 on the growth of *ped2* mutant. Wild-type *Arabidopsis* (WT/air) and *ped2* mutant (*ped2*/air) were grown for 8 weeks in a normal atmosphere (36 Pa CO_2) under constant illumination (100 μE/m²/s). The *ped2* mutant was also grown for 8 weeks in an atmosphere containing 1000 Pa CO_2 (*ped2*/CO_2) under constant illumination (50 μE/m²/s). (**B**) Effect of strong irradiation on maximal quantum yield of photosystem II (F_v/F_m). Wild-type *Arabidopsis* (filled squares), *ped2* mutant (open circles) and the *stm* mutant (filled triangles) were grown for 3 weeks in an atmosphere containing 1000 Pa CO_2 under low light (50 μE/m²/s). These plants were illuminated with strong light (450 μE/m²/s) in a normal atmosphere (36 Pa CO_2). Maximum quantum yield of photosystem II (F_v/F_m) of the leaves at each defined time was measured after these plants were kept for 30 min in darkness. Each point represents the average F_v/F_m measured in six leaves of independent plants. The standard error of each point is <0.01.

the photorespiration enzymes, and finally returned to the Calvin–Benson cycle. Therefore, the F_v/F_m of the wild-type plants would not be expected to change after the strong illumination, since photorespiration operates properly and photoinhibition is not induced under such conditions. This is what was observed (Figure 8B, filled squares). In contrast, the F_v/F_m ratios of the *ped2* and *stm* mutants decreased after the transfer to the same conditions (Figure 8B, open circles and filled triangles). These mutants were unable to maintain sufficient activity of the Calvin–Benson cycle under these conditions, because they could not metabolize phosphoglycolate due to the defect in photorespiration. The reduced activity of the Calvin–Benson cycle induced an excessive supply of energy from the light reaction of photosynthesis, and caused photoinhibition under high light irradiation. The imbalance between the light reaction and the Calvin–Benson cycle might have been responsible for the observed reduction of F_v/F_m. After 120 min of illumination, F_v/F_m of the *ped2* mutant reached a plateau (F_v/F_m = 0.64), while that of the *stm* mutant kept decreasing. These results suggest that the activity for photorespiration in the *ped2* mutant is partially inhibited, but is stronger than that in the *stm* mutant.

Discussion

The chemically induced *ped2* strain is one of a series of *Arabidopsis thaliana* mutants that has defects in glyoxysomal fatty acid β-oxidation. Positional cloning and subsequent analyses revealed that the *PED2* gene encodes *At*Pex14p, a 75 kDa peroxisomal membrane protein, whose amino acid sequence is most similar to human Pex14p. At present, there is no other gene that encodes a protein similar to *At*Pex14p in *Arabidopsis* genome database. Recently, Lopez-Huertas *et al.* (1999) reported that antibody raised against human Pex14p recognizes a 66 kDa protein in the sunflower glyoxysomal membrane.

Recent analyses of yeast mutants allowed the identification of >20 PEX genes and their products, peroxins (Subramani, 1998). Among these peroxins, it has been suggested that Pex14p forms a protein complex in the peroxisomal membrane with other peroxins, such as Pex13p and Pex17p (Albertini *et al.*, 1997; Huhse *et al.*, 1998). This protein complex is sometimes called a docking protein complex, since it may control intracellular transport of both PTS1- and PTS2-containing proteins (Subramani, 1998). Pex14p binds directly to both PTS1 receptor (Pex5p) and PTS2 receptor (Pex7p) (Albertini *et al.*, 1997). Thus, Pex14p is believed to be a point of convergence of the PTS1-dependent and PTS2-dependent peroxisomal protein import pathway in mammalian and fungal cells. The present data strongly suggest that the *At*Pex14p is a key component of the peroxisomal protein import machinery that determines the intracellular transport of both PTS1-containing and PTS2-containing proteins in plant cells. PTS1 receptors have been identified from several plants (Brickner *et al.*, 1998; Kragler *et al.*, 1998; Wimmer *et al.*, 1998), and a PTS2 receptor has been identified from *Arabidopsis* (Schumann *et al.*, 1999). Whether *At*Pex14p binds directly to both PTS1 and PTS2 receptors remains to be tested.

In higher plant cells, all enzymes involved in fatty acid β-oxidation and the glyoxylate cycle except cytosolic aconitase are localized predominantly in glyoxysomes (Hayashi, 2000). Among these enzymes, short-chain acyl CoA oxidase, multifunctional enzyme, malate synthase and isocitrate lyase are PTS1-containing proteins, whereas long-chain acyl CoA oxidase, 3-ketoacyl CoA thiolase, malate dehydrogenase and citrate synthase are PTS2-containing proteins (Hayashi, 2000). The defect in the *PED2* gene resulted in reduced amounts of enzymes in glyoxysomes, which reduced the ability of glyoxysomes to carry out fatty acid β-oxidation. The loss of glyoxysomal matrix proteins also caused a defect in the morphology of the glyoxysomes. The *PEX14* disruption mutant of *Hansenula polymorpha* was also shown to lack intact peroxisomes but it contained several small membranous vesicles (Komori *et al.*, 1997).

Fatty acid β-oxidation is an important physiological function of glyoxysomes during germination and the early stage of post-germinative growth, since it metabolizes lipid reserves in the seeds to produce sucrose, which is necessary for seedling growth (Beevers, 1982). However, this activity decreases rapidly along with the functional transformation of glyoxysomes into leaf peroxisomes that occurs during subsequent seedling growth. Since the *ped2* mutant has been identified by its defect in fatty acid β-oxidation, we had assumed that the defect was limited to glyoxysomes. However, electron microscopic analyses indicated that the *ped2* mutant had morphological defects not only in glyoxysomes but also in leaf peroxisomes and unspecialized peroxisomes. In addition, we found that the *ped2* mutant had defects in the physiological function of leaf peroxisomes, i.e. in photorespiration. Measurements of maximal quantum yield of photosystem II suggested that the activity of photorespiration in the *ped2* mutant is lower than that in wild-type plants but higher than that in the *stm* mutant. Leaf peroxisomes contain enzymes for photorespiration such as hydroxypyruvate reductase and glycolate oxidase (Tolbert, 1982). These enzymes contain PTS1 at their C-termini (Tsugeki *et al.*, 1993; Hayashi *et al.*, 1996b; Mano *et al.*, 1997, 1999). Since the *ped2* mutant has a weakened ability to import PTS1-containing proteins, leaf peroxisomes in the mutant contain reduced amounts of these enzymes. Although photorespiration consists of many enzymic reactions located not only in leaf peroxisomes, but also in chloroplasts and mitochondria (Tolbert, 1982), reduced amounts of leaf peroxisomal enzymes diminish the overall activity of photorespiration in the *ped2* mutant. The partial inhibition of photorespiration in the *ped2* mutant is in good agreement with the observation that the *ped2* mutant has a reduced ability to import PTS1- and PTS2-containing proteins.

Functional differentiation is a remarkable feature of peroxisomes in higher plant cells (Nishimura *et al.*, 1996). In order to perform different physiological functions, glyoxysomes, leaf peroxisomes and unspecialized peroxisomes contain different sets of enzymes (Beevers, 1979; Tolbert, 1982). However, the present data suggest that each of the plant peroxisomes imports these enzymes using the same protein import machinery that involves *At*Pex14p, and that the pleiotropic phenotype of the *ped2* mutant is caused by a defect in a single gene product, *At*Pex14p.

Materials and methods

Plant materials and growth conditions

Identification of the *ped2* mutant of *Arabidopsis thaliana* has been described previously (Hayashi *et al.*, 1998). Progenies that had been back-crossed twice were used in this study. *Arabidopsis thaliana* ecotype Landsberg *erecta* was used as the wild-type plant. Seeds of the *stm* mutant were kindly provided by the *Arabidopsis* Biological Resource Center, Ohio State University. Plants were grown under a 16 h light (100 $\mu E/m^2/s$)/8 h dark cycle at 22°C.

Fine mapping of the PED2 gene

The *ped2* mutant was outcrossed to the wild-type plant [ecotype Columbia (Col-0)]. F_2 progeny, obtained by self-fertilization of the F_1 plants, were germinated on growth medium without sucrose (Hayashi *et al.*, 1998). Three hundred and ten seedlings that could not expand green cotyledons and leaves on the growth medium were recovered after transferring these seedlings to medium containing sucrose. The genomic DNA of these F_2 plants was individually isolated. Recombinations that occurred between the *PED2* locus and the molecular markers were scored by using the CAPS mapping procedure (Konieczny and Ausubel, 1993). The molecular marker, LFY3, has been described previously (Konieczny and Ausubel, 1993). The nucleotide sequences of the primers and the enzymes for other molecular markers are as follows. MRG21-3: GAGCATCGAAATGCGTCACG and GTCTTCTTTGATCCGATT-AGACCG, *Rsa*I; MQB2-1: TGACTTGCTGTCTGAGGTTCC and TCACTGATTCCACCGATTCC, *Rsa*I; MQB2-4: CGCCTTGATTGT-TGCTTCTACC and CGTGTCAAGGCCAATAGTCC, *Hin*fI; MHJ24-4: TGGTCCATATTCCTGAAGACG and CGCTCTTCACAATGATC-TGC, *Nco*I.

DNA sequencing analyses

DNA and RNA extraction, sequence determination and routine molecular biological techniques were performed by standard techniques (Sambrook *et al.*, 1989). For identification of the *PED2* gene, the DNA fragments were amplified by the PCR using 100 ng of genomic DNA isolated from wild-type plants and the *ped2* mutant as templates, a 5′ primer (CTTCCAAGGTTAGTGAGCTGC) and a 3′ primer (GGCTCTTCACT-CATGCTTCC). A *PED2* cDNA clone was generated by RT–PCR with total RNA isolated from 7-day-old cotyledons of wild-type plants using a 5′ primer (CTTCCAAGGTTAGTGAGCTGC) and a 3′ primer (GTT-TTTAGTTCCCTTCCTGGC). Analysis of the nucleotide sequences of those DNA fragments was performed according to a previous report (Hayashi *et al.*, 1998).

Construction of clone for complementation studies and plant transformation

The P1 clone, MQB2, which contains the *PED2* gene was kindly sent from the Kazusa DNA Institute, Chiba, Japan. *Xho*I fragments obtained after complete digestion of MQB2 DNA were subcloned into the *Xho*I site of Bluescript KS+. The *Xho*I fragment (7734 bp) that had been inserted in the vector was recovered, and then ligated to the *Xho*I site of pBI121Δ35S. A plant binary vector, pBI121Δ35S, was constructed from pBI121 (Clontech, Palo Alto, CA) by replacing a *Hin*dIII–*Sac*I fragment with a polylinker consisting of *Hin*dIII, *Xho*I, *Sma*I, *Spe*I and *Sac*I sites. The vector containing the *Xho*I fragment was designated as pBI-PED2. pBI-PED2 was introduced into the *ped2* mutant by the vacuum infiltration method (Bechtold *et al.*, 1993) using *Agrobacterium tumefaciens* (strain C58C1Rif^R) harboring pBI-PED2. T_3 transformants harboring homozygous transgenes were analyzed by plating on either growth medium containing 0.2 μg/ml 2,4-DB or growth medium without sucrose.

Immunoblotting

A DNA fragment encoding from Met1 to Pro100 of *At*Pex14p was amplified from the *PED2* cDNA by PCR using a 5′ primer (GGGAGC-TCGCTGCTATGGCGACT) and a 3′ primer (CCCTCGAGTTAAG-GAACACGGCGGAAAGCTT). The amplified DNA was inserted into the pET32 vector (Novagen, Madison, WI). A fusion protein was synthesized in *Escherichia coli* cells, and used for the production of rabbit antibody raised against *At*Pex14p according to the method reported previously (Hayashi *et al.*, 1999). We also used antibodies raised against pumpkin 3-ketoacyl CoA thiolase (Kato *et al.*, 1996b), pumpkin malate dehydrogenase (Kato *et al.*, 1998), caster bean isocitrate lyase (Maeshima *et al.*, 1988) and pumpkin ascorbate peroxidase (Yamaguchi *et al.*, 1995). Immunoblot analyses were performed according to protocols described previously (Hayashi *et al.*, 1998).

Subcellular fractionation of etiolated pumpkin cotyledons and analyses of the intact glyoxysomes

Subcellular fractionation of 5-day-old pumpkin etiolated cotyledons (2 g, fresh weight) was performed using 30–60% (w/w) sucrose density gradient centrifugation according to the method previously reported (Hayashi *et al.*, 1999). After the centrifugation, fractions of 0.5 ml were collected, and used for immunoblot analyses and enzyme assays.

Isolation of intact glyoxysomes from 5-day-old pumpkin etiolated cotyledons (100 g, fresh weight) by Percoll density gradient centrifugation has also been reported previously (Yamaguchi *et al.*, 1995). The intact glyoxysomes (250 μg total protein) were resuspended in 200 μl of either low salt buffer, high salt buffer or alkaline solution. Each solution consists of 10 mM HEPES–KOH pH 7.2, 500 mM KCl with 10 mM HEPES–KOH pH 7.2 and 0.1 M Na_2CO_3 pH 11, respectively. After centrifugation at 100 000 *g* for 30 min, these samples were separated into supernatant and pellet. The pellets were resuspended in 200 μl of 100 mM HEPES–KOH pH 7.2. In some experiments, the intact glyoxysomes (250 μg total protein) were incubated in buffer containing 10 mM HEPES–KOH pH 7.2, 1 mM EDTA and 0.3 M mannitol with an appropriate concentration of proteinase K for 30 min at 4°C in the presence or absence of 5% Triton X-100. The reactions were terminated by the addition of 5 mM phenylmethylsulfonyl fluoride.

Detection of fluorescence in ped2 mutants expressing GFP–PTS1 and GFP

To produce *ped2* mutants expressing GFP–PTS1 and GFP, *ped2* mutants were outcrossed to transgenic *Arabidopsis* expressing GFP–PTS1 or GFP. Generation of these kanamycin-resistant transgenic plants was reported previously (Mano *et al.*, 1999). Homozygous F_3 plants (*ped2*/*ped2*, GFP–PTS1/GFP–PTS1 and *ped2*/*ped2*, GFP/GFP) were identified by determining the sucrose requirement and the kanamycin resistance during post-germinative growth. The homozygous F_3 plants and transgenic wild-type plant expressing GFP were grown for 10 days on growth medium under constant illumination. Roots of these plants were mounted under coverslips with phosphate-buffered saline. The specimens were examined using a TCS NT laser-scanning confocal microscope under the same condition with ×40 objective lens and an FITC filter set (Leica Japan, Tokyo, Japan).

Immunoelectron microscopic analysis

Five-day-old etiolated cotyledons, 7-day-old green cotyledons, 14-day-old leaves and 14-day-old roots were harvested from plants that were grown for the appropriate number of days in darkness or under constant illumination. Preparation of the ultrathin sections, and the immuno-electron microscopic analyses were performed according to the protocol described previously (Hayashi *et al.*, 1998).

Measurements of maximum quantum yield of photosystem II (F_v/F_m)

To reduce the effect of photoinhibition, plants were grown for 4 weeks in an atmosphere containing 1000 Pa CO_2 under low light (50 $\mu E/m^2/s$). These plants were then illuminated with strong light (450 $\mu E/m^2/s$) for 0, 30, 60, 120 and 240 min in a normal atmosphere (36 Pa CO_2). After the end of each illumination period, plants were kept for 30 min in the dark. The ratio of variable fluorescence to maximum fluorescence (F_v/F_m) was automatically calculated from the result of the modulated chlorophyll fluorescence emission from the upper surface of dark-adapted leaves, which was measured using a pulse amplitude modulation fluorometer (Mini-PAM; H.Walz, Effeltrich, Germany).

Acknowledgements

This work was supported in part by a grant from the Research for the Future Program of the Japanese Society for the Promotion of Science (JSPS-RFTF96L00407), and by grants-in-aid for scientific research from the Ministry of Education, Science and Culture of Japan (12440231 to M.N. and 12640625 to M.H.) and by a grant from the Nissan Science Foundation (Tokyo, Japan) to M.H.

References

Albertini,M., Rehling,P., Erdmann,R., Girzalsky,W., Kiel,J.A.K.W., Veenhuis,M. and Kunau,W.H. (1997) Pex14p, a peroxisomal membrane protein binding both receptors of the two PTS-dependent import pathways. *Cell*, **89**, 83–92.

Bechtold,N., Ellis,J. and Pelletier,G. (1993) *In planta Agrobacterium* mediated gene transfer by infiltration of adult *Arabidopsis thaliana* plants. *C. R. Acad. Sci.*, **316**, 1194–1199.

Beevers,H. (1979) Microbodies in higher plants. *Annu. Rev. Plant Physiol.*, **30**, 159–193.

Beevers,H. (1982) Glyoxysomes in higher plants. *Ann. N Y Acad. Sci.*, **386**, 243–251.

Brickner,D.G., Brickner,J.H. and Olsen,J.J. (1998) Sequence analysis of a cDNA encoding Pex5p, a peroxisomal targeting signal type 1 receptor from *Arabidopsis*. *Plant Physiol.*, **118**, 330.

Brocard,C., Lametschwandtner,G., Koudelka,R. and Hartig,A. (1997) Pex14p is a member of the protein linkage map of Pex5p. *EMBO J.*, **16**, 5491–5500.

De Bellis,L. and Nishimura,M. (1991) Development of enzymes of the glyoxylate cycle during senescence of pumpkin cotyledons. *Plant Cell Physiol.*, **32**, 555–561.

Flynn,C.R., Mullen,R.T. and Trelease,R.N. (1998) Mutational analyses of a type 2 peroxisomal targeting signal that is capable of directing oligomeric protein import into tobacco BY-2 glyoxysomes. *Plant J.*, **16**, 709–720.

Franklin,L.A., Levavasseur,G., Osmond,C.B., Henley,W.J. and Ramus,J. (1992) Two components of onset and recovery during photoinhibition of *Ulva rotundata*. *Planta*, **187**, 399–408.

Gietl,C., Faber,K.N., Vanderklei,I.J. and Veenhuis,M. (1994) Mutational analysis of the N-terminal topogenic signal of watermelon glyoxysomal malate dehydrogenase using the heterologous host *Hansenula polymorpha*. *Proc. Natl Acad. Sci. USA*, **91**, 3151–3155.

Hayashi,H., De Bellis,L., Ciurli,A., Kondo,M., Hayashi,M. and Nishimura,M. (1999) A novel acyl-CoA oxidase that can oxidize short-chain acyl-CoA in plant peroxisomes. *J. Biol. Chem.*, **274**, 12715–12721.

Hayashi,M. (2000) Plant peroxisomes: molecular basis of the regulation of their functions. *J. Plant Res.*, **113**, 103–109.

Hayashi,M., Aoki,M., Kato,A., Kondo,M. and Nishimura,M. (1996a) Transport of chimeric proteins that contain a carboxy-terminal targeting signal into plant microbodies. *Plant J.*, **10**, 225–234.

Hayashi,M., Tsugeki,R., Kondo,M., Mori,H. and Nishimura,M. (1996b) Pumpkin hydroxypyruvate reductases with and without a putative C-terminal signal for targeting to microbodies may be produced by alternative splicing. *Plant Mol. Biol.*, **30**, 183–189.

Hayashi,M., Aoki,M., Kondo,M. and Nishimura,M. (1997) Changes in targeting efficiencies of proteins to plant microbodies caused by amino acid substitutions in the carboxy-terminal tripeptide. *Plant Cell Physiol.*, **38**, 759–768.

Hayashi,M., Toriyama,K., Kondo,M. and Nishimura,M. (1998) 2,4-dichlorophenoxybutyric acid-resistant mutants of *Arabidopsis* have defects in glyoxysomal fatty acid β-oxidation. *Plant Cell*, **10**, 183–195.

Huhse,B., Rehling,P., Albertini,M., Blank,L., Meller,K. and Kunau,W.H. (1998) Pex17p of *Saccharomyces cerevisiae* is a novel peroxin and component of the peroxisomal protein translocation machinery. *J. Cell Biol.*, **140**, 49–60.

Kato,A., Hayashi,M., Kondo,M. and Nishimura,M. (1996a) Targeting and processing of a chimeric protein with the N-terminal presequence of the precursor to glyoxysomal citrate synthase. *Plant Cell*, **8**, 1601–1611.

Kato,A., Hayashi,M., Takeuchi,Y. and Nishimura,M. (1996b) cDNA cloning and expression of a gene for 3-ketoacyl-CoA thiolase in pumpkin cotyledons. *Plant Mol. Biol.*, **31**, 843–852.

Kato,A., Takeda-Yoshikawa,Y., Hayashi,M., Kondo,M., Hara-Nishimura,I. and Nishimura,M. (1998) Glyoxysomal malate dehydrogenase in pumpkin: cloning of a cDNA and functional analysis of its presequence. *Plant Cell Physiol.*, **39**, 186–195.

Kato,A., Hayashi,M. and Nishimura,M. (1999) Oligomeric proteins containing N-terminal targeting signals are imported into peroxisomes in transgenic *Arabidopsis*. *Plant Cell Physiol.*, **40**, 586–591.

Komori,M., Rasmussen,S.W., Kiel,J.A.K.W., Baerends,R.J.S., Cregg,J.M., Van der Klei,I.J. and Veenhuis,M. (1997) The *Hansenula polymorpha PEX14* gene encodes a novel peroxisomal membrane protein essential for peroxisome biogenesis. *EMBO J.*, **16**, 44–53.

Konieczny,A. and Ausubel,F.M. (1993) A procedure for mapping *Arabidopsis* mutations using co-dominant ecotype-specific PCR-based markers. *Plant J.*, **4**, 403–410.

Kragler,F., Lametschwandtner,G., Christmann,J., Hartig,A. and Harada,J.J. (1998) Identification and analysis of the plant peroxisomal targeting signal 1 receptor NtPEX5. *Proc. Natl Acad. Sci. USA*, **95**, 13336–13341.

Krause,G.H. (1988) Photoinhibition of photosynthesis. An evaluation of damaging and protective mechanisms. *Physiol. Plant.*, **74**, 566–574.

Lee,M.S., Mullen,R.T. and Trelease,R.N. (1997) Oilseed isocitrate lyases lacking their essential type 1 peroxisomal targeting signal are piggybacked to glyoxysomes. *Plant Cell*, **9**, 185–197.

Lopez-Huertas,E., Oh,J.S. and Baker,A. (1999) Antibodies against Pex14p block ATP-independent binding of matrix proteins to peroxisomes *in vitro*. *FEBS Lett.*, **459**, 227–229.

Maeshima,M., Yokoi,H. and Asahi,T. (1988) Evidence for no proteolytic processing during transport of isocitrate lyase into glyoxysomes in castor bean endosperm. *Plant Cell Physiol.*, **29**, 381–384.

Mano,S., Hayashi,M., Kondo,M. and Nishimura,M. (1997) Hydroxypyruvate reductase with a carboxy-terminal targeting signal to microbodies is expressed in *Arabidopsis*. *Plant Cell Physiol.*, **38**, 449–455.

Mano,S., Hayashi,M. and Nishimura,M. (1999) Light regulates alternative splicing of hydroxypyruvate reductase in pumpkin. *Plant J.*, **17**, 309–320.

Mori,H. and Nishimura,M. (1989) Glyoxysomal malate synthase is specifically degraded in microbodies during greening of pumpkin cotyledons. *FEBS Lett.*, **244**, 163–166.

Nishimura,M., Yamaguchi,J., Mori,H., Akazawa,T. and Yokota,S. (1986) Immunocytochemical analysis shows that glyoxysomes are directly transformed to leaf peroxisomes during greening of pumpkin cotyledons. *Plant Physiol.*, **80**, 313–316.

Nishimura,M., Takeuchi,Y., De Bellis,L. and Hara-Nishimura,I. (1993) Leaf peroxisomes are directly transformed to glyoxysomes during senescence of pumpkin cotyledons. *Protoplasma*, **175**, 131–137.

Nishimura,M., Hayashi,M., Kato,A., Yamaguchi,K. and Mano,S. (1996) Functional transformation of microbodies in higher plant cells. *Cell Struct. Funct.*, **21**, 387–393.

Öquist,G., Chow,W.S. and Andersson,J.M. (1992) Photoinhibition of photosynthesis represents a mechanism for the long term regulation of photosystem II. *Planta*, **186**, 450–460.

Sambrook,J., Fritsch,E.F. and Maniatis,T. (1989) *Molecular Cloning: A Laboratory Manual*. Cold Spring Harbor Laboratory Press, Cold Spring Harbor, NY.

Schumann,U., Gietl,C. and Schmid,M. (1999) Sequence analysis of a cDNA encoding Pex7p, a peroxisomal targeting signal 2 receptor from *Arabidopsis*. *Plant Physiol.*, **120**, 339.

Shimizu,N. *et al.* (1999) The peroxin Pex14p—cDNA cloning by functional complementation on a Chinese hamster ovary cell mutant, characterization and functional analysis. *J. Biol. Chem.*, **274**, 12593–12604.

Somerville,C.R. and Ogren,W.L. (1981) Photorespiration-deficient mutants of *Arabidopsis thaliana* lacking mitochondrial serine transhydroxymethylase activity. *Plant Physiol.*, **67**, 666–671.

Somerville,C.R. and Ogren,W.L. (1982) Genetic modification of photorespiration. *Trends Biochem. Sci.*, **7**, 171–174.

Subramani,S. (1998) Components involved in peroxisome import, biogenesis, proliferation, turnover and movement. *Physiol. Rev.*, **78**, 171–188.

Titus,D.E. and Becker,W.M. (1985) Investigation of the glyoxysome–peroxisome transition in germinating cucumber cotyledons using double-label immunoelectron microscopy. *J. Cell Biol.*, **101**, 1288–1299.

Tolbert,N.E. (1982) Leaf peroxisomes. *Ann. N Y Acad. Sci.*, **386**, 254–268.

Trelease,R.N., Lee,M.S., Banjoko,A. and Bunkelmann,J. (1996) C-terminal polypeptides are necessary and sufficient for *in vivo* targeting of transiently-expressed proteins to peroxisomes in suspension-cultured plant cells. *Protoplasma*, **195**, 156–167.

Tsugeki,R., Hara-Nishimura,I., Mori,H. and Nishimura,M. (1993) Cloning and sequencing of cDNA for glycolate oxidase from pumpkin cotyledons and Northern blot analysis. *Plant Cell Physiol.*, **34**, 51–57.

Will,G.K., Soukupova,M., Hong,X., Erdmann,K.S., Kiel,J., Dodt,G., Kunau,W.H. and Erdmann,R. (1999) Identification and characterization of the human orthologue of yeast pex14p. *Mol. Cell. Biol.*, **19**, 2265–2277.

Wimmer,C., Schmid,M., Veenhuis,M. and Gietl,C. (1998) The plant PTS1 receptor: similarities and differences to its human and yeast counterparts. *Plant J.*, **16**, 453–464.

Yamaguchi,K., Mori,H. and Nishimura,M. (1995) A novel isoenzyme of ascorbate peroxidase localized on glyoxysomal and leaf peroxisomal membranes in pumpkin. *Plant Cell Physiol.*, **36**, 1157–1162.

Received June 26, 2000; revised August 14, 2000; accepted September 15, 2000

Plant Cell Physiol. 42(1): 20–27 (2001)

Pumpkin Peroxisomal Ascorbate Peroxidase is Localized on Peroxisomal Membranes and Unknown Membranous Structures

Kazumasa Nito [1, 2], Katsushi Yamaguchi [1], Maki Kondo [1], Makoto Hayashi [1] and Mikio Nishimura [1, 2, 3]

[1] *Department of Cell Biology, National Institute for Basic Biology, Okazaki, 444-8585 Japan*

[2] *Department of Molecular Biomechanics, School of Life Science, the Graduate University for Advanced Studies, Okazaki, 444-8585 Japan*

To investigate the roles of peroxisomal membrane proteins in the reversible conversion of glyoxysomes to leaf peroxisomes, we characterized several membrane proteins of glyoxysomes. One of them was identified as an ascorbate peroxidase (pAPX) that is localized on glyoxysomal membranes. Its cDNA was isolated by immunoscreening. The deduced amino acid sequence encoded by the cDNA insert does not have a peroxisomal targeting signal (PTS), suggesting that pAPX is imported by one or more PTS-independent pathways. Subcellular fractionation of 3- and 5-d-old cotyledons of pumpkin revealed that pAPX was localized not only in the glyoxysomal fraction, but also in the ER fraction. A magnesium shift experiment showed that the density of pAPX in the ER fraction did not increase in the presence of Mg^{2+}, indicating that pAPX is not localized in the rough ER. Immunocytochemical analysis using a transgenic Arabidopsis which expressed pumpkin pAPX showed that pAPX was localized on peroxisomal membranes, and also on a unknown membranous structure in green cotyledons. The overall results suggested that pAPX is transported to glyoxysomal membranes via this unknown membranous structure.

Key words: Ascorbate peroxidase — Endoplasmic reticulum — Hydrogen peroxide — Peroxisome — Protein transport — Pumpkin.

Abbreviations: cAPX, cytosolic ascorbate peroxidase; pAPX, peroxisomal ascorbate peroxidase; BiP, binding protein; CAT, catalase; ER, endoplasmic reticulum; HPR, hydroxypyruvate reductase; ICL, isocitrate lyase; PTS, peroxisome targeting signal.

Introduction

Peroxisomes are organelles about 1 μm in diameter that occur in cells of all eukaryotic organisms. Peroxisomes are bounded by a single membrane and do not have their own DNA. These characteristics are clearly different from those of chloroplasts and mitochondria. Therefore, the biogenesis of peroxisomes is completely regulated by nuclear DNA. In higher plants, germinating seedlings require sucrose to obtain energy for seedling growth. In this germinating stage, peroxisomes possess enzymes for β-oxidation of fatty acids and the glyoxylate cycle in storage tissues of oilseeds. These specialized peroxisomes have been called glyoxysomes. After greening, plants do not need to produce sucrose from storage oil as photosynthesis supplies the energy for growth (Beevers 1979). These metabolic changes correspond to the functional transition of glyoxysomes to leaf peroxisomes. Some of the enzymes in leaf peroxisomes are involved in photorespiration. Glyoxysomes have been reported to be directly transformed into leaf peroxisomes in greening cotyledons (Nishimura et al. 1986, Sautter 1986, Titus and Becker 1985). The reverse process, the conversion of leaf peroxisomes to glyoxysomes, has been observed in senescing cotyledons of the same plants (De Bellis et al. 1991) and has also been reported to occur directly (Nishimura et al. 1993).

Peroxisomal matrix proteins have been reported to be translated on free polysomes in the cytosol and then imported to peroxisomes (Lazarow and Fujiki 1985). Two types of peroxisomal targeting signals (PTSs) of matrix enzymes (PTS1 and PTS2) have been identified. PTS1 is found in the C-terminus of proteins, such as isocitrate lyase and malate synthase (Gould et al. 1990, Hayashi et al. 1996, Hayashi et al. 1997, Mano et al. 1996, Subramani 1993). PTS2 is located in the N-terminus of large molecular weight precursors such as the precursors of thiolase, citrate synthase and malate dehydrogenase (Gietl 1990, Hayashi et al. 1999, Kato et al. 1996a, Kato et al. 1996b, Kato et al. 1999). However, the targeting signal for peroxisomal membrane proteins is not known.

Ascorbate peroxidase, which is a peroxisomal membrane protein (designated pAPX), has been found in pumpkin, cucumber and spinach, and has been characterized enzymatically and biochemically (Francisco and Richard 1998, Ishikawa et al. 1998, Yamaguchi et al. 1995b). These studies have suggested that H_2O_2 produced in peroxisomes might be scavenged by the cooperative efforts of CAT and APX, because the K_m of APX for H_2O_2 (30–80 μM) is much lower than that of CAT (Chen and Asada 1989, Koshiba 1993).

In this study, we investigated the level of pAPX at various growth stages of pumpkin seedlings and its physiological role on peroxisomal membranes. We report evidence that pAPX is localized on peroxisomal membranes and also on unknown membranous structures, suggesting that pAPX is translocated to peroxisomes via these membranous structures.

[3] Corresponding author: E-mail, mikosome@nibb.ac.jp; Fax, +81-564-55-7505.

Materials and Methods

Plant materials

Pumpkin (*Cucurbita* sp. cv. Kurokawa Amakuri) seeds were soaked overnight, planted in moist rock fiber (66R; Nitto Bouseki, Chiba, Japan) and allowed to germinate at 25°C in darkness. *Arabidopsis thaliana* (ecotype Colombia) seeds were surface sterilized in 2% NaClO, 0.02% Triton X-100, and grown on germination media (2.3 mg ml^{-1} MS salt (Wako, Osaka, Japan), 1% sucrose, 100 μg ml^{-1} myo-inositol, 1 μg ml^{-1} thiamine-HCl, 0.5 μg ml^{-1} pyridoxine, 0.5 μg ml^{-1} nicotinic acid, 0.5 mg ml^{-1} MES-KOH (pH 5.7), 0.2% INA agar (Ina Shokuhin, Nagano, Japan) at 22°C under continuous light.

Preparation of peroxisomes

Pumpkin seedlings were grown for 5 d in darkness to produce etiolated cotyledons (70 g FW). The etiolated cotyledons were homogenized for 3 s twice with 200 ml of grinding medium that contained 20 mM pyrophosphate-HCl, pH 7.5, 1 mM EDTA and 0.3 M mannitol in a chilled Waring blender. The filtrates were combined and centrifuged at 1,500×*g* for 20 min. The pellet was resuspended in 150 ml of grinding medium, and the differential centrifugation steps were repeated. The resultant pellet was then resuspended in 5 ml of buffer A (10 mM HEPES-KOH, pH 7.2, 1 mM EDTA and 0.3 M mannitol) and was subjected to centrifugation in Percoll. A 4- ml aliquot of the suspension was layered directly on top of 30 ml of a 28% (v/v) solution of Percoll in 10 mM HEPES-KOH (pH 7.2), 1 mM EDTA and 0.3 M raffinose and was centrifuged at 40,000×*g* for 30 min with slow acceleration and deceleration. Peroxisomes sedimented near the bottom of the self-generated gradient and were collected with a Pasteur pipette. To remove the Percoll, peroxisomes were washed by centrifugation at 5,000×*g* for 10 min after the addition of 4 volumes of buffer A. The pellet was suspended carefully in 1 ml of buffer A and was used as purified peroxisomes for subsequent analysis (Yamaguchi et al. 1995a).

Characterization of glyoxysomal membrane proteins

Purified peroxisomes were pelleted again by centrifugation at 5,000×*g* for 10 min and were suspended in 200 μl of 10 mM HEPES-KOH buffer (pH 7.2). After centrifugation at 100,000×*g* for 30 min, the supernatant was analyzed as the water-soluble fraction. The pellet was resuspended in 0.2 M KCl in 10 mM HEPES-KOH buffer (pH 7.2), and was centrifuged again at 100,000×*g* for 30 min to yield a salt-soluble fraction. The pellet was then extracted with 0.1 M Na_2CO_3 to remove peripheral membrane proteins (Fujiki et al. 1982). After centrifugation at 100,000×*g* for 30 min, the supernatant was neutralized by the addition of 1 M HCl and was analyzed as the alkali-soluble fraction. The pellet was resuspended in 100 mM HEPES-KOH (pH 7.2), and was used as the alkali-insoluble fraction.

Preparation of total homogenates from pumpkin cotyledons

Total homogenates of pumpkin cotyledons at various stages of growth were prepared as follows. Cotyledons were homogenized with 50 mM Tris-HCl (pH 8.0), 1 mM EDTA, 10% glycerol and 1% SDS as a detergent. The homogenates were centrifuged at 12,000×*g* for 10 min and the supernatants were used for assays and immunoblotting with anti-pAPX, anti-ICL (Mano et al. 1996) and anti-HPR (Mano et al. 1997a).

Treatment of in vitro senescence

Green cotyledons of pumpkin grown in a greenhouse for 20 d were harvested and were placed on moistened discs of filter paper in a plastic petri dishes. Petri dishes were incubated in permanent darkness at 25°C for 0, 2, 4, 6 and 8 d. Total homogenates from cotyledons were subjected to SDS-PAGE (10 μg each) and analyzed by immunoblotting.

Expression of fusion proteins and preparation of specific antibodies

Standard procedures for expression of fusion proteins and preparation of specific antibodies were described previously (Hayashi et al. 1998). The two DNA fragments corresponding to the N-terminal 90-residue polypeptide and the C-terminal 140-residue polypeptide of pAPX were produced by PCR. These primers, mAE-1 (sense, 5′-GGCCATGGCGTTACCGGTCGTAGACA-3′) and mAE-4 (antisense, 5′-CCGAATTCTTAAGTAATCTTCGGATGTTTAG-3′) for the N-terminal 90-residue polypeptide, mAE-3 (sense, 5′-GGCCATGGGCCT-GTCTGACAAGGATATT-3′) and mAE-2 (antisense, 5′-CCGAAT-TCTTACTTCAAATTTTTGCGAA-3′) for the C-terminal 140-residue polypeptide, were conjugated with the *Nco*I and *Eco*RI restriction sites, respectively.

The antiserum against the N-terminal 90-residue polypeptide showed a specific immunoreactivity to pumpkin pAPX and did not cross-react with the other APX in pumpkin and pAPX of Arabidopsis. The antiserum against the C-terminal 140-residue polypeptide reacted with cAPX in addition to pAPX. Therefore, the antibodies against the N-terminal and C-terminal domains were used for detection of pAPX and cAPX, respectively.

Generation of transgenic Arabidopsis plants

The *Sma*I-*Hin*dIII full length cDNA fragment of pAPX was blunted by T4 DNA polymerase and subcloned into the *Sma*I site of Ti-plasmid pBI121-Hm, a derivative of pBI-121. The inserted cDNA was expressed by the cauliflower mosaic virus 35S promoter. Standard procedures were used for all these manipulations (Sambrook et al. 1989). The Ti-plasmids were then introduced to *Agrobacterium tumefaciens* (strain EHA101) by electroporation (Nagel et al. 1990). Using this *A. tumefaciens*, *Arabidopsis thaliana* (ecotype Colombia) was transformed by the protocol of Valvekens et al. (1988). Primary transformants were designated T0 plants. T1 seeds collected from T0 plants were grown on germination medium that contained 100 mg ml^{-1} kanamycin. A cotyledon was removed from a kanamycin-resistant plant and the amount of the product of pAPX was analyzed by immunoblotting. A 7-d-old cotyledon from transgenic Arabidopsis that accumulated the largest amount of pAPX was used for immunoelectron microscopy.

Immunoelectron microscopy

The green cotyledons of transgenic Arabidopsis and pumpkin, were harvested and were vacuum-infiltrated for 1 h with a fixative that consisted of 4% paraformaldehyde, 1% glutaraldehyde and 0.06 M sucrose in 0.05 M cacodylate buffer (pH 7.4). The fixed samples were then cut into slices of less than 1 mM in thickness and treated for another 2 h with freshly prepared fixative. After washing with the same buffer, the samples were dehydrated in a graded dimethylformamide series at –20°C and embedded in LR-White resin (London Resin Co. Ltd., Basingstoke, Hampshire, U.K.). Blocks were polymerized under a UV lamp at –20°C for 24 h. Ultrathin sections were mounted on uncoated nickel grids. The sections were treated with blocking solution (1% bovine serum albumin in phosphate-buffered saline) for 1 h at room temperature. Then they were incubated overnight at 4°C in a solution of pAPX-specific antibodies that had been diluted in 1 : 200 in blocking solution at 4°C. Sections washed with phosphate-buffered saline, were incubated for 30 min at room temperature in a solution of protein A-gold (15 nm; Amersham Japan) that had been diluted 1 : 20 in the blocking solution. The sections were washed with distilled water and then stained with 4% uranyl acetate and lead citrate. All sections

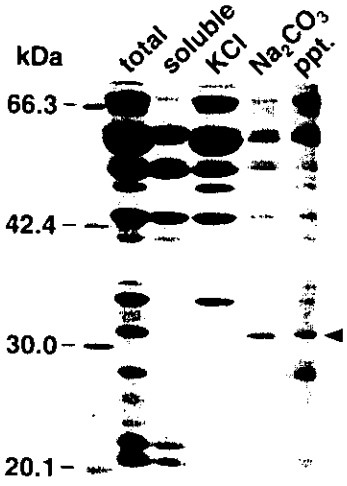

Fig. 1 SDS-PAGE of major membrane proteins of glyoxysomes isolated from germinating pumpkin cotyledons. Total, water-soluble (soluble), salt-soluble (KCl), alkali-soluble (Na_2CO_3) and alkali-insoluble (ppt.) fractions of glyoxysomal membrane proteins were prepared as described in "Materials and Methods" and were subjected to SDS-PAGE. Arrowhead indicates ascorbate peroxidase localized on glyoxysomal membranes.

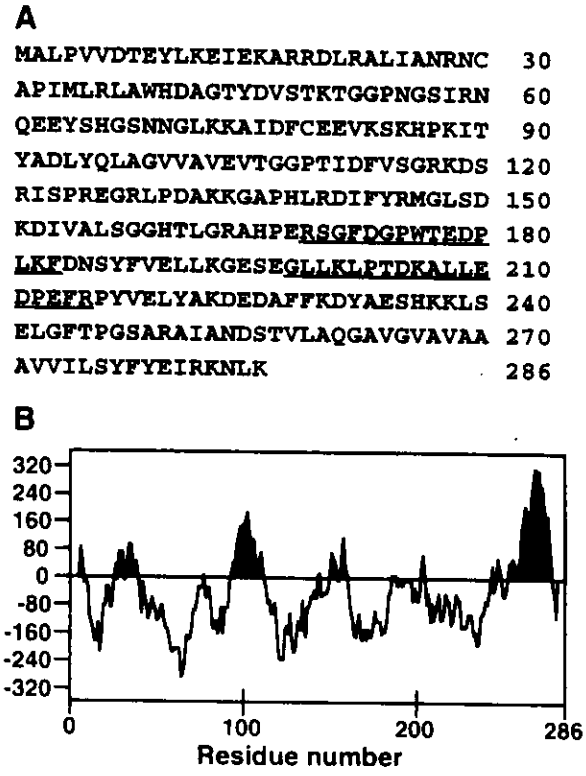

Fig. 2 Deduced amino acid sequence of pumpkin pAPX cDNA (A) and hydropathy profile of pAPX (B). Internal amino acid sequences of pAPX that were determined directly are underlined. Hydropathy indexes were calculated according to Kyte and Doolittle (1982).

were stained and examined under a transmission electron microscope (1200EX; JEOL, Tokyo, Japan) operated at 80 kV.

Subcellular fractionation of pumpkin cotyledons

Etiolated cotyledons from 3- or 5-d-old pumpkin seedlings (2 g) were homogenized with 3 ml of chopping buffer [150 mM Tricine-KOH (pH 7.5), 1 mM EDTA and 13% (w/w) sucrose] and filtered through three layers of cheesecloth. A portion of the filtrate (1 ml) was layered on a sucrose gradient that consisted of 2 ml 20% sucrose followed by a 13-ml linear gradient of 30–60% (w/w) sucrose and centrifuged at 110,000×*g* and 4°C for 2.5 h in a SW28.1 rotor (Beckman, Palo Alto, CA, U.S.A.). Each fraction (0.5 ml) was collected and used for immunoblot analysis with anti-pAPX, anti-cAPX, anti-CAT (Yamaguchi et al. 1984), anti-ICL (Maeshima et al. 1988) and anti-BiP (Hatano et al. 1997) antibodies.

Mg^{2+}-induced shift experiment

Etiolated cotyledons from 5-d-old pumpkin seedlings (5 g) were homogenized with 20 ml of extraction buffer [50 mM HEPES-NaOH (pH 7.0), 10% (w/w) sucrose, 2 mM EDTA or 5 mM $MgCl_2$] and filtered through three layers of cheesecloth. Portions of the filtrates were centrifuged at 10,000×*g* and 4°C for 10 min. The supernatants were centrifuged at 100,000×*g* and 4°C for 1 h. The precipitates were resuspended with 0.5 ml of extraction buffer and then layered onto a linear gradient of 15–45% (w/w) sucrose that contained 2 mM EDTA or 5 mM $MgCl_2$. The samples were centrifuged at 110,000×*g* and 4°C for 2.5 h in the SW28.1 rotor. Each fraction (0.5 ml) was collected and used for immunoblot analysis with anti-pAPX and anti-BiP antibodies.

Results

Isolation of peroxisomal ascorbate peroxidase

To characterize the functions of the glyoxysomal membrane proteins in pumpkin, we isolated glyoxysomes from etiolated cotyledons. Isolated glyoxysomes were sequentially extracted with 10 mM HEPES-KOH (pH 7.2), the same buffer plus 0.2 M KCl, and 0.1 M Na_2CO_3. Few proteins were extractable from glyoxysomes even after the treatment with 0.1 M Na_2CO_3 (Fig. 1; ppt.), suggesting that they are glyoxysomal membrane-bound proteins. Among these proteins, we characterized a 31-kDa protein in this study (Fig. 1; arrowhead).

A cDNA library for poly $(A)^+$-RNA from etiolated cotyledons was constructed by the modified vector-primer method of Mori et al. (1991), with plasmid pTTQ18. Immunoscreening was carried out as described previously (Mori et al. 1991). To isolate cDNA clones with longer inserts of the 31-kDa protein, the same library was screened by colony hybridization. The clone containing the longest cDNA insert was selected and sequenced. This cDNA consisted of 1,133 bp, and contained an open reading frame of 858 bp. The deduced amino acid sequence consisted of 286 amino acids with a calculated molecular mass of 31,527 Da (Fig. 2A). There is an in frame stop codon in the 5′ untranslated region. To further characterize the 31-kDa protein, we digested it with trypsin and sequenced the fragments. The amino acid sequences of two peptides derived from the 31-kDa protein were determined as

```
pAPX                                                                                                    MALPVVDTEYLKEIEKARRDLRALIANRN  29
sAPX  MAATALGSVAASSASSTTRFLSTATRATLPFSSRSSSLSSFKFLRSAPLISHLFLNQGRPSSCVSIRRFNAASHPKCLASDPEQLKSAREDIKELLKTTF 100
tAPX  MAATALGSVAASSASSTTRFLSTATRATLPFSSRSSSLSSFKFLRSAPLISHLFLNQGRPSSCVSIRRFNAASHPKCLASDPEQLKSAREDIKELLKTTF 100
cAPX                                                                                                    MTKNYPTVSEDYKKAVEKCRKLRGLIAEKN  31

pAPX  GAPIMLRLAWHDAGTYDVSTKTG----GPNGSIRNQEEYSHGSNNGLKKAIDFCEEVKSKHPKITYADLYQLAGVVAVEVTGGPTIDFVSGRKDSRIS--  123
sAPX  CHPILVRLGWHDAGTYNKNIEEWPQRGGANGSLRFDVELGHGANAGLVNALKLIEPIKKKYSNVTYADLFQLASATAIEEAGGPKIPMKYGRVDVVGPEQ  200
tAPX  CHPILVRLGWHDAGTYNKNIEEWPQRGGANGSLRFDVELGHGANAGLVNALKLIEPIKKKYSNVTYADLFQLASATAIEEAGGPKIPMKYGRVDVVGPEQ  200
cAPX  GAPIMVRLAWHSAGTFDCQSRTG----GPFGTMRFDAEQAHGANSGIHIALRLLDPIREQFPTISFADFHQLAGVVAVEVTGGPDIPFHPGREDKPQP--  125

pAPX  -PREGRLPDAKKG--APHLRDIFYR-MGLSDKDIVALSGGHTLGRAHPERSGFDGP----------------WTEDPLKFDNSYFVELLKGESEGLLKLP  203
sAPX  CPEEGRLPDAGPPSPAAHLREVFYR-MGLNDREIVALSGAHTLGRSRPERSGWGKPETKYTKDGPGAPGGQSWTVQWLKFNNSYFKDIKERRDEELLVLP  299
tAPX  CPEEGRLPDAGPPSPAAHLREVFYR-MGLNDREIVALSGAHTLGRSRPERSGWGKPETKYTKDGPGAPGGQSWTVQWLKFNNSYFKDIKERRDEELLVLP  299
cAPX  -PPEGRLPDATKG--CDHLRDVFAKQMGLSDKDIVALSGAHTLGRCHKDRSGFEGA----------------WTSNPLIFDNSYFKELLSGEKEGLLQLV  206

pAPX  TDKALLEDPEFRPYVELYAKDEDAFFKDYAESHKKLSELGFTPGSARAIANDSTVLAQGAVGVAVAAAVVILSYFYEIRKNLK                    286
sAPX  TDAALFEDPSFKVYAEKYVEDQEAFFKDYAEAHAKLSNLGAKFDPPEGIVIDDASSKPAGEKFDAAKYSYGKD                               372
tAPX  TDAALFEDPSFKVYAEKYVEDQEAFFKDYAEAHAKLSNLGAKFDPPEGIVIDDASSKPAGEKFDAAKYSYGKRELSDSMKQKIRAEYESFGGSPDKPLPT 399
cAPX  SDKALLDDPVFRPLVEKYAADEDAFFADYAEAHMKLSELGFADA                                                           250

pAPX                          286
sAPX                          372
tAPX  NYFLNIILVIAVLAILTSLLGN 421
cAPX                          250
```

Fig. 3 Alignment of pAPX with stroma (sAPX) and thylakoid-bound (tAPX) ascorbate peroxidases of pumpkin, and cytosolic ascorbate peroxidase (cAPX) of Arabidopsis.

described previously (Yamaguchi et al. 1995b). These sequences were shown to be identical with parts of the deduced amino acid sequence encoded in the cDNA clone (underlines in Fig. 2A). Therefore, we concluded that this cDNA clone contained the cDNA of the 31-kDa protein.

The deduced amino acid sequence of the 31-kDa protein shows a high similarity to ascorbate peroxidases (APX) of plants. Since the 31-kDa protein has ascorbate peroxidase activity (Yamaguchi et al. 1995b), we concluded that the 31-kDa protein was peroxisomal ascorbate peroxidase (pAPX) in pumpkin. The amino acid sequence of pAPX had 30% identity to thylakoid-APX (tAPX) (Yamaguchi et al. 1996), 34% identity to stromal APX (sAPX) (Mano et al. 1997b) of pumpkin and 53% identity to cytosolic APX (cAPX) (Kubo et al. 1992) of Arabidopsis (Fig. 3). Despite its high similarity to cAPX, pAPX possesses the extended carboxy-terminus (248–286). A Kyte-Doolittle hydrophobicity plot of pAPX revealed the presence of a hydrophobic region located at the carboxy-terminus (amino acids 254–282) which is a putative transmembrane domain (Fig. 2B) (Kyte and Doolittle 1982). This suggests that pAPX is anchored to the peroxisomal membranes with its carboxy-terminus.

Developmental changes in the level of pAPX in germination and senescence

When seedlings were grown in darkness, the levels of pAPX protein reached a maximum after five days and then gradually decreased (Fig. 4). However, the amount of pAPX protein decreased rapidly when 5-d-old seedlings were transferred to the light. The levels of other glyoxysomal enzymes in

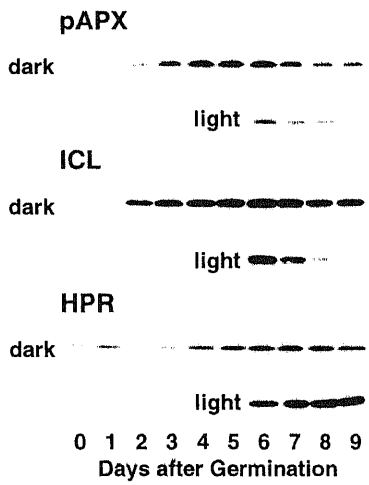

Fig. 4 Developmental changes in the levels of peroxisomal proteins in pumpkin cotyledons during the peroxisomal transition from glyoxysomes to leaf peroxisomes. Immunoblot analysis of homogenates from cotyledons at various stages was carried out using antibodies against pAPX, ICL and HPR.

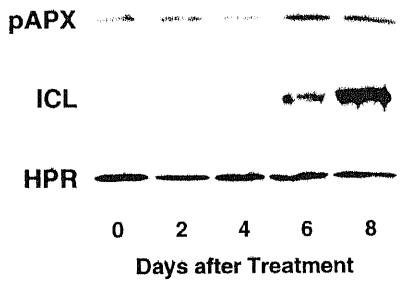

Fig. 5 Developmental changes in the levels of peroxisomal proteins in pumpkin cotyledons after induction of in vitro senescence. Green cotyledons of pumpkin were harvested and were incubated in continuous darkness for 0, 2, 4, 6 and 8 d. Total homogenates from senescent cotyledons were subjected to SDS-PAGE (10 μg each), which were followed by immunoblotting using antibodies against pAPX, ICL and HPR.

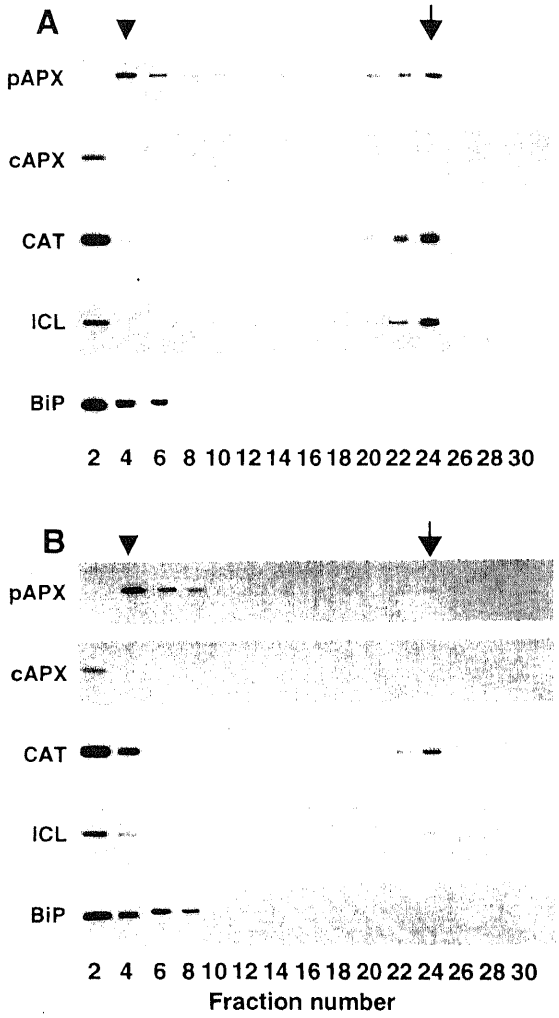

Fig. 6 Subcellular distribution of pAPX in pumpkin etiolated cotyledons. Homogenates of cotyledons that were grown in the dark for 5 d (A) or 3 d (B) were layered on top of a sucrose density gradient (30–60%, w/w) and centrifuged. Fractions were numbered from the top of the gradient. Each fraction of the gradient was subjected to SDS-PAGE followed by immunoblotting using antibodies against pAPX, cAPX, CAT, ICL and BiP. Arrows indicate the peak of the peroxisome. Arrowheads indicate the peak of the ER.

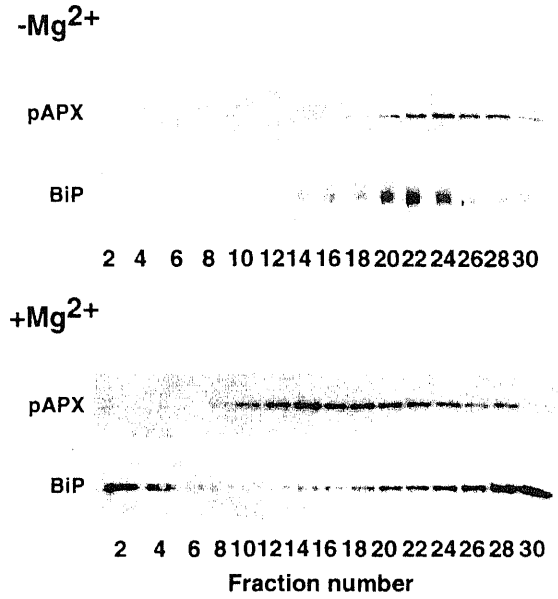

Fig. 7 Mg^{2+}-induced shift analysis of microsomal fraction from pumpkin etiolated cotyledons. Microsomal membrane fractions were prepared under 2 mM EDTA ($-Mg^{2+}$) or 5 mM $MgCl_2$ ($+Mg^{2+}$) conditions. Fractions were numbered from the top of the gradient. Each fraction of the gradient was subjected to SDS-PAGE followed by immunoblotting using antibodies against pAPX and BiP.

pumpkin cotyledons, such as ICL and citrate synthase, undergo similar developmental changes during the transformation of glyoxysomes to leaf peroxisomes (Kato et al. 1995, Mano et al. 1996). These results suggest that the amount of pumpkin pAPX is regulated in the cotyledons, as are the amounts of other glyoxysomal matrix enzymes.

After greening, cotyledons gradually undergo senescence. Gut and Matile (1988) have shown that glyoxysomal enzymes are detectable in detached senescent leaves. Glyoxysomal enzymes also appear during the reverse transition of leaf peroxisomes to glyoxysomes that occurs in senescence (De Bellis et al. 1991). We investigated the changes in the levels of pAPX protein during senescence in vitro (Fig. 5). After incubation of 20-d-old cotyledons in continuous darkness, the amount of pAPX protein did not change whereas the leaf peroxisomal enzyme, HPR decreased slightly. By contrast, ICL, which is a glyoxysomal enzyme, increased markedly.

Subcellular localization of pAPX in pumpkin etiolated cotyledons

To analyze the subcellular localization of pAPX, we carried out subcellular fractionation of 5-d-old etiolated cotyledons of pumpkin (Fig. 6A). The distribution of pAPX and various marker enzymes on a sucrose density gradient was detected by an immunoblot analysis with each antibody. From the distribution of marker enzymes, the glyoxysomes were clearly separated from the cytosol and ER. The peaks of CAT, ICL and BiP found in the top fraction of the sucrose gradient were released from organelles damaged during homogenization of the samples. As shown by the immunoreactive bands in Fig. 6A, pAPX peaked in fraction 24 of the gradient (i.e. near the bottom of the gradient). This peak coincided with those of CAT and ICL, which are glyoxysomal marker enzymes (arrow), indicating that these fractions contained glyoxysomes. Another pAPX peak was found in fraction 4 (arrowhead), which is not a glyoxysomal fraction. Although a part of BiP, an ER marker enzyme, was solubilized and was detected in the cytosolic fraction, frac-

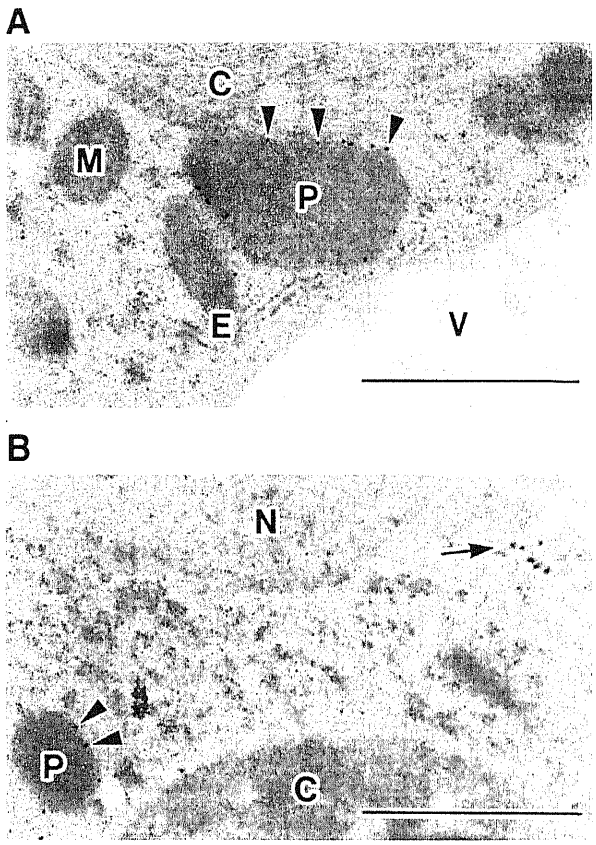

Fig. 8 Immunocytochemical localization of pAPX in transgenic Arabidopsis that expressed pumpkin pAPX. Ultra-thin sections of cotyledons of Arabidopsis were immunogold labeled with an antibody against pAPX. Arrowheads indicate gold particles on peroxisomal membranes (A and B). Arrows indicate gold particles localized on the unknown membranous structure (B). C, chloroplast; E, rough ER; M, mitochondrion; N, nucleus; P, peroxisome; V, vacuole. Bars represent 1 μm.

tions 4 to 6 appear to be the ER fractions because marker enzymes such as CAT and ICL released from damaged organelles were found only in fraction 2.

Biogenesis of glyoxysomes is more active in the earlier germinating stages. To compare the distributions of pAPX in the ER and glyoxysomal fractions of the earlier germinating stages, 3-d-old etiolated cotyledons of pumpkin were fractionated and analyzed by the same method (Fig. 6B). The immunoblotting showed that the ratio of the amount of pAPX in ER to the amount of pAPX in glyoxysomes is larger in 3-d-old etiolated cotyledons than in 5-d-old etiolated cotyledons. These results suggest that pAPX is transported via the ER to glyoxysomes during germination.

pAPX is localized in a unknown membranous structure

To further define the endomembrane localization of pAPX in the ER fraction, microsomal membranes were fractionated on sucrose density gradients with a magnesium-induced shift, and characterized by an immunoblot analysis (Fig. 7). In gradients without magnesium (i.e. +2 mM EDTA), pAPX was the most abundant at a sucrose density of 35% (w/w). On the immunoblot (Fig. 7, upper panels), BiP was localized at roughly the same density. In gradients with 5 mM $MgCl_2$ (lower panels), the pAPX peak shifted to a lower sucrose density (29%), whereas the BiP peak shifted to a higher sucrose density (>42%). A magnesium-dependent density shift is one of the characteristics of the rough ER and the density of the rough ER increases in the presence of Mg^{2+}. These results indicate that pAPX is localized in membranous structures other than the rough ER.

In an immunoblot study using the homogenate from Arabidopsis, the antibody against pumpkin pAPX did not crossreact with pAPX in Arabidopsis and specific gold particles were not detected in an immunogold study using pumpkin and Arabidopsis cotyledons (data not shown). Therefore, we performed an immunocytochemical study using a transgenic Arabidopsis overexpressing pAPX of pumpkin. Ultrathin sections were prepared from the cotyledons of an 8-d-old transgenic Arabidopsis. Figure 8A shows the localization of pAPX in transgenic Arabidopsis, as determined by immunogold labeling with pAPX antiserum. Gold particles were localized on peroxisomal membranes and also on unknown membranous structures in green cotyledons (Fig. 8B), but were not found in other organelles including the rough ER, mitochondria and chloroplasts. These results support the findings of the subcellular fractionation (Fig. 6, 7) that pAPX is localized not only in peroxisomes but also in unknown membranous structures other than the rough ER.

Discussion

Previous studies on plant peroxisomes have mainly focused on matrix enzymes and so little is known of membrane proteins in these organelles. We have been characterizing the proteins that are bound to pumpkin glyoxysomal membranes. In this study, we have partially characterized one of these proteins, pAPX, which is found in pumpkin glyoxysomal membranes.

In germinating oil seedlings, glyoxysomes play an important role in the process of converting storage lipids to sucrose. In the germinating stage, the expression levels of glyoxylate cycle enzymes, such as ICL and malate synthetase, are elevated in glyoxysomes. On the other hand, hydrogen peroxide, which is toxic to the cell, is generated in the glyoxysomes. Therefore, peroxisomes have a scavenging mechanism for hydrogen peroxide. The scavenging of hydrogen peroxide in the glyoxysomes is mainly carried out by CAT, which is highly expressed in the germination stages. However, CAT is not suitable for scavenging low concentrations of hydrogen peroxide because of its high K_m value (Huang et al. 1983).

The K_m value of pAPX, approximately 30–80 μM, is

lower than that of CAT (Chen and Asada 1989, Koshiba 1993). This means that pAPX is better adapted to scavenging low concentrations of hydrogen peroxide. The C-terminus of pAPX appears to have an extension sequence based on the hydropathy profile of the transmembrane domain that is not present in cAPX (Fig. 3). Latency experiments using isolated glyoxysomes have shown that the catalytic site of pAPX is exposed to the cytosol (Yamaguchi et al. 1995b). Therefore, these results suggest that pAPX is present on the outer surface of glyoxysomes, and is anchored to the membrane with its C-terminus. We speculate that one of the functions of pAPX is to be the scavenging of hydrogen peroxide which escaped from scavenging by CAT and leaked out to the cytosol.

The transition from glyoxysomes to leaf peroxisomes occurs in response to irradiation of light. The main function of peroxisomes changes from fatty acid β-oxidation to photorespiration as a result of the transition. In green leaves, the expression level of pAPX decreased but low levels were maintained (Fig. 4). As mentioned above, the reverse transition from leaf peroxisomes to glyoxysomes occurs in senescing cotyledons, as shown by the accumulation of glyoxysomal enzymes in the organelles during senescence. This suggests that one of the functions of glyoxysomes is to translocate the nutrients of senescing leaves to other vegetative tissues. Though its role in senescent organs is not well understood, pAPX seems to protect the enzymes that are involved in this translocation from hydrogen peroxide.

Peroxisomal matrix enzymes are known to be transported directly to peroxisomes post-translationally. Two kinds of amino acid sequences have been shown to act as a peroxisomal targeting signal (PTS) so far. One is PTS1, which has a SKL-like motif localized in the C-terminus of the protein ([A/C/P/S] – [K/R] – [I/L/M/]). Another is PTS2, which is localized in the N-terminus of proteins as an extension polypeptide (R- [I/L/Q] -X_5-HL). However, these signals are responsible for the transport of only some of the peroxisomal proteins. For example, the targeting signal for the peroxisomal membrane has still not been identified, but it is known that it is not PTS1 or PTS2. pAPX has neither PTS1 nor PTS2 and thus its transport should be independent of these signals (Fig. 2). Recent studies have shown that peroxins, which are involved in biogenesis and maintenance of peroxisomes, are present in yeast and mammals (Subramani 1993). Targeting signals have been identified in some of the peroxins, such as Pex3p and Pex22p, that are bound to the peroxisomal membranes of *Pichia pastoris* (Koller et al. 1999, Wiemer et al. 1996). However, these targeting signals have no consensus sequences and there is no homologous sequence in pAPX. Further analysis is necessary to clarify the targeting signal of pAPX.

The subcellular fractionation experiments showed that pAPX is present in the fractions that contain the ER and peroxisomes (Fig. 6). This suggests that pAPX is transported via other membranous structures to the peroxisomes. As shown in Figure 7, pAPX is not localized in the main fraction associated with the rough ER. Thus, we performed immunoelectron microscopy to analyze the localization of pAPX, but it was difficult to detect the immunogold particles in pumpkin, because of the low contents of the protein. Therefore, we generated transgenic Arabidopsis plants which overexpressed pumpkin pAPX. The antibody against pumpkin pAPX showed a specific immunoreactivity to pumpkin pAPX and did not cross-react with Arabidopsis pAPX on immunoblotting. Specific gold particles were bound on the peroxisomal membranes, indicating that expressed pAPX is localized on peroxisomal membranes (Fig. 8). This demonstrates that pAPX is transported to peroxisomes in Arabidopsis as in pumpkin. Immunoelectron microscopy revealed pAPX accumulated on unknown membranous structures besides the peroxisomal membranes (Fig. 8B). No immunogold particles were detected on typical rough ER. It is still not clear whether these unknown membranous structures are present in pumpkin because no immunogold particles were observed in pumpkin. One possibility is that these unknown membranous structures are the smooth ER or are specialized ER domains. Mullen et al. (1999) reported that pAPX is co-localized in the reticular/circular network and does not co-localize with the immunofluorescence of BiP, calreticulin or calnexin, all of which are marker proteins of ER. They suggested that pAPX is transported to peroxisomes via a subdomain of the ER. These unknown membranous structures may be subdomains of the ER. Thus, the present results suggest that ER or a subdomain of ER is involved in the transport of pAPX to the peroxisomal membrane. Further analysis of these unknown membranous structures will provide valuable information on the biogenesis of peroxisomes in higher plants.

Acknowledgements

The authors thank Dr. M. Maeshima (Nagoya University) for the antibody against isocitrate lyase. This work was supported in part by a grant from the Research for the Future Program of the Japanese Society for the Promotion of Science (JSPS-RFTF96L00407), and by grants-in-aid for scientific research from the Ministry of Education, Science and Culture of Japan (12440231).

References

Beevers, H. (1979) Microbodies in higher plants. *Annu. Rev. Plant Physiol.* 30: 159–193.

Chen, G. and Asada, K. (1989) Ascorbate peroxidase in tea leaves: occurrence of two isozymes and the differences in their enzymatic and molecular properties. *Plant Cell Physiol.* 30: 987–998.

De Bellis, L., Baden, C.S. and Nishimura, M. (1991) Development of enzymes of the glyoxylate cycle during senescence of pumpkin cotyledons. *Plant Cell Physiol.* 32: 555–561.

Francisco, J.C. and Richard, N.T. (1998) Differential expression of ascorbate peroxidase and a putative molecular chaperone in the boundary membrane of differentiating cucumber seedling peroxisomes. *J. Plant Physiol.* 153: 332–338.

Fujiki, Y., Fowler, S., Shio, H., Hubbard, A.L. and Lazarow, P.B. (1982) Polypeptide and phospholipid composition of the membrane of rat liver peroxisomes: comparison with endoplasmic reticulum and mitochondrial membrane. *J. Cell Biol.* 93: 103–110.

Gietl, C. (1990) Glyoxysomal malate dehydrogenase from watermelon is synthesized with an amino-terminal transit peptide. *Proc. Natl. Acad. Sci. USA* 87: 5773–5777.

Gould, S.J., Keller, G.-A., Schneider, M., Howell, S.H., Garrard, L.J., Goodman, J.M., Distel, B., Tabak, H. and Subramani, S. (1990) Peroxisomal protein import is conserved between yeast, plants, insects and mammals. *EMBO J.* 9: 85–90.

Gut, H. and Matile, P. (1988) Apparent induction of key enzymes of the glyoxylic acid cycle in senescent barley leaves. *Planta* 176: 548–550.

Hatano, K., Shimada, T., Hiraiwa, N., Nishimura, M. and Hara-Nishimura, I. (1997) A rapid increase in the level of binding protein (BiP) is accompanied by synthesis and degradation of storage proteins in pumpkin cotyledons. *Plant Cell Physiol.* 38: 344–351.

Hayashi, M., Aoki, M., Kato, A., Kondo, M. and Nishimura, M. (1996) Transport of chimeric proteins that contain a carboxy-terminal targeting signal into plant microbodies. *Plant J.* 10: 225–234.

Hayashi, M., Aoki, M., Kondo, M. and Nishimura, M. (1997) Changes in targeting efficiencies of proteins to plant microbodies caused by amino acid substitutions in the carboxy-terminal tripeptide. *Plant Cell Physiol.* 38: 759–768.

Hayashi, H., De Bellis, L., Yamaguchi, K., Kato, A., Hayashi, M. and Nishimura, M. (1998) Molecular characterization of a glyoxysomal long chain acyl-CoA oxidase that is synthesized as a precursor of higher molecular mass in pumpkin. *J. Biol. Chem.* 273: 8301–8307.

Hayashi, H., De Bellis, L., Ciurli, A., Kondo, M., Hayashi, M. and Nishimura, M. (1999) A novel acyl-CoA oxidase that can oxidize short-chain acyl-CoA in plant peroxisomes. *J. Biol. Chem.* 274: 12715–12721.

Huang, A.H.C., Trelease, R.N. and Moore, T.S. (1983) *Plant Peroxisomes*. pp. 89–94. Academic Press, New York.

Ishikawa, T., Yoshimura, K., Sakai, K., Tamoi, M., Takeda, T. and Shigeoka, S. (1998) Molecular characterization and physiological role of a glyoxysome-bound ascorbate peroxidase from spinach. *Plant Cell Physiol.* 39: 23–34.

Kato, A., Hayashi, M., Mori, H. and Nishimura, M. (1995) Molecular characterization of a glyoxysomal citrate synthase that is synthesized as a precursor of higher molecular mass in pumpkin. *Plant Mol. Biol.* 27: 377–390.

Kato, A., Hayashi, M., Kondo, M. and Nishimura, M. (1996a) Targeting and processing of a chimeric protein with the N-terminal presequence of the precursor to glyoxysomal citrate synthase. *Plant Cell* 8: 1601–1611.

Kato, A., Hayashi, M., Takeuchi, Y. and Nishimura, M. (1996b) cDNA cloning and expression of a gene for 3-ketoacyl-CoA thiolase in pumpkin cotyledons. *Plant Mol. Biol.* 31: 843–852.

Kato, A., Hayashi, M. and Nishimura, M. (1999) Oligomeric proteins containing N-terminal targeting signals are imported into peroxisomes in transgenic Arabidopsis. *Plant Cell Physiol.* 40: 586–591.

Koller, A., Snyder, W.B., Faber, K.N., Wenzel, T.J., Rangell, L., Keller, G.A. and Subramani, S. (1999) Pex22p of Pichia pastoris, essential for peroxisomal matrix protein import, anchors the ubiquitin-conjugating enzyme, Pex4p, on the peroxisomal membrane. *J. Cell Biol.* 146: 99–112.

Koshiba, T. (1993) Cytosolic ascorbate peroxidase in seedlings and leaves of maize. *Plant Cell Physiol.* 34: 713–721.

Kubo, A., Saji, H., Tanaka, K. and Kondo, N. (1992) Cloning and sequencing of a cDNA encoding ascorbate peroxidase from *Arabidopsis thaliana*. *Plant Mol. Biol.* 18: 691–701.

Kyte, J. and Doolittle, R.F. (1982) A simple method for displaying the hydropathic character of a protein. *J. Mol. Biol.* 157: 105–132.

Lazarow, P.B. and Fujiki, Y. (1985) Biogenesis of peroxisomes. *Annu. Rev. Cell. Biol.* 1: 489–530.

Maeshima, M., Yokoi, H. and Asahi, T. (1988) Evidence for no proteolytic processing during transport of isocitrate lyase into glyoxysomes in castor bean endosperm. *Plant Cell Physiol.* 29: 381–384.

Mano, S., Hayashi, M., Kondo, M. and Nishimura, M. (1996) cDNA cloning and expression of a gene for isocitrate lyase in pumpkin cotyledons. *Plant Cell Physiol.* 37: 941–948.

Mano, S., Hayashi, M., Kondo, M. and Nishimura, M. (1997a) Hydroxypyruvate reductase with a carboxy-terminal targeting signal to microbodies is expressed in Arabidopsis. *Plant Cell Physiol.* 38: 449–455.

Mano, S., Yamaguchi, K., Hayashi, M. and Nishimura, M. (1997b) Stromal and thylakoid-bound ascorbate peroxidases are produced by alternative splicing in pumpkin. *FEBS Lett.* 413: 21–26.

Mori, H., Takeda-Yoshikawa, Y., Hara-Nishimura, I. and Nishimura, M. (1991) Pumpkin malate synthase. *Eur. J. Biochem.* 197: 331–336.

Mullen, R.T., Lisenbee, C.S., Miernyk, J.A. and Trelease, R.N. (1999) Peroxisomal membrane ascorbate peroxidase is sorted to a membranous network that resembles a subdomain of the endoplasmic reticulum [In Process Citation]. *Plant Cell* 11: 2167–2186.

Nagel, A., Elliot, A., Masel, A., Birch, R.G. and Manners, J.M. (1990) Electroporation of binary Ti plasmid vector into *Agrobacterium tumefaciens* and *Agrobacterium rhizogenes*. *FEMS Microbiol. Lett.* 67: 325–328.

Nishimura, M., Yamaguchi, J., Mori, H., Akazawa, T. and Yokota, S. (1986) Immunocytochemical analysis shows that glyoxysomes are directly transformed to leaf peroxisomes during greening of pumpkin cotyledons. *Plant Physiol.* 80: 313–316.

Nishimura, N., Takeuchi, Y., De Bellis, L. and Hara-Nishimura, I. (1993) Leaf peroxisomes are directly transformed to glyoxysomes during senescence of pumpkin cotyledons. *Protoplasma* 175: 131–137.

Sambrook, J., Fritsch, E.F. and Maniatis, T. (1989) *Molecular Cloning: A Laboratory Manual*, 2nd edn. Cold Spring Harbor, NY: Cold Spring Harbor Laboratory Press.

Sautter, C. (1986) Microbody transition in greening watermelon cotyledons. Double immunocytochemical labeling of isocitrate lyase and hydroxypyruvate reductase. *Planta* 167: 491–503.

Subramani, S. (1993) Protein import into peroxisomes and biogenesis of the organelle. *Annu. Rev. Cell. Biol.* 9: 445–478.

Titus, D.E. and Becker, W.M. (1985) Investigation of the glyoxysome-peroxisome transition in germinating cucumber cotyledons using double-label immunoelectron microscopy. *J. Cell Biol.* 101: 1288–1299.

Valvekens, K., Montagu, M.V. and Lijsebettens, M.V. (1988) *Agrobacterium tumefaciens*-mediated transformation of *Arabidopsis thaliana* root explants by using kanamycin selection. *Proc. Natl. Acad. Sci. USA* 85: 5536–5540.

Wiemer, E., Luerst, G., Faber, K.N., Veenhuis, M. and Subramani, S. (1996) Isolation and characterization of Pas2p, a peroxisomal membrane protein essential for peroxisome biogenesis in the methylotrophic yeast *Pichia pastoris*. *J. Biol. Chem.* 271: 18973–18980.

Yamaguchi, J., Nishimura, M. and Akazawa, T. (1984) Maturation of catalase precursor proceeds to a different extent in glyoxysomes and leaf peroxisomes of pumpkin cotyledons. *Proc. Natl. Acad. Sci. USA* 81: 4809–4813.

Yamaguchi, K., Takeuchi, Y., Mori, H. and Nishimura, M. (1995a) Development of microbody membrane proteins during the transformation of glyoxysomes to leaf peroxisomes in pumpkin cotyledons. *Plant Cell Physiol.* 36: 455–464.

Yamaguchi, K., Mori, H. and Nishimura, M. (1995b) A novel isoenzyme of ascorbate peroxidase localized on glyoxysomal and leaf peroxisomal membranes in pumpkin. *Plant Cell Physiol.* 36: 1157–1162.

Yamaguchi, K., Hayashi, M. and Nishimura, M. (1996) cDNA cloning of thylakoid-bound ascorbate peroxidase in pumpkin and its characterization. *Plant Cell Physiol.* 37: 405–409.

(Received July 14, 2000; Accepted October 18, 2000)

Plant Cell Physiol. 43(4): 355–366 (2002)

Rapid Paper

Direct Interaction and Determination of Binding Domains among Peroxisomal Import Factors in *Arabidopsis thaliana*

Kazumasa Nito [1, 2], Makoto Hayashi [1] and Mikio Nishimura [1, 2, 3]

[1] *Department of Cell Biology, National Institute for Basic Biology, Okazaki, 444-8585 Japan*
[2] *Department of Molecular Biomechanics, School of Life Science, The Graduate University for Advanced Studies, Okazaki, 444-8585 Japan*

We analyzed the role of Arabidopsis orthologues of human Pex14p, Pex5p and Pex7p that are central components of peroxisomal protein import machinery. Immunoblot analysis showed that *At*Pex14p and *At*Pex5p were present in most organs in Arabidopsis, suggesting that these factors play a role in the main protein import pathways for plant peroxisomes. Two-hybrid analysis showed that *At*Pex14p interacted with *At*Pex5p, but not with *At*Pex7p. In addition, *At*Pex7p was bound to *At*Pex5p, indicating that the PTS2 pathway depends on the PTS1 pathway in Arabidopsis. Further analysis showed that the nine WXXXF/Y repeats in the amino acids ^{231}K-^{450}D and ^{1}M-^{230}V of *At*Pex5p are bound to two N-terminal domains, amino acids ^{58}I-^{65}L and ^{78}R-^{97}R of *At*Pex14p and the C-terminal amino acids ^{266}Y-^{317}S of *At*Pex7p, respectively. Since the binding domains of *At*Pex5p to *At*Pex14p and *At*Pex7p do not overlap, *At*Pex14p, *At*Pex5p and *At*Pex7p might form their complex and function cooperatively in peroxisomal protein import.

Key words: Arabidopsis — Peroxin — Peroxisome — Protein import — Protein–protein interaction.

Abbreviation: GFP, green fluorescent protein; GST, glutathione S-transferase; HPR, hydroxypyruvate reductase; ICL, isocitrate lyase; IgG, immunoglobulin G; PTS, peroxisome targeting signal; TPR, tetratricopeptide repeat; Trx, thioredoxin.

Introduction

Peroxisomes, organelles about 1 μm in diameter and found in cells of all eukaryotic organisms, are enveloped in a single membrane and do not have their own DNA. These characteristics are clearly different from those of chloroplasts and mitochondria. Therefore, the biogenesis of peroxisomes is completely regulated by nuclear DNA. In higher plants, germinating seedlings require sucrose to obtain the energy for seedling growth. In the germinating stage, peroxisomes possess enzymes for β-oxidation of fatty acids and the glyoxylate cycle in storage tissues of oilseeds. These specialized peroxisomes have been called glyoxysomes. After greening, plants do not need to produce sucrose from storage oil as photosynthesis supplies the energy for growth (Beevers 1979). These metabolic changes correspond to the functional peroxisomal transition, in which glyoxysomes are transformed into leaf peroxisomes that play a role in photorespiration. Glyoxysomes have been reported to transform directly into leaf peroxisomes in greening cotyledons (Nishimura et al. 1986, Sautter 1986, Titus and Becker 1985). The reverse process, the conversion of leaf peroxisomes to glyoxysomes, has been observed in senescing cotyledons of the same plants (De Bellis and Nishimura 1991) and has also been reported to occur directly (Nishimura et al. 1993).

Peroxisomal matrix proteins are translated on free polysomes in the cytosol and then imported to peroxisomes (Lazarow and Fujiki 1985). Two types of peroxisomal targeting signals (PTS1 and PTS2) of matrix enzymes have been identified. PTS1 is found in the C-terminus of proteins, such as ICL, HPR, glycolate oxidase, short-chain acyl CoA oxidase and malate synthase (Hayashi et al. 1999, Hayashi et al. 1996, Lee et al. 1997, Mano et al. 1996, Mori et al. 1991, Tsugeki et al. 1993, Volokita 1991). PTS2 is located in the N-terminus of large molecular weight precursors to thiolase, citrate synthase, malate dehydrogenase and long-chain acyl CoA oxidase (Gietl 1990, Hayashi et al. 1998, Kato et al. 1996a, Kato et al. 1996b, Kato et al. 1999).

Recent studies on peroxisomal biogenesis using *ped2* mutant analysis revealed that *At*Pex14p functions as a key protein for peroxisomal matrix protein import in higher plants (Hayashi et al. 2000). Neither PTS1 or PTS2 targeted proteins could be imported into the peroxisomal matrix in *ped2* mutant. These findings indicated that *At*Pex14p plays important roles for peroxisomal protein import of both PTS1- and PTS2-containing proteins. The PTS1 receptor, Pex5p, from tobacco bound specifically to the peroxisomal targeting signal PTS1 (Kragler et al. 1998) and seemed to serve as a specific recognition receptor. Among other higher plants, Pex5p has been reported from watermelon and Arabidopsis (Brickner et al. 1998, Wimmer et al. 1998). Only the cDNA sequence has been reported for the PTS2 receptor, *At*Pex7p, in Arabidopsis (Schumann et al. 1999).

[3] Corresponding author: E-mail, mikosome@nibb.ac.jp; Fax, +81-564-55-7505.

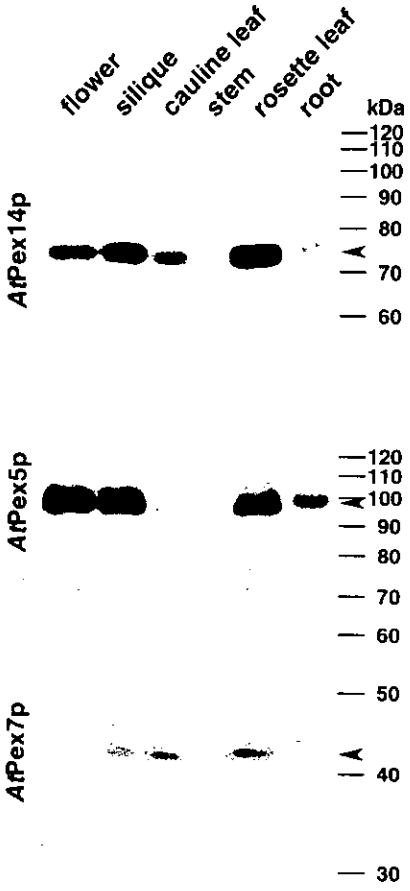

Fig. 1 Organ specificity of *At*Pex14p, *At*Pex5p and *At*Pex7p. Immunoblot analysis of homogenates from various organs was carried out using antibodies against *At*Pex14p, *At*Pex5p and *At*Pex7p. Crude extracts were prepared from the flower, silique, cauline leaf, stem, rosette leaf and root, respectively. Equal amounts of total protein, 10 μg for *At*Pex14p and *At*Pex5p and 50 μg for *At*Pex7p, were loaded in each lane. Markers are shown on the right with molecular masses in kDa.

In this study, we investigated the interactions among the peroxisomal import factors, *At*Pex14p, *At*Pex5p and *At*Pex7p, and the PTS1- and PTS2-containing proteins and determined the binding domains by two-hybrid analysis. On the basis of these results, we analyzed the mechanism of the peroxisomal protein import pathways, namely the PTS1 pathway and PTS2 pathway and interaction of the two pathways. Furthermore, we clarified the expression pattern of peroxisomal import factors, *At*Pex14p, *At*Pex5p and *At*Pex7p, and characterized the spatial and developmental expression of the PTS1 and PTS2 pathways.

Results

Peroxisomal import factors AtPex5p and AtPex7p were detected as a 99 kDa protein and 43 kDa protein, respectively

We have identified from *ped2* mutant analysis that *At*Pex14p functions in the peroxisomal protein import machinery of Arabidopsis (Hayashi et al. 2000). As peroxisomal import machinery other than *At*Pex14p, *At*Pex5p and *At*Pex7p have been reported as Arabidopsis orthologues of yeast and mammal peroxins (Brickner et al. 1998, Schumann et al. 1999). Pex5p and Pex7p in yeast and mammals operate as PTS1 receptor and PTS2 receptor in peroxisomal protein import, respectively. In higher plants, however, Brickner et al. (1998) and Schumann et al. (1999) reported only the cDNA sequences of *At*Pex5p and *At*Pex7p, and no experimental evidence has been reported to confirm their functional roles. We prepared the specific antibodies against *At*Pex5p and *At*Pex7p (see Materials and Methods). To clarify the functional roles of *At*Pex5p and *At*Pex7p in addition to *At*Pex14p, we analyzed their expression pattern by immunoblotting using their antibodies. The antibodies showed a specific immunoreactivity to the 99kDa and 43kDa monospecific bands, respectively (Fig. 1). A search of Arabidopsis genome databases with the PEDANT BLAST Network Service (http://pedant.gsf.de/) revealed no other homologous proteins for *At*Pex14p, *At*Pex5p or *At*Pex7p in the Arabidopsis genome. Therefore, it was indicated that the Arabidopsis genome contains a single copy of these peroxisomal import factors.

The peroxisomal import factors AtPex14p and AtPex5p were coordinately expressed in various organs but AtPex7p was not

To investigate the expression pattern of the peroxisomal protein import factors, *At*Pex14p, *At*Pex5p and *At*Pex7p, immunoblot analysis of homogenates from various organs of Arabidopsis grown for 4 weeks was carried out using antibodies against *At*Pex14p, *At*Pex5p and *At*Pex7p (Fig. 1). As shown in Fig. 1, flower, silique, cauline leaf, rosette leaf and root exhibits high expression of *At*Pex14p. *At*Pex5p was also detected in most of organs and the expression pattern of *At*Pex5p was similar to that of *At*Pex14p. These import factors were not detectable in the stem. However, small amounts of these import factors were observed in extracts of stem under the prolonged exposure (data not shown). The expression pattern of *At*Pex7p differed from those of *At*Pex14p and *At*Pex5p. The 43 kDa band of *At*Pex7p was detected markedly in silique, cauline leaf and rosette leaf, but was barely detectable in the flower, stem and root.

Studies on the *ped2* mutant have shown that *At*Pex14p is essential for both PTS1-dependent and PTS2-dependent protein import (Hayashi et al. 2000). As shown in Fig. 1, the expression pattern of *At*Pex5p, PTS1 receptor, is almost the same as that of *At*Pex14p. Most plant peroxisomal proteins identified contain a PTS1 signal. This suggests that the PTS1-pathway is a major protein import pathway for plant peroxisomes.

During the transition of plant peroxisomes, the peroxisomal import factors AtPex14p and AtPex5p were markedly accumulated but AtPex7p was decreased

Peroxisomes change their function accompanying the development of the plant. Especially, the functional transition of glyoxysomes to leaf peroxisomes occurs directly in greening

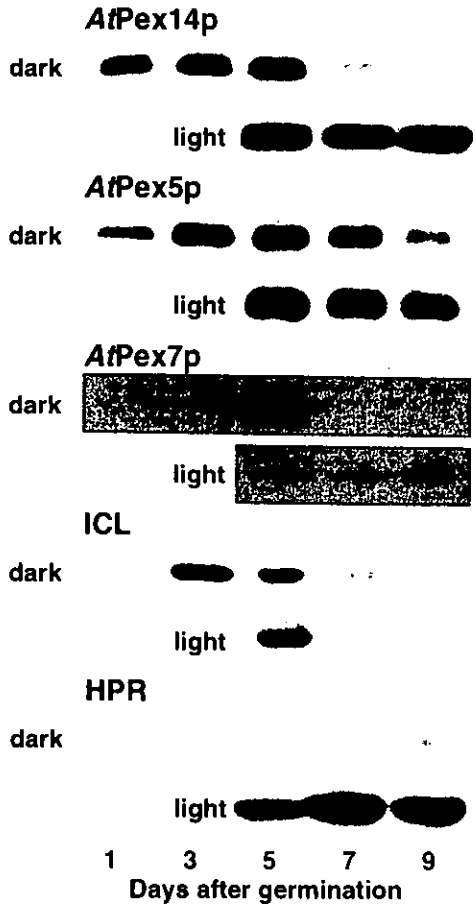

Fig. 2 Developmental changes in the levels of *At*Pex14p, *At*Pex5p and *At*Pex7p during germination. Arabidopsis seeds were grown in continuous darkness for 9 d or in darkness for 4 d then under continuous illumination for 5 d. Immunoblot analysis of homogenates prepared from cotyledons at various stages was carried out using antibodies against *At*Pex14p, *At*Pex5p, *At*Pex7p, ICL, and HPR. Equal amounts of total protein, 10 μg for *At*Pex14p, *At*Pex5p, ICL and HPR and 50 μg for *At*Pex7p, were loaded in each lane. Number of days after germination is shown at the bottom of each lane.

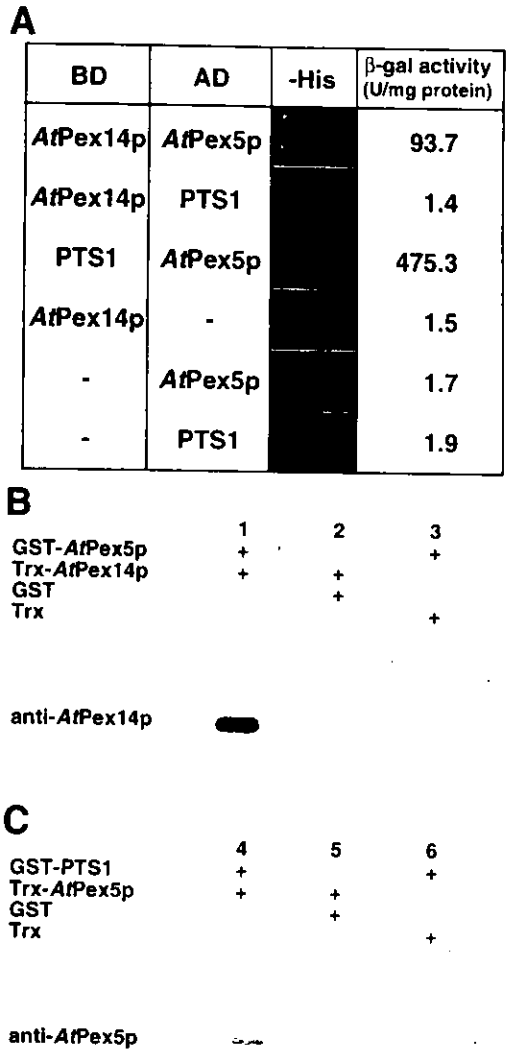

Fig. 3 Detection of interaction among *At*Pex14p, *At*Pex5p and PTS1-containing protein. (A) Two-hybrid analysis of *At*Pex14p, *At*Pex5p and PTS1-containing protein. Proteins were fused to Gal4 BD or AD as indicated. Transformants were tested for growth on synthetic medium without histidine (–His) and assayed for quantitative β-galactosidase activity. (B) and (C) In vitro binding experiments of between *At*Pex14p and *At*Pex5p, *At*Pex5p and PTS1-containing protein. Immunoblots (antibodies are indicated) of proteins recovered in glutathione Sepharose 4B are shown. The fusion proteins added in each experiment were as indicated.

cotyledons of fatty seedlings (Nishimura et al. 1986, Sautter 1986, Titus and Becker 1985). In greening cotyledons, matrix proteins are also replaced from glyoxysomal enzymes, such as ICL, to leaf peroxisomal enzymes, such as HPR (Fig. 2). We analyzed the developmental changes in the levels of peroxisomal protein import factors during the functional transition (Fig. 2).

When seedlings were grown in darkness, *At*Pex14p was expressed at the early stage of germination. *At*Pex14p was accumulated up to 5 d and then rapidly decreased. By contrast, when 4-day-old seedlings were transferred to the light, the amount of *At*Pex14p was kept constant in the green cotyledons. Although expression of *At*Pex5p was slightly delayed compared with that of *At*Pex14p, the level of *At*Pex5p reached a maximum after 3 to 5 d and then gradually decreased in etiolated cotyledons. When seedlings were illuminated, the amount of *At*Pex5p was also kept constant like that of *At*Pex14p. The developmental changes of these import factors, *At*Pex14p and *At*Pex5p, coincided with the accumulation of glyoxysomal enzymes and of leaf peroxisomal enzymes, such as ICL in etiolated cotyledons, and HPR in greening cotyledons. From the results of the analysis of the developmental changes, we concluded that *At*Pex14p and *At*Pex5p are responsible for protein

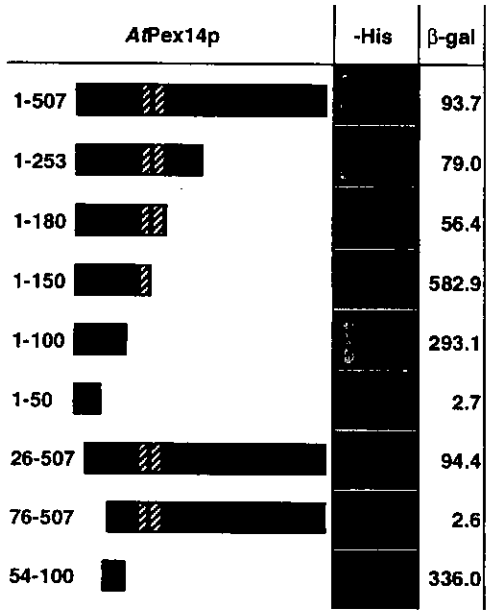

Fig. 4 The amino acids ^{54}R-^{100}P of *At*Pex14p interacts with *At*Pex5p. Various truncated *At*Pex14p were fused to the Gal4p DNA-binding domain and tested for binding activity to *At*Pex5p. Hatched boxes indicate the putative transmembrane domains. Numbers on the indicate each length of amino acid sequence. Transformants were tested for growth on synthetic medium without histidine (–His) and assayed for quantitative β-galactosidase activity.

import of two kinds of peroxisomes, glyoxysomes and leaf peroxisomes. The overall results of immunoblot analysis suggest that expression of *At*Pex14p or *At*Pex5p is a marker for high ability of peroxisomal protein import in biogenesis of peroxisomes. In contrast, the level of *At*Pex7p reached a maximum after 5 d and then rapidly decreased in etiolated cotyledons. The amount of *At*Pex7p was kept at a much lower level than that of *At*Pex14p and *At*Pex5p, when seedlings were illuminated.

AtPex14p interacts with AtPex5p, but not with PTS1-containing protein

Previously, we showed that *At*Pex14p is localized on the peroxisomal membrane and is exposed to the cytosolic surface (Hayashi et al. 2000). Pex5p from tobacco (Kragler et al. 1998) is localized in the cytosol and identified with PTS1-receptor of peroxisomal protein import. To investigate the interactions of *At*Pex14p, *At*Pex5p and PTS1-containing protein in the process of peroxisomal protein import, we carried out yeast two-hybrid analysis.

Each protein was fused to Gal4 AD or Gal4 BD and expressed in a tester strain PJ69–4A (James et al. 1996). The binding activity of protein–protein interactions was analyzed by its auxotrophy (–histidine + 3-AT 50 mM) and β-galactosidase activity. In the yeast two-hybrid analysis, *At*Pex14p interacted with *At*Pex5p, and but not directly with the PTS1-containing protein (Fig. 3A), leading to transcriptional activation of the *HIS3* and *LacZ*/β-galactosidase reporter genes in yeast tester strain. These interactions were shown in interchanges of each fused protein (data not shown). When each protein alone was expressed, the tester strain did not activate transcription of the reporter genes. Since *At*Pex5p fused to Gal4 DNA-binding domain auto-activated the reporter genes, these interactions were only tested with the Gal4 activation domain constructs of *At*Pex5p. The supporting evidence was provided by an in vitro binding assay. Each protein was fused to Trx or GST and was expressed in the *E. coli* expression system (Novagen). Two proteins were mixed with glutathione Sepharose 4B (Amersham), and the elution protein from glutathione Sepharose 4B was analyzed by immunoblotting. In this experiment, GST-fused or Trx-fused *At*Pex5p was shown to have a specific and direct interaction with Trx-fused *At*Pex14p (Fig. 3B, lane 1) and PTS1-conjugated GST (Fig. 3C, lane 4). Interactions were not observed with Trx and GST alone. These results showed that *At*Pex5p really functions as a PTS1 receptor. Since *At*Pex14p has binding activity to *At*Pex5p, we concluded that *At*Pex14p functions as an *At*Pex5p receptor for the *At*Pex5p-PTS1-containing protein complex on the peroxisomal membrane.

Two domains, ^{58}I-^{65}L and ^{78}R-^{97}R of AtPex14p interact with AtPex5p

To determine the binding domain of *At*Pex14p to *At*Pex5p, we prepared various truncated *At*Pex14ps-fused Gal4 DNA-binding domains, and analyzed the binding activities to the full length of *At*Pex5p (Fig. 4). When *At*Pex14p was truncated from its C-terminus, the tester strain, which expressed the N-terminus from amino acids ^{1}M-^{100}P of *At*Pex14p, showed transcriptional activation of reporter genes. Truncation of *At*Pex14p carried out from its N-terminus, showed that the C-terminus from amino acids ^{26}A-^{507}N of *At*Pex14p led to the activation of transcription. Furthermore, amino acids ^{54}R-^{100}P of *At*Pex14p, which showed a high homology domain among the Pex14ps from other species (Fig. 5, top column), also activated transcription of reporter genes. Therefore, it is concluded that amino acids ^{54}R-^{100}P in the N-terminus of *At*Pex14p has binding activity to *At*Pex5p. Interestingly, the amino acids ^{1}M-^{253}V of *At*Pex14p that was the same length of translation product in the *ped2* mutant also has binding activity to *At*Pex5p (Fig. 4).

Furthermore, to determine the amino acid residues important for binding in amino acids ^{54}R-^{100}P of *At*Pex14p, amino acid substitutions were introduced in which four amino acids were changed to four of alanine or glycine (Fig. 5, middle column). The mutated amino acids ^{54}R-^{100}P of *At*Pex14p was tested for binding activity to the full length of *At*Pex5p. As a result, peptides mutated in two domains; amino acids ^{58}I-^{65}L or ^{78}R-^{97}R of *At*Pex14p lost binding activity to *At*Pex5p (Fig. 5, bottom column). Therefore, protein–protein interaction between *At*Pex14p and *At*Pex5p required two domains; namely amino acids ^{58}I-^{65}L and ^{78}R-^{97}R of *At*Pex14p. N-terminal regions of Pex14p from various species were compared (Fig. 5, top column). Although the amino acid sequence of *At*Pex14p has

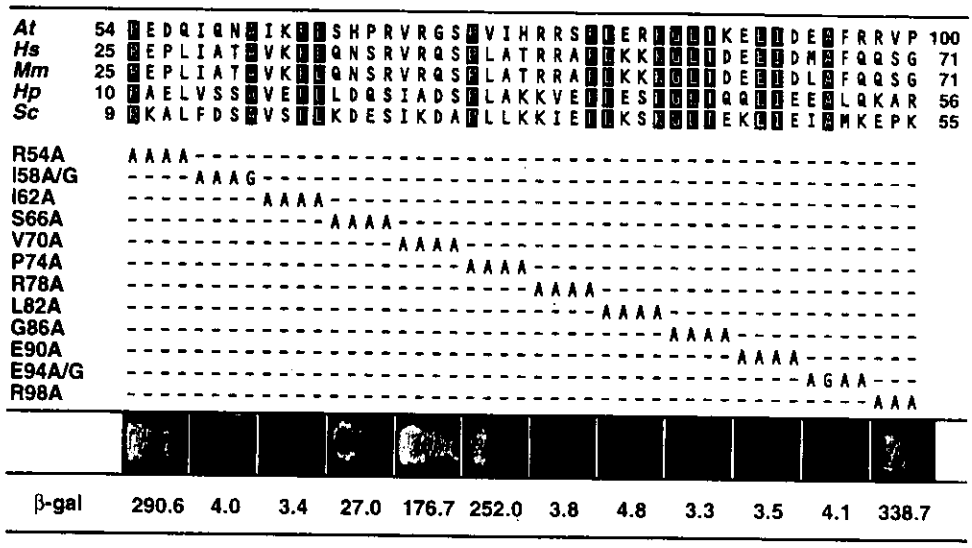

Fig. 5 Determination of binding domain in *At*Pex14p by introducing amino acid substitution within ^{54}R-^{100}P. Top column: alignment of *At*Pex14p with Pex14ps identified from various species. *At*, *Arabidopsis thaliana*; *Hs*, *Homo sapiens*; *Mm*, *Mus muscuris*; *Hp*, *Hansenula polymorpha*; *Sc*, *Saccharomyces cerevisiae*. Conserved amino acids are highlighted. Middle column: amino acid sequences of mutated *At*Pex14ps fused to the Gal4p DNA-binding domain. Amino acid substitutions introduced into the fusion proteins are indicated on the right. The name of each fusion protein is indicated on the left. Bottom column: result of binding assay for mutated *At*Pex14ps and mutated *At*Pex5p. Transformants were tested for growth on synthetic medium without histidine (–His) and assayed for quantitative β-galactosidase activity.

low identity to Pex14p from other species (to human; 29.6%) (Will et al. 1999), amino acids ^{54}R-^{100}P of *At*Pex14p has relatively high identity to N-terminus of Pex14p from other species (to human; 53.2%). We concluded that these two domains of *At*Pex14p were conserved and were common binding domains for *At*Pex5p among all species.

WXXXF motifs in amino acids ^{231}K-^{450}D of AtPex5p are required for binding to AtPex14p

We carried out the next experiments to determine the binding domain of *At*Pex5p to *At*Pex14p. *At*Pex5p has two unique motifs. One is the TPR motif previously reported as a binding domain for PTS1-containing protein (Brocard et al. 1994). The other is a WXXXF/Y repeat that existed in Pex5p from various species. This repeat is found in each Pex5p, but differs in number and spacing (Schliebs et al. 1999). For example, Pex5p of yeast (*S. cerevisiae*) possesses only two of these repeats whereas *At*Pex5p contains nine in amino acids ^{231}K-^{450}D. These nine repeats separately exist as three N-terminal repeats and six C-terminal repeats in amino acids ^{231}K-^{450}D of *At*Pex5p.

To determine the binding domain of *At*Pex5p to *At*Pex14p, we prepared various truncated *At*Pex5ps-fused Gal4 activation domains, and analyzed the binding activities to the amino acids ^{54}R-^{100}P of *At*Pex14p (Fig. 6A). The amino acids ^{231}K-^{450}D of *At*Pex5p, including the nine WXXXF/Y repeats, had binding activity to *At*Pex14p. The amino acids ^{457}H-^{728}L of *At*Pex5p, containing the TPR motifs, show binding activity to PTS1-containing protein (data not shown). Each binding domain for *At*Pex14p and PTS1-containing protein did not overlap in the amino acid region of *At*Pex5p. This implies that *At*Pex14p, *At*Pex5p and PTS1-containing protein form an import complex that functions in peroxisomal protein import.

To investigate whether the nine WXXXF/Y repeats were used properly, we substituted each WXXXF/Y with AXXXA and analyzed the binding activities to *At*Pex14p. All mutated WXXXF/Y showed binding activity to *At*Pex14p, but transcriptional activation of the *LacZ*/β-galactosidase reporter gene decreased slightly (data not shown). The *LacZ*/β-galactosidase reporter gene activity was significantly decreased by mutation of the eighth WXXXF (Fig. 6A). Deletion of the eighth WXXXF repeat also exhibited the same level of binding activity as the mutated repeat.

To demonstrate that WXXXF/Y repeats are the binding site for *At*Pex14p, the eighth WXXXF including five amino acids each before and behind was linked tandem. These two to four tandem repeats of WXXXF showed a gradual increase of β-galactosidase activity (Fig. 6B). In addition to this, β-galactosidase activity of amino acids ^{336}E-^{450}D of *At*Pex5p including six WXXXF/Y repeats was much higher than those of the two to four tandem repeats, showing that the number of repeats is responsible for the efficiency of the binding. The mutated eighth AXXXA did not show the binding activity. These findings indicate that WXXXF is required for binding to *At*Pex14p.

AtPex7p interacts with AtPex5p, but not with AtPex14p

In addition to Pex14p and Pex5p, Pex7p is known as a PTS2 receptor in peroxisomal protein import from studies of

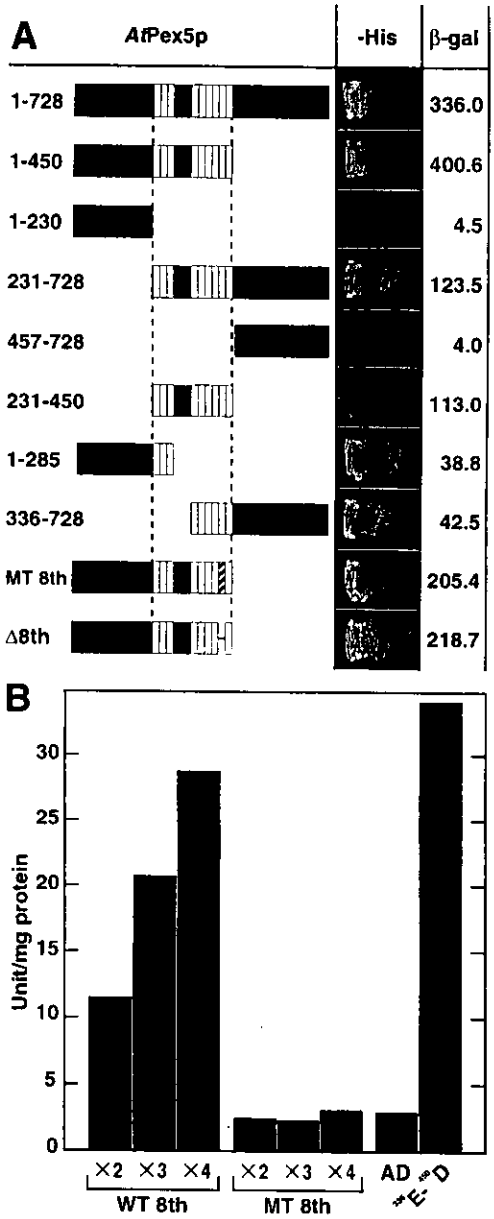

Fig. 6 WXXXF/Y repeats in the amino acids ^{231}K-^{450}D of *At*Pex5p are required for binding to *At*Pex14p. (A) Various truncated *At*Pex5p were fused to the Gal4p activation domain and tested for binding activity to the amino acids ^{54}R-^{100}P of *At*Pex14p. Numbers on the left indicate length of each amino acid sequence. Open boxes indicate WXXXF/Y of the consensus amino acid sequence. Hatched box indicates amino acid substitution of 8th WXXXF to AXXXA. (B) Artificial tandem repeats of 8th WXXXF sequence were tested for binding activity to *At*Pex14p-(^{54}R-^{100}P). WT 8th indicates tandem repeats linked with eighth WXXXF sequence of wild-type. MT 8th indicates tandem repeats linked with AXXXA sequence substituted from eighth WXXXF sequence. AD indicates expression of only Gal4 AD in tester strain. ^{336}E-^{450}D indicates the amino acids ^{336}E-^{450}D of *At*Pex5p including six WXXXF/Y repeats. Transformants were tested for growth on synthetic medium without histidine (–His) and assayed for quantitative β-galactosidase activity.

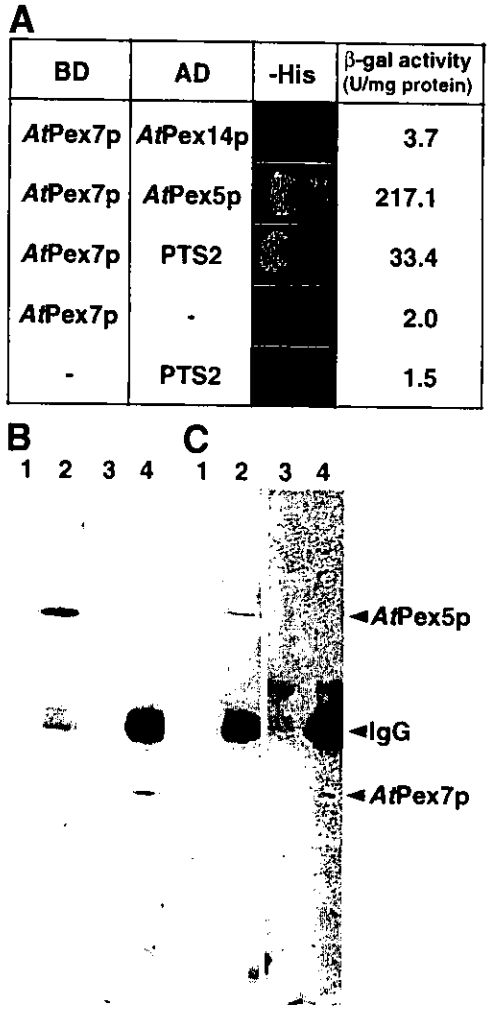

Fig. 7 *At*Pex7p interacts with *At*Pex5p and PTS2-containing protein. (A) Two-hybrid analysis of *At*Pex14p, *At*Pex5p, *At*Pex7p and PTS2-containing protein. Proteins were fused to Gal4 BD or AD as indicated. Transformants were tested for growth on synthetic medium without histidine (–His) and assayed for quantitative β-galactosidase activity. (B) and (C) Co-immunoprecipitation of *At*Pex5p and *At*Pex7p. Antibodies against *At*Pex5p (B) and *At*Pex7p (C) were immobilized on column. After total homogenates from etiolated cotyledons were passed over, the columns were washed and then eluted. Wash fraction (odd lanes) and elution fraction (even lanes) were subjected by SDS-PAGE and immunoblotting using antibodies against *At*Pex5p (lane 1, 2) and *At*Pex7p (lane 3, 4). Arrowheads on the right indicate specific bands.

yeast and mammals. To investigate the interactions of *At*Pex7p, *At*Pex14p, *At*Pex5p and PTS2-containing protein, yeast two-hybrid analysis was also carried out. The interaction was analyzed as shown in Fig. 3A.

The results of yeast two-hybrid analysis showed that *At*Pex7p interacts with PTS2-containing protein, leading to transcriptional activation of the *HIS3* and *LacZ*/β-galactosidase reporter genes in yeast tester strain (Fig. 7A). This shows that the amino acid sequence encoded for cDNA of *At*Pex7p

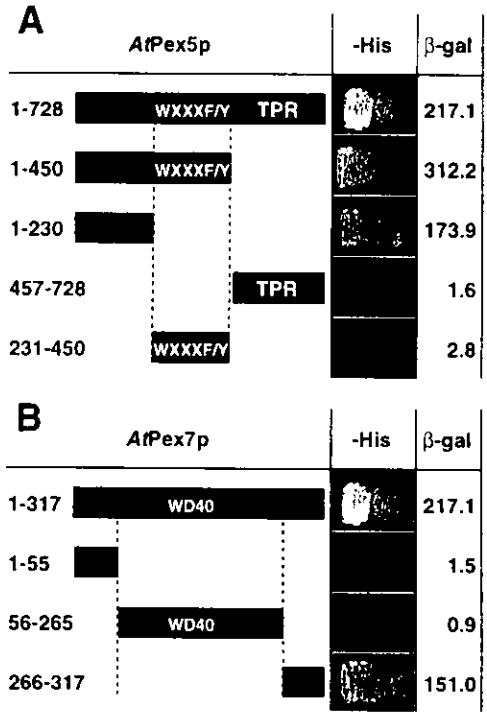

Fig. 8 The amino acids ^{1}M-^{230}V of *At*Pex5p interacts with amino acids ^{266}Y-^{317}S of *At*Pex7p. (A) Various truncated *At*Pex5p were fused to the Gal4p activation domain and tested for binding activity to *At*Pex7p. WXXXF/Y indicates nine repeats of the consensus amino acid sequence. TPR indicates four TPR motifs. (B) Various truncated *At*Pex7p were fused to the Gal4p DNA binding domain and tested for binding activity to *At*Pex5p. WD40 indicates four WD40 repeats. Numbers on the left indicate length of each amino acid sequence. Transformants were tested for growth on synthetic medium without histidine (–His) and assayed for quantitative β-galactosidase activity.

reported by Schumann et al. (1999) maintains the function of a PTS2 receptor. Furthermore, Fig. 7A shows that *At*Pex7p interacts with *At*Pex5p but not with *At*Pex14p directly. This was also supported by a co-immunoprecipitation assay. The antibody against either *At*Pex5p (Fig. 7B) or *At*Pex7p (Fig. 7C) was immobilized on the column. Then, total homogenates from 4-day-old Arabidopsis seedlings were passed through, and the eluted proteins were analyzed by immunoblotting. In this experiment, both proteins were detected in only elution fractions from both columns (Fig. 7B, C, even lanes), indicating that *At*Pex5p and *At*Pex7p interact with each other. *At*Pex5p and *At*Pex7p were not eluted from column that were immobilized with preimmune serums (data not shown). Since a part of the immobilized antibodies were eluted, the IgG bands were detected in all eluted fractions. We demonstrate that *At*Pex7p has binding activity to *At*Pex5p.

The amino acids ^{266}Y-^{317}S of AtPex7p interacts with the amino acids ^{1}M-^{230}V of AtPex5p

To determine the binding domain of *At*Pex5p to *At*Pex7p, we prepared various truncated *At*Pex5ps-fused Gal4 activation domains, and analyzed the binding activities to the full length of *At*Pex7p (Fig. 8A). The results showed that the binding domain of *At*Pex5p was specific to the N-terminal region, amino acid ^{1}M-^{230}V of *At*Pex5p. This N-terminal region did not overlap with the binding domain for either *At*Pex14p (amino acids ^{231}K-^{450}D) or PTS1-containing protein (amino acids ^{457}H-^{728}L). To determine the binding domain of *At*Pex7p to *At*Pex5p, we prepared various truncated *At*Pex7ps-fused Gal4 DNA-binding domains, and analyzed the binding activities to full length *At*Pex5p (Fig. 8B). The results show that the binding domain of *At*Pex7p was restricted to the C-terminal region, especially, amino acid ^{266}Y-^{317}S of *At*Pex7p. This C-terminal region does not include with WD40 repeats (amino acids ^{56}S-^{265}D) that was identified as the binding domain for PTS2-containing proteins (Zhang and Lazarow 1994).

Discussion

More than 20 PEX genes and their products, peroxins, have been identified in yeast and mammals (Subramani et al. 2000). Some of these factors, including Pex14p, Pex5p and Pex7p, contain members of the peroxisomal protein import apparatus (Albertini et al. 1997, Marzioch et al. 1994, Van der Leij et al. 1993), but the details of the protein import mechanisms are still unclear. Studies in yeast showed that Pex14p interacts with both Pex5p and Pex7p (Albertini et al. 1997), but, there is no binding activity between Pex5p and Pex7p. Yeast mutants defective in abilities of Pex5p and Pex7p lose PTS1 and PTS2 pathways, respectively (Marzioch et al. 1994, McCollum et al. 1993). These findings suggested that the PTS1 pathway and PTS2 pathway are independent in yeast. By contrast, the nonsense mutation R390ter of Pex5p in human invites to defect in both PTS1 and PTS2 pathways (Braverman et al. 1998). This suggested that human Pex5p was involved not only in PTS1 pathway but also in PTS2 pathway. Two isoforms of human and Chinese hamster ovary cell Pex5p were produced by alternative splicing (Braverman et al. 1998, Otera et al. 1998). Each of the Pex5p isoforms are called short-form and long-form of Pex5p. Transfection of mutant cells, R390ter of Pex5p, with the long-form of Pex5p restores both PTS1 and PTS2 pathways, however, the short-form of Pex5p restores only the PTS1 pathway. Furthermore, transfection of mutant cells, R390ter of Pex5p, with the long-form of Pex5p containing a mutation in the binding domains for PTS1-containing protein restores the PTS2 pathway but not the PTS1 pathway. These findings suggested that the long-form of Pex5p is responsible for the PTS2 pathway, but the short form of Pex5p is not (Braverman et al. 1998, Otera et al. 1998). Therefore, it is indicated that the human PTS2 pathway is partially independent of the Pex5p, PTS1 receptor. In this report, we demonstrated by two-hybrid analysis that *At*Pex5p binds to both *At*Pex14p and *At*Pex7p, but that *At*Pex14p does not bind to *At*Pex7p. This binding pattern in Arabidopsis peroxisomal import factors is similar to that of long-form of Pex5p in

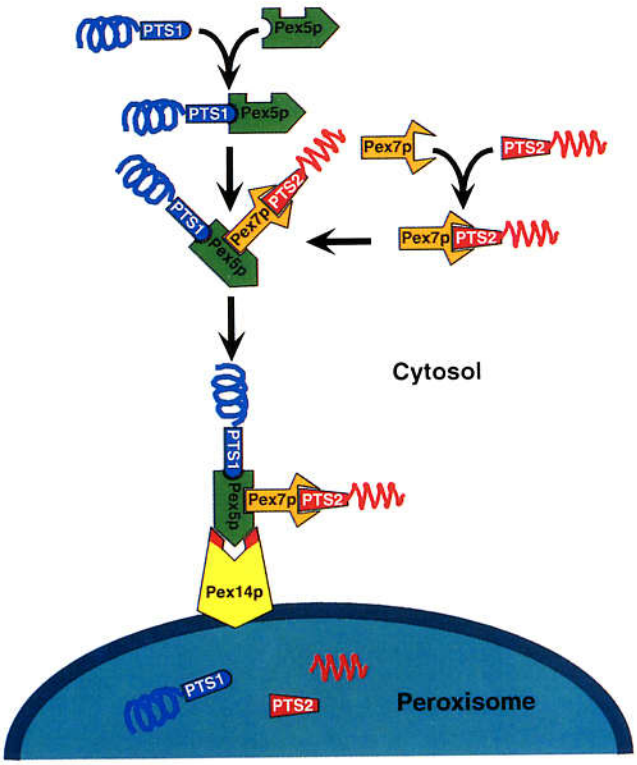

Fig. 9 A schematic model of peroxisomal protein import in Arabidopsis. Pex5p and Pex7p, PTS1 receptor and PTS2 receptor, which are localized in the cytosol are bound to PTS1- and PTS2-containing proteins (cargo), respectively. Both protein complexes bind between amino acids ^{1}M-^{230}V of *At*Pex5p and amino acids ^{266}Y-^{317}S of *At*Pex7p. The receptor-cargo import complex consisting of Pex5p, Pex7p, PTS1- and PTS2-containing protein binds then to the peroxisomal membrane via interaction between WXXXF/Y repeats of *At*Pex5p and amino acids ^{58}I-^{65}L and ^{78}R-^{97}R of *At*Pex14p. All binding domains do not overlap in the process of peroxisomal protein import.

humans. However, in the immunoblot analysis (Fig. 1, 2) and RT-PCR (data not shown), *At*Pex5p was detected as a monospecific band. Therefore, there is little possibility that the multiple *At*Pex5p isoforms are produced by alternative splicing in Arabidopsis. These findings implied that the PTS2 pathway in Arabidopsis is completely dependent on the *At*Pex5p, PTS1 receptor (Fig. 9).

Most peroxisomal matrix proteins possess either PTS1 or PTS2 as the targeting signal (PTS) in various species (Olsen 1998). Our results suggest that the PTS1 pathway, dependent on *At*Pex5p, is the main import pathway expressed in most organs from the expression of *At*Pex5p (Fig. 1). This finding is in agreement with the fact that human Pex14p and Pex5p are expressed in most tissues (Wiemer et al. 1995, Will et al. 1999). Since *At*Pex7p that is the PTS2 receptor is expressed in limited organs in comparison with that of *At*Pex5p, it is speculated that the PTS2-dependent import pathway is an additional transport pathway for peroxisomes, and that the expression of the PTS2-containing protein is more specific among the organs than that of the PTS1-containing protein. At present, most peroxisomal matrix proteins including glyoxysomal and leaf peroxisomal proteins possess PTS1. In contrast with this, PTS2-containing proteins in higher plants, namely thiolase (Kato et al. 1996b), malate dehydrogenase (Kato et al. 1998), citrate synthase (Kato et al. 1995) and long-chain acyl-CoA oxidase (Hayashi et al. 1998), are mainly accumulated in glyoxysomes, but not in leaf peroxisomes. Although leaf peroxisomal enzymes containing PTS2 have not been identified at present in higher plants, as Fig. 1 shows, *At*Pex7p is expressed in cauline leaves and rosette leaves. A search of Arabidopsis genome databases with PEDANT BLAST Network Service (http://pedant.gsf.de/) revealed that 49 genes of unidentified PTS2-containing proteins exist in the Arabidopsis genome. This suggests that unidentified PTS2-containing proteins are expressed in these organs and plays a role in unidentified metabolic pathways of plant peroxisomes.

The data obtained with yeast and mammals indicated that Pex14p is localized on peroxisomal membrane, and is a central receptor for Pex5p, which captures the PTS1-containing protein (Brocard et al. 1997, Will et al. 1999). In human Pex14p it has been determined that the amino acids ^{1}M-^{78}S is a binding domain for Pex5p (Schliebs et al. 1999). The amino acid sequence of *At*Pex14p is longer than that of human Pex14p. Sequence homology showed that the amino acids ^{1}M-^{100}P of *At*Pex14p correspond with amino acids ^{1}M-^{71}G of human Pex14p (Fig. 5, top column). In this study, we found two binding domains of *At*Pex14p for Pex5p, ^{58}I-^{65}L and ^{78}R-^{97}R in 100 N-terminal amino acids (Fig. 5, bottom column). Secondary structure prediction (Garnier et al. 1978) for the amino acid sequence of *At*Pex14p showed that these two N-terminal domains might form a binding pocket (data not shown). This binding pocket of *At*Pex14p may hold *At*Pex5p on its peroxisomal membrane.

Previous studies showed that a nucleotide substitution occurred in the *ped2* mutant, converting a CAA codon encoding ^{254}Q of the gene product to a stop codon (TAA), and that the protein import activities of PTS1- and PTS2-containing proteins partially remained in the *ped2* mutant (Hayashi et al. 2000). In this paper, we showed that the amino acids ^{1}M-^{253}V of *At*Pex14p corresponding to deduced polypeptide in *ped2* mutant possessed binding activity to *At*Pex5p, indicating that the N-terminal region of *At*Pex14p is essential for import of PTS1- and PTS2-containing proteins (Fig. 4). Although these N-terminal amino acids ^{1}M-^{253}V of *At*Pex14p could not be detected by immunoblotting in *ped2* mutant (data not shown), it is likely that the truncated *At*Pex14p is expressed in small amounts in *ped2* mutant and still partially retains the ability of translocation of PTS1- and PTS2-containing proteins. If this polypeptide does not exist in *ped2* mutant, small amounts of PTS1- and PTS2-containing proteins may be imported to peroxisomes via another import pathway that is independent of *At*Pex14p in Arabidopsis.

We determined the domain binding *At*Pex14p and

*At*Pex5p. The binding domain of *At*Pex5p is WXXXF/Y repeats and the number of WXXXF/Y repeats affects the affinity between *At*Pex14p and *At*Pex5p (Fig. 6). This binding activity between *At*Pex14p and *At*Pex5p increased proportionally with the number of WXXXF/Y repeats (Fig. 6B). These repeats are found in the amino acid sequence of Pex5p from various species as the consensus sequences different in number and spacing (Schliebs et al. 1999). For example, Pex5p from Arabidopsis and watermelon possesses nine of these repeats whereas Pex5p from *S. cerevisiae* contains only two. In this manner, the number of repeats from higher plants tend to be more than those of other species. Furthermore, a recent study showed that human Pex5p forms a tetrameric structure (Schliebs et al. 1999). If this is also the case in *At*Pex5p, the receptor complex of *At*Pex5p possesses 36 WXXXF/Y repeats, which is the binding domain for *At*Pex14p. This fact suggests that Pex5p from higher plants has higher affinity with Pex14p than other species. Higher plants need to degrade storage lipid rapidly, and obtained the energy for growth. Moreover, peroxisomes underwent the functional transition and obtain photorespiratory activity in higher plants. This functional transition of peroxisomes is observed in plants, but not in yeast or mammals. Therefore, higher plants can adapt to a change a large quantity of metabolic enzymes rapidly, and produce Pex5p that possesses high protein import activity.

Pex5p and Pex7p are localized in the cytosol and have been identified as the PTS1 receptor and PTS2 receptor, respectively, in various species (Subramani 1998). These receptors are reported to be important factors for peroxisomal protein import. In this paper, we suggest that *At*Pex5p and *At*Pex7p form a PTS1-PTS2 receptor complex in the peroxisomal protein import pathway, and that the PTS2 pathway is dependent on the PTS1 pathway in higher plants. Therefore, the PTS2 pathway may be an additional pathway in peroxisomal protein import. Furthermore, their binding domains are N-terminal amino acids ^{1}M-^{230}V of *At*Pex5p and C-terminal amino acids ^{266}Y-^{317}S of *At*Pex7p, respectively (Fig. 8). Each receptor possesses binding domains for PTS1- and PTS2-containing proteins that are cargo proteins. In Pex5p, the binding domain is a TPR motif (Gatto et al. 2000) located in the amino acids ^{457}H-^{728}L of *At*Pex5p. In Pex7p, the binding domains are WD40 repeats (Shimozawa et al. 1999) located in the amino acids ^{56}S-^{265}D of *At*Pex7p. These binding domains do not overlap at least on amino acid sequences, including the binding domain for *At*Pex14p (amino acids ^{231}K-^{450}D of *At*Pex5p). In addition to these results, some peroxisomal proteins containing PTS1 or PTS2 have been shown to form an oligomer in the cytosol (Kato et al. 1999, Subramani 1998). These findings suggest that interaction of peroxisomal import factors, *At*Pex14p, *At*Pex5p and *At*Pex7p, with cargo protein, PTS1- and PTS2-containing proteins, is not competitive in peroxisomal protein import, and imply that these proteins form a huge import complex on the peroxisomal membrane. The protein import system toward peroxisomes is different from that of mitochondria and chloroplasts, and possesses the unique ability that even a huge gold particle containing PTS can be introduced into the peroxisomal matrix through the membrane (Walton et al. 1995). The peroxisomal unique protein import may reflect the introduction ability of a huge import complex that is formed with three import factors in addition to PTS1- and PTS2-containing proteins (Fig. 9).

We found that the binding domains among peroxisomal import factors, *At*Pex14p, *At*Pex5p and *At*Pex7p do not overlap. It is still unclear whether the binding between *At*Pex14p, *At*Pex5p and *At*Pex7p is not redundant in the three-dimensional structure. Further analysis of the three-dimensional structures of binding sites for these import factors will provide information on the co-operativity of these import factors in the process of the import of these proteins. In this paper, we suggest the schematic model of peroxisomal protein import in Arabidopsis (Fig. 9). In this model, import factors and cargo proteins form the huge protein complex. However, we could not detect the import complex of *At*Pex14p, *At*Pex5p and *At*Pex7p in in vitro binding experiments. As a reason for this failure, it is likely that binding efficiencies of these factors are probably low. In fact, we showed the interaction between not only *At*Pex14p and *At*Pex5p but also *At*Pex5p and PTS1-containing protein in in vitro binding experiments in Fig. 3, however, the complex of three proteins could not be detected when *At*Pex14p, *At*Pex5p and PTS1-containing protein were mixed at the same time. It is necessary to clarify in further studies whether huge protein complex are formed on peroxisomal membrane and their affinities are changed by interaction among more than two factors. Pex5p has been shown to be translocated into the peroxisomal matrix with cargo proteins, and recycled to the cytosol in the process of protein import (Dammai and Subramani 2001). However, the mechanism of association and dissociation between PTS receptors and cargo proteins is still unclear with respect to peroxisomal protein import machinery. It is possible that of other peroxisomal import factors beside *At*Pex14p, *At*Pex5p and *At*Pex7p exist, and their interaction may regulate the mechanism of association and dissociation. In fact, Pex13p and Pex17p have been characterized as protein import factors on peroxisomal membranes from analyses of yeast and mammals. Arabidopsis Pex13p and Pex17p have not yet been identified functionally. Characterization of other import factors such as Pex13p and Pex17p, and clarification of the changes in the affinity between peroxisomal import complexes and cargo proteins remain for future studies.

Materials and Methods

Plant materials

Arabidopsis thaliana (ecotype Landsberg *erecta* and Colombia) seeds were surface sterilized in 2% NaClO, 0.02% Triton X-100, and were grown on germination media (2.3 mg ml^{-1} Murashige and Skoog salts (Wako, Osaka, Japan), 1% sucrose, 100 μg ml^{-1} myo-inositol,

1 μg ml^{-1} thiamine-HCl, 0.5 μg ml^{-1} pyridoxine, 0.5 μg ml^{-1} nicotinic acid, 0.5 mg ml^{-1} MES-KOH (pH 5.7), 0.2% INA agar (Ina Shokuhin, Nagano, Japan)) at 22°C under continuous illumination or darkness. Some 7-day-old seedlings were transferred from the medium to a 1 : 1 mixture of perlite and vermiculite and grown for 4 weeks at 22°C. Plants were harvested and homogenates prepared from various organs and germinating seedlings.

Preparation of total homogenates from Arabidopsis

Total homogenates from cotyledons and other various organs of Arabidopsis were prepared as follows. Cotyledons and various organs were homogenized with 50 mM Tris-HCl, pH 8.0, 1 mM EDTA, 10% glycerol and 1% SDS as a detergent. The homogenates were centrifuged at 12,000×*g* for 10 min and the supernatants were measured using the Bio-Rad Protein Assay (Bio-Rad, Hercules, CA, U.S.A.) and then were subjected to SDS-PAGE and subsequent immunoblotting.

Expression of fusion proteins and preparation of their specific antibodies

Standard procedures for expression of fusion proteins and preparation of specific antibodies were described previously (Nito et al. 2001). Two DNA fragments corresponding to the amino acids ^{231}K-^{450}D of *At*Pex5p and full-length polypeptide of *At*Pex7p were produced by PCR. The DNA fragment obtained after PCR was ligated into the T-vector and used to transform *E. coli*. After plasmid extraction, the DNA fragments were digested with the appropriate restriction enzymes and ligated into the multiple cloning site of pET32a vector (Novagen, Madison, WI, U.S.A.). The fusion proteins, consisting of Trx and the sequence of each peptide were expressed in *E. coli* BL21(DE3) and purified by column chromatography on a Ni^+-chelating column (Amersham Pharmacia, Tokyo). The purified fusion proteins in 1 ml of sterilized water were emulsified with an equal volume of Freund's complete adjuvant (DIFCO, Detroit, MI, U.S.A.). The emulsion was injected subcutaneously into the back of a rabbit. Four weeks later, a booster injection (about 0.5 mg of protein with incomplete adjuvant) was given in the same way. Blood was taken from a vein in the ear 3 d after the second booster injection. Since antibodies prepared with other amino acid regions of *At*Pex5p and *At*Pex7p also detected immunoreactive bands with the same molecular weight (data not shown), these antibodies were considered to recognize *At*Pex5p and *At*Pex7p, respectively.

In vitro binding experiments

The preparation of Trx-fused the amino acids ^{1}M-^{100}P of *At*Pex14p was as described previously (Hayashi et al. 2000). GST-fused and Trx-fused *At*Pex5p, and GST-fused PTS1-containing protein were prepared in this study. The DNA fragment corresponding to the full length of *At*Pex5p was amplified by RT-PCR. The PCR product was subcloned into pET41a vector and pET32a vector (Novagen, Madison, WI, U.S.A.). The oligo DNAs corresponding to the C-terminal 10 residue (GSVVVARSRM) of ICL, which is a PTS1-containing protein, were synthesized and inserted to pGEX vector (Amersham Pharmacia, Tokyo). The fusion proteins, consisting of GST or Trx alone, GST- or Trx-fused *At*Pex5p and GST-fused PTS1-containing protein were expressed and purified by the same strategy as described above. Two of these proteins were mixed with glutathione Sepharose 4B for 1 h and then were centrifuged. Proteins recovered in the precipitate were eluted with 10 mM glutathione and were subjected to immunoblot analysis using antibodies against *At*Pex14p or *At*Pex5p.

Co-immunoprecipitation experiments

Fusion proteins used for preparation of antibodies were immobilized on an NHS-activated column (Amersham Pharmacia, Tokyo). Then, we carried out affinity purification of antibodies against *At*Pex5p and *At*Pex7p using these columns. Purified antibodies were immobilized on NHS-activated column. The crude homogenate from etiolated Arabidopsis cotyledons grown for 4 d were prepared with 50 mM phosphate buffer (pH 7.5), 100 mM sodium chloride, and then passed over the columns. The columns were washed with ten column volumes of the same buffer and fractionated. Bound proteins were eluted with glycine-HCl (pH 2.0). Washed fractions and elution fractions were analyzed by SDS-PAGE and subsequent immunoblotting using antibodies against *At*Pex5p and *At*Pex7p.

Immunoblotting

Ten to fifty μg of total protein were applied onto lanes of SDS-polyacrylamide gel. After electrophoresis, proteins were transferred to a PVDF membrane (MILLIPORE, Tokyo, Japan) in a semi-dry electroblotting system. The membrane was blocked with 5% non-fat dry milk, 3% BSA in Tris-buffered saline, pH 7.4 and immunoblotted with 1 : 5,000 to 10,000 dilution of antibodies against anti-*At*Pex14p, anti-*At*Pex5p, anti-*At*Pex7p, anti-ICL (Maeshima et al. 1988, Mano et al. 1996), or anti-HPR (Mano et al. 1997). Bands were visualized with an ECL Western blotting detection kit (Amersham Japan, Tokyo, Japan) using a 1 : 5,000 dilution of peroxidase-conjugated goat antibodies against rabbit IgG following the instructions of the manufacturer.

Two-hybrid analysis

The two-hybrid system was based on the method of Fields and Song (Field and Song 1989). The tested genes were fused to the Gal4p DNA-binding domain (BD) or activation domain (AD) in the vectors pGBD-C1 and pGAD-C1 (James et al. 1996). To construct various lengths of DNA fragments encoding the truncated *At*Pex14p, DNA fragments conjugated at the *ClaI*/*SalI* sites were amplified by PCR. The artificial tandem repeats of WXXXF were also constructed by PCR (Nakajima and Yaoita 1997). After PCR, DNA fragments were then subcloned into a T-vector prepared with Bluescript KS^+ (Stratagene, La Jolla, CA, U.S.A.) as described in a previously (Marchuk et al. 1990). After digestion with individual restriction enzymes, DNA fragments were inserted into a suitable restriction site on pGBD-C1 and pGAD-C1. In the same way, *At*Pex5p DNA fragments of various lengths conjugated at the *Bam*HI/*Sal*I sites were subcloned into pGAD-C1. Likewise, *At*Pex7p DNA fragments of various lengths conjugated at the *Sal*I/*Bgl*II sites were subcloned into pGBD-C1. To generate the constructs for Gal4 BD and AD-fused PTS1 protein, the plasmid encoding the GFP conjugated to the PTS1 signal (Mano et al. 1999) was digested by *Bam*HI/*Pst*I, and then the DNA fragment was inserted in the pGBD-C1 and pGAD-C1 vector. All amino acid substitutions in *At*Pex14p were performed by PCR-based mutagenesis. The open reading frames were sequenced and it was confirmed that no mutations were introduced other than the desired ones.

The two-hybrid vectors were co-transformed into tester strain PJ69–4A (James et al. 1996) according to an established protocol (Gietz et al. 1995). Yeast transformants were selected and grown on complete synthesized media containing 2% glucose, 0.67% yeast nitrogen base without amino acid (DIFCO) and amino acids as needed. Two-hybrid interactions were assayed using both the His3 reporter and LacZ reporter. Quantitative β-galactosidase activity was measured according to an established protocol (Miller 1972). The mean β-galactosidase activity (unit (mg protein)$^{-1}$) measured in the lysate of three transformants was calculated.

Acknowledgment

The authors thank Dr. P. James (University of Wisconsin) for kindly providing the host strain and cloning vectors for two-hybrid

analysis and Dr. M. Maeshima (Nagoya University) for antibody against ICL. This work was supported in part by grants-in-aid for scientific research from the Ministry of Education, Science and Culture of Japan (12440231 to M.N. and 12640625 to M.H.), and by a grant from CREST of JST (Japan Science and Technology) to M.H.

References

Albertini, M., Rehling, P., Erdmann, R., Girzalsky, W., Kiel, J.A., Veenhuis, M. and Kunau, W.H. (1997) Pex14p, a peroxisomal membrane protein binding both receptors of the two PTS-dependent import pathways. *Cell* 89: 83–92.

Beevers, H. (1979) Microbodies in higher plants. *Annu. Rev. Plant Physiol.* 30: 159–193.

Braverman, N., Dodt, G., Gould, S.J. and Valle, D. (1998) An isoform of Pex5p, the human PTS1 receptor, is required for the import of PTS2 proteins into peroxisomes. *Hum. Mol. Genet.* 7: 1195–1205.

Brickner, D.G., Brickner, J.H. and Olsen, L.J. (1998) Sequence analysis of a cDNA encoding Pex5p, a peroxisomal targeting signal type 1 receptor from *Arabidopsis thaliana*. *Plant Physiol.* 118: 330.

Brocard, C., Kragler, F., Simon, M.M., Schuster, T. and Hartig, A. (1994) The tetratricopeptide repeat-domain of the PAS10 protein of *Saccharomyces cerevisiae* is essential for binding the peroxisomal targeting signal -SKL. *Biochem. Biophys. Res. Commun.* 204: 1016–1022.

Brocard, C., Lametschwandtner, G., Koudelka, R. and Hartig, A. (1997) Pex14p is a member of the protein linkage map of Pex5p. *EMBO J.* 16: 5491–5500.

Dammai, V. and Subramani, S. (2001) The human peroxisomal targeting signal receptor, Pex5p, is translocated into the peroxisomal matrix and recycled to the cytosol. *Cell* 105: 187–196.

De Bellis, L. and Nishimura, M. (1991) Development of enzymes of the glyoxylate cycle during senescence of pumpkin cotyledons. *Plant Cell Physiol.* 32: 555–561.

Field, S. and Song, O.K. (1989) A novel genetic system to detect protein-protein interactions. *Nature* 340: 245–246.

Garnier, J., Osguthorpe, D.J. and Robson, B. (1978) Analysis of the accuracy and implication of simple methods for predicting the secondary structure of globular proteins. *J. Mol. Biol.* 120: 97–120.

Gatto, G.J., Geisberecht, B.V., Gould, S.J. and Berg, J.M. (2000) Peroxisomal targeting signal-1 recognition by the TPR domains of human PEX5. *Nat. Struct. Biol.* 7: 1091–1095.

Gietl, C. (1990) Glyoxysomal malate dehydrogenase from watermelon is synthesized with an amino-terminal transit peptide. *Proc. Natl. Acad. Sci. USA* 87: 5773–5777.

Gietz, R.D., Schiestl, R.H., Willems, A.R. and Woods, R.A. (1995) Studies on the Transformation of intact yeast cells by the LiAc/SS-DNA/PEG procedure. *YEAST* 11: 355–360.

Hayashi, H., De Bellis, L., Ciurli, A., Kondo, M., Hayashi, M. and Nishimura, M. (1999) A novel acyl-CoA oxidase that can oxidize short-chain acyl-CoA in plant peroxisomes. *J. Biol. Chem.* 274: 12715–12721.

Hayashi, H., De Bellis, L., Yamaguchi, K., Kato, A., Hayashi, M. and Nishimura, M. (1998) Molecular characterization of a glyoxisomal long chain acyl-CoA oxidase that is synthesized as a precursor of higher molecular mass in pumpkin. *J. Biol. Chem.* 273: 8301–8307.

Hayashi, M., Nito, K., Toriyama-Kato, K., Kondo, M., Yamaya, T. and Nishimura, M. (2000) *At*Pex14p maintains peroxisomal functions by determining protein targeting to three kinds of plant peroxisomes. *EMBO J.* 19: 5701–5710.

Hayashi, M., Tsugeki, R., Kondo, M., Mori, H. and Nishimura, M. (1996) Pumpkin hydroxypyruvate reductases with and without a putative C-terminal signal for targeting to microbodies may be produced by alternative splicing. *Plant Mol. Biol.* 30: 183–189.

James, P., Halladay, J. and Craig, E.A. (1996) Genomic libraries and a host strain designed for highly efficient two-hybrid selection in yeast. *Genetics* 144: 1425–1436.

Kato, A., Hayashi, M., Kondo, M. and Nishimura, M. (1996a) Targeting and processing of a chimeric protein with the N-terminal presequence of the precursor to glyoxysomal citrate synthase. *Plant Cell* 8: 1601–1611.

Kato, A., Hayashi, M., Mori, H. and Nishimura, M. (1995) Molecular characterization of a glyoxysomal citrate synthase that is synthesized as a precursor of higher molecular mass in pumpkin. *Plant Mol. Biol.* 27: 377–390.

Kato, A., Hayashi, M. and Nishimura, M. (1999) Oligomeric proteins containing N-terminal targeting signals are imported into peroxisomes in transgenic *Arabidopsis*. *Plant Cell Physiol.* 40: 586–591.

Kato, A., Hayashi, M., Takeuchi, Y. and Nishimura, M. (1996b) cDNA cloning and expression of a gene for 3-ketoacyl-CoA thiolase in pumpkin cotyledons. *Plant Mol. Biol.* 31: 843–852.

Kato, A., Takeda-Yoshikawa, Y., Hayashi, M., Kondo, M., Hara-Nishimura, I. and Nishimura, M. (1998) Glyoxysomal malate dehydrogenase in pumpkin: cloning of a cDNA and functional analysis of its presequence. *Plant Cell Physiol.* 39: 186–195.

Kragler, F., Lametschwandtner, G., Christmann, J., Hartig, A. and Harada, J.J. (1998) Identification and analysis of the plant peroxisomal targeting signal 1 receptor NtPEX5. *Proc. Natl. Acad. Sci. USA* 95: 13336–13341.

Lazarow, P.B. and Fujiki, Y. (1985) Biogenesis of peroxisomes. *Annu. Rev. Cell. Biol.* 1: 489–530.

Lee, M.S., Mullen, R.T. and Trelease, R.N. (1997) Oilseed isocitrate lyases lacking their essential type 1 peroxisomal targeting signal are piggybacked to glyoxysomes. *Plant Cell* 9: 185–197

Maeshima, M., Yokoi, H. and Asahi, T. (1988) Evidence for no proteolytic processing during transport of isocitrate lyase into glyoxysomes in caster bean endosperm. *Plant Cell Physiol.* 29: 381–384.

Mano, S., Hayashi, M., Kondo, M. and Nishimura, M. (1996) cDNA cloning and expression of a gene for isocitrate lyase in pumpkin cotyledons. *Plant Cell Physiol.* 37: 941–948.

Mano, S., Hayashi, M., Kondo, M. and Nishimura, M. (1997) Hydroxypyruvate reductase with a carboxy-terminal targeting signal to microbodies is expressed in *Arabidopsis*. *Plant Cell Physiol.* 38: 449–455.

Mano, S., Hayashi, M. and Nishimura, M. (1999) Light regulates alternative splicing of hydroxypyruvate reductase in pumpkin. *Plant J.* 17: 309–320.

Marchuk, D., Drumm, M., Saulino, A. and Collins, F.S. (1990) Construction of T-vectors, a rapid and general system for direct cloning of unmodified PCR products. *Nucl. Acids Res.* 19: 1154.

Marzioch, M., Erdmann, K.S., Veenhuis, M. and Kunau, W.-H. (1994) PAS7 encodes a novel yeast member of the WD-40 protein family essential for import of 3-oxoacyl-CoA thiolase, a PTS2-containing protein, into peroxisomes. *EMBO J.* 13: 4908–4918.

McCollum, D., Monosov, E. and Subramani, S. (1993) The pas8 mutant of *Pichia pastoris* exhibit the peroxisomal protein import deficiencies of Zellweger syndrome cells–the PAS8 protein binds to the COOH-terminal tripeptide peroxisomal targeting signal, and is a member of the TPR protein family. *J. Cell Biol.* 121: 761–774.

Miller, J.H. (1972) *Experiments in Molecular Genetics*. Cold Spring Harbor Laboratory, Cold Spring Harbor, NY.

Mori, H., Takeda-Yoshikawa, Y., Hara-Nishimura, I. and Nishimura, M. (1991) Pumpkin malate synthase. *Eur. J. Biochem.* 197: 331–336.

Nakajima, K. and Yaoita, T. (1997) Construction of multiple-epitope tag sequence by PCR for sensitive Western blot analysis. *Nucl. Acids Res.* 25: 2231–2232.

Nishimura, M., Yamaguchi, J., Mori, H., Akazawa, T. and Yokota, S. (1986) Immunocytochemical analysis shows that glyoxysomes are directly transformed to leaf peroxisomes during greening of pumpkin cotyledons. *Plant Physiol.* 80: 313–316.

Nishimura, N., Takeuchi, Y., De Bellis, L. and Hara-Nishimura, I. (1993) Leaf peroxisomes are directly transformed to glyoxysomes during senescence of pumpkin cotyledons. *Protoplasma* 175: 131–137.

Nito, K., Yamaguchi, K., Kondo, M., Hayashi, M. and Nishimura, M. (2001) Pumpkin peroxisomal ascorbate peroxidase is localized on peroxisomal membranes and unknown membranous structures. *Plant Cell Physiol.* 42: 20–27.

Olsen, L.J. (1998) The surprising complexity of peroxisome biogenesis. *Plant Mol. Biol.* 38: 163–189.

Otera, H., Okumoto, K., Tateishi, K., Ikoma, Y., Matsuda, E., Nishimura, M., Tsukamoto, T., Osumi, T., Ohashi, K., Higuchi, O. and Fujiki, Y. (1998) Peroxisome targeting signal type 1 (PTS1) receptor is involved in import of both PTS1 and PTS2: studies with *PEX5*-defective CHO cell mutants. *Mol. Cell. Biol.* 18: 388–399.

Sautter, C. (1986) Microbody transition in greening watermelon cotyledons. Double immunocytochemical labeling of isocitrate lyase and hydroxypyruvate reductase. *Planta* 167: 491–503.

Schliebs, W., Saidowsky, J., Agianian, B., Dodt, G., Herberg, F.W. and Kunau, W.-H. (1999) Recombinant human peroxisomal targeting signal receptor

PEX5. *J. Biol. Chem.* 274: 5666–5673.

Schumann, U., Gietl, C. and Schmid, M. (1999) Sequence analysis of a cDNA encoding Pex7p, a peroxisomal targeting signal 2 receptor from *Arabidopsis thaliana*. *Plant Physiol.* 120: 339.

Shimozawa, N., Suzuki, Y., Zhang, Z., Miura, K., Matsumoto, A., Nagaya, M., Castillo-Taucher, S. and Kondo, N. (1999) A novel nonsense mutation of the PEX7 gene in a patient with rhizomelic chondrodysplasia punctata. *J. Hum. Genet.* 44: 123–125.

Subramani, S. (1998) Components involved in peroxisome import, biogenesis, proliferation, turnover, and movement. *Physiol. Rev.* 78: 171–188.

Subramani, S., Koller, A. and Snyder, W.B. (2000) Import of peroxisomal matrix and membrane proteins. *Annu. Rev. Biochem.* 69: 399–418.

Titus, D.E. and Becker, W.M. (1985) Investigation of the glyoxysome-peroxisome transition in germinating cucumber cotyledons using double-label immunoelectron microscopy. *J. Cell Biol.* 101: 1288–1299.

Tsugeki, R., Hara-Nishimura, I., Mori, H. and Nishimura, M. (1993) Cloning and Sequencing of cDNA for glycolate oxidase from pumpkin cotyledons and northern blot analysis. *Plant Cell Physiol.* 34: 51–57.

Van der Leij, I., Franse, M.M., Elgersma, Y., Distel, B. and Tabak, H.F. (1993) PAS10 is tetratricopeptide-repeat protein that is essential for the import of most matrix proteins into peroxisomes of *Saccharomyces cerevisiae*. *Proc. Natl. Acad. Sci. USA* 90: 11782–11786.

Volokita, M. (1991) The carboxy-terminal end of glycolate oxidase directs a foreign protein into tobacco leaf peroxisomes. *Plant J.* 1: 361–366.

Walton, P.A., Hill, P.E. and Subramani, S. (1995) Import of stably folded proteins into peroxisomes. *Mol. Biol. Cell* 6: 675–683.

Wiemer, E.A.C., Nuttley, W.M., Bertolaet, B.L., Li, X., Francke, U., Wheelock, M.J., Anne, U.K., Johnson, K.R. and Subramani, S. (1995) Human peroxisomal targeting signal-1 receptor restores peroxisomal protein import in cells from patients with fatal peroxisomal disorders. *J. Cell Biol.* 130: 51–65.

Will, G.K., Soukupova, M., Hong, X., Erdmann, K.S., Kiel, J.A.K.W., Dodt, G., Kunau, W.-H. and Erdmann, R. (1999) Identification and characterization of the human orthologue of yeast Pex14p. *Mol. Cell. Biol.* 19: 2265–2277.

Wimmer, C., Schmid, M., Veenhuis, M. and Gietl, C. (1998) The plant PTS1 receptor: similarities and differences to its human and yeast counterparts. *Plant J.* 16: 453–464.

Zhang, J.W. and Lazarow, P.B. (1994) PEB1 (PAS7) in *Saccharomyces cerevisiae* encodes a hydrophilic, intraperoxisomal protein which is a member of the WD repeat family and is essential for the import of thiolase into peroxisomes. *J. Cell Biol.* 129: 65–80.

(Received January 10, 2002; Accepted February 14, 2002)

参考論文目録

Hayashi, M., Nito, K., Takei-Hoshi R., Yagi, M., Kondo, M., Suenaga, A., Yamaya, T. and Nishimura, M. (2002).

Ped3p is a peroxisomal ATP-binding cassette transporter that might supply substrates for fatty acid β-oxidation, Plant Cell Physiol. 43, 1-11

Plant & Cell Physiology

WT *ped3*

WT *ped1*

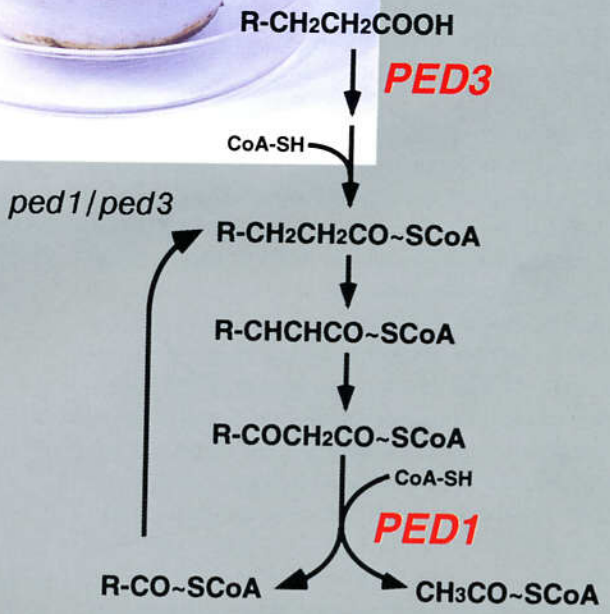

January
2002 Vol. 43 1

Plant Cell Physiol. 43(1): 1–11 (2002)

Rapid Paper

Ped3p is a Peroxisomal ATP-Binding Cassette Transporter that might Supply Substrates for Fatty Acid β-Oxidation

Makoto Hayashi [1, 5], Kazumasa Nito [1, 2], Rie Takei-Hoshi [1], Mina Yagi [1], Maki Kondo [1], Arata Suenaga [3], Tomoyuki Yamaya [3, 4] and Mikio Nishimura [1, 2]

[1] *Department of Cell Biology, National Institute for Basic Biology, Okazaki, 444-8585 Japan*
[2] *Department of Molecular Biomechanics, School of Life Science, Graduate University of Advanced Studies, Okazaki, 444-8585 Japan*
[3] *Department of Applied Plant Science, Graduate School of Agricultural Sciences, Tohoku University, 1-1 Tsutsumidori-Amamiyamachi, Aoba-ku, Sendai, 981-8555 Japan*
[4] *Plant Science Center, RIKEN, 2-1 Hirosawa, Wako, 351-0198 Japan*

Glyoxysomes, a group of specialized peroxisomes, are organelles that degrade fatty acids by the combination of fatty acid β-oxidation and glyoxylate cycle. However, the mechanism underlying the transport of the fatty acids across the peroxisomal membrane is still obscure in higher plant cells. We identified and analyzed the *PED3* gene and its gene product, Ped3p. The phenotype of the Arabidopsis *ped3* mutant indicated that the mutation in the *PED3* gene inhibits the activity of fatty acid β-oxidation. Ped3p is a 149-kDa protein that exists in peroxisomal membranes. The amino acid sequence of Ped3p had a typical characteristic for "full-size" ATP-binding cassette (ABC) transporter consisting of two transmembrane regions and two ATP-binding regions. This protein was divided into two parts, that had 32% identical amino acid sequences. Each part showed a significant sequence similarity with peroxisomal "half" ABC transporters so far identified in mammals and yeast. Ped3p may contribute to the transport of fatty acids and their derivatives across the peroxisomal membrane.

Key words: ABC transporter — *Arabidopsis thaliana* — Fatty acid β-oxidation — Glyoxysome — Leaf peroxisome — Peroxisome.

Abbreviations: 2,4-D, 2,4-dichlorophenoxyacetic acid; 2,4-DB, 2,4-dichlorophenoxybutyric acid.

The nucleotide sequence reported in this paper has been submitted to the DDBJ, EMBL and GenBank under accession numbers AB070615 (*PED3*) and AB070616 (*PED3* cDNA).

Introduction

Peroxisomes in higher plant cells are known to differentiate into at least three different classes, namely glyoxysomes, leaf peroxisomes and unspecialized peroxisomes (Beevers 1982). Each organelle contains a unique set of enzymes that provides special functions in various organs in higher plants. Glyoxysomes are present in cells of storage organs, such as endosperms and cotyledons during post-germinative growth of oil-seed plants, as well as in senescent organs (Nishimura et al. 1986, Nishimura et al. 1993, Nishimura et al. 1996). They contain enzymes for fatty acid β-oxidation and the glyoxylate cycle, and play a pivotal role in the conversion of seed-reserved lipids into sucrose. The seed-reserved lipids are deposited in lipid bodies as triacylglycerols. In general, these triacylglycerols mainly contain long-chain fatty acids such as palmitic acid, stearic acid, oleic acid, linoleic acid and linolenic acid (Trelease and Doman 1984). The fatty acids produced from the seed-reserved lipids are thought to be exclusively degraded in glyoxysomes (i.e. not in mitochondria) during germination and post-germinative growth (Beevers 1982). By contrast, leaf peroxisomes are widely found in cells of photosynthetic organs. Some of the enzymes responsible for photorespiration are localized in leaf peroxisomes even though the entire photorespiratory process involves a combination of enzymatic reactions that occur in chloroplasts, leaf peroxisomes and mitochondria (Tolbert 1982).

To identify the genes regulating the peroxisomal function in plant cells, we isolated mutants with defective peroxisomes. To screen such mutants, we used 2,4-dichlorophenoxybutyric acid (2,4-DB) as a compound for detecting Arabidopsis mutants with defects in glyoxysomal fatty acid β-oxidation (Hayashi et al. 1998b). We expected that two methylene groups of the butyric side chain in 2,4-DB would be removed by the action of glyoxysomal fatty acid β-oxidation to produce a herbicide, 2,4-dichlorophenoxyacetic acid (2,4-D), in wild-type plants, whereas the mutants no longer produce a toxic level of 2,4-D from 2,4-DB, because of the defect in fatty acid β-oxidation. We succeeded in identifying four mutants that were classified as carrying alleles at three independent loci. These loci were designated as *ped1*, *ped2*, and *ped3*, respectively, where *ped* stands for peroxisome defective.

Extensive studies of *ped2* mutant revealed that the *PED2* gene encodes Arabidopsis ortholog of *PEX14* (Hayashi et al.

[5] Corresponding author: E-mail, makoto@nibb.ac.jp; Fax, +81-564-55-7505.

2000). *At*Pex14p, a *PED2* gene product, is involved in the peroxisomal protein import machinery, and maintains peroxisomal functions by determining protein targeting to all kinds of plant peroxisomes. Therefore, the *ped2* mutant has deduced activity of not only glyoxysomal function but also leaf peroxisomal function, i.e. photorespiration. By contrast, it has been known that *ped1* mutant has a defect in a gene encoding one of the enzymes for fatty acid β-oxidation, 3-ketoacyl CoA thiolase (Hayashi et al. 1998b). The loss of 3-ketoacyl-CoA thiolase in the *ped1* mutant has recently been reported to affect the morphology of the glyoxysomes, while leaf peroxisomes and unspecialized peroxisomes are normal (Hayashi et al. 2001). Ultrastructural analyses revealed that glyoxysomes in the *ped1* mutant become enlarged organelles, probably because of accumulation of a metabolic intermediate induced by the lack of 3-ketoacyl-CoA thiolase. Detailed morphological observations suggested a direct interaction between glyoxysomes and lipid bodies during the post-germinative growth of the seedlings. The direct interaction is implicated in incorporating the fatty acids produced from the seed-reserved lipids into glyoxysomes. However, the mechanism underlying the transport of the fatty acids across the glyoxysomal membrane is still obscure in cells of higher plants.

In mammalian and yeast cells, it has been speculated that the peroxisomal half ATP-binding cassette (ABC) transporter plays an important role for the transport of fatty acids across peroxisomal membranes (Shani and Valle 1998). The existence of an ABC transporter in peroxisomal membranes was first elucidated in mammalian cells. Kamijo et al. (1990) cloned the rat PMP70 gene, and showed that it encoded a 70-kDa polypeptide containing one transmembrane region and one cytosolic ATP binding region, so-called peroxisomal "half" ABC transporter. Since then, attention has been paid to the peroxisomal ABC transporter, especially in relation to the human peroxisomal disorder. Mosser et al. (1993) reported a gene responsible for a human peroxisomal disorder, X-linked adrenoleukodystrophy. ALDP, a product of the gene, is a second "half" peroxisomal ABC transporter that has significant similarity to PMP70, more so than any other ABC transporter known at the time. At present, four peroxisomal ABC transporters have been identified in mammals. They are PMP70, ALDP and their homologues P70R and ALDR (Lombardplatet et al. 1996, Shani et al. 1997). In addition to these mammalian proteins, two orthologs of yeast, *Saccharomyces cerevisiae*, peroxisomal ABC transporters have been identified and characterized. They are called *PXA1* and *PXA2* (also called *PAT2* and *PAT1*, respectively) (Shani et al. 1995, Hettema et al. 1996, Shani and Valle 1998).

Here we report the identification the *PED3* gene. The *PED3* gene encodes a novel type of peroxisomal ABC transporter with a molecular mass of 149 kDa. Ped3p, a *PED3* gene product, exists in the glyoxysomal membrane, and is involved in the mechanism for transporting fatty acids produced from the seed-reserved lipids. We also discuss the possibility of a broad substrate specificity of Ped3p.

Results

Identification and characterization of four ped3 alleles

We previously identified two allelic mutations in *PED3* locus that are *ped3-1* and *ped3-2* on an *Arabidopsis thaliana*, ecotype Landsberg *erecta* background (Hayashi et al. 1998b). These mutant lines were identified by their resistance to the presence of the toxic level of 2,4-DB. By employing the same screening technique, we identified two additional alleles, which we designated as *ped3-3* and *ped3-4*. These *ped3* mutants showed resistance specifically to 2,4-DB (Fig. 1A) but not to 2,4-D (data not shown). By contrast, 2,4-DB inhibits the growth of wild-type Arabidopsis, because 2,4-DB is metabolized to produce a herbicide, 2,4-D, by the action of peroxisomal fatty acid β-oxidation (Fig. 1A). This suggests that the mutations in *PED3* locus reduce or inhibit the activity of peroxisomal fatty acid β-oxidation.

In oil-seed plants, the most important physiological function of fatty acid β-oxidation is a gluconeogenesis from seed-reserved lipids during post-germinative growth. To determine the activity of fatty acid β-oxidation, we examined the effect of sucrose on growth of these mutant lines (Fig. 1B), because defects in fatty acid β-oxidation seem to inhibit the conversion of seed-reserved lipids into sucrose that is required for heterotrophic growth. The wild-type Arabidopsis seedlings germinated and grew normally regardless of the presence or absence of sucrose in the growth medium. None of the *ped3* mutants could expand their green cotyledons and leaves when sucrose was removed from the growth medium (Fig. 1B). The inhibitory effects on germination and post-germinative growth varied depending on the mutant. Germination of *ped3-1* and *ped3-3* embryos was most severely inhibited, and seedlings never emerged from their seed coats on growth medium without sucrose. By contrast, *ped3-2* and *ped3-4* seedlings emerged from their seed coats but could no longer grow further. Roots of these mutants did not elongate and their leaves did not develop.

The growth inhibition that occurred in the absence of sucrose may be due to the suppression of gluconeogenesis from seed-reserved lipids during post-germinative growth. A mature seed of Arabidopsis contains approximately 5 μg of triacylglycerol as seed-reserved lipids (Fig. 1C). Seed-reserved lipids in the wild-type seed were rapidly degraded within 5 d after germination and used for gluconeogenesis (Fig. 1C). By contrast, seedlings of all the *ped3* mutants grown for 5 d still contained a significant amount of seed-reserved lipids (Fig. 1C). This suggests that all the *ped3* mutants have a defect in degrading the seed-reserved lipids. These findings indicated that all *ped3* mutant lines have a defect in gluconeogenesis from the seed-reserved lipids that is necessary for the post-germinative growth.

Despite the requirement of sucrose for germination and post-germinative growth, none of the *ped3* mutants required

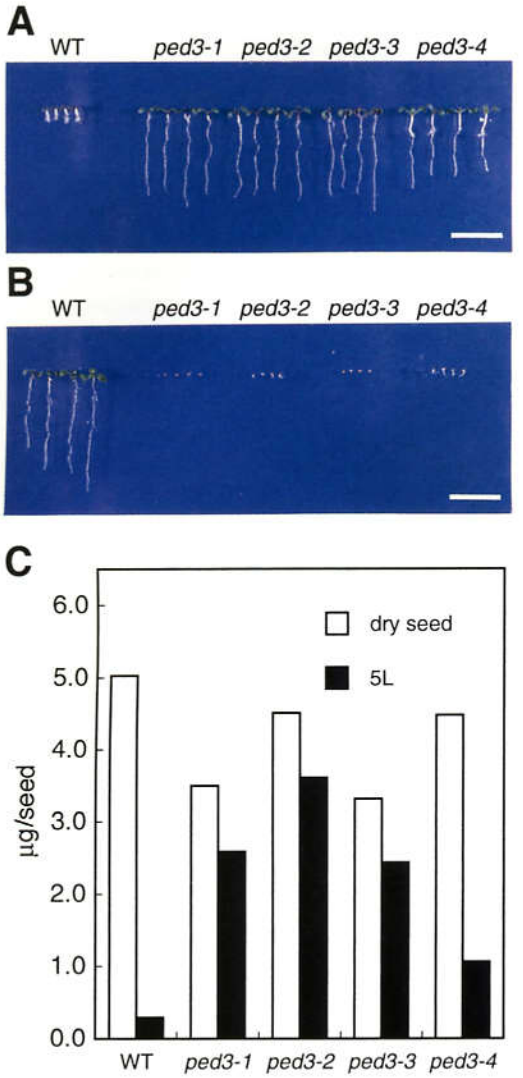

Fig. 1 Phenotypes of four *ped3* mutant lines. (A) Effects of 2,4-dichlorophenoxybutyric acid (2,4-DB) on the growth of four *ped3* mutant lines. Wild-type Arabidopsis (WT), *ped3-1*, *ped3-2*, *ped3-3* and *ped3-4* were grown for 7 d on growth medium containing 0.25 µg ml^{-1} of 2,4-DB under constant illumination. Photographs were taken after the seedlings were removed from the medium and rearranged on agar plates. (B) Effects of sucrose on the growth of four *ped3* mutant lines. Wild-type Arabidopsis (WT), *ped3-1*, *ped3-2*, *ped3-3* and *ped3-4* were grown for 7 d on growth medium without sucrose under constant illumination. Photographs were taken after the seedlings were removed from the medium and rearranged on agar plates. (C) Four *ped3* mutant lines have defect in degrading seed-reserved lipids during post-germinative growth. The amount of seed-reserved lipids remaining in a 5-day-old seedling grown under constant illumination (black bar) is compared with that in a dry seed (white bar). Wild-type Arabidopsis rapidly degrades seed-reserved lipids, while all *ped3* mutants (*ped3-1*, *ped3-2*, *ped3-3* and *ped3-4*) still contained larger amount of seed-reserved lipids 5 d after germination.

sucrose after they expanded green leaves on the growth medium containing sucrose. Therefore, they could grow and

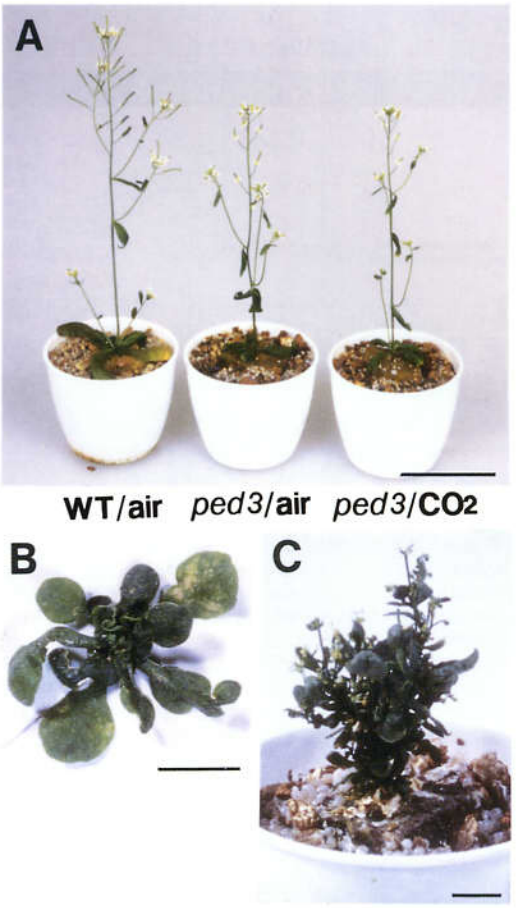

Fig. 2 Phenotypes of the *ped3* mutant and *ped1*/*ped3* double mutant. (A) Wild-type Arabidopsis (WT/air), and *ped3-2* mutant (ped3/air) were grown for 6 weeks in a normal atmosphere (36 Pa CO_2). The *ped3-2* mutant was also grown for 6 weeks in an atmosphere containing 1,000 Pa CO_2 (ped3/CO_2). Bar = 5 cm. (B) Rosette leaves of the *ped1*/*ped3* double mutant grown for 3 weeks. Bar = 1 cm. (C) *ped1*/*ped3* double mutant was grown for 6 weeks. Bar = 1 cm.

produce seeds on soil without supplying sucrose (Fig. 2A). *ped3* mutants grew equally under a normal atmosphere and an atmosphere enriched to 1% CO_2, suggesting that the *ped3* mutants do not have defects in leaf peroxisomal function (Fig. 2A). By contrast, the *ped2* mutant, that has a defect in the gene encoding the Arabidopsis ortholog of *PEX14*, has reduced activity of not only glyoxysomal function but also leaf peroxisomal function. Because of this defect, the *ped2* mutant showed a growth defect and has yellowish leaves in a normal atmosphere, but grew normally in a high CO_2 concentration (Hayashi et al. 2000).

To investigate the functional relationship between the *PED3* gene and fatty acid β-oxidation, we generated a *ped1*/*ped3* double mutant by outcrossing the *ped3-2* mutant to the *ped1* mutant that has a defect in 3-ketoacyl CoA thiolase. In the F3 generation, we identified 11 *ped1*/*ped3* double mutants. All these mutants showed similar vegetative and reproductive phe-

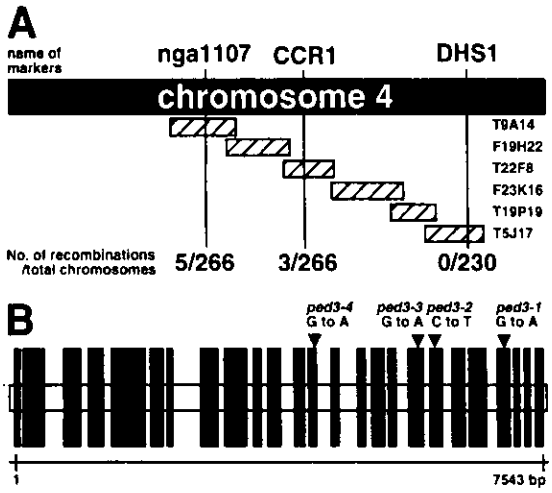

C

```
MPSLQLLQLTERGRGLVASRRKSILLAAGIVAAGGTAVYL      40
KSRVASRRPDSSRLCNGQSDDDEALEKLTATDQNAKITIK      80
KKKGGGLKSLQVLTAILLSQMGKMGARDLLALVATVVFRT     120
ALSNRLAKVQGFLFRAAFLRRAPLFLRLISENIMLCFMLS     160
TLHSTSKYITGALSLRFRKILTKIIHSHYFENMVYYKISH     200
VDGRITHPEQRIASDVPRFSSELSDLILDDLTAVTDGILY     240
AWRLCSYASPKYIFWILAYVLGAGTAIRNFSPSFGKLMSK     280
EQQLEGEYRQLHSRLRTHSESIAFYGGETREESHIQQKFK     320
NLVSHMSHVLHDHWFGMIQDFLLKYLGATVAVILIIEPF     360
FSGHLRPDDSTLGRAEMLSNIRYHTSVIISLFQALGTLSI     400
SSRRLNRLSGYADRIHELMAVSRELSGDDKSSFQRNRSRN     440
YLSEANYVEFSDVKVVTPTGNVLVEDLTLRVEQGSNLLIT     480
GPNGSGKSSLFRVLGGLWPLVSGHIVKPGVGSDLNKEIFY     520
VPQRPYMAVGTLRDQLIYPLTSGQESELLTEIGMVELLKN     560
VDLEYLLDRYQPEKEVNWGDELSLGEQQRLGMARLFYHKP     600
KFAILDECTSAVTTDMEERFAAKVRAMGTSCITISHRPAL     640
VAFHDVVLSLDGEGGWSVHYKRDDSALLTDAEIDSVKSSD     680
TDRQNDAMVVQRAFAAARKESATNSKAQSYQTQLIARSPV     720
VDKSVVLPRFPQPQTSQRALPSRVAAMLNVLIPTIFDKQG     760
AQLLAVACLVVSRTLISDRIASLNGTTVKYVLEQDKAAFV     800
RLIGLSVLQSGASSIIAPSLRHLTQRLALGWRIRLTQHLL     840
        (N; ped3-4)
RNYLRNNAFYKVFHMSGNSIDADQRLTRDLEKLTADLSGL     880
LTGMVKPSVDILWFIWRMKLLTGQRGVAILYTYMLLGLGF     920
LRRVAPDFGDLAGEEQQLEGKFRFMHERLNTHAESIAFFG     960
GGAREKAMVDKKFRALLDHSLMLLRKKWLYGILDDFVTKQ    1000
LPNNVIWGLSLLYALEHKGDRALVSTQGELAHALRYLASV    1040
        (X; ped3-3)                (W; ped3-2)
VSQSFMAFGDILELHKKFLELSGGINRIFELDEFLDASQS    1080
GVTSENQTSRLDSQDLLSFSEVDIITPAQKLMASKLSCEI    1120
VSGKSLLVTGPNGSGKTSVFRVLRDIWPTVCGRLTKPSLD    1160
IKELGSGNGMFFVPQRPYTCLGTLRDQIIYPLSKEEAEKR    1200
AAKLYTSGESSTEAGSILDSHLKTILENVRLVYLLERDVG    1240
GWDATTNWEDILSLGEQQRLGMARLFFHRPKFGVLDECTN    1280
(X; ped3-1)
ATSVDVEEQLYRVARDMGVTFITSSQRPALIPFHSLELRL    1320
IDGEGNWELRSIEQTTE                           1337
```

D

```
Ped3p  (298-312)   HSESIAFYGGETREE
Ped3p  (952-966)   HAESIAFFGGGARER
Pxa1p  (292-306)   NSEEIAFYQGTAVER
Pxa2p  (320-334)   SNEEIALLRGQKREL
PMP70 (275-289)    NSEEIAFYNGNKREK
ALDP   (289-303)   NSEEIAFYGGHEVEL
Consensus            E IA   G   E
```

notypes. They had wavy leaves with irregular shapes (Fig. 2B). Influorescence of the double mutants was difficult to develop, but they occasionally had dwarf inflorescences with abnormal structure (Fig. 2C). Although the inflorescences had some flowers, they were sterile. These phenotypes were not found in their parents.

High-resolution mapping of PED3 locus

We outcrossed the *ped3-2* mutant that has a Landsberg *erecta* ecotype background to wild-type Arabidopsis, ecotype Columbia, and identified 133 F2 progenies that have homozygous *ped3-2* alleles for high-resolution mapping. These progenies were subsequently scored according to their genetic background with a series of molecular markers (Fig. 3A). The number of chromosomes that showed a Colombia background represents the number of recombinations that occurred between the *PED3* locus and the position of each molecular marker, since the genomic DNA of the *ped3* mutant has a Landsberg *erecta* background. As summarized in Fig. 3A, high-resolution mapping revealed that the *PED3* locus is located on the right side of CCR1. The nearest marker to the *PED3* locus is DHS1 that is known to contain a BAC clone, T5J17 (accession no. AL035708). T5J17 represents the terminal end sequence of the lower arm of chromosome 4 in the Arabidopsis genome sequencing project (http://www.arabidopsis.org/). We searched for nucleotide sequences of T5J17, as well as T19P19, F23K16 and T22F8. These BAC clones are known to represent the

Fig. 3 Positional cloning of the *PED3* gene. (A) High-resolution mapping of *PED3* on chromosome 4. Names and positions of the molecular markers used in this study are indicated at the top of the illustration. Hatched bars represent the regions covered by BAC clones. We analyzed 133 F_2 progenies (266 chromosomes) having homozygous *ped3-2* alleles. The numbers of recombinations that occurred between the *PED3* locus and the molecular markers are indicated at the bottom of the illustration. Mapping results with molecular markers, nga1107, CCR1 and DHS1 are summarized schematically and indicate that the *PED3* locus is most likely to be located within a single BAC clone, T5J17. (B) Schematic diagram of a 7,543-bp genomic DNA fragment that is involved in the BAC clone, T5J17. The twenty five black bars represent protein coding regions determined from the cDNA sequence. Four arrowheads on the black bars indicate single nucleotide substitutions that occur in *ped3-1*, *ped3-2*, *ped3-3* and *ped3-4* alleles. Nucleotide residue 1 corresponds to an adenine of the first methionine codon. (C) Amino acid sequence of Ped3p. Amino acid sequence of Ped3p deduced from the nucleotide sequence of the *PED3* cDNA is indicated as single letter codes. Underlines indicate ATP/GTP-binding site motif A (P-loop) (prosite accession no. PS00017), while two double underlines indicate ABC transporters family signature (prosite accession no. PS00211). ^{810}Ser, ^{1007}Trp, ^{1035}Arg and ^{1242}Trp are substituted to Asn in *ped3-4*, stop codon (X) in *ped3-3*, Trp in *ped3-2*, and stop codon (X) in *ped3-1*, respectively. (D) Alignment of EAA-like motifs found in peroxisomal ABC transporters. Amino acid sequences of Ped3p, *S. cerevisiae* Pxa1p and Pex2p, human PMP70 and ALDP are shown with the number of amino acid residues. Similar amino acids are boxed in black, and identical amino acids are indicated as consensus.

genomic sequence for the right side of CCR1 (Fig. 3A). Based on these nucleotide sequences, we designed a set of oligonucleotide primers that could amplify one of the predicted genes by using the polymerase chain reaction (PCR). This gene is located within the 7543-bp DNA fragment contained in T5J17 (Fig. 3B). DNA fragments corresponding to this region were amplified from genomic DNAs of wild-type Arabidopsis, *ped3-1*, *ped3-2*, *ped3-3* and *ped3-4* mutants using the same primer set, and were fully sequenced. The nucleotide sequences of these DNA fragments are identical except for single nucleotide substitutions from ^{6999}G in the wild-type plant to A in the *ped3-1* mutant, ^{5986}C to T in *ped3-2* mutant, ^{5805}G to A in *ped3-3* mutant, ^{4352}G to A in *ped3-4* mutant (Fig. 3B, arrowheads). These results strongly indicated that the 7,543-bp DNA fragment contained the *PED3* gene (accession No. AB070615).

PED3 gene encodes an ABC transporter

To deduce the amino acid sequence of the *PED3* gene product, Ped3p, we searched the Arabidopsis expressed sequence tag (EST) database (http://www.kazusa.or.jp/) for the nucleotide sequence of the *PED3* gene, and found an EST clone called APZL37d10 (GenBank accession no. AV523713). This clone contained a partial cDNA encoding a peptide starting from Phe^{336} to the carboxy-terminal end. Therefore, we generated the full-length cDNA using reverse transcriptase-PCR with total RNA isolated from wild-type plants. We determined the nucleotide sequence of the cDNA (accession No. AB070616). Comparison of the nucleotide sequences for the cDNA and genomic DNA revealed that the *PED3* gene contains at least 25 exons (Fig. 3B). The deduced amino acid sequence of the Ped3p is composed of 1,337 amino acid residues with calculated a molecular mass of 149.4 kDa (Fig. 3C). Two alleles, *ped3-1* and *ped3-3*, have a nonsense mutation at the codon encoding ^{1242}Trp and ^{1007}Trp, respectively, while other alleles, *ped3-2* and *ped3-4*, have an amino acid substitution of ^{1035}Arg to Trp, and ^{810}Ser to Asn, respectively (Fig. 3C). It is worth emphasizing that germination of *ped3-1* and *ped3-3* embryos, that have a nonsense mutation in *PED3* locus, was the most severely inhibited, while *ped3-2* and *ped3-4* seedlings, that have a missense mutation at the *PED3* locus, showed milder phenotypes on the growth medium without sucrose (Fig. 3C).

Analyses of the amino acid sequence revealed that Ped3p could be divided into two parts at around ^{668}Cys. The amino acid sequences of these repeat sequences were 32% identical. In addition, each repeat has significant similarity with peroxisomal membrane proteins identified in mammals and yeast, such as PMP70, ALDP, and Pxa1p. The highest similarity was found in Rat PMP70 (Fig. 4A). Each repeat was further divided into two regions. One corresponds to the amino-terminal two thirds of the repeat (Fig. 4B, C; thick bars), while the other corresponds to the rest (Fig. 4B, C; open boxes). The former region is highly hydrophobic, and contains approximately six putative membrane-spanning segments. It also contains an

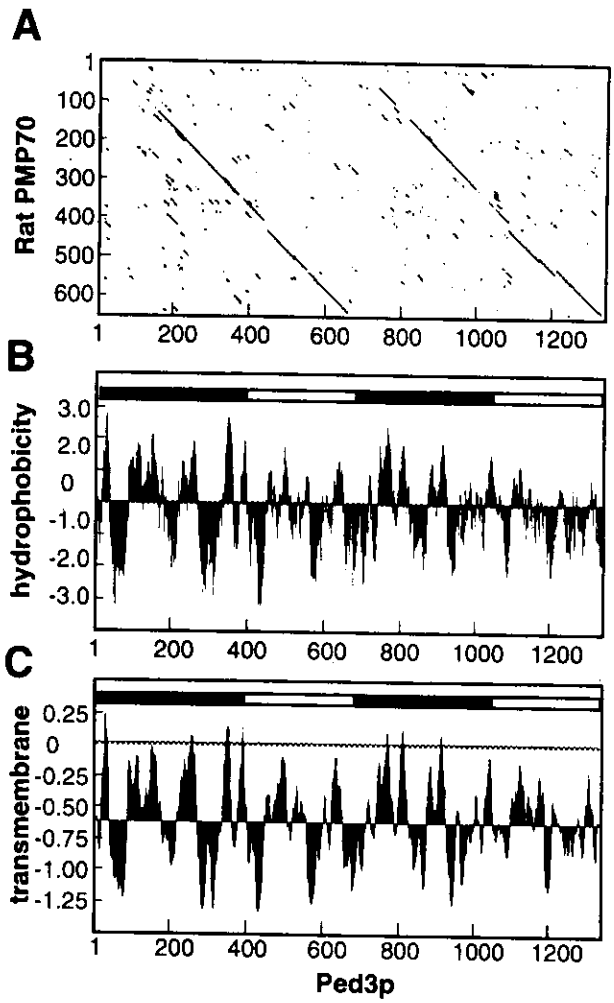

Fig. 4 Characterization of amino acid sequence of Ped3p. (A) Graphical comparison between amino acid sequences of Ped3p (vertical line) and rat PMP70 (horizontal line). A dot represents a stretch of 30 amino acids that aligned at least 11 similar amino acids. Numbers on each axis represent numbers of amino acid residues. (B) Hydropathy profile of Ped3p. The spots are generated using the algorithm of Kyte and Doolittle with a window size of 16 amino acid residues. Thick bars and open boxes in the panel represent two hydrophobic regions containing putative transmembrane segments, and two hydrophilic regions containing ATP-binding site, respectively. (C) Prediction of transmembrane helices in Ped3p. The spots are generated using the algorithm of von Heijne. Thick bars and open boxes in the panel represent two hydrophobic regions containing putative transmembrane segments, and two hydrophilic regions containing ATP-binding site, respectively.

EAA-like motif highly conserved among peroxisomal ABC transporters (Fig. 4D). EAA-like motif is similar in sequence and location to a motif previously described only in prokaryotic ABC transporters known as the EAA motif (Shani et al. 1996). Two missense and two single codon deletions were found within the EAA-like motif of ALDP (^{291}Glu) in four unrelated X-linked adrenoleukodystrophy patients. It has also been demonstrated that the yeast possessing missense mutation

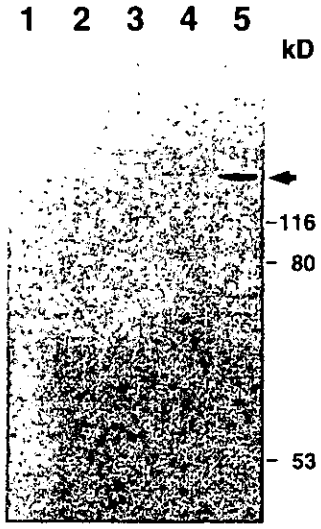

Fig. 5. Immunodetection of Ped3p in etiolated cotyledons of wild-type Arabidopsis and the *ped3* mutants. Extracts were prepared from etiolated cotyledons of *ped3-1* (line 1), *ped3-2* (lane 2), *ped3-3* (lane 3), *ped3-4* (lane 4), and wild-type Arabidopsis (lane 5). For each sample, 10 μg of total protein was subjected to SDS-PAGE. Immunoblot analysis was performed using an antibody raised against Ped3p. Arrow indicates the position of Ped3p. Positions of molecular markers are shown on the right with molecular masses in kDa.

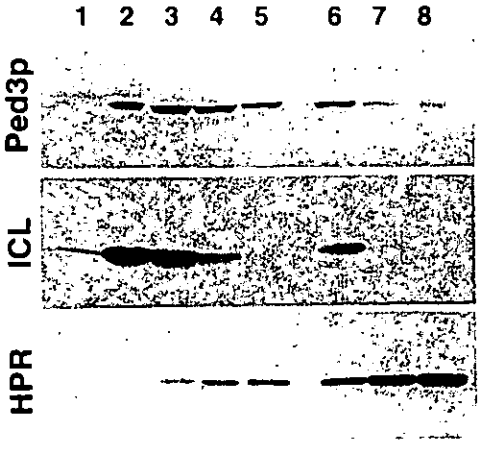

Fig. 6 Developmental changes of the Ped3p. The samples contained in each lane were prepared from etiolated cotyledons grown for 1 d in the dark (lane 1), 3 d in the dark (lane 2), 5 d in the dark (lane 3), 7 d in the dark (lane 4), 9 d in the dark. Green cotyledons obtained from the seedlings grown 4 d in the dark followed by 1 d in the light (lane 6), 4 d in the dark followed by 3 d in the light (lane 7), 4 d in the dark followed by 5 d in the light (lane 8) were also analyzed. For each sample, 10 μg of total protein prepared from cotyledons was subjected to SDS-PAGE. Immunoblot analyses were performed using the antibodies raised against Ped3p, isocitrate lyase (ICL) and hydroxypyruvate reductase (HPR).

in the EAA-like motif of PXA1 (^{294}Glu and ^{301}Gly) could not grow on medium containing 0.1% oleic acid as a sole carbon source, and had reduced fatty acid β-oxidation activity. These results indicated that the EAA-like motif is important for the

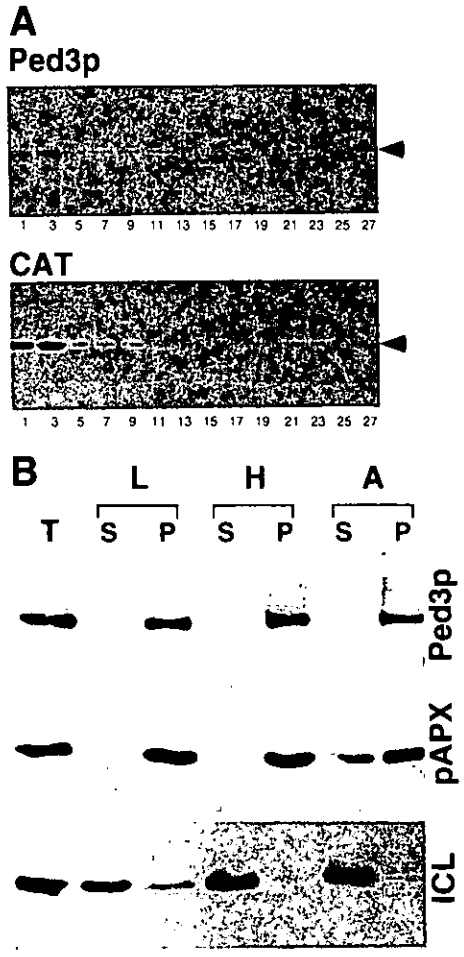

Fig. 7 Subcellular localization of Ped3p. (A) Subcellular fractionation of Arabidopsis etiolated cotyledons was performed by 30–60% sucrose density gradient centrifugation. Fraction number 1 represents the top fraction of the gradient. Ped3p and catalase in each fraction were detected by immunoblot analyses using antibodies raised against Ped3p and catalase (CAT). (B) Intact glyoxysomes isolated from pumpkin etiolated cotyledons were resuspended in either low salt buffer (L), high salt buffer (H) or alkaline solution (A). Each buffer consists of 10 mM HEPES-KOH (pH 7.2), 500 mM KCl with 10 mM HEPES-KOH (pH 7.2), and 0.1 M Na_2CO_3, respectively. These samples were then centrifuged, and separated into soluble (S) and insoluble (P) fractions. T represents total proteins of the intact glyoxysomes. Ped3p, peroxisomal ascorbate peroxidase (pAPX) and isocitrate lyase (ICL) were detected by immunoblot analysis.

function of peroxisomal ABC transporters, although the precise function of the EAA-like motif in peroxisomal ABC transporters remains to be determined. From these observation, conserved amino acid residues in the EAA-like motif of Ped3p, such as ^{300}Glu, ^{954}Glu, ^{307}Gly and ^{961}Gly, seemed to be important for its function as a peroxisomal ABC transporter. The latter region contains an ATP-binding site (Fig. 3C). It is hydrophilic, and may exist in cytosolic surface of the peroxisomal membrane (Fig. 4B).

Ped3p is abundant during post-germinative growth

To analyze Ped3p, a *PED3* gene product, we prepared an antiserum raised against a fusion protein containing a partial amino acid sequence of Ped3p (^{384}His-^{780}Ile). This antiserum recognized an ~149-kD protein in the wild-type plant (Fig. 5; lane 5), while no cross-reactive band that exhibited the comparable intensity was detected in the *ped3* mutants (Fig. 5; lanes 1–4). These data indicate that Ped3p is the 149-kDa protein.

Immunoblot analyses revealed that the amount of Ped3p in Arabidopsis etiolated cotyledons increased until 5 d after germination, and then declined during seedling growth under constant darkness (Fig. 6; Ped3p, lanes 1–5). The amount of Ped3p in the seedlings germinated in the dark decreased rapidly by illumination from the 4th day after germination (Fig. 6; Ped3p, lanes 6–8). The appearance and disappearance of Ped3p during post-germinative growth of the wild-type plant is similar to that of other glyoxysomal matrix proteins such as isocitrate lyase (Fig. 6; ICL), and different from leaf peroxisomal enzymes, such as hydroxypyruvate reductase (Fig. 6; HPR).

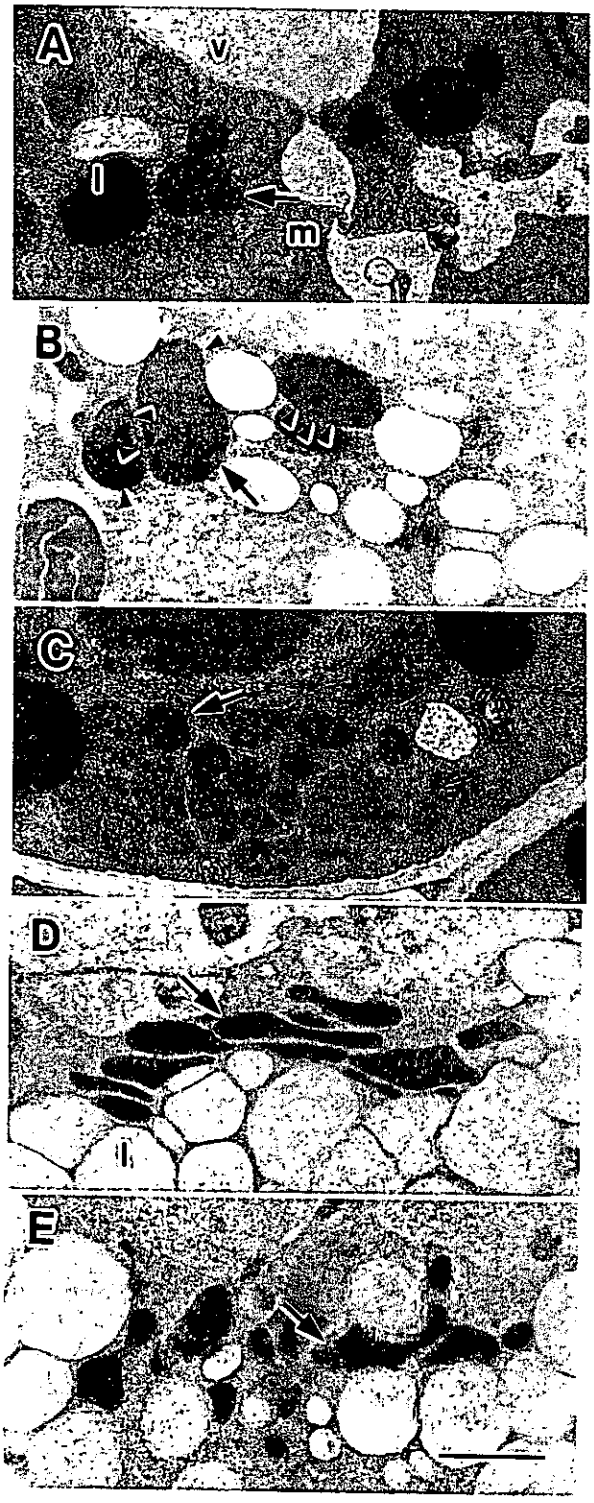

Ped3p is a glyoxysomal integral membrane protein

To investigate the subcellular localization of the Ped3p in wild-type plant cells, we subjected homogenates prepared from etiolated Arabidopsis cotyledons to sucrose density gradient centrifugation. Fractions thus obtained were analyzed using an immunoblot technique with an antibody raised against Ped3p. The 149-kDa protein was detected in fractions 21–23, whose densities were 1.25 g cm^{-3} (Fig. 7A). These fractions also contained other glyoxysomal marker enzymes, such as catalase (Fig. 7A) and isocitrate lyase (data not shown).

Fig. 7B represents the result of the extensive subfractionation studies performed by the treatment of intact glyoxysomes isolated from etiolated pumpkin cotyledons with various solutions. Isocitrate lyase, a marker enzyme for glyoxysomal matrix, was completely dissolved both in high-salt buffer and alkaline solution. By contrast, Ped3p were found only in the insoluble fraction even after the treatment with alkaline solution. This suggests the tight integration of Ped3p into the glyoxysomal membrane, since ascorbate peroxidase, a marker enzyme for peroxisomal membranes (Yamaguchi et al. 1995, Bunkelmann and Trelease 1996, Nito et al. 2001), was detected both in soluble and insoluble fractions after the treatment with an alkaline solution.

Morphology of glyoxysomes in the ped3 mutant

Fig. 8 shows an electron microscopic analysis of glyoxysomes in wild-type plants and the *ped3* mutants. As shown in Fig. 8A, glyoxysomes found in the 5-day-old etiolated cotyledons of wild-type plants are approximately 0.5 μm in diame-

Fig. 8 Electron microscopic analyses of glyoxysomes in the cells of 5-day-old etiolated cotyledons. (A) A cotyledonary cell of wild-type plant. (B) Immunogold labeling of wild-type plant using an antibody raised against Ped3p. (C) A cotyledonary cell of *ped3-2*. (D) Immunogold labeling of *ped3-2* using an antibody raised against 3-ketoacyl CoA thiolase. (E) Immunogold labeling of *ped3-2* using an antibody raised against isocitrate lyase. Arrowhead, peroxisome; m, mitochondrion; I, lipid body. Bar in (D) = 1 μm. Magnification of (A) to (E) is the same.

ter, and have a round or oval shape containing a uniform matrix. When the cells were immunogold-labeled using antibodies raised against Ped3p, the gold particles were mostly localized on the glyoxysomal membrane (Fig. 8B, arrowheads). Glyoxysomes in the *ped3* mutant are morphologically normal (Fig. 8C), while other 2,4DB-resistant mutants, such as *ped1* and *ped2* have glyoxysomes with abnormal structures (Hayashi et al. 1998b, Hayashi et al. 2000, Hayashi et al. 2001). The glyoxysomes in the *ped3* mutants contain detectable amounts of enzymes for fatty acid β-oxidation and glyoxylate cycle, such as 3-ketoacyl CoA thiolase (Fig. 8D) and isocitrate lyase (Fig. 8E), respectively.

Discussion

The chemically induced *ped3* mutant lines belong to a series of *A. thaliana* mutants that has defects in peroxisomal fatty acid β-oxidation. Positional cloning and subsequent analyses revealed that the *PED3* gene encodes a 149-kDa glyoxysomal membrane protein that possesses a typical characteristic of ABC transporter. Present data indicated that two *ped3* alleles, *ped3-1* and *ped3-3*, with nonsense mutations in *PED3* locus showed a stronger defect than the rest of two alleles, *ped3-2* and *ped3-4*, that have missense mutations during postgerminative growth without supplemental sucrose (Fig. 1B, 3C). In addition, analyses of the Arabidopsis genome sequence near the end of the lower arm of chromosome 4 revealed that there are no putative genes encoding a polypeptide that has similarity to the known enzymes for fatty acid β-oxidation, such as acyl CoA synthetase, acyl CoA oxidase, the bifunctional enzyme, 3-ketoacyl CoA thiolase (http://pedant.mips.biochem.mpg.de/, data not shown). These data strongly support the conclusion that the loss of the 149-kDa peroxisomal ABC transporter reduces the activity for fatty acid β-oxidation in the *ped3* mutants.

Many ABC transporters have been identified to date, in taxa ranging from bacteria to higher organisms. These proteins have been known to transport a variety of substrates across various membranes by utilizing the energy of ATP hydrolysis, and are grouped into the ABC superfamily (Higgins 1992). The designation of ABC transporters recognizes a highly conserved ATP-binding cassette, which is the most characteristic feature of this superfamily. The typical transporter consists of two copies each of two structural units. One of these domains is highly hydrophobic and each consists of six membrane-spanning segments. These domains form a pathway through which the substrate crosses the membrane and are believed to determine the substrate specificity of the transporter. The other domains are peripherally located at the cytoplasmic face of the membrane, bind ATP, and couple ATP hydrolysis to the transport process. The domain organization of ABC transporters is various. The most frequent arrangement is four domains fused in a single polypeptide, referred to herein as "full-size" ABC transporter. However, there are many ABC transporters that are expressed as separate subunits, which contains a single repeat sequence or a single domain.

Several peroxisomal ABC transporters in mammalian and yeast cells have been identified: PMP70, ALDP, P70R, ALDR, *PXA1* and *PXA2* (Shani and Valle 1998). All these proteins have a molecular mass near 70 kDa, and contain one transmembrane domain and one ATP-binding region. Because of this unique structure, these proteins are often called peroxisomal "half" ABC transporters. By contrast, analysis of the amino acid sequence revealed that Ped3p is grouped into the "full-size" ABC transporter in spite of the fact that it exists in peroxisomal membranes. Ped3p is the first "full-size" ABC transporter so far identified in peroxisomal membranes. A BLAST search failed to reveal an Arabidopsis "half" ABC transporter that is more similar to rat PMP70 than Ped3p. We also failed to find a peroxisomal candidate for "full-size" ABC transporter in other organisms, including the yeast genome, which has sequence similarity to Ped3p. Therefore, it is possible that the domain structure of the peroxisomal ABC transporters varies depending on the organisms. Since the ABC transporters are thought to have a common evolutionary origin (Ames and Higgins 1983, Ames 1986), the difference of the domain structure in peroxisomal ABC transporters may reflect the evolution of peroxisomes. Since peroxisomal ABC transporters have been identified from only a limited number of organisms at present, further identification and detailed structural comparison of the peroxisomal ABC transporters from various organisms may help to clarify the evolution of the peroxisomes.

A human peroxisomal disorder, X-linked adrenoleukodystrophy is known to be induced by a defect in the peroxisomal half ABC transporter, ALDP. This genetic disease is characterized by the accumulation of very long-chain fatty acids (VLCFA) in serum due to a decreased peroxisomal VLCFA β-oxidation capacity. Because of its characteristic of ABC transporter and symptoms of the disease as well as the existence of VLCFA CoA synthetase activity on the cytoplasmic side of the peroxisomal membrane, ALDP is anticipated to be involved in the transport of CoA-esterified VLCFA across the peroxisomal membrane (Shani and Valle 1998). In yeast, two peroxisomal ABC transporters, Pxa1p and Pxa2p, form a heterodimer (Shani and Valle 1996), and are involved in the transport of CoA-esterified VLCFA (Hettema et al. 1996, Verleur et al. 1997). By inference, the Ped3p may function as a transporter of either fatty acids or CoA-esterified fatty acids across the peroxisomal membrane in higher plants. In the life cycle of the higher plants, fatty acids are most actively produced from seed-reserved lipids deposited in lipid bodies during post-germinative growth of the seedlings, when peroxisomes are functionally differentiated into glyoxysomes. These fatty acids or CoA-esterified fatty acids may be imported into the glyoxysomes by the action of Ped3p. The loss of Ped3p prevents the import of fatty acids into glyoxysomes, and subsequent gluconeogenesis that is necessary for the growth of the seedlings. The observed

phenotypes in the *ped3* mutants support this conclusion.

This assumption is also supported by the morphological difference of glyoxysomes in the *ped3* and *ped1* mutants. It has been known that glyoxysomes in the *ped1* mutant become enlarged organelles with abnormal structure (Hayashi et al. 1998b, Hayashi et al. 2001). Although fatty acids are imported into the glyoxysomes, the loss of 3-ketoacyl-CoA thiolase may induce the enlargement of the glyoxysomes by the accumulation of a metabolic intermediate for fatty acid β-oxidation. A similar phenomenon is induced by a deletion of another enzyme for fatty acid β-oxidation, the multifunctional enzyme, in yeast *Yarrowia lipolytica* (Smith et al. 2000). By contrast, glyoxysomes in *ped3* mutants did not show any morphological defect. One possible interpretation is that import the incompetency of fatty acids prevents subsequent metabolism, but does not affect the environment inside the glyoxysomes of the *ped3* mutant.

The *ped3* mutant showed not only a defect in fatty acid β-oxidation but also resistance to a toxic level of 2,4DB, that possesses the butyric side chain within the molecule. This result suggests that Ped3p transports 2,4DB into glyoxysomes, and may function as a transporter with broad substrate specificity from long-chain fatty acids to short-chain fatty acids, and their derivatives. The vegetative and reproductive phenotypes observed only in the *ped1/ped3* double mutant may support this idea. Future analyses of the substrate specificity may help to understand the function of Ped3p.

Materials and Methods

Plant materials and growth conditions

Identification of *ped3* mutant lines of *A. thaliana* has been previously described (Hayashi et al. 1998b). Progenies that had been backcrossed three times were used in this study. Arabidopsis ecotype Landsberg *erecta* was used as the wild-type plant. All seeds were surface sterilized in 2% NaClO, 0.02% Triton X-100, and germinated on growth media (2.3 mg ml^{-1} MS salt (Wako, Osaka, Japan), 1% sucrose, 100 μg ml^{-1} myo-inositol, 1 μg ml^{-1} thiamine-HCl, 0.5 μg ml^{-1} pyridoxine, 0.5 μg ml^{-1} nicotinic acid, 0.5 mg ml^{-1} MES-KOH (pH 5.7), 0.8% agar. Seedlings grown for 2 weeks on the growth medium were transferred into a 1 : 1 mixture of perlite and vermiculite. Plants were grown under a 16-h-light (100 μE m^{-2} s^{-1})/8-h-dark cycle at 22°C.

Quantitative analyses of total triacylglycerols

Amount of seed-reserved lipids contained in dry seeds and 5-day-old etiolated seedlings was measured as the amount of total triacylglycerol by using the assay kit, TRIGRYLCERIDE-TEST (Wako, Osaka, Japan). Either 10 dry seeds or 10 seedlings were homogenized in a mortar in 200 μl of water. Homogenates obtained were mixed with 3 ml isopropanol. Free glycerol and other compounds showing a similar color reaction in the sample was removed by an absorbent accompanying with the kit. The amount of triacylglycerols in the sample was measured according to the manufacturer's protocol. The amount of seed-reserved lipids was calculated as the amount of triolein.

Isolation of ped1/ped3 double mutant

The *ped3-2* mutant was outcrossed to *ped1* mutant. F2 progenies, obtained by self-fertilization of the F1 plants, were germinated on growth medium without sucrose. Seedlings that could not grow without sucrose were recovered after transferring these seedlings to medium containing sucrose. The genomic DNA of these F2 plants was individually isolated. The DNA fragment contained in the *PED1* locus was amplified by PCR using the 5′ primer (TGCTCCTGCCTTGAGACACC) and the 3′ primer (CTGCATATCAGAGGACCTCT). The polymorphism between *PED1* and *ped1* alleles was detected by the digestion of the DNA fragment with a restriction enzyme, *Nla*III. We identified one line that had heterozygous *PED1* allele (*PED1/ped1*) and homozygous *PED3* allele (*ped3-2/ped3-2*), and obtained F3 progenies by self-fertilization. We analyzed the allele at the *PED1* locus of the F3 progenies by the same procedure, and identified the *ped1/ped3* double mutant (*ped1/ped1*, *ped3-2/ped3-2*).

High-resolution mapping of PED3 locus

The *ped3-2* mutant was outcrossed to the wild-type plant (ecotype Columbia [Col-0]). F2 progenies, obtained by self-fertilization of the F1 plants, were germinated on growth medium without sucrose. One hundred thirty three seedlings that could not grow without sucrose recovered growth after they were transferred to medium containing sucrose. The genomic DNA of these F2 plants was individually isolated. Recombinations that occurred between the *PED3* locus and the molecular markers were scored by using the cleaved amplified polymorphic sequence (CAPS) mapping procedure (Konieczny and Ausubel 1993) and simple sequence length polymorphisms (SSLP) mapping procedure described previously (Bell and Ecker 1994).

Sequencing analyses

DNA and RNA extraction, sequence determination, and routine molecular biological techniques were performed by standard techniques (Sambrook et al. 1989). For identification of the *PED3* gene, the DNA fragments were amplified by the polymerase chain reaction (PCR) using 100 ng of genomic DNAs isolated from wild-type plants, *ped3-1*, *ped3-2*, *ped3-3* and *ped3-4* as templates, together with a 5′ primer (TACTCAATTCCAGGCCATGC), and a 3′ primer (TCACTCTGTTGTCTGTTCGATCGAACGG). A *PED3* cDNA clone was generated by reverse transcriptase-PCR with total RNA isolated from 7-day-old cotyledons of wild-type plants using the same primer set. The nucleotide sequences of those DNA fragments were analyzed as reported previously (Hayashi et al. 1998b). DNA and amino acid sequences were analyzed using MacVector and GCG Wisconsin package (Oxford Molecular Group, Inc., Oxford, U.K.).

Immunoblotting

A DNA fragment encoding from ^{384}His to ^{780}Ile of Ped3p was amplified from the *PED3* cDNA by PCR. The amplified DNA was inserted into the pET32 vector (Novagen, Madison, WI, U.S.A.). A fusion protein was synthesized in *Escherichia coli* cells, and used for the production of rabbit antibody raised against Ped3p according to the method previously reported (Hayashi et al. 1999). We also used antibodies raised against caster bean isocitrate lyase (Maeshima et al. 1988), spinach hydroxypyruvate reductase (Mano et al. 1999), pumpkin catalase (Yamaguchi and Nishimura 1984), pumpkin ascorbate peroxidase (Yamaguchi et al. 1995) and pumpkin 3-ketoacyl CoA thiolase (Kato et al. 1996). Immunoblots were analyzed according to protocols described previously (Hayashi et al. 1998a).

Subcellular fractionation and analyses of the intact glyoxysomes

One hundred mg of Arabidopsis seeds were grown on growth medium for 5 d in darkness at 22°C. Subcellular fractionation of 5-day-old etiolated cotyledons was performed using a 30–60% (w/w) sucrose density gradient centrifugation as previously reported (Hayashi et al. 1998b). After the centrifugation, 0.5 ml fractions were col-

lected, and used for immunoblot analyses.

Isolation of intact glyoxysomes from 5-day-old pumpkin etiolated cotyledons (100 g FW) by Percoll density gradient centrifugation has been also reported previously (Hayashi et al. 2000). The intact glyoxysomes (250 μg total protein) were resuspended in 200 μl of either low salt buffer, high salt buffer or alkaline solution. Each solution consisted of 10 mM HEPES-KOH (pH 7.2), 500 mM KCl with 10 mM HEPES-KOH (pH 7.2), and 0.1 M Na_2CO_3 (pH 11), respectively. After centrifugation at 100,000×*g* for 30 min, these samples were separated into the supernatants and the pellets. The pellets were resuspended in 200 μl of 100 mM HEPES-KOH (pH 7.2).

Electron microscopic analysis

Etiolated cotyledons were harvested from plants that were grown for 5 d in the dark. The ultrathin sections, the microscopic analysis and immunogold-labeling technique were prepared according to the protocol described previously (Hayashi et al. 1998b).

Acknowledgments

The authors thank Kazusa DNA Research Institute for kindly providing an EST clone, Dr. M. Maeshima (Nagoya University) for the antibody against isocitrate lyase, and K. Toriyama-Kato for technical assistance. This work was supported in part by a grant from the Research for the Future Program of the Japanese Society for the Promotion of Science (JSPS-RFTF96L00407), and by grants-in-aid for scientific research from the Ministry of Education, Science and Culture of Japan (12440231 to M.N. and 12640625 to M.H.) and by a grant from CREST of JST (Japan Science and Technology) to M.H and T.Y.

Note Added in Proof

During the reviewing process, the same gene was reported by Zolman et al. (2001) *Plant Physiol.* 127: 1266–1278. The authors designated the gene as *PXA1*.

References

Ames, G.F.-L. (1986) Bacterial periplasmic transport systems: structure, mechanism and evolution. *Annu. Rev. Biochem.* 55: 397–425.

Ames, G.F.-L. and Higgins, C.F. (1983) The organization, mechanism of action and evolution of periplasmic transport systems. *Trends Biochem. Sci.* 8: 97–100.

Beevers, H. (1982) Glyoxysomes in higher plants. *Ann. NY Acad. Sci.* 386: 243–251.

Bell, C.J. and Ecker, J.R. (1994) Assignment of 30 microsatellite loci to the linkage map of *Arabidopsis*. *Genomics* 19: 137–144.

Bunkelmann, J.R. and Trelease, R.N. (1996) Ascorbate peroxidase – A prominent membrane protein in oilseed glyoxysomes. *Plant Physiol.* 110: 589–598.

Hayashi, H., De Bellis, L., Ciurli, A., Kondo, M., Hayashi, M. and Nishimura, M. (1999). A novel acyl-CoA oxidase that can oxidize short-chain acyl-CoA in plant peroxisomes. *J. Biol. Chem.* 274: 12715–12721.

Hayashi, H., DeBellis, L., Yamaguchi, K., Kato, A., Hayashi, M. and Nishimura, M. (1998a) Molecular characterization of a glyoxysomal long chain acyl-CoA oxidase that is synthesized as a precursor of higher molecular mass in pumpkin. *J. Biol. Chem.* 273: 8301–8307.

Hayashi, M., Nito, K., Toriyama-Kato, K., Kondo, M., Yamaya, T. and Nishimura, M. (2000) AtPex14p maintains peroxisomal functions by determining protein targeting to three kinds of plant peroxisomes. *EMBO J.* 19: 5701–5710.

Hayashi, M., Toriyama, K., Kondo, M. and Nishimura, M. (1998b) 2, 4-dichlorophenoxybutyric acid-resistant mutants of Arabidopsis have defects in glyoxysomal fatty acid β-oxidation. *Plant Cell* 10: 183–195.

Hayashi, Y., Hayashi, H., Hayashi, M., Hara-Nishimura, I. and Nishimura, M. (2001) Direct interaction between glyoxysomes and lipid bodies in cotyledons of the *Arabidopsis thaliana ped1* mutant. *Protoplasma* 218: 83–94.

Hettema, E.H., van Roermund, C.W., Distel, B., van den Berg, M., Vilela, C., Rodrigues-Pousada, C., Wanders, R.J. and Tabak, H.F. (1996) The ABC transporter proteins Pat1 and Pat2 are required for import of long-chain fatty acids into peroxisomes of *Saccharomyces cerevisiae*. *EMBO J.* 15: 3813–3822.

Higgins, C.F. (1992) ABC transporters: from microorganisms to man. *Annu. Rev. Cell. Biol.* 8: 67–113.

Kamijo, K., Taketani, S., Yokota, S., Osumi, T. and Hashimoto, T. (1990) The 70-kDa peroxisomal membrane protein is a member of the Mdr (P-glycoprotein)-related ATP-binding protein superfamily. *J. Biol. Chem.* 265: 4534–4540.

Kato, A., Hayashi, M., Takeuchi, Y. and Nishimura, M. (1996) cDNA cloning and expression of a gene for 3-ketoacyl-CoA thiolase in pumpkin cotyledons. *Plant Mol. Biol.* 31: 843–852.

Konieczny, A. and Ausubel, F.M. (1993) A procedure for mapping *Arabidopsis* mutations using co-dominant ecotype-specific PCR-based markers. *Plant J.* 4: 403–410.

Lombardplatet, G., Savary, S., Sarde, C.O., Mandel, J.L. and Chimini, G. (1996) A close relative of the adrenoleukodystrophy (ALD) gene codes for a peroxisomal protein with a specific expression pattern. *Proc. Natl. Acad. Sci. USA* 93: 1265–1269.

Maeshima, M., Yokoi, H. and Asahi, T. (1988) Evidence for no proteolytic processing during transport of isocitrate lyase into glyoxysomes in castor bean endosperm. *Plant Cell Physiol.* 29: 381–384.

Mano, S., Hayashi, M. and Nishimura, M. (1999) Light regulates alternative splicing of hydroxypyruvate reductase in pumpkin. *Plant J.* 17: 309–320.

Mosser, J., Douar, A., Sarde, C., Kioschis, P., Feil, R., Moser, H., Poustka, A., Mandel, J. and P, A. (1993) Putative X-linked adrenoleukodystrophy gene shares unexpected homology with ABC transporters. *Nature* 361: 726–730.

Nishimura, M., Hayashi, M., Kato, A., Yamaguchi, K. and Mano, S. (1996) Functional transformation of microbodies in higher plant cells. *Cell Struct. Funct.* 21: 387–393.

Nishimura, M., Takeuchi, Y., De Bellis, L. and Hara-Nishimura, I. (1993) Leaf peroxisomes are directly transformed to glyoxysomes during senescence of pumpkin cotyledons. *Protoplasma* 175: 131–137.

Nishimura, M., Yamaguchi, J., Mori, H., Akazawa, T. and Yokota, S. (1986) Immunocytochemical analysis shows that glyoxysomes are directly transformed to leaf peroxisomes during greening of pumpkin cotyledons. *Plant Physiol.* 80: 313–316.

Nito, K., Yamaguchi, K., Kondo, M., Hayashi, M. and Nishimura, M. (2001) Pumpkin peroxisomal ascorbate peroxidase is localized on peroxisomal membranes and unknown membranous structures. *Plant Cell Physiol.* 42: 20–27.

Sambrook, J., Fritsch, E.F. and Maniatis, T. (1989) Molecular cloning: A laboratory manual. Cold Spring Harbor, NY: Cold Spring Harbor Laboratory Press.

Shani, N., Jimenez-Sanchez, G., Steel, G., Dean, M. and Valle, D. (1997) Identification of a fourth half ABC transporter in the human peroxisomal membrane. *Hum. Mol. Genet.* 6: 1925–1931.

Shani, N., Sapag, A. and Valle, D. (1996) Characterization and analysis of conserved motifs in a peroxisomal ATP-binding cassette transporter. *J. Biol. Chem.* 271: 8725–8730.

Shani, N. and Valle, D. (1996) A *Saccharomyces cerevisiae* homolog of the human adrenoleukodystrophy transporter is a heterodimer of two half ATP-binding cassette transporters. *Proc. Natl. Acad. Sci. USA* 93: 11901–11906.

Shani, N. and Valle, D. (1998) Peroxisomal ABC transporters. *Methods Enzymol.* 292: 753–776.

Shani, N., Watkins, P.A. and Valle, D. (1995) *PXA1*, a possible *Saccharomyces cerevisiae* ortholog of the human adrenoleukodystrophy gene. *Proc. Natl. Acad. Sci. USA* 92: 6012–6016.

Smith, J.J., Brown, T.W., Eitzen, G.A. and Rachubinski, R.A. (2000) Regulation of peroxisome size and number by fatty acid β-oxidation in the yeast *Yarrowia lipolytica*. *J. Biol. Chem.* 275: 20168–20178.

Tolbert, N.E. (1982) Leaf peroxisomes. *Ann. NY Acad. Sci.* 386: 254–268.

Trelease, R.N. and Doman, D.C. (1984) Mobilization of oil and wax reserves. *In* Seed Physiology vol. 2 Germination and Reserve Mobilization. Edited by Murray, D.R. pp. 201–245. Academic Press, New York.

Verleur, N., Hettema, E.H., van Roermund, C.W., Tabak, H.F. and Wanders, R.J. (1997) Transport of activated fatty acids by the peroxisomal ATP-binding-cassette transporter Pxa2 in a semi-intact yeast cell system. *Eur. J. Biochem.* 249: 657–661.

Yamaguchi, J. and Nishimura, M. (1984) Purification of glyoxysomal catalase and immunochemical comparison of glyoxysomal and leaf peroxisomal catalase in germinating pumpkin cotyledons. *Plant Physiol.* 74: 261–267.

Yamaguchi, K., Mori, H. and Nishimura, M. (1995) A novel isoenzyme of ascorbate peroxidase localized on glyoxysomal and leaf peroxisomal membranes in pumpkin. *Plant Cell Physiol.* 36: 1157–1162.

(Received November 7, 2001; Accepted December 7, 2001)